Andreas Hirsch

WILEY-VCH

The Chemistry of the Fullerenes

Andreas Hirsch

The Chemistry of the Fullerenes

Andreas Hirsch

The Chemistry of the Fullerenes

WILEY-VCH Verlag GmbH & Co. KGaA

Library of Congress Card No.:
applied for

British Library Cataloguing-in-Publication Data
A catalogue record for this book is available from the British Library.

Bibliographic information published by the Deutsche Nationalbibliothek
Die Deutsche Nationalbibliothek lists this publication in the Deutsche Nationalbibliografie; detailed bibliographic data are available in the Internet at <http://dnb.d-nb.de>.

Printed in the Federal Republic of Germany
Printed on acid-free paper

ISBN: 978-3-527-30890-3

.

Dedicated to my wife Almut

Preface

"Buckminsterfullerene: Is it a real thing?" This question was in our heads that evening in November 1990, when Fred Wudl came into the lab and showed us the first 50 mg sample of C_{60}. Although at that time there was evidence for the geometrical structures of this soccer ball shaped molecule and his bigger brother the "American football" C_{70}, no one knew what the chemical and physical properties of these fascinating molecular allotropes of carbon would be. On that same night we started to work on C_{60} and three reversible one electron reductions of the carbon sphere were found – one more than already detected by the Rice group. We were all enthusiastic and Fred projected possible chemical transformations and proposed remarkable electronic properties of fulleride salts – a prediction that shortly thereafter became reality by the discovery of the superconductivity of K_3C_{60} in the Bell labs. It was one of the greatest opportunities in my scientific life, that Fred asked me to participate in the ball game and to investigate organic fullerene chemistry. He also encouraged me to carry on this work in Germany, once I had finished my postdoctoral time in his group in Santa Barbara. The pioneering research of these early days is still a basis of my present work. Fullerene chemistry, which is unique in many respects, has meanwhile exploded. In a very short period of time a huge number of chemical transformations of the "real thing" C_{60} and outstanding properties of fullerene derivatives have been discovered. Many principles of fullerene chemistry are understood. The fullerenes are now an established compound class in organic chemistry.

It is therefore the right time to give a first comprehensive overview of fullerene chemistry, which is the aim of this book. This summary addresses chemists, material scientists and a broad readership in industry and the scientific community. The number of publications in this field meanwhile gains such dimensions that for nonspecialists it is very difficult to obtain a facile access to the topics of interest. In this book, which contains the complete important literature, the reader will find all aspects of fullerene chemistry as well as the properties of fullerene derivatives. After a short description of the discovery of the fullerenes all methods of the production and isolation of the parent fullerenes and endohedrals are discussed in detail (Chapter 1). In this first chapter the mechanism of the fullerene formation, the physical properties, for example the molecular structure, the thermodynamic, electronic and spectroscopic properties as well as solubilities are also summarized. This knowledge is necessary to understand the chemical behavior of the fullerenes. The description of the chemistry of the fullerenes themselves is organized according to the type of chemical transformation, starting from the reduction (Chapter 2), nucleophilic additions (Chapter 3), cycloadditions (Chapter 4), hydrogenation (Chapter 5), radical additions (Chapter 6), transition metal complex formation (Chapter 7) through oxidation and reactions with electrophiles (Chapter 8). Most of the examples presented in these chapters are reactions with C_{60}, since only very little work has been published on C_{70} and the higher fullerenes. It is the aim to provide an understanding of the basic characteristics of fullerene chemistry. This is achieved by a comparative description of both experimental and theoretical investigations in each of these chapters. It is also emphasized in each chapter wherever a reaction type leads to a fullerene derivative with a potential for practical application. In the last chapter (Chapter 9) the emerging principles of fullerene chemistry, such as reactivity and regiochemistry, are evaluated and summarized. The fullerene chemistry is still in an early stage of development. For synthetic chemists a lot of challenging work remains to be done. A prediction of the future directions of fullerene chemistry is therefore also given in Chapter 9 and finally, since from the beginning of the fullerene era many practical uses have been proposed, perspectives for applications are evaluated.

Writing this book prevented me for some time from carrying out practical work with my own hands. Nevertheless, since I have had co-workers like Thomas Grösser, Iris Lamparth, Andreas Skiebe and Antonio Soi, the experimental work on fullerenes in my lab has proceeded, even with much success. I am also indebted to my co-workers for their assistance in preparing figures and illustrations presented in this book. I thank Dr. L. R. Subramanian for reading the entire manuscript and for useful suggestions.

From Georg Thieme Verlag I thank Dr. J. P. Richmond for the excellent co-operation, which enabled the fast realization of this book project.

I am very grateful to my teacher Prof. Dr. Dr. h.c. M. Hanack, who has been supporting me for many years and who provided the starting conditions for writing this book.

It was Prof. Dr. F. Wudl who introduced me to the art of fullerene chemistry and who inspired me to continue with this work, for which I want to thank him very much. On reviewing the manuscript he came up with cogent comments and suggestions.

My special thanks go to my wife Almut, who, despite the fact that for several months she was very often deprived of the company of her husband, responded with warmth and understanding.

Andreas Hirsch
Tübingen, May 1994

Contents

Chapter 1 The Parent Fullerenes 1

1.1 The Fullerenes: Molecular Allotropes of Carbon 2
1.2 The Discovery of the Fullerenes 5
1.3 Fullerene Production 7
1.3.1 Fullerene Generation by Vaporization of Graphite 7
1.3.1.1 Resitive Heating of Graphite 7
13.1.2 Arc heating of Graphite 10
13.1.3 Solar Generators 10
13.1.4 Inductive Heating of Graphite 11
1.3.2 Fullerene Synthesis in Combustion 11
1.3.3 Formation of Fullerenes by Pyrolysis of Naphthalene 12
1.3.4 Endohedrals 12
1.3.5 The Formation Process 15
1.4 Separation and Purification 21
1.5 Properties 25
1.5.1 Structures 25
1.5.2 Physical and Spectroscopic Properties. 29
References 33

Chapter 2 Reduction 37

2.1 Introduction 38
2.2 Fulleride Anions 38
2.3 Reductive Electrosynthesis 42
2.3.1 Electrocrystallization 42
2.3.2 Electrophilic Additions to Fulleride Anions 43
2.4 Reduction with Metals 44
2.4.1 Alkali Metal Fullerides 44
2.4.1.1 Generation in Solution and Quenching Experiments 44
2.4.1.2 Synthesis and Properties of Alkali Metal Fulleride Solids 45
2.4.2 Alkaline Earth Metal Fullerides 50
2.4.3 Reduction with Mercury 51
2.5 Reduction with Organic Donor Molecules 51
References 53

Chapter 3 Nucleophilic Additions 56

3.1 Introduction 57
3.2 Addition of Carbon Nucleophiles 57
3.2.1 Hydroalkylation and Hydroarylation of C_{60} and C_{70} 57
3.2.2 Langmuir – Blodgett Films of $C_{60}H$*t*-Bu 63

3.2.3 Addition of Macromolecular Carbanions - Fullerene Polymers 64
3.2.4 Cyclopropanation of C_{60} and C_{70} 66
3.3 Addition of Amines 73
3.4 Addition of Hydroxide 76
References 77

Chapter 4 Cycloadditions 79

4.1 Introduction 80
4.2 [4+2] Cycloadditions 80
4.3 [3+2] Cycloadditions 87
4.3.1 Addition of Diazomethanes, Diazoacetates and Diazoamides 87
4.3.2 Addition of Azides 99
4.3.3 Addition of Trimethylenemethanes 99
4.3.4 Addition of Azomethine Ylides 103
4.3.5 Addition of Nitrile Oxides 105
4.3.6 Addition of Sulfinimides 106
4.3.7 Addition of Disiliranes 106
4.4 [2+2] Cycloadditions 107
4.4.1 Addition of Benzyne 107
4.4.2 Addition of Enones 107
4.4.3 Addition of Quadricyclane 108
4.4.4 Addition of Electron Rich Alkynes 109
4.4.5 Photopolymerization of C_{60} 110
4.5 [2+1] Cycloadditions 111
4.5.1 Addition of Carbenes 111
4.5.2 Addition of Silylenes 111
References 112

Chapter 5 Hydrogenation 115

5.1 Introduction 116
5.2 Oligohydrofullerenes $C_{60}H_{2n}$ and $C_{70}H_{2n}$ (n = 1 - 6) 116
5.2.1 Hydrogenation via Hydroboration, Hydrozirconation and Zinc/Acid Reduction 117
5.2.2 Theoretical Investigations 119
5.3 Polyhydrofullerenes $C_{60}H_{2n}$ and $C_{70}H_{2n}$ (n = 7 - 70) 125
5.3.1 Birch – Hückel Reduction 125
5.3.2 Transfer Hydrogenation of C_{60} and C_{70} 127
5.3.3 Catalytic Hydrogenation 129
5.3.4 Theoretical Investigations 129
References 134

Chapter 6 Radical Additions 136

6.1 Introduction 137
6.2 ESR Investigations of Radical Additions 137

6.2.1 Addition of Single Radicals ... 137
6.2.2 Multiple Radical Additions ... 143
6.3 Metalation of C_{60} with Pentacarbonylrhenium Radicals ... 146
6.4 Hydrostannylation of C_{60} ... 147
6.5 Addition of Bis(trifluoromethyl)nitroxide ... 147
6.6 Radical Copolymerization of C_{60} and Paracyclophane ... 147
References ... 148

Chapter 7 Transition Metal Complex Formation ... 150

7.1 Introduction ... 151
7.2 (η^2-C_{60}) Transition Metal Complexes ... 151
7.3 Hydrometalation Reactions ... 159
7.4 Organopalladium Polymers of C_{60} ... 160
References ... 160

Chapter 8 Oxidation and Reactions with Electrophiles ... 162

8.1 Introduction ... 163
8.2 Electrochemical Oxidation of C_{60} and C_{70} ... 163
8.3 Oxygenation ... 163
8.4 Osmylation ... 166
8.5 Halogenation ... 172
8.5.1 Fluorination ... 172
8.5.2 Chlorination ... 175
8.5.3 Bromination ... 177
8.5.4 Reaction with Iodine ... 180
8.6 Reactions with Strong Oxidizing Reagents and Acids ... 180
8.7 Reaction with Lewis Acids and Fullerenation of Aromatics ... 182
References ... 183

Chapter 9 Principles and Perspectives of Fullerene Chemistry ... 185

9.1 Introduction ... 186
9.2 Reactivity ... 186
9.3 Regiochemistry of Addition Reactions ... 190
9.4 The Future of Fullerene Chemistry ... 195
9.4.1 Multiple Addition Products with a Defined Three-Dimensional Structure ... 195
9.4.2 Heterofullerenes ... 196
9.4.3 Ring-Opening and Degradation Reactions - Synthesis of Endohedrals ... 196
9.4.4 Chemistry with Higher Fullerenes ... 197
9.5 Perspectives for Practical Applications ... 197
9.6 Concluding Remarks ... 199
References ... 200

Index ... 202

Chapter 1 The Parent Fullerenes

1.1 The Fullerenes: Molecular Allotropes of Carbon

1.2 The Discovery of the Fullerenes

1.3 Fullerene Production
1.3.1 Fullerene Generation by Vaporization of Graphite
1.3.1.1 Resitive Heating of Graphite
1.3.1.2 Arc Heating of Graphite
1.3.1.3 Solar Generators
1.3.1.4 Inductive Heating of Graphite
1.3.2 Fullerene Synthesis in Combustion
1.3.3 Formation of Fullerenes by Pyrolysis of Naphthalene
1.3.4 Endohedrals
1.3.5 The Formation Process

1.4 Separation and Purification

1.5 Properties
1.5.1 Structures
1.5.2 Physical and Spectroscopic Properties

References

1.1 The Fullerenes: Molecular Allotropes of Carbon

For synthetic chemists, who are interested in the transformation of known and the creation of new matter, elemental carbon as starting material played a minor role in the past. This situation changed dramatically, when the family of carbon allotropes consisting of the classical forms graphite and diamond, became enriched by the fullerenes. In contrast to graphite and diamond, with extended solid state structures, the fullerenes are spherical molecules and are soluble in a variety of organic solvents, an important requirement for chemical manipulations.

The fullerenes are built up of fused pentagons and hexagons. The pentagons, absent in graphite, provide the curvature. The smallest stable and at the same time the most abundant fullerene, obtained by usual preparation methods, is the I_h-symmetrical buckminsterfullerene C_{60} [Fig 1.1]. Buckminsterfullerene has the shape of a soccer ball. The next stable homologue is C_{70} [Fig 1.2] followed by the higher fullerenes C_{76}, C_{78}, C_{82}, C_{84}, C_{90}, C_{94} and C_{96}. The building principle of the fullerenes is a consequence of the Euler theorem which says that for the closure of each spherical network of n hexagons, 12 pentagons are required, with the exception of n =1.

Compared to small two-dimensional molecules, for example the planar benzene, the structures of these three-dimensional systems additionally appeal from an aesthetic point of view. The beauty and the unprecedented spherical architecture of these molecular cages immediately attracted the attention of many scientists. In a very fast development buckminsterfullerene C_{60} became one of the most intensively investigated molecules. For the synthetic chemists the challenge arose to synthesize exohedrally modified derivatives, in which the properties of fullerenes can be combined with those of other classes of materials. The following questions concerning the derivatization of fullerenes have been asked from the beginning: What kind of reactivity do the fullerenes have? Do they behave like a three-dimensional "superbenzene"? What are the structures of exohedral fullerene derivatives and how stable are they?

The IUPAC nomenclature method of buckminsterfullerene given below is too lengthly and complicated for general use[1]:

Hentriacontacyclo[29.29.0.0.^{2,14}.0^{3,12}.0^{4,59}.0^{5,10}.0^{6,58}.0^{7,55}.0^{8,53}.0^{9,21}.0^{11,20}.0^{13,18}.0^{15,30}.0^{16,28}.
0^{17,25}.0^{19,24}.0^{22,52}.0^{23,50}.0^{26,49}.0^{27,47}.0^{29,45}.0^{32,44}.0^{33,60}.0^{34,57}.0^{35,43}.0^{36,56}.0^{37,41}.0^{38,54}.0^{39,51}.
0^{40,48}.0^{42,46}]hexaconta-1,3,5(10),6,8,11,13(18),14,16,19,21,23,25,27,29(45),30,32,(44),33,
35(43),36,38(54),39(51),40(48),41,46,49,52,55,57,59-triacontaene.

Furthermore, the enormous number of derivatives including the multitude of possible regioisomers, available by chemical modifications requires the introduction of a simple nomenclature. Already by naming the soccer ball shaped C_{60} as [5,6]-fullerene-60-I_h, its structure is sufficiently described[2]. Thereby the numbers 5 and 6 denote, that C_{60} consists of pentagons and hexagons and the number 60 indicates the number of C-atoms. For [5,6]-fullerene-60-I_h and [5,6]-fullerene-70-D_{5h} there exists only one stable isomer of each, which further simplifies their name to fullerene-60 and fullerene-70. The indication of the symmetry groups however becomes important for the description of the higher fullerenes, where different isomers, for example [5,6]-fullerene-78-D_3 and [5,6]-fullerene-78-C_{2v} coexist. An unambiguous description of exohedrally modified derivatives also requires to introduce a numbering system for the C-atoms in each fullerene[3]. Thereby, the C-atoms are numbered in a spiral clockwise fashion, commencing in a hexagon. This is shown in Figure 1.1 and 1.2 for C_{60} and C_{70}. Although the axis of highest symmetry in C_{60} as well as in C_{70} (S_{10} and C_5) goes through pentagons, it is useful to start the numbering in a hexagon, since none of the other fullerenes have five-fold

symmetry and the bonds of the highest priority (reactivity) in C_{60} and C_{70} are those at the junction of two hexagons [Fig 1.1, Fig 1.2].

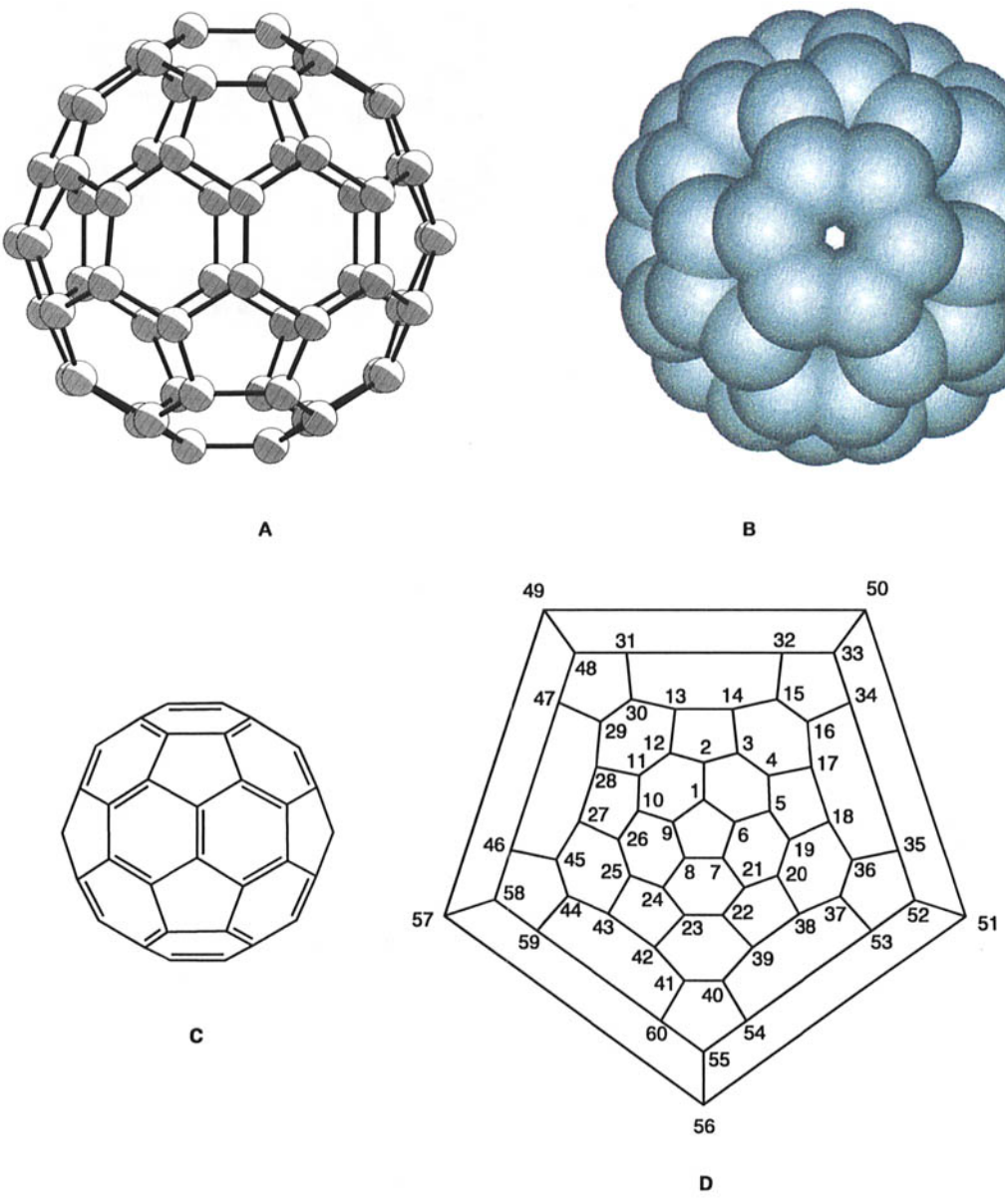

Figure 1.1 Schematic representations of C_{60} (A) ball and stick model, (B) space filling model, (C) front view diagram and (D) Schlegel diagram with numbering of the C-atoms

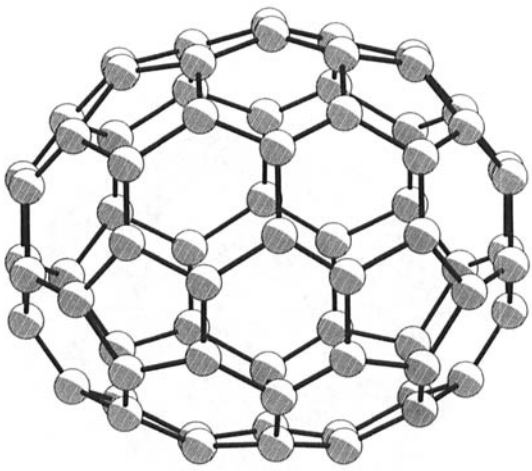

A

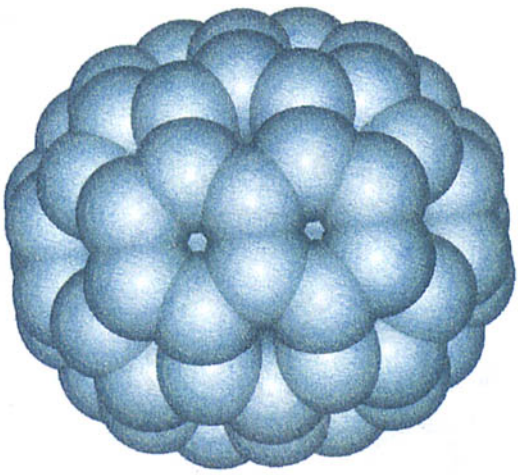

B

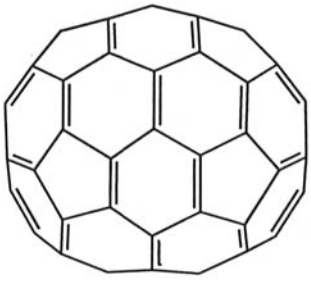

C

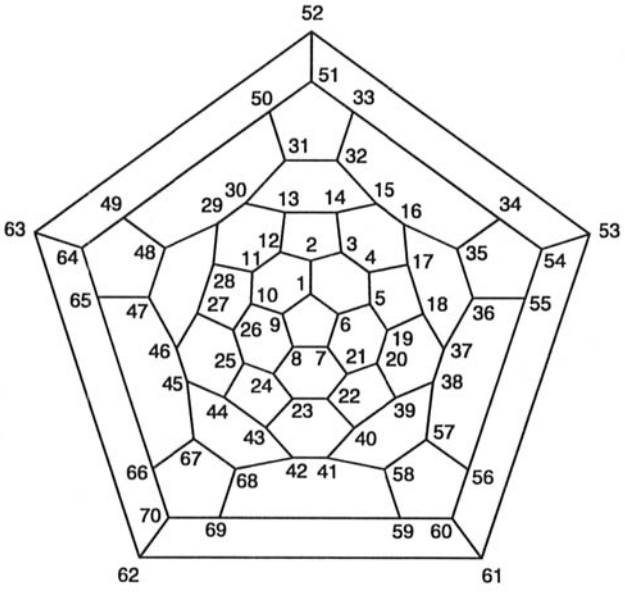

D

Figure 1.2 Schematic representations of C_{70} (A) ball and stick model, (B) space filling model, (C) front view diagram and (D) Schlegel diagram with numbering of the C-atoms

For simple schematic representations of fullerenes and their derivatives front view formulas or Schlegel diagrams are useful. The front view formulas give a quick impression of the geometry and the bonding situation (double bonds, single bonds) projected in two dimensions. The bonds at the back of the molecule are omitted for clarity. This kind of representation is often used for derivatives with only few adducts bound to the fullerene core. The Schlegel diagram shows each C-atom of the fullerene, which is flattened out in two dimensions. This model is suitable for the consideration of polyadducts for example polyhydrofullerenes.

The main type of chemical fullerene derivatizations are addition reactions. Regardless of the relatively large number of possible reaction sites, addition reactions show a remarkable regioselectivity, especially when the number of addents is small. This is another fulfilled requirement, which makes these molecular spheres exciting objects for the work of synthetic chemists.

1.2 The Discovery of the Fullerenes

In 1966 Deadalus alias D. E. H. Jones considered the possibility of making large hollow carbon cages, structures, that nowadays are called giant fullerenes[4,5]. This suggestion did not elicit any reaction from the scientific community. Four years later in 1970, simulated by the synthesis of the bowl shaped corannulene **1**[6], Osawa for the first time proposed the spherical I_h-symmetric football structure for the C_{60} molecule (**2**)[7,8]. In the course of his efforts to find new three-dimensional superaromatic π-systems, he recognized the corannulene to be a part of the football framework. Subsequently some theoretical papers of other groups appeared, in which inter alia Hückel calculations on C_{60} have been reported[9,10,11,12].

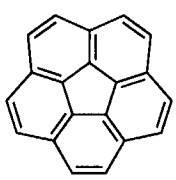

1

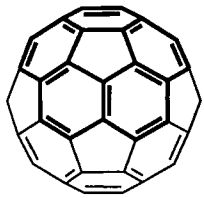

2

In 1984 it was observed, that upon laser vaporization of graphite, large carbon-only clusters C_n with n = 30-190 can be produced[13]. The mass distribution of the carbon clusters was determined by time-of-flight mass spectrometry. Only ions with even numbers of carbon atoms were observable in the spectra of large carbon clusters ($n \geq 30$). Although C_{60} and C_{70} were among these clusters, their identity was not recognized at this time. The breakthrough in the experimental discovery of the fullerenes came in 1985[14] when Kroto visited the Rice University in Houston. Here, Smalley and co-workers developed a technique[15] for studying refractory clusters by mass spectrometry, generated in a plasma by focusing a pulsed laser on a solid, in this case graphite. The original goal of the investigations of Kroto and Smalley was to simulate the conditions under which carbon nucleates in the atmospheres of red giant stars. Indeed, the cluster beam studies showed that the formation of species such as the cyanopolyynes HC_7N and HC_9N, which have been detected in space[16,17] can be simulated by laboratory experiments[18]. During the course of these studies, it was observed, that under

specific clustering conditions the 720 mass peak attributed to C_{60} and to a lesser extent the peak attributed to C_{70} exhibit a pronounced intensity in the spectra [Fig. 1.3]. Conditions could be found, for which the mass spectra were completely dominated by the C_{60} signal. Kroto and Smalley immediately drew the right conclusion of these experimental findings. The extra stability of C_{60} is due to its spherical structure, which is that of a truncated icosahedron with I_h symmetry[14]. This molecule was named after the architect Buckminster Fuller, whose geodesic domes obey similar building principles. Retrospectively, the enhanced intensity of the peak of C_{70}, which is also a stable fullerene, became understandable as well. Although buckminsterfullerene C_{60} was discovered, a method for a synthesis in macroscopic amounts needed to be found.

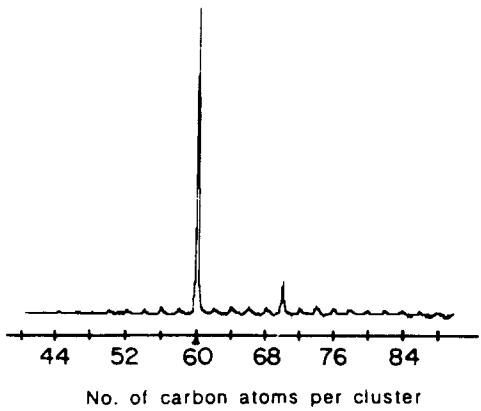

Figure 1.3 Time-of-flight mass spectrum of carbon cluster produced by laser vaporization of graphite under the optimum conditions for observation of a dominant C_{60} signal[14].

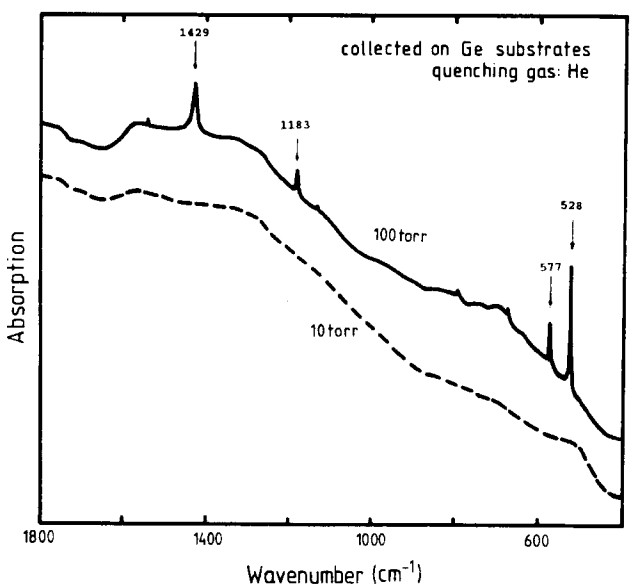

Figure 1.4 IR-spectra of soot particles produced by evaporation of graphite under different helium quenching gas pressures. The occurrence of the four additional sharp peaks at elevated helium pressures turned out to originate from buckminsterfullerene (C_{60})[19].

This second breakthrough in the fullerene research was achieved by Krätschmer and Huffman[19]. Their intention was to produce laboratory analogues of interstellar dust by vaporization of graphite rods in a helium atmosphere[20]. They observed, that upon choosing the right helium pressure, the IR-spectra of the soot, generated by the graphite vaporization, show four sharp stronger absorptions, together with those of the continuum of regular soot [Fig. 1.4][21]. These absorptions were close to the positions predicted by theory for buckminsterfullerene[22]. The isolation of the fullerenes from the soot was then accomplished by sublimation or extraction with benzene. This allowed the verification of their identity by spectroscopic and crystallographic methods as well as by control experiments with ^{13}C-enriched material. Next to buckminsterfullerene C_{60}, higher homolgues are also obtained by this technique. Now, the fullerenes were available for the scientific community.

1.3 Fullerene Production

1.3.1 Fullerene Generation by Vaporization of Graphite

1.3.1.1 Resistive Heating of Graphite

The generation of fullerenes by resistive heating of graphite was the first technique to produce macroscopic quantities[19]. This method is based on the technique for the production of amorphous carbon films in a vacuum evaporator[23]. The apparatus [Fig. 1.5] that Krätschmer and Fostiropoulos used for the first production of fullerenes consisted of a bell jar as recipient, which is connected to a pump system and a gas inlet. In the interior of the recipient two graphite rod are kept in contact by a soft spring. Thereby, one graphite rod is sharpened to a conical point, whereas the end of the other is flat. The graphite rods are connected to copper electrodes.

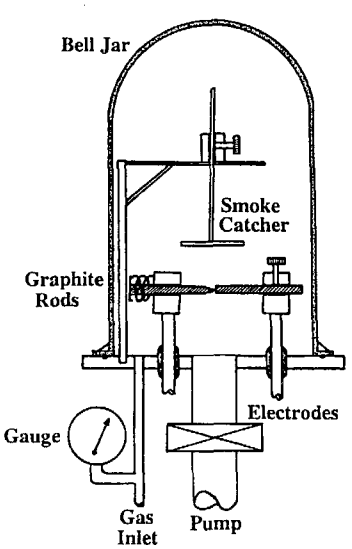

Figure 1.5 Fullerene generator originally used by Krätschmer[19,24].

For the production of soot, the apparatus is repeatedly evacuated and purged with helium and finally filled with about 140 mbar of helium. After applying a voltage, the electric current passing through the rods dissipates most of its Ohmic power heating at the narrow point of contact. This leads to a bright glowing in this area at temperatures of about 2500 - 3000 °C. At the same time a smoke develops at the contact zone, being transported away by convection and collected on the cooler areas (bell jar and smoke catcher) of the apparatus. The evaporation of the graphite is most efficient at the sharpened end of the rod. After the reaction is over, the fullerenes are extracted from the soot for example with toluene. The yield of extract (fullerenes) obtained by this technique is about 10-15 %.

Modifications of this type of fullerene reactor are gravity feed generators[25,26,27]. The advantage of these generators is their simple construction principle. This, together with the low costs make them attractive for synthetic chemists. A schematic representation of such a simple benchtop reactor, developed by Wudl[27] is given in Fig. 1.6. A thin 3 mm graphite rod, guided by a copper sleeve, with a sharpened tip is placed on a thick 12 mm rod. A commercially available arc welder serves as power supply. After applying a current (AC or DC) of about 40-60 A, only the material of the thin rod evaporates, whereupon it slips downward, guided by the copper sleeve which keeps the electrical contact. After a few minutes the rod is consumed to the point that it can not any longer make contact with the 12 mm rod. Then, the power is shut off. The yield of fullerenes based on evaporated graphite obtained by this method lies in the range of 5-10 %[27,28].

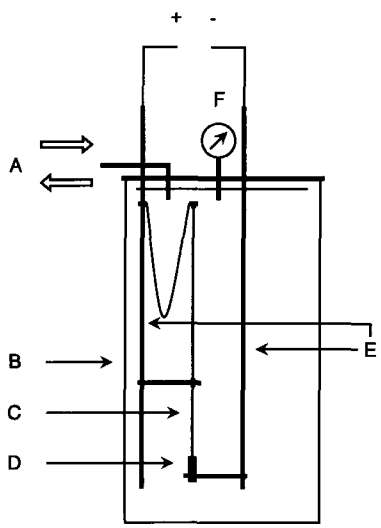

Figure 1.6 Simple benchtop reactor developed by Wudl[27]. Helium supply and connection to a vacuum system (A), pyrex bell jar (B), graphite rod (3 mm) (C), graphite rod (10 mm) (D), copper electrode (E), manometer (F).

The role of the buffer gas is to cool the plasma by collisions with the carbon vapor. The gas has to be inert, because otherwise reactions with smaller carbon clusters or atoms, initially formed by the evaporation will take place. Already using N_2 dramatically reduces the yield of fullerenes, presumably due to nitrogen atoms, formed in the hot zone of the generator, reacting with the carbon fragments[28].

The highest yields of fullerenes are obtained if helium is used as buffer gas. Also the concentration of the buffer gas is important [Fig 1.7]. Maximum yields are obtained by pressures ranging between 140 and 160 mbar[28]. With a very low buffer gas pressure the carbon radicals diffuse far away from the hot zone and the cluster continue to grow in an area which is too cool to allow an annealing to spherical carbon molecules. On the other hand, if the pressure of the buffer gas is too high, a very high concentration of carbon radicals results in the hot reaction zone. This leads to a fast growth of particles far beyond 60 C-atoms and the annealing process to fullerenes cannot compete[29].

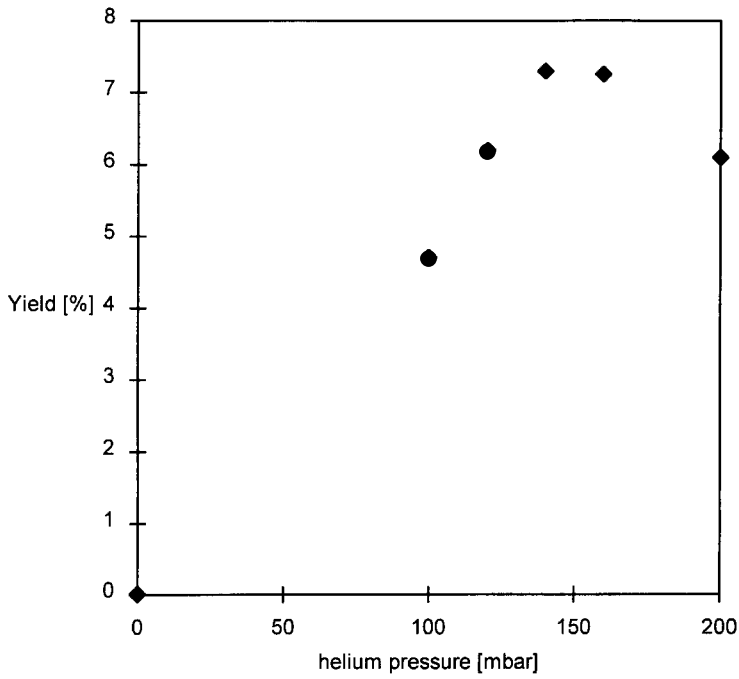

Figure 1.7 Dependence of the fullerene yield on the helium gas pressure in the fullerene generator

During these resistive heating procedures the formation of slag, depositing on the thicker graphite rod can be observed after some time of evaporation. As long as this vapor-deposited boundary layer remains between the two electrodes in a sufficiently thick and resistive form, the electrical power continues to be dissipated just in this small zone, and carbon vaporization from the end of the thin graphite rod proceeds efficiently[30]. Thus the formation of such a resistive layer may be an important requirement for the continuation of smoke production. In the beginning of the reaction this was guaranteed by the sharpened thin graphite rod (heat dissipation in this small resistive zone). For graphite rods, with diameters of 6 mm or greater, the resistive layer does not remain sufficiently resistive and the entire length of the graphite rod eventually begins to glow. This causes an inefficient evaporation of carbon from the center of the rod. Therefore, only comparatively thin graphite rod can be used for efficient fullerene production by the resistive heating technique.

1.3.1.2 Arc Heating of Graphite

An alternative for the resistive heating is the arc vaporization[29,31,32,33] of graphite first developed by Smalley[31]. If the tips of two sharpened graphite rods are kept in close proximity but not in a direct contact, the bulk of the electrical power is dissipated in an arc and not in Ohmic heating. In an original generator a spring tension was adjusted to maintain the arc between the nearly contacting graphite electrodes. The most efficient operation occurs when the electrodes are just barely touching, which lead to the formulation of the term "contact-arcing"[31]. This method allows an efficient evaporation of carbon, also with somewhat thicker, for example 6 mm rods. The yield of fullerenes obtained by this technique was found to be about 15 %. However, by increasing the rod diameter the yield decreases almost linearly[31], which also prevents an upscaling to very large rod sizes. The reason for the low yields of fullerenes, observed by using larger rod-sizes is their sensitivity towards UV-radiation. Very intense UV-radiation originates from the central portion of the arc plasma. While the newly formed fullerenes are moving away from the region around the arc, they are exposed to this intense light flux. The absorption of UV-light produces a triplet state (T_1), which lives for a few microseconds [Scheme 1.1][34].

$$C_{60}\,(S_0) + h\upsilon \rightarrow C_{60}^{*}\,(T_1)$$

Scheme 1.1

In this T_1 state the fullerene is an open shell system and very susceptible to other carbon species C_n. As a result of such a reaction a nonvaporizable insoluble product may be formed [Scheme 1.2][31].

$$C_{60}^{*}\,(T_1) + C_x \rightarrow \text{insoluble carbon}$$

Scheme 1.2

The effect of increased rod sizes is a larger photochemical danger zone. The rate of the migration of the newly formed fullerenes through this zone however remains constant. Therefore, the yield of fullerenes, which migrate through this region without reacting with other carbon species linearly decreases with the rod diameter[31].

1.3.1.3 Solar Generators

The problem of intense UV-radiation is avoided by the use of solar furnaces as fullerene generators[31,35]. Although sun light is used for the evaporation of graphite the exposure of generated fullerenes to radiation is far less extensive than using resistive heating or arc vaporization techniques. As an example for a solar generator, "Solar 1" developed by Smalley[31] will be discussed [Fig. 1.8].

The sunlight is collected by parabolic mirrors and focused onto a tip of a graphite rod. This rod is mounted inside a Pyrex tube. To minimize the extent of conductive heat loss and to provide suitable conditions for the annealing process of the carbon clusters, the graphite rod was enclosed by a helical tungsten preheater. After degassing the system with the preheater, it is filled with about 50 Torr of

argon and sealed off. For running the reaction the apparatus is adjusted so that the sunlight is focused directly on the tip of the graphite target. The argon gas heated by the tungsten preheater is efficiently carried up over the solar-irradiated carbon tip by convection (solar flux: 800-900 W/m^2). The condensing carbon vapor quickly moves away from the intensive sunlight, cools in the upper regions of the Pyrex tube and subsequently deposits on the upper walls. Although fullerenes can be obtained in this way, the efficiency of the prototype "Solar-1" generator is not very high.

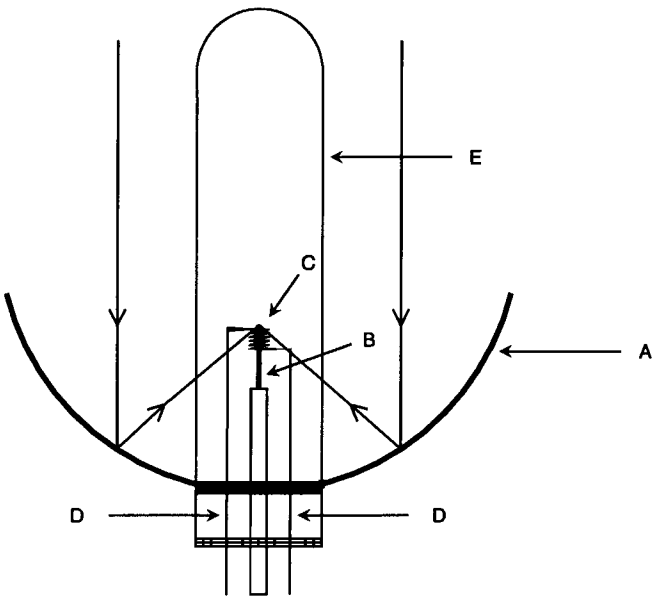

Figure 1.8 Schematic representation of the "Solar 1" fullerene generator[30]. (A) Parabolic mirror, (B) graphite target, (C) preheater, (D) insulated preheater connectors and (E) glass tube.

1.3.1.4 Inductive Heating of Graphite

Fullerenes can also be produced by direct inductive heating of a carbon sample, held in a boron nitride support[36]. Evaporations carried out at 2700 °C in a helium atmosphere, lead to the formation of fullerene containing soot. The soot is collected on the cold Pyrex glass of the reaction tube. This method allows a continuous operation by keeping the graphite sample in the heating zone. Upon evaporating 1 g of graphite 80 to 120 mg of fullerene extract can be obtained in 10 minutes.

1.3.2 Fullerene Synthesis in Combustion

The existence of fullerenes in sooting flames has been revealed for the first time by mass spectrometry studies[37,38]. Also the production of fullerenes in optimized sooting flames was shown to be possible[39,40,41,42]. For this purpose premixed laminar benzene/oxygen/argon flames operated under ranges of conditions including different pressures, temperatures and carbon to oxygen ratios have been used. Next to fullerenes and soot, polyaromatic hydrocarbons (PAHs) are formed simultaneously. The

yield of the fullerenes, as well as the C_{70}/C_{60} ratio strongly depend on the operation mode. The amount of C_{60} and C_{70}, produced under different sooting flame condition is in the range 0.003 - 9 % of the soot mass. Expressed as percentage of fuel carbon, the yield varies from 2 x 10^{-4} to 0.3 % for a non-sooting flame, obtained at optimum conditions, at a pressure of 20 Torr, a carbon to oxygen ratio of 0.995 with 10 % argon and a flame temperature of about 1800 K. The C_{70}/C_{60} ratio varies over the range 0.26 to 5.7, which is much larger than that observed for graphite vaporization methods (0.02 - 0.18) [319]. This ratio tends to increase with increasing pressure.

1.3.3 Formation of Fullerenes by Pyrolysis of Naphthalene

Fullerenes can also be obtained by pyrolysis of naphthalene at 1000 °C in an argon stream[43]. The naphthalene skeleton is a monomer of the C_{60} structure. The fullerenes are formed by dehydrogenative coupling reactions. Primary reaction products are polynaphthyls with up to seven naphthalene moieties joined together. The full dehydrogenation leads to both C_{60} as well as C_{70} in yields less than 0.5 %. As side products hydrofullerenes, for example $C_{60}H_{36}$, have also been observed by mass spectrometry.

1.3.4 Endohedrals

Since the fullerenes are hollow molecules, it was expected immediately that it should be possible to trap atoms inside the cage. Within one week after the initial discovery of C_{60}, evidence for an endohedral lanthanum complex of C_{60} was obtained[44]. The laser vaporization of a graphite disk, soaked in $LaCl_3$ solution allowed the observation of an additional peak in the time-of-flight (TOF) mass spectrum due to La encapsulated by C_{60}. Evidence, that indeed endohedral complexes are formed in this way came from "shrink-wrap" experiments showing that these complexes can loose successively C_2 fragments without bursting the cluster or loosing the incorporated metal [Scheme 1.3][45]. This is valid up to a certain limit, dictated by the ionic radius of the internal atom. For example, it was found to be difficult, to fragment past LaC_{44}^+ and impossible to go past LaC_{36}^+, without bursting the cluster [46].

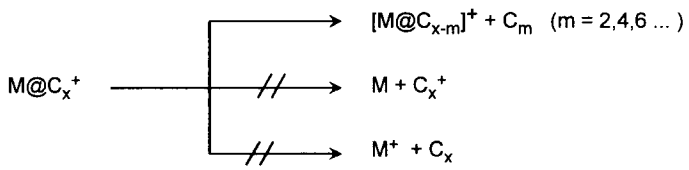

Scheme 1.3

To facilitate the discussion of these somewhat more complicated fullerenes with one or more atoms inside the cage, a special symbolism and nomenclature was introduced[46]. Thereby the symbol @ is used, to indicate the atoms in the interior of the fullerene. All atoms, that are listed to the left of the @ symbol are located inside the cage and all atoms to the right are a part of the cage structure, which includes heterofullerenes for example $C_{59}B$. A C_{60}-caged metal species is then written as M@C_{60}, expanded as "metal at C_{60}".

The production of endohedral fullerene complexes in visible amounts was first accomplished by a pulsed laser vaporization of a lanthanum oxide/graphite composite rod in a flow of argon gas at 1200°C[46]. In this procedure, the newly formed endohedrals together with empty fullerenes sublime readily and

are carried away in the flowing gas, depositing on the cool surfaces of the apparatus. This sublimate contains the complexes La@C_{60}, La@C_{70}, La@C_{74} and La@C_{82}. Among these, the endohedral molecule La@C_{82} exhibits an extra stability. It can be dissolved in toluene or carbon disulfide and exposed to the air [Fig. 1.9]. The smaller lanthanum fullerenes are less stable and do not survive a hot extraction with toluene on air. The laser vaporization technique was also successful for the production of yttrium fullerenes such as Y@C_{60}, Y@C_{70} and Y_2@C_{82} in addition to Y@C_{82}[47].

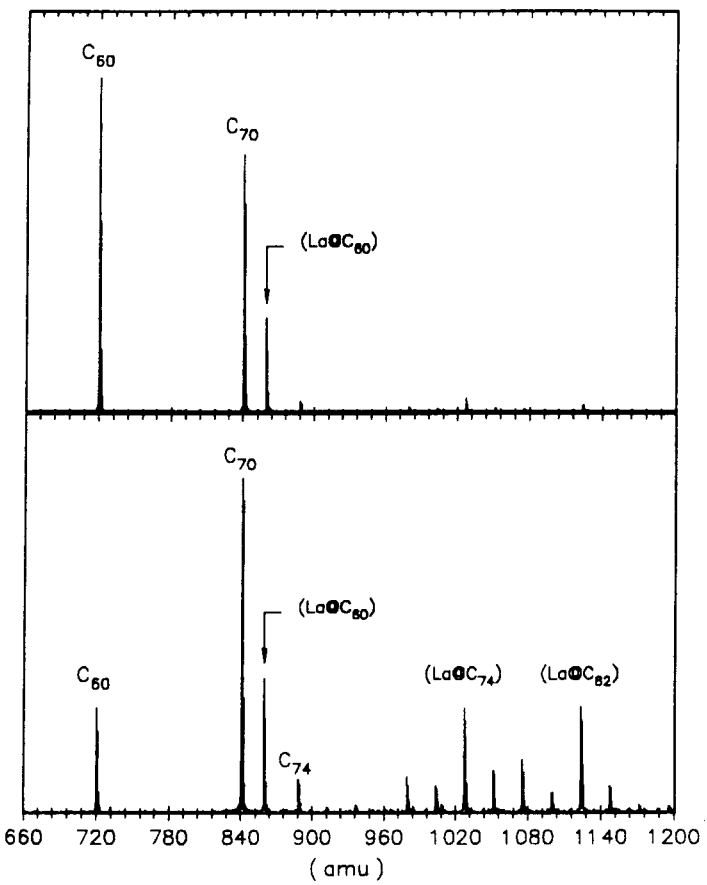

Figure 1.9 FT-ICR mass spectrum of hot toluene fullerene extract produced by laser vaporization of a lanthanum oxide/graphite composite rod[46].

Endohedral fullerene complexes can also be produced by arc vaporization of graphite, impregnated with a variety of metal oxides [46,48,49,50,51,52,53,54] or rare earth metal carbides[55]. The yield of the lanthanofullerene La@C_{82} for example increases by a factor of 10, when instead of the metal oxide the metal carbide enriched composite graphite rods are used for the generation of soot[55]. In general, the endohedral complexes M_n@C_{82} (n = 1,2,3) are the most abundant in the toluene or carbon disulfide extracts. But also metals, encapsulated in C_{76}, C_{80}, C_{84} have been extracted. Endohedral complexes of inter alia La, Y, Sc, Ce, Nd, Sm, Eu, Gd, Tb, Dy, Ho and Er can be prepared in this way. The interior of C_{82}, which is approximately 8 Å in diameter, can readily accommodate three rare earth trivalent ions which have average diameters ranging from 2.06 to 2.34 Å[49]. The yield of dimetallo- or trimetallofullerenes depends on the metal-to-carbon ratio, whereas higher yields of multiple metal

species are obtained by a higher metal content in the composite. Significantly, metallofullerenes encaged by C_{60} are not found in the solvent-extractable material. Possible reasons for this phenomenon are[52]: (i) the $M@C_{60}$ fullerenes are unstable and destroyed upon exposure to air or moisture; (ii) the $M@C_{60}$ fullerenes are insoluble in organic solvents and (iii) the $M@C_{60}$ fullerenes are not formed by this production method.

Another point of interest is that the $M_n@C_{82}$ fullerenes are the most abundant, although empty C_{82} is not a dominant species formed under normal conditions. The fact that also C_{80}, which in the empty case is an open shell system and therefore very unstable, efficiently encapsulates rare earth metals, to form stable endohedrals $M_2@C_{80}$ suggests, that the electronic structure of the fullerene shell is dramatically influenced by the central metals. This, on the other hand can be a reason for the possible instability of $M@C_{60}$. ESR studies on $M@C_{82}$ (M = Sc, Y, La) demonstrate that the metals are in the +3 oxidation state[48,53,54], which leaves the fullerene to be in the trianionic state. This finding is corroborated by cyclic voltammetry studies on HPLC purified $La@C_{82}$[56]. The cyclic voltammogram of dark green dichlorobenzene solutions of $La@C_{82}$ shows one reversible oxidation peak. The value of the oxidation potential being approximately equal to that of ferrocene implies, that the complex is a moderate electron donor and therefore an oxygen-stable molecule. In addition, five reversible reductions are observed, showing that $La@C_{82}$ is a stronger electron acceptor than empty fullerenes, with the first reduction potential being especially low lying. These findings can be interpreted with the proposed molecular orbital diagram [Fig. 1.10]. The removal of the radical electron corresponds to the first oxidation process. The resulting cation should be diamagnetic. The first reduction is relatively easy, because the filling of the HOMO leads to the closed shell species $La@C_{82}^-$. It was predicted by theoretical calculations, that the location of the lanthanum within the cage is off-center, which allows a stronger interaction with carbon atoms of the fullerene sphere[57,58,59].

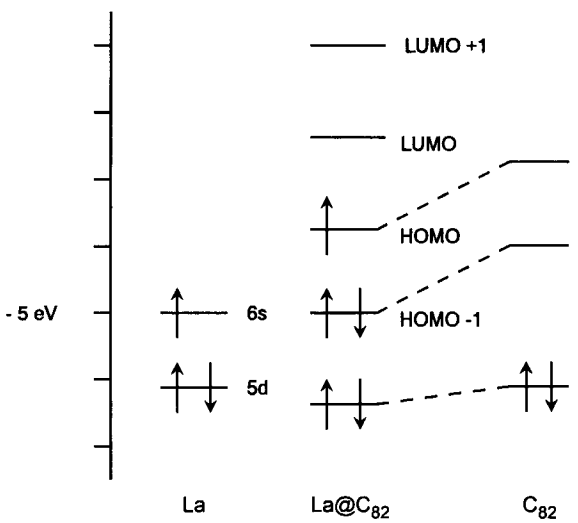

Figure 1.10 Schematic molecular orbital diagram of $La@C_{82}$[56]

Although electropositive metals form endohedral complexes with fullerenes during their formation in macroscopic quantities, this is not the case with helium, the buffer gas used for the fullerene synthesis. It was demonstrated that among 880,000 fullerene molecules generated by the arc-vaporization method only one contains a helium atom[60]. On the other hand, it could be shown by mass spectrometry studies, that an intact empty fullerene can be penetrated by the noble gas atoms He and Ne[61,62,63,64,65,66,67]. For this purpose singly and multiply charged C_x^{n+} fullerene molecules (x = 60, 70; n = 1-3) are shot through a stationary noble gas atmosphere in a molecular beam experiment. The resulting $M@C_{60}^+$ species show the "shrink-wrap" behavior with retention of M and successive elimination of C_2 [Scheme 1.3], which is typical for endohedral complexes. Upon reduction of $He@C_{60}^+$ the neutral complex $He@C_{60}$ can be obtained, which has a finite lifetime of >90 μs[64]. This provides further evidence, that the noble gas is physically trapped inside the fullerene cage. The endohedral complex $He@C_{60}$ is the first noble gas-carbon compound.

For the investigation of the properties of endohedral noble gas fullerene compounds it is necessary to increase the fraction of the molecules occupied. This has been done by heating C_{60} or C_{70} in a noble gas atmosphere at high pressures (e.g. 2700 bar) and temperatures (e.g. 600 °C)[68,69]. Next to helium also neon, argon, krypton and xenon have been incorporated into fullerenes by this method. Mole fractions of $X@C_{60}$ and $X@C_{70}$ (X = Ne, Ar, Kr, Xe) in the range between 0.04 and 0.3 % have been estimated by mass spectrometry[69]. Since the abundance of C_{60} and C_{70} with four ^{13}C atoms is high enough to interfere with the peaks of $He@C_{60}^+$ and $He@C_{70}^+$ it is difficult to measure the extent of helium incorporation by mass spectrometric methods. The use of ^3He however allows to record ^3He NMR spectra since ^3He has spin = 1/2. The ^3He NMR spectra of $^3He@C_{60}$ and $^3He@C_{70}$ show that the incorporation fraction is about 0.1 %[69]. ^3He NMR spectroscopy can also be used to measure the shielding environment inside the fullerene cavity. It has been shown that the ^3He nuclei encapsulated in C_{60} and C_{70} are shielded by 6 and 29 ppm respectively relative to free ^3He[68]. These shieldings indicate significant diamagnetic ring currents in C_{60} and very large ones in C_{70}.

Since the penetration of a noble gas atom through a six-membered ring would afford a very high activation energy[68], the formation of $X@C_{60}$ or $X@C_{70}$ (X = noble gas) must be accompanied by the breaking of at least one bond of the fullerene core. A window mechanism has been proposed to explain the penetration of noble gases into the fullerene cages [68,70]. The energetics of opening both the 6-6 bond and the 5-6 bond have been calculated[70]. A comparison of the reaction coordinates for the processes of breaking a 6-6 bond in the C_{60} singlet ground state and a 5-6 bond in the triplet state reveals an energetic preference of the latter process. The opening of one 5-6 bond leads to the formation of a nine membered ring, which is expected to be large enough for atoms to pass in or out. After the thermal breaking of a bond the fullerene, either filled with a noble gas atom or empty, can reform by closing the opened bond or it can react further, via another irreversible pathway, to form degraded fullerenes. Degradation products have indeed been found by the synthesis of $X@C_{60}$ or $X@C_{60}$[68].

1.3.5 The Formation Process

Despite the fact that the fullerenes are significantly destabilized with respect to graphite[71], they are readily formed out of a chaotic carbon plasma at temperatures of about 3000 K. A thermodynamically controlled pathway leading to highly symmetric fullerenes can be ruled out. If the fullerene formation would be thermodynamically controlled, then for example, the yield of C_{70}, which is more stable than C_{60}[72,73], should be much higher as it is found in extracts from graphitic soot. The toluene extract of soot, obtained by carbon vaporization, contains predominantly C_{60} followed by C_{70}. The ratio C_{60}/C_{70}

is about 85:15[74]. It must therefore be kinetic factors that govern the fullerene generation. The buckminsterfullerene ([5,6]-fullerene-60-I_h) is the most stable C_{60} fullerene isomer. Furthermore, the energy per carbon of [5,6]-fullerene-60-I_h is much lower than any isomer of C_{58} and C_{62}. Locally, [5,6]-fullerene-60-I_h is in a deep potential well and if once formed from clustering carbon it is chemically inert. This explains the much lower abundance of the higher fullerenes. One reason for the stability of C_{60} is that it obeys the "isolated pentagon rule" (IPR), which allows only fullerenes in which all pentagons are completely separated from each other by hexagons[75,76]. [5,6]-Fullerene-60-I_h at the same time is the smallest possible fullerene, which obeys the IPR. The next most stable isomer of C_{60} has two pairs of adjacent pentagons and has been calculated to be 2 eV higher in energy[77]. These stability considerations already imply that if clusters smaller than C_{60} are formed they will undergo further reactions in the plasma and if those being a little bit larger than C_{60} are formed, for example C_{62}, they can be stabilized by loss of small fragments (C_2) and rearrangements leading to the survivor [5,6]-fullerene-60-I_h. Analogous processes should be valid for the higher fullerenes.

A mechanism for the fullerene generation[78] by vaporization of graphite has to consider three major stages: (i) the vaporization itself and the nature of the initially formed intermediates; (ii) the structure of the growing clusters and (iii) the annealing to the fullerenes. The first step in the fullerene generation by evaporation of graphite is the formation of carbon atoms. This has been shown experimentally by $^{12}C/^{13}C$ isotope scrambling measurements[79,80,81]. The distribution of ^{13}C among the C_{60} molecules follows exactly Poisson statistics. The next step is the clustering of the carbon atoms. The smaller clusters are linear carbon chains or carbon rings. This was concluded by mass spectrometry studies of carbon clusters generated by laser desorption[82,83,84,85] and is supported by calculations[86,87]. If reactive components are added to the buffer gas during the graphite vaporization such early intermediates can be quenched and the fullerene formation is suppressed [Scheme 1.4][88,89,90,91]. The laser desorption of graphite in the presence of H_2 allowed the mass spectrometric observation of polyynes[88]. Similar rod-shaped molecules, the dicyanopolyynes NC-$(C{\equiv}C)_n$-CN (n = 3-7) are obtained in high yields upon vaporization of graphite in a He/$(CN)_2$ atmosphere [Scheme 1.4][90]. Obviously, in both cases irreversible additions of H atoms and CN-radicals to the ends of linear carbon chain intermediates occur. If Cl_2 is added to the buffer gas, instead of linear chains, perchlorinated cyclic compounds are found in the toluene extract of the soot [Scheme 1.4]. The amount of fullerenes in the extract is less than 5 %. Each carbon framework of the cyclic compounds **1-3** represents a part of the C_{60}-structure. Thereby, it is remarkable, that already structures containing pentagons, for example the decachlorocorannulene are formed. Polyaromatic hydrocarbons (PAHs) like **4-5** can be isolated, if the vaporization of graphite is carried out in an atmosphere of He/propene or He/methanol [Scheme 1.4]. Systems with a similar carbon framework are suggested to be present as intermediates during the formation of fullerenes in benzene flames[42]. However, it can not be concluded from the quenching experiments alone, whether clusters with structures like **1-5** are indeed predominant intermediates in the fullerene formation, since the presence of reactive species has an influence on the growth process. It has also to be stated, that the mechanisms of the fullerene formation by graphite evaporation and by combustion or pyrolysis of naphthalene are very likely different.

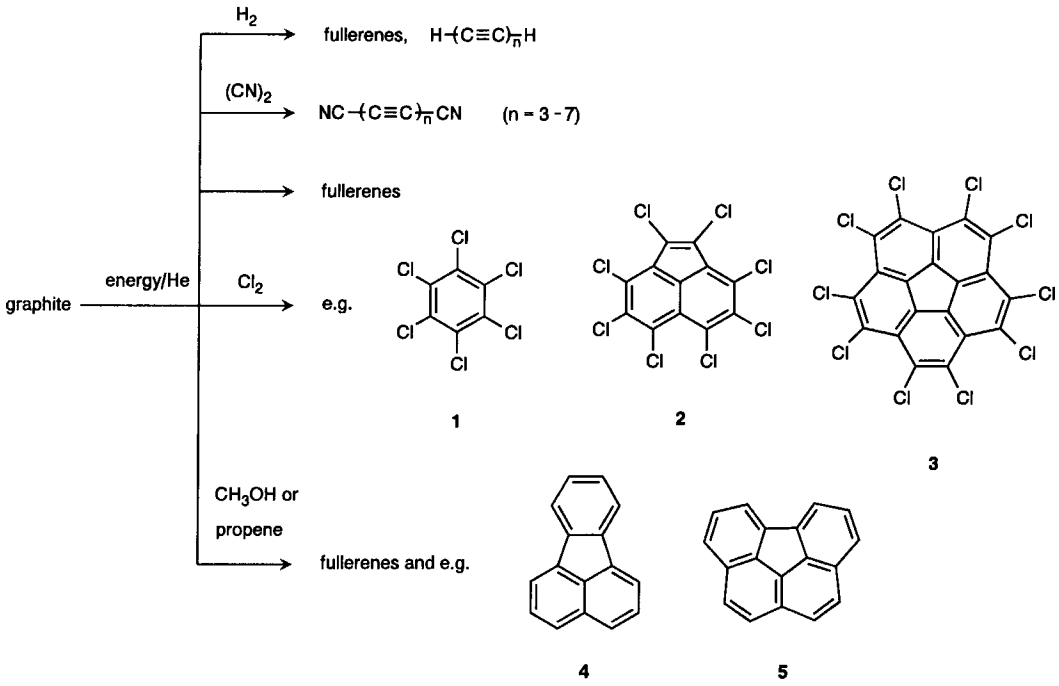

Scheme 1.4

Graphitic sheets as intermediates for cluster sizes of 30 or more carbon atoms are proposed in the "pentagon road" model[92,93]. Thereby it is emphasized, that the growth process of the graphitic sheet follows a low energy path by minimizing the number of dangling bonds. This can be achieved by the introduction of pentagons accompanied by a curling process [Fig. 1.11]. A complete closure to a fullerene reduces the number of dangling bonds to zero. This model also takes into account that high energy adjacent pentagon structures are avoided and also explains (i) the need for an elevated temperature for effective fullerene formation, because prior to a further growth an annealing process leads to an isolated pentagon network and (ii) the role of the buffer gas as well as the pressure dependence on the fullerene yield, because the helium concentration controls the diffusion of the C_n species from the hot into cooler zones of the plasma. Higher buffer gas pressures lead to an increase of the concentration of reactive C_n, which causes the annealing process to be not competitive with the cluster growth. During the annealing process the formation of a low energy structure obeying the IPR could be accomplished inter alia by the Stone-Wales rearrangement [Scheme 1.5][94]. This is a concerted process, which involves a Hückel four-center transition state.

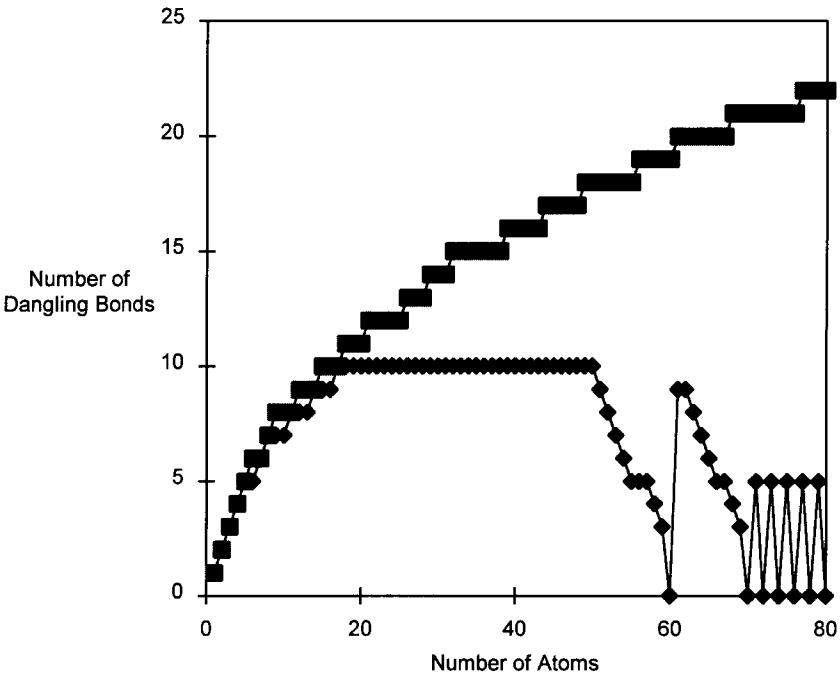

Figure 1.11 Number of dangling bonds in the best possible structure for a graphitic sheet with (top) all hexagons, compared to (bottom) those which obey the IPR, as a function of the number of atoms in the sheet[93].

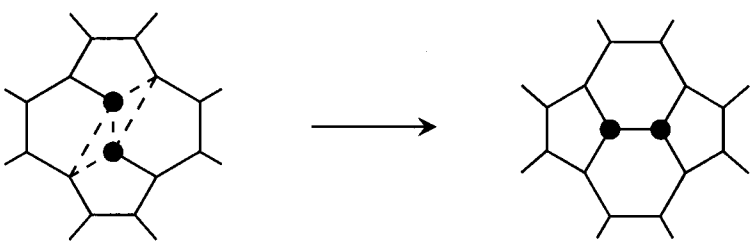

Scheme 1.5

Graphitic sheets however are not detectable in the carbon-plasma by ion chromatography (IC)[85,95,96,97]. This method provides a means for separating carbon cluster ions with different structures because the reciprocal of the ion mobility is proportional to the collision cross-section. It was found that several species C_n^+ with different structures coexist and their relative amount depends on the cluster size. Small clusters C_n^+ ($n < 7$) are linear. In the range of $n = 7\text{-}10$ chains as well as monocycles coexist. The clusters C_{11}^+ - C_{20}^+ are exclusively monocycles and the range between C_{21}^+ and C_{28}^+ is characterized by planar mono- and bicyclic systems. The first three-dimensional structure is detected at C_{29}^+ and the first fullerenes appear at C_{30}^+ and dominate from C_{50}^+.

Therefore, the growth pattern for carbon in the plasma starting from atoms is linear → monocyclic rings → polycyclic rings and finally → fullerenes.

If such mixtures of ions, generated by laser desorption of graphite are annealed by collisions, predominantly monocyclic rings are formed upon isomerization of the initial structures. At very high collision energies an isomerization to fullerenes occur. The fullerenes C_n^+ obtained in this way carry an enormous amount of internal energy, which can be dissipated by the cleavage of C_1- or C_3- (for odd n) or C_2-fragments (for even n) [Fig 1.12].

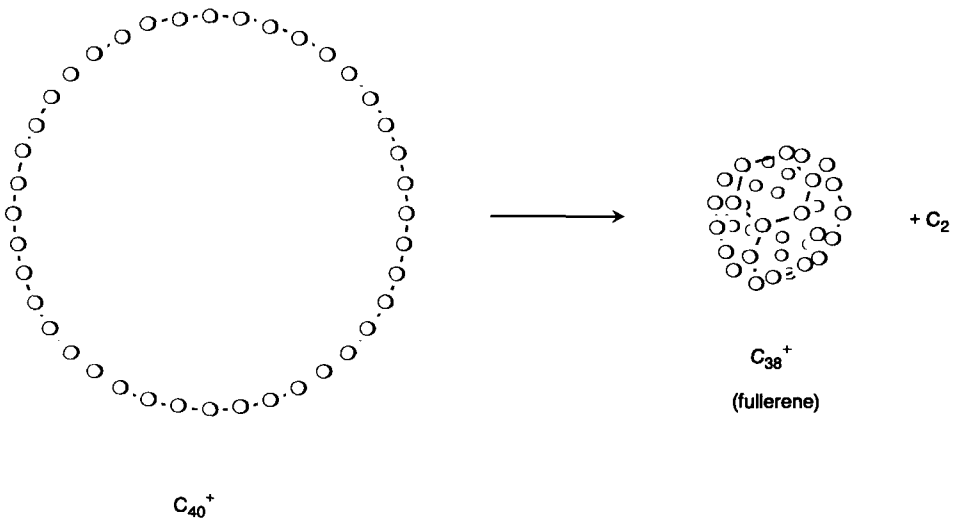

Figure 1.12 Generation of the fullerene C_{38}^+ by collision induced heating of the monocyclic C_{40}^+.

In another important series of experiments it has been shown by ion-cyclotron-resonance (ICR) studies that monocyclic carbon rings can coalesce very efficiently to fullerenes [Scheme 1.6][98]. The carbon rings are obtained by laser desorption of carbon oxide $C_n(CO)_{n/3}$ precursors, out of which upon loss of CO the cyclo[n]carbons C_{18}, C_{24} and C_{30} are generated. Fullerene formation proceeds via collisions of positively charged cluster ions C_n^+ with the corresponding neutrals. In the positive ion mode reactions between cations and neutral molecules of the cyclo[n]carbons lead to fullerene ions. Remarkably, the cyclocarbons C_{18} and C_{24} predominantly lead via C_{72}^+ to C_{70}^+ and no signal for C_{60}^+ is observed. On the other hand the C_{30} precursors coalesce almost exclusively to C_{60}. Subsequent losses of C_2 fragments demonstrate the fullerene nature of the products. The distribution of fullerenes can therefore be directly affected by the size of the precursors.

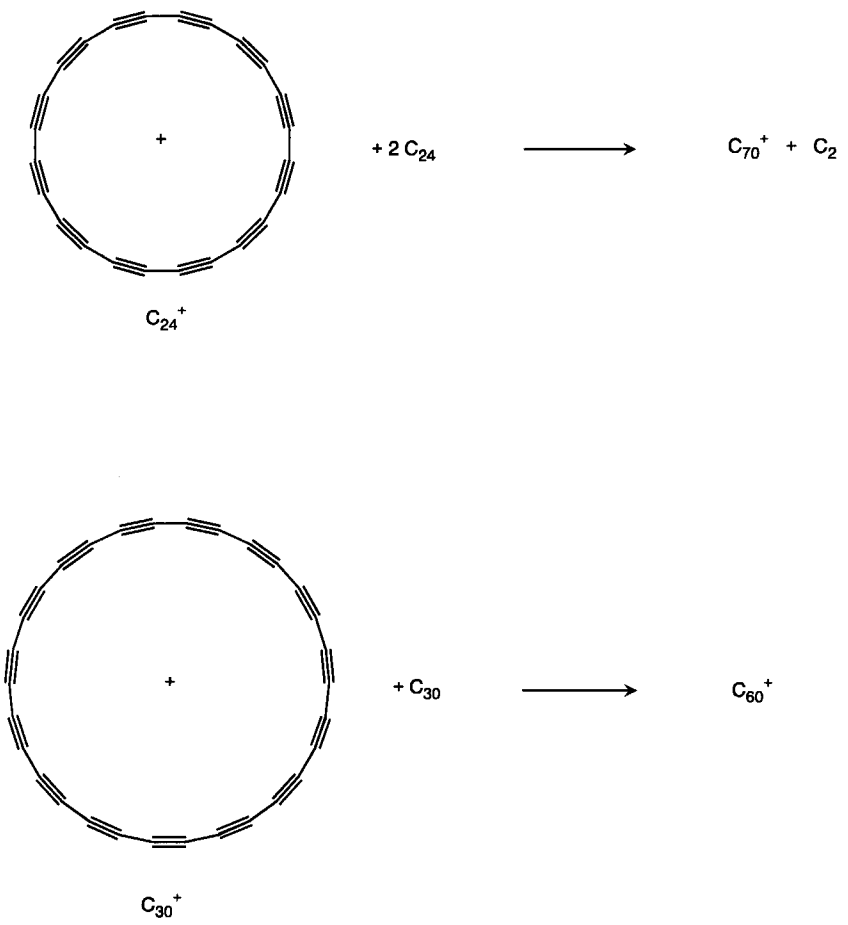

Scheme 1.6

These investigations impressively demonstrate, that fullerenes can form through excitation or coalescence of relatively large monocyclic precursors. A growth mechanism of smaller fullerenes by subsequent incorporation of C_2- or C_3-units is not necessarily required. In the excitation experiments of C_n^+ clusters as well as the coalescence studies of cyclocarbons a scenario is investigated, which comes close to the situation in a carbon plasma generated by Krätschmer-Huffman graphite evaporation. Based on the experimental data available, the fullerene generation is schematically summarized in Scheme 1.7. Upon vaporization of graphite carbon atoms are formed, which subsequently cluster to a mixture of chains, monocyclic rings, polycyclic rings and fullerenes. In an annealing process these clusters rearrange, especially efficiently via monocyclic rings to fullerenes. During this annealing, stable fullerenes can be formed by loss of small fragments (e.g. C_2, C_3) and by ring rearrangements (e.g. Stone-Wales rearrangement). The fact however that fullerenes are available by several methods implies the existence of different mechanisms, which may also operate simultaneously.

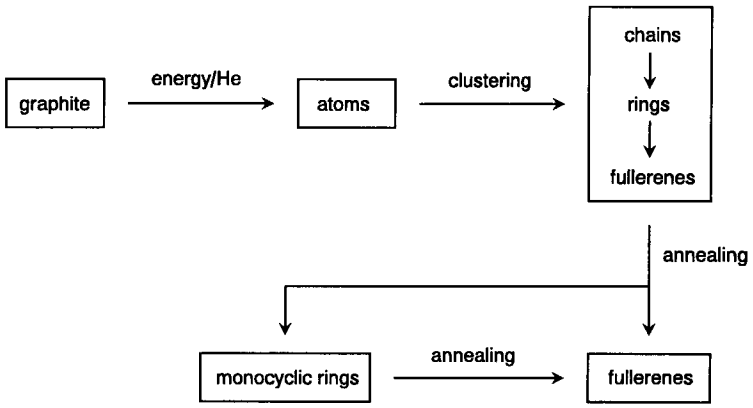

Scheme 1.7

1.4 Separation and Purification

The raw product obtained by the evaporation of graphite is soot and slag. Next to soluble fullerenes the soot and slag contain other kinds of closed carbon structures for example giant fullerenes[99] and nano-tubes[100,101]. The rest is amorphous carbon. The fullerenes can be isolated from the soot either by sublimation or by extraction. The first isolation of fullerenes was achieved by a simple sublimation with a Bunsen burner as heat source[24]. In a more controlled procedure the sublimation from soot can be carried out by gradient sublimation[102]. Thereby, the fullerenes are deposited on a quartz rod along a temperature gradient. With this method a partial separation or enrichment of the different fullerenes is possible. In addition, endohedrals can be enriched and C_{74}, not obtainable by extraction, sublimes out of the soot. A disadvantage of these methods is the thermal stress on the fullerenes leading to partial decomposition. This problem has been overcome, at least partly, by using microwave-aided sublimation[103].

The most common method for the isolation of the fullerenes from soot is the extraction with organic solvents[19,25,99]. In general toluene is used as solvent since it provides a sufficient solubility and is less toxic than benzene or carbon disulfide. Either a hot extraction of the soot followed by filtration or a Soxhlet extraction is possible. It has been shown that longer extraction times lead to higher yields of fullerenes[99]. Alternatively, also hexane or heptane can be used as solvents for this method. Fullerene yields of up to 26% from the soot are reported for Soxhlet extractions[99]. The typical color of toluene extract is red to red brown. It contains next to C_{60} and C_{70} higher fullerenes, for example C_{76}, C_{78}, C_{84}, C_{90} and C_{96}. Buckminsterfullerene C_{60} is the most abundant species. Upon further extractions of soot with other solvents, for example pyridine or 1,2,3,5-tetramethylbenzene, additional soluble material is accessible. In such fractions clusters with very high masses (giant fullerenes) up to C_{466} are detectable by mass spectrometry[99]. However, under these more drastic extraction conditions, chemical reactions between fullerenes and the solvent have been observed[99]. The preferred method of isolating fullerenes from the soot is Soxhlet extraction with toluene.

For the separation of the fullerenes predominantly chromatographic methods are used. A clean separation of C_{60} as the first fullerene fraction is obtained by column chromatography with alumina as stationary phase with either pure hexane or hexane/toluene (95:5) as eluent[25,104,105]. However, since the fullerenes are not very soluble in hexane, enormous amounts of alumina and solvents are needed, which makes this method inefficient. Also a one-step separation of the higher fullerenes is impossible, because of the pronounced tailing effect of the preceding fullerenes. The use of solvents providing a higher solubility, for example toluene cause the fullerenes to elute together without retention on alumina. The efficiency of the separation of fullerenes on alumina with hexane as mobile phase has been dramatically improved by using Soxhlet-chromatography [Fig 1.13][106,107].

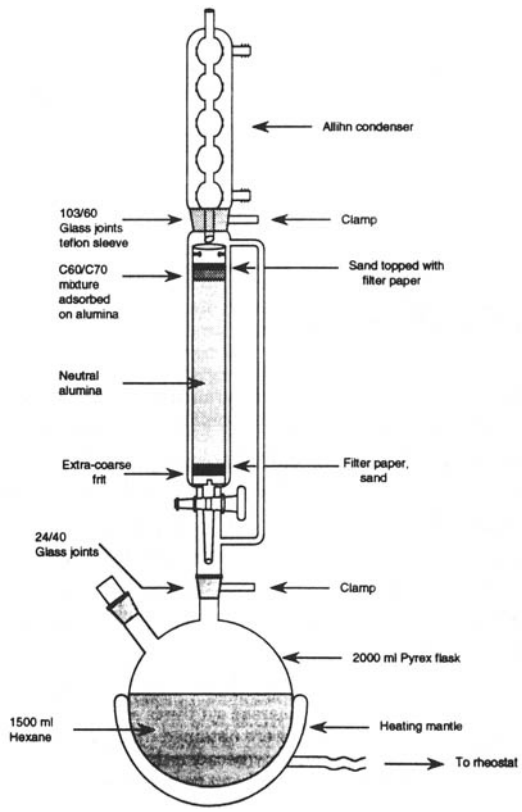

Figure 1.13 Schematic representation of the modified Soxhlet chromatography apparatus[107].

This method combines distillation or Soxhlet extraction with chromatography and therefore does not require large quantities of solvent as well as constant monitoring. Gram quantities of pure C_{60} can be obtained in reasonable periods of time. After the C_{60} is eluted, simply a new hexane containing flask is used for the collection of eluting C_{70}.

With chromatography on graphite higher amounts of toluene in the hexane/toluene mixture improving the solubility can be used[108,109]. The major breakthrough however, allowing the use of pure toluene as mobile phase has been achieved by chromatography on mixtures of charcoal and silica gel[110,111]. This is the most inexpensive and efficient method for a fast separation of C_{60}. A flash

chromatography- or even simpler a plug filtration setup can be used. For example[111] a fritted funnel (10 cm diameter) is covered with a slurry of 63 g charcoal and 125 g silica gel, which gives a plug of 5.5 cm height. A concentrated toluene solution of fullerene extract is loaded and eluted by the application of a slight vacuum at the filter flask. After a few minutes a dark purple solution of 1.5 g of C_{60} starting from 2.5 g extract can be obtained.

Although the Soxhlet chromatography on alumina as well as the chromatography on charcoal are very simple and efficient methods, a certain amount of the fullerene decomposes or irreversibly adsorbs on these stationary phases. Especially higher fullerenes hardly elute from charcoal columns. Upon chromatography on alumina light-catalysed degradation of the fullerenes was observed[112]. A material, which is completely unreactive towards fullerenes is polystyrene gel. Also on this stationary phase a good separation of fullerenes can be obtained with toluene as mobile phase [Fig. 1.14][113,114,115].

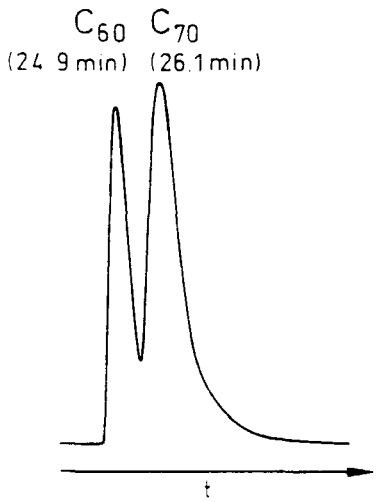

Figure 1.14 Separation of C_{60} and C_{70} on polystyrene gel column with toluene as mobile phase[115].

A completely automated system with reinjection/sample collection and solvent recovery allows the separation of up to 10 g of extract a day. The C_{60} is obtained in a very high purity and the recovery is nearly 100 %.

A variety of other packing materials including C_{18} reversed phase[116,117,118], Pirkle-type phases[119,120,121] and γ-cyclodextrine phases[122] and reversed phases containing polycyclic aromatics[123] or multi-legged phenyl groups[124] have been used for the separation of fullerenes both by analytical and preparative HPLC. The eluent most commonly used is hexane, either pure or in combination with more polar components like CH_2Cl_2, Et_2O, THF or toluene. For HPLC on C_{18}-reversed phase silica gel, toluene/MeCN 75:25 or $CHCl_3$/MeCN 60:40 for example are suitable mobile phases. Although the solubility of parent fullerenes is very low in these combinations of solvents, such HPLC methods are useful for analytical purposes or for the separation of higher fullerenes[117,118]. A complete protocol for the isolation of fullerenes from soot and their separation by column chromatography and HPLC elaborated by Diederich is represented in Figure 1.15[125].

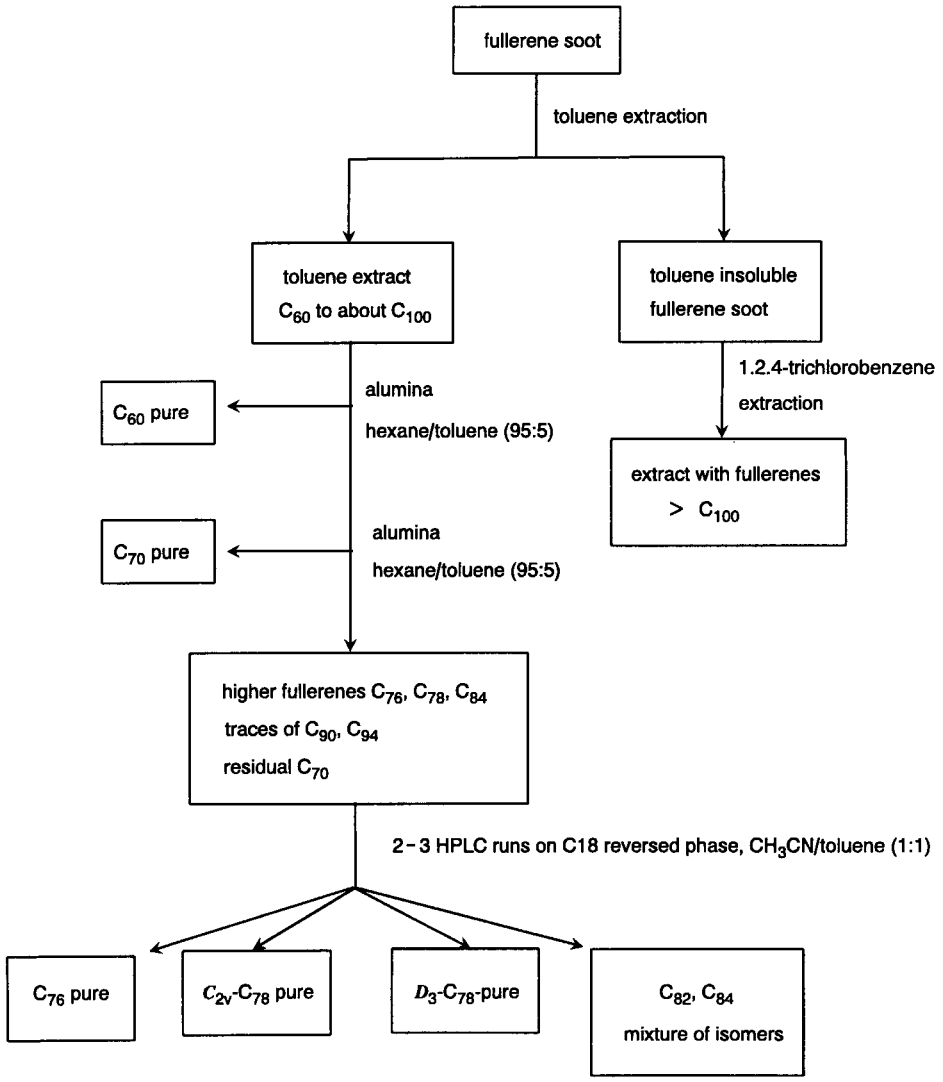

Figure 1.15 A protocol for fullerene separation and isolation[125]

For the separation of fullerene derivatives containing covalently bound groups, HPLC methods are also very important. Addents on the fullerene core have a dramatic influence on the solubility properties and the retention behavior. In many cases more polar eluents in mixtures or in a pure form can be used and efficient separations on silica gel or several reversed phases (medium polarity), even of different regioisomers of addition products, are possible[126,127].

A separation of C_{60} from C_{70} has also been achieved on the basis of the small difference in their chemical reactivity[128]. Treatment of carbon disulfide solution of a C_{60}/C_{70} mixture with $AlCl_3$ leads to a preferred precipitation of a $C_{70}[AlCl_3]_n$ complex, whereas the purple C_{60} is mostly unaffected and

its solution can be separated by filtration from the precipitate. The parent fullerenes can be recovered from the C_{70} enriched precipitate by treatment with water.

1.5 Properties

1.5.1 Structures

Each fullerene contains $2(10 + M)$ carbon atoms corresponding to exactly 12 pentagons and M hexagons. This building principle is a simple consequence of the Euler's theorem. Hence, the smallest fullerene that can be imagined is C_{20}. Starting at C_{20} any even-membered carbon cluster, except C_{22}, can form at least one fullerene structure. With increasing M the number of possible fullerene isomers rises dramatically, from only 1 for M = 0 to over 20.000 for $M = 29$ and so on[129,130]. The soccer-ball shaped C_{60} isomer [5,6]-fullerene-60-I_h is the smallest stable fullerene. The structure of [5,6]-fullerene-60-I_h was determined theoretically[131,132,133,134,135] and experimentally[136,137,138,139] [Table 1.1]. These investigations confirm the icosahedral structure of [5,6]-fullerene-60-I_h. Two features of this C_{60} structure are of special significance: (i) all the twelve pentagons are isolated by hexagons and (ii) the bonds at the junctions of two hexagons (6-6 bonds) are shorter than the bonds at the junctions of a hexagon and a pentagon (5-6 bonds) [Tab. 1.1; Fig 1.16].

[5,6]-Fullerene-60-I_h is the only C_{60} isomer and at the same time the smallest possible fullerene, which obeys the "isolated pentagon rule" (IPR)[75,76]. The IPR predicts fullerene structures with all the pentagons isolated by hexagons to be stabilized against structures with adjacent pentagons. A destabilization caused by adjacent pentagons is (i) due to pentalene-type 8π-electron systems, leading to resonance destabilization and (ii) due to an increase of strain energy, as a consequence of the enforced bond angles. The formation of IPR structures is accompanied with an enhancement of the sphericity of the molecules. A spherical shape distributes the strain as evenly as possible and minimizes the anisotropic contribution to the strain energy[140]. The bond length alternation in [5,6]-fullerene-60-I_h shows that in the lowest energy Kekulé stucture, the double bonds are located at the junctions of the hexagons (6-6 double bonds) and there are no double bonds in the pentagonal rings. Each hexagon in [5,6]-fullerene-60-I_h exhibits a cyclohexatriene- and each pentagon a [5]radialene character.

Table 1.1 Calculated and measured bond distances in [5,6]-fullerene-60-I_h in Å

Method	5-6 bonds	6-6 bonds	Ref.
HF(STO-3G)	1.465	1.376	131
HF(7*s*3*p*/4*s*2*p*)	1.453	1.369	132
LDF(11*s*6*p*)	1.43	1.39	133
HF	1.448	1.37	134
MP2	1.446	1.406	135
NMR	1.448	1.370	136
neutron diffraction	1.444	1.391	137
electron diffraction	1.458	1.401	138
X-ray	1.467	1.355	139

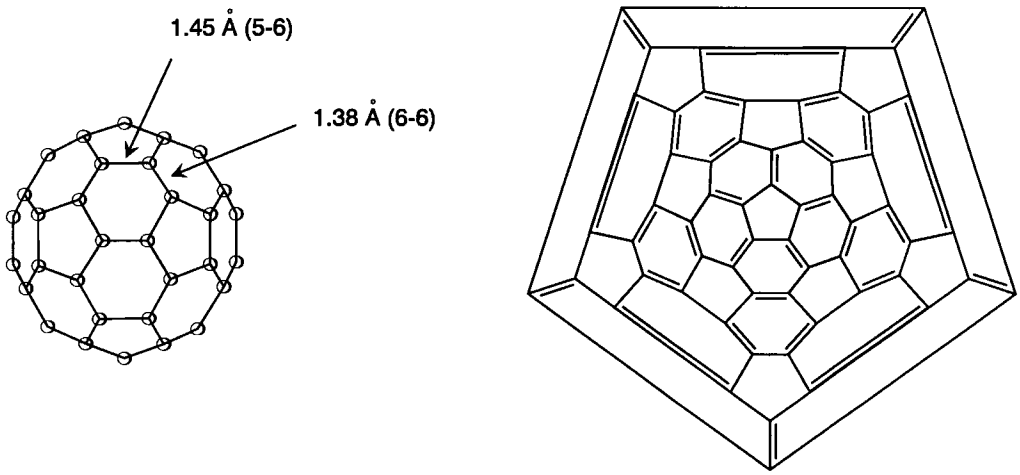

Figure 1.16 Schematic representation of [5,6]-fullerene-60-I_h with the lengths of the two different bonds in the molecule and Schlegel diagram of the lowest energy Kekulé structure.

The next higher stable and IPR satisfying fullerene is [5,6]-fullerene-70-D_{5h}[25]. Its structure was calculated[141] and determined by X-ray crystallography[142,143] [Fig. 1.17; Tab. 1.2]. The geometry at the poles (highest curvature) of [5,6]-fullerene-C_{70}-D_{5h} is very similar to that of [5,6]-fullerene-60-I_h. The corannulene subunits (bonds 5,6,7,8) have the same type of bond length alternation. In contrast to [5,6]-fullerene-60-I_h this fullerene has an equatorial belt consisting of fused hexagons.

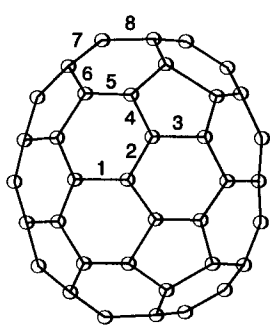

Figure 1.17 Bond type definitions for the [5,6]-fullerene-C_{70}-D_{5h} molecule.

Table 1.2 The calculated and experimental structure of [5,6]-fullerene-C_{70}-D_{5h}

Bond type	Bond length (Å) Experiment a	b	Bond length (Å) Theory (dzp/SCF)[141]
1	1.462	1.462	1.475
2	1.423	1.414	1.407
3	1.441	1.426	1.415
4	1.432	1.447	1.457
5	1.372	1.378	1.361
6	1.453	1.445	1.446
7	1.381	1.387	1.375
8	1.463	1.543	1.451

[a] data were taken from the crystal structure of the complex $(\eta^2\text{-}C_{70})Ir(CO)Cl(PPh_3)_2$[142].
[b] data were taken from the crystal structure of $C_{70} \cdot 6\ (S_8)$[143].

The number of fullerene isomers that are possible without any constraints reduces considerably if only IPR structures are allowed. Taking into account that open-shell structures are avoided[130,144,145] and that the number of double bonds in pentagons is minimized[146], which favours a *meta* over a *para* relationship of the pentagons[147], the number of allowed isomers is further reduced.

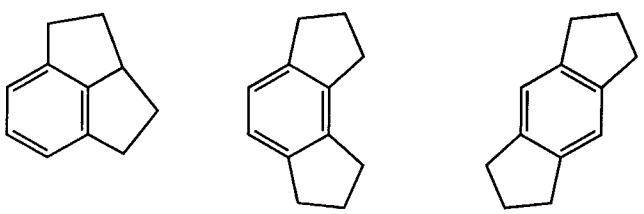

ortho (IPR "forbidden") ***meta*** ***para***

With these constraints magic numbers n for stable fullerenes C_n can be predicted, which are n = 60, 70, 72, 76, 78, 84 ...[130]. All of these fullerenes with the exception of C_{72} have now been produced by the evaporation of graphite. The number of allowed fullerene isomers are then one for C_{60}, one for C_{70}, one for C_{76} (D_2), five for C_{78} (D_{3h} (1), D_{3h} (2), D_3, C_{2v} (1), C_{2v} (2)), 24 for C_{84} and 46 for C_{90}[130,148]. The interplay between theoretical predictions and ^{13}C NMR experiments was the key for the structure elucidation of some principle isomers of the higher fullerenes C_{76}, and C_{78}, C_{82} and C_{84}[117,118,125,149,150,151,152]. The structure assignments have been accomplished by comparing the ^{13}C NMR spectra (number and intensity of lines) of given isomers, isolated or enriched by HPLC, to the theoretical possible structures, suggested by Manolopoulos and Fowler[130]. In addition, the number of lines in different chemical shift regions provide further useful information for the structure

determination. In this way [5,6]-fullerene-C_{76}-D_2 [Fig. 1.18], [5,6]-fullerene-C_{78}-C_{2v} (1) [Fig. 1.18], [5,6]-fullerene-C_{78}-C_{2v} (2), [5,6]-fullerene-C_{78}-D_3, [5,6]-fullerene-C_{82}-C_2, [5,6]-fullerene-C_{82}-C_{2v}, [5,6]-fullerene-C_{82}-C_{3v}, [5,6]-fullerene-C_{84}-D_2 and [5,6]-fullerene-C_{84}-D_{2d} could be characterized.

Since only one isomer of each C_{60}, C_{70} and C_{76} is formed, in the following the indication of symmetry and building motif ([5,6]-fullerene) will be omitted.

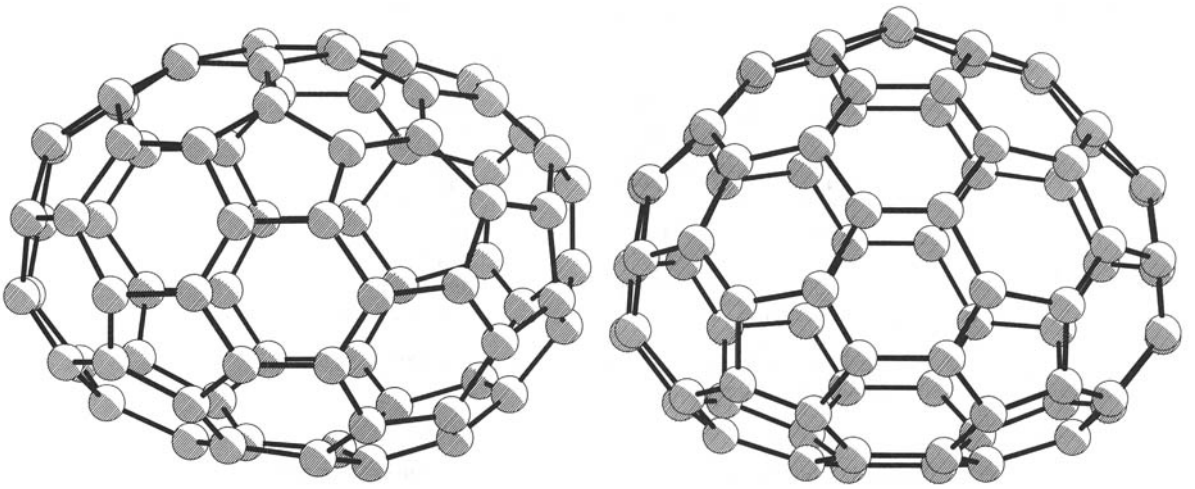

Figure 1.18 Computer models of [5,6]-fullerene-C_{76}-D_2 and [5,6]-fullerene-C_{78}-C_{2v}.

The fact that in the case of C_{78} the most symmetrical D_{3h} isomer is not favored implies that an important stabilizing factor is the maximization of the sphericity rather than symmetry. Interestingly, some of the fullerenes, for example [5,6]-fullerene-C_{76}-D_2 are chiral. This chirality is based on the helical arrangement of the sp^2-atoms in space [Fig. 1. 19].

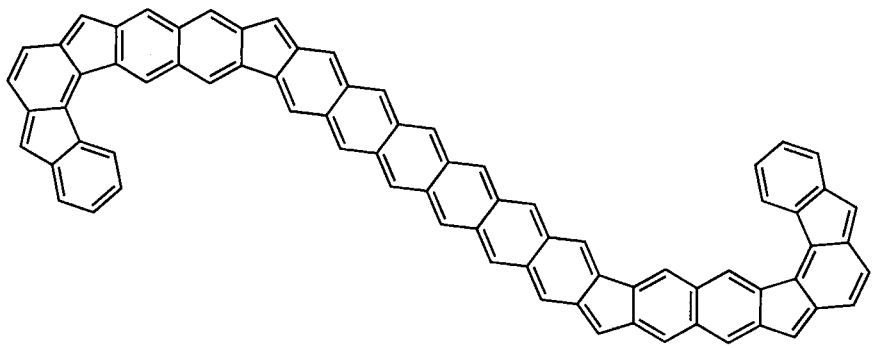

Figure 1.19 Helix motif in double-helical [5,6]-fullerene-C_{76}-D_2.

1.5.2 Physical and Spectroscopic Properties

Physical properties investigations in solution as well as in the solid state have been predominantly carried out on C_{60} and to a minor extent on C_{70}, since these are the most abundant fullerenes. At the moment there is only little material available for the higher fullerenes or endohedrals, because it takes about 250 hours of work to produce 1 mg of any of these[153].

The heat of formation of C_{60} and C_{70} have been determined experimentally by calorimetry to be 10.16 kcal/mol per C-atom for C_{60} and 9.65 kcal/mol per C-atom for C_{70}[71,70]. The fullerenes are therefore thermodynamically less stable than graphite and diamond, which exhibit heats of formation of zero and 0.4 kcal/mol, respectively. It is expected that upon increasing the size of the fullerene the energy content of the spheres asymptotically reaches that of graphite[154,155].

In order to chemically modify fullerenes, in most cases it is necessary that they are in the solution state. Also for extractions or chromatographic separations the solubility plays a crucial role. The solubility of C_{60} in a variety of organic solvents has been investigated systematically [Tab. 1.3][156,157,158].

Table 1.3 Solubility of C_{60} in various solvents[157]

solvent	$[C_{60}]$, mg/mL	mole fraction (x 10^4)	*n*
n-pentane	0.005	0.008	1.36
n-hexane	0.043	0.073	1.38
cyclohexane	0.036	0.059	1.43
n-decane	0.071	0.19	1.41
decalines	4.6	9.8	1.48
carbon disulfide	7.9	6.6	1.63
dichloromethane	0.26	0.27	1.42
chloroform	0.16	0.22	1.45
tetrachloromethane	0.32	0.40	1.46
tetrahydrofuran	0.000	0.000	1.41
benzene	1.7	2.1	1.50
toluene	2.8	4.0	1.50
tetraline	16	31	1.54
benzonitrile	0.41	0.71	1.53
anisole	5.6	8.4	1.52
chlorobenzene	7.0	9.9	1.52
1,2-dichlorobenzene	27	53	1.55
1-methylnaphthalene	33	68	1.62
1-chloronaphthalene	51	97	1.63
acetone	0.001	0.001	1.36
methanol	0.000	0.000	1.33

In polar and H-bonding solvents like acetone, tetrahydrofuran or methanol C_{60} is essentially insoluble. It is sparingly soluble in alkanes with the solubility increasing with the number of atoms. In aromatic solvents and in carbon disulfide, in general appreciable solubilities are observed. A significant increase of the solubility takes place on going from the benzenes to naphthalenes. Although there are trends for the solution behavior of C_{60}, there is no direct dependence of the solubility on a certain solvent parameter like the index of refraction *n*. When the solubility is expressed in mole fraction units it is

evident that C_{60} is not very soluble even in the best solvents listed in Table 1.3. The solubility of C_{70} follows qualitatively similar trends.

The electronic absorption spectra[25] of C_{60} and C_{70} are characterized by several stronger absorptions between 190 and 410 nm as well as by some forbidden transitions in the visible part of the spectrum [Fig. 1.20; Fig 1.21]. For C_{60}, the assignment of the transitions has been carried out using the results of theoretical calculations[159,160]. The absorptions between 190 and 410 nm are due to allowed $^1T_{1u}$-^1A_g-transitions, whereas those between 410 and 620 nm due to orbitally forbidden singlet-singlet transitions. These latter absorptions in the visible are responsible for the purple color of C_{60} and the red color of C_{70}.

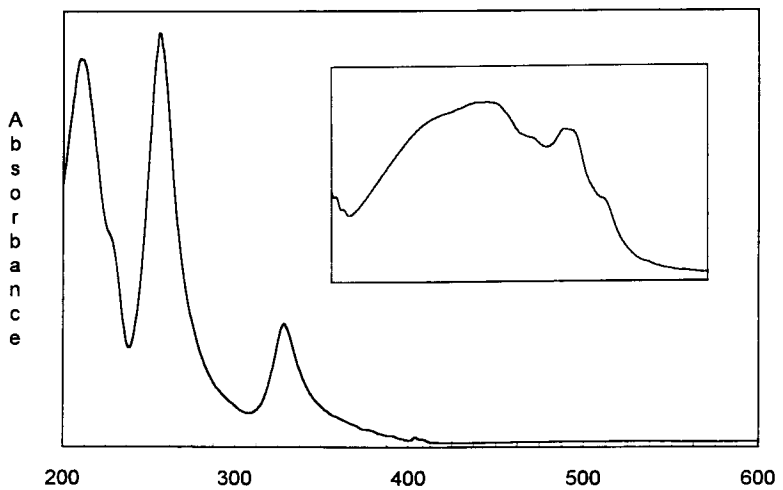

Figure 1.20 Electronic absorption spectrum of C_{60} in hexane. The inset is the 420-700 nm region.

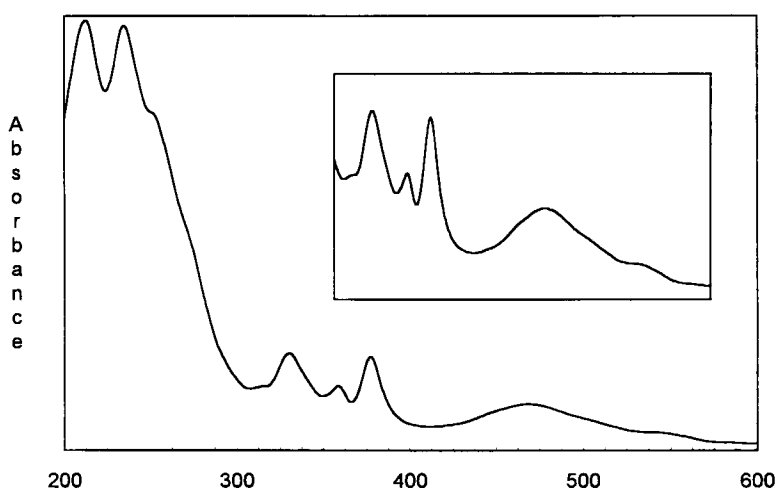

Figure 1.21 Electronic absorption spectrum of C_{70} in hexane. The inset is the 300-600 nm region.

As expected for the icosahedral symmetry the ^{13}C NMR spectrum of C_{60} [Fig. 1.22] shows one signal at 143.2 ppm[25]. Since the amount of fullerene in the NMR samples is small due to low solubility and the spin-lattice relaxation times are quite long (≥ 20 s for C_{60}[25]), a comparatively large number of accumulations are necessary. The ^{13}C NMR spectrum of C_{70} [Fig. 1.23] shows five peaks[25] in the intensity ratio of 1:2:1:2:1, which have been attributed to the five different sets of C-atoms by 2D NMR analysis[161]. The center of gravity of the ^{13}C resonances shifts continuously towards higher field on going from C_{70} to the higher fullerenes C_{76}, C_{78}, C_{82} and C_{84}[125]. This can be interpreted in terms of an increase of the more benzoid pyrene-type carbons with increasing size of the carbon spheres.

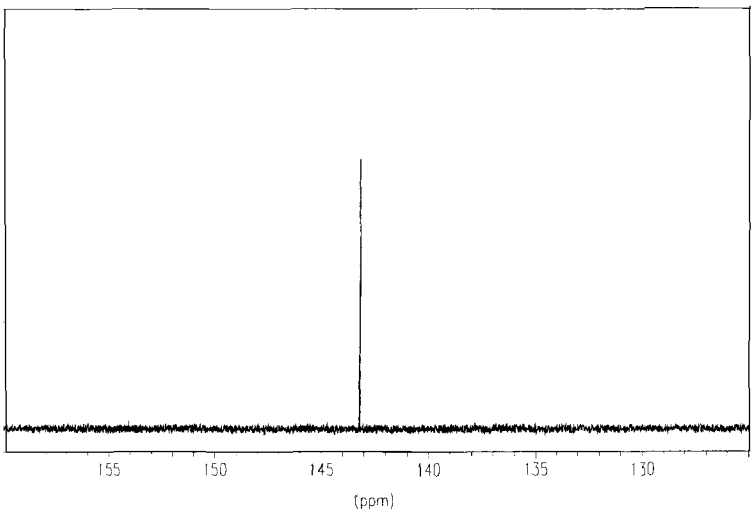

Figure 1.22 ^{13}C NMR spectrum of C_{60}.

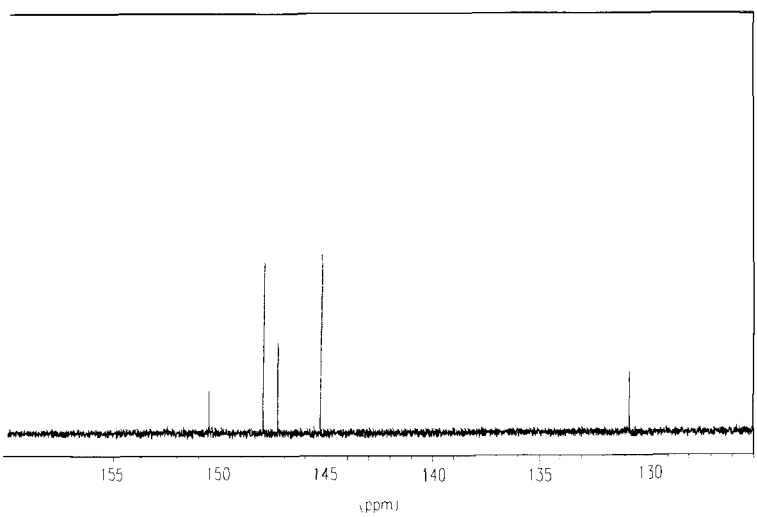

Figure 1.23 ^{13}C NMR spectrum of C_{70}.

Out of the 174 vibrational modes[22] for C_{60} giving rise to 42 fundamentals of various symmetries, four have t_{1u} symmetry and are IR active [Fig 1.24]. This fact has historical significance in the first detection of C_{60}[19].

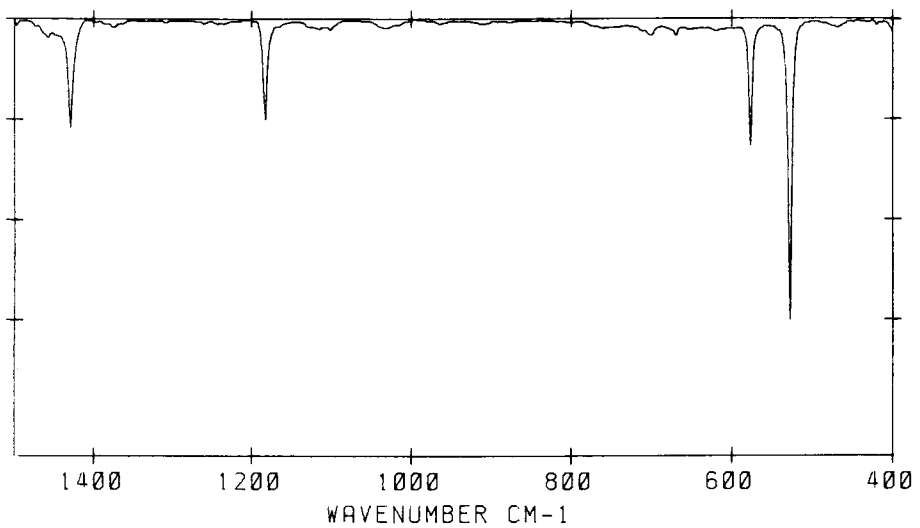

Figure 1.24 IR spectrum (KBr) of C_{60}.

Solid C_{60} forms a face-centered-cubic (FCC) structure at room temperature[162]. The density in the solid sate d_{ffc} is 1.68 g cm^{-3} [19]. Four equivalent molecules are contained in a unit cube with edge length a = 14.198 Å, at the origin and face centers. Due to weak intermolecular interactions the spherical molecules in this "plastic crystal" almost freely rotate at room temperature. As determined by solid state NMR measurements[163,164,165,166] the C_{60} molecules reorient with rotational diffusion constant of 10 x 10^{10} s^{-1}. Below 255 K, a first order phase transition to a simple-cubic (SC) structure takes place[167,168,169]. Also C_{70} is rotationally disordered at room temperature and undergoes a phase transition to a low temperature phase[170].

A slow crystallization from benzene gives a solvate $C_{60}(C_6H_6)_4$ in which the rotation is slowed considerably. This allowed the determination of the crystal structure by X-ray crystallography[171,172]. Also cocrystallates with other molecules for example cyclohexane[173], ferrocene[174], [bis(ethylenedithio)tetrathiafulvalene][175], $[Fe_4(CO)_{4(}\eta^5\text{-}C_5H_5)_4]$[176] and iodine[177] have been characterized. In addition, C_{60} forms host-guest complexes with 1,4-hydroquinone[178], sulfur (S_8)[143,179] and γ-cyclodextrine[180] to give the water-soluble complex C_{60}(γ-cyclodextrine)$_2$.

References

1 H. W. Kroto, A. W. Allaf, S. P. Balm *Chem. Rev.* **1991**, *91*, 1213.
2 This nomenclature is suggested by the Chemical Abstracts Service.
3 R. Taylor *J. Chem. Soc., Perkin Trans 2* **1993**, 813.
4 D. E. H. Jones *New Scientist* **1966**, *35 (519)*, 245.
5 D. E. H. Jones *The Inventions of Daedalus;* Freeman: Oxford, 1982 pp 118.
6 W. E. Barth, R. G. Lawton *J. Am. Chem. Soc.* **1966**, *88*, 380.
7 E. Osawa *Kagaku* **1970**, *25*, 854.
8 Z. Yoshida, E. Osawa *Aromaticity;* Kagakudojin: Kyoto, 1971 pp 174.
9 D. A. Bochvar, E. G. Gal'pern *Dokl. Akad. Nauk SSSR* **1973**, *209*, 610.
10 I. V. Stankevich, M. V. Nikerov, D. A. Bochvar *Russ. Chem. Rev.* **1984**, *53(7)*, 640.
11 R. A. Davidson *Theor. Chim. Acta* **1981**, *58*, 193.
12 A. D. J. Haymet *Chem. Phys. Lett.* **1985**, *122*, 421.
13 E. A. Rohlfing, D. M. Cox, A. Kaldor *J. Chem. Phys.* **1984**, *81*, 3322.
14 H. W. Kroto, J. R. Heath, S. C. O'Brien, R. F. Curl, R. E. Smalley *Nature* **1985**, *318*, 162.
15 T. G. Dietz, M. A. Duncan, D. E. Powers, R. E. Smalley *J. Chem. Phys.* **1981**, *74*, 6511.
16 L. W. Avery, N. W. Broten, J. M. Mcleod, T. Oka, H. W. Kroto *Astrophys. J.* **1976**, *205*, L173.
17 H. W. Kroto, C. Kirby, D. R. M. Walton, L. W. Avery, N. W. Broten, J. M. Mcleod, T. Oka *Astrophys. J.* **1978**, *219*, L133.
18 J. R. Heath, Q. Zhang, S. C. O'Brien, R. F. Curl, H. Kroto, R. E. Smalley *J. Am. Chem. Soc.* **1987**, *109*, 359.
19 W. Krätschmer, L. D. Lamb, K. Fostiropoulos, D. R. Huffman *Nature* **1990**, *347*, 354.
20 D. R. Huffman *Adv. Phys.* **1977**, *26*, 129.
21 W. Krätschmer, K. Fostiropoulos, D. R. Huffman *Chem. Phys. Lett.* **1990**, *170*, 167.
22 S. J. Cyvin, E. Brendsdal, B. N. Cyvin, J. Brunvoll *Chem. Phys. Lett.* **1988**, *143*, 377.
23 D. E. Bradley *Br. J. Appl. Phys.* **1954**, *5*, 65.
24 K. Fostiropoulos *Ph.D. Dissertation*, University of Heidelberg, 1991.
25 H. Ajie, M. M. Alvarez, S. J. Anz, R. D. Beck, F. Diederich, K. Fostiropoulos, R. Huffman, W. Krätschmer, Y. Rubin, K. E. Schriver, D. Sensharma, R. L. Whetten *J. Phys. Chem.* **1990**, *94*, 8630.
26 R. L. Whetten, M. M. Alvarez, S. J. Anz, K. E. Schriver, R. D. Beck, F. Diederich, Y. Rubin, R. Ettl, C. S. Foote, A. P. Darmanyan, J. W. Arbogast *Mater. Res. Soc., Symp. Proc.* **1990**, *206*, 639.
27 A. S. Koch, K. C. Khemani, F. Wudl *J. Org. Chem* **1991**, *56*, 4543.
28 T. Grösser *Diplom Disseration*, University of Tübingen, 1992.
29 R. E. Haufler, Y. Chai, L. P. F. Chibante, J. Conceicao, C. Jin, L. S. Wang, S. Maruyama, R. E. Smalley *Mater. Res. Symp. Proc.* **1991**, *206*, 627.
30 L. P. F. Chibante, A. Thess, J. M. Alford, M. D. Diener, R. E. Smalley *J. Phys. Chem.* **1993**, *97*, 8696.
31 R. E. Haufler, J. Conceicao, L. P. F. Chibante, Y. Chai, N. E. Byrne, S. Flanagan, M. M. Haley, S.C. O'Brian, C. Pan, Z. Xiao, W. E. Billups, M. A. Ciufolini, R. H. Hauge, J. L. Margrave, L. J. Wilson, R. F. Curl, R. E. Smalley *J. Phys. Chem.* **1990**, *94*, 8634.
32 W. A. Scrivens, J. M. Tour *J. Org. Chem.* **1992**, *57*, 6932.
33 K. Kikuchi, N. Nahahara, M. Honda, S. Suzuki, K. Saito, H. Shiromaru, K. Yamauchi, I. Ikemoto, T. Kuramochi, S. Hino, Y. Achiba *Chem. Lett.* **1991**, 1607.
34 R. E. Haufler, L. S. Wang, L. P. F. Chibante, C. Jin, J. Conceicao, Y. Chai, R. E. Smalley *Chem. Phys. Lett.* **1991**, *179*, 449.
35 C. L. Fields, J. R. Pitts, M. J. Hale, C. Bingham, A. Lewandowski, D. E. King *J. Phys. Chem.* **1993**, *97*, 8701.
36 G. Peters, M. Jansen *Angew. Chem.* **1992**, *104*, 240; *ibid. Int. Ed. Engl.* **1992**, *31*, 223.
37 P. Gerhardt, S. Löffler, K. H. Homann *Chem. Phys. Lett.* **1987**, *137*, 316.
38 P. Gerhardt, K. H. Homann *J. Phys. Chem.* **1990**, *94*, 5381.
39 J. B. Howard, J. T. McKinnon, Y. Makarovsky, A. Lafleur, M. E. Johnson *Nature* **1991**, *352*, 139.
40 J. B. Howard, J. T. McKinnon, M. E. Johnson Y. Makarovsky, A. Lafleur *J. Phys. Chem.* **1992**, *96*, 6657.
41 J. B. Howard, A. Lafleur, Y. Makarovsky, S. Mitra, C. J. Pope, T. K. Yadav *Carbon* **1992**, *30*, 1183.
42 C. J. Pope, J. A. Marr, J. B. Howard *J. Phys. Chem.* **1993**, *97*, 11001.
43 R. Taylor, G. J. Langley, H. W. Kroto, D. R. M. Walton *Nature* **1993**, *366*, 728.
44 J. R. Heath, S. C. O'Brien, Q. Zhang, Y. Liu, R. F. Curl, H. W. Kroto, F. K. Tittel, R. E. Smalley *J. Am. Chem. Soc.* **1985**, *107*, 7779.

45 F. D. Weiss, S. C. O'Brien, J. L. Eklind, R. F. Curl, R. E. Smalley *J. Am. Chem. Soc.* **1988**, *110*, 4464.
46 Y. Cai, T. Guo, C. Jin, R. E. Haufler, L. P. F. Chibante, J. Fure, L. Wang, J. M. Alford, R. Smalley *J. Phys. Chem.* **1991**, *95*, 7564.
47 J. H. Weaver, Y. Chai, G. H. Kroll, C. Jin, T. R. Ohno, R. E. Haufler, T. Guo, J. M. Alford, J. Conceicao, L. P. F. Chibante, A. Jain, G. Palmer, R. E. Smalley *Chem. Phys. Lett.* **1992**, *190*, 460.
48 H. Shinohara, H. Sato, Y. Saito, M. Ohkohchi, Y. Ando *J. Phys. Chem.* **1992**, *96*, 3571.
49 E. G. Gillan, C. Yeretzian, K. S. Min, M. M. Alvarez, R. L. Whetten, R. B. Kaner *J. Phys. Chem.* **1992**, *96*, 6869.
50 M. M. Alvarez, E. G. Gillan, K. Holczer, R. B. Kaner, K. S. Min, R. L. Whetten *J. Phys. Chem.* **1991**, *95*, 10561.
51 S. Suzuki, S. Kawata, H. Shiromaru, K. Yamauchi, K. Kikuchi, T. Kato, Y. Achiba *J. Phys. Chem.* **1992**, ***96***, 7159.
52 S. Bandow, H. Kitagawa, T. Mitani, H. Inokuchi, Y. Saito, H. Yamaguchi, N. Hayashi, H. Sato, H. Shinohara *J. Phys. Chem.* **1992**, *96*, 9609.
53 R. D. Johnston, M. S. de Vries, J. Salem, D. S. Bethune, C. S. Yannoni *Nature* **1992**, *355*, 239.
54 H. Shinohara, H. Sato, M. Ohkohchi, Y. Ando, T. Kodama, T. Shida, T. Kato, Y. Saito *Nature* **1992**, *357*, 52.
55 S. Bandow, H. Shinohara, Y. Saito, M. Ohkohchi, Y. Ando *J. Phys. Chem.* **1993**, *97*, 6101.
56 T. Suzuki, Y. Maruyama, T. Kato, K. Kikuchi, Y. Achiba *J. Am. Chem. Soc.* **1993**, *115*, 11006.
57 K. Laasonen, W. Andreoni, M. Parrinello *Science* **1992**, *258*, 1916.
58 S. Nagase, K. Kobayashi, T. Kato, Y. Achiba *Chem. Phys. Lett.* **1993**, *201*, 475.
59 S. Saito, S. Sawada *Chem. Phys. Lett.* **1992**, *198*, 466.
60 M. Saunders, H. A. Jimenez-Vazquez, R. J. Cross, R. J. Poreda *Science* **1993**, *259*, 1428.
61 T. Weiske, D. K. Böhme, J. Hrusak, W. Krätschmer, H. Schwarz *Angew. Chem.* **1991**, *103*, 898.; *ibid. Int. Ed. Engl.* **1991**, *30*, 884.
62 T. Weiske, J. Hrusak, D. K. Böhme, H. Schwarz *Chem. Phys. Lett.* **1991**, *186*, 459.
63 T. Weiske, D. K. Böhme, H. Schwarz *J. Phys. Chem.* **1991**, *95*, 8451.
64 T. Weiske, T. Wong, W. Krätschmer, J. K. Terlouv, H. Schwarz *Angew. Chem.* **1992**, *104*, 242 *ibid Int. Ed. Engl.* **1992**, *31*, 183.
65 T. Weiske, H. Schwarz, A. Hirsch, T. Grösser *Chem. Phys. Lett.* **1992**, *199*, 640.
66 M. M. Ross, J. H. Callahan *J. Phys. Chem.* **1991**, *95*, 5720.
67 K. A. Caldwell, D. H. Giblin, C. S. Hsu, D. Cox, M. L. Gross *J. Am. Chem. Soc.* **1991**, *113*, 8519.
68 M. Saunders, H. A. Jimenez-Vazquez, R. James Cross, S. Mroczkowski, D. I. Freedberg, F. A. L. Anet *Science* **1994**, *367*, 256.
69 M. Saunders, H. A. Jimenez-Vazquez, R. James Cross, S. Mroczkowski, M. L. Gross, D. E. Giblin, R. J. Poreda *J. Am. Chem. Soc.* **1994**, *116*, 2193.
70 R. L. Murry, G. E. Scuseria *Science* **1994**, *263*, 791.
71 H. D. Beckhaus, C. Rüchardt, M. Kao, F. Diederich, C. S. Foote *Angew. Chem.* **1992**, *104*, 69; *ibid Int. Ed. Engl.* **1992**, *31*. 63.
72 R. F. Curl *Philos. Trans. R. Soc. London A*, **1993**, *343*, 19.
73 H. D. Beckhaus, S. Verevkin, C. Rüchardt, F. Diederich, C. Thilgen, H. U. ter Meer, H. Moon, W. Müller *Angew. Chem.* in press.
74 H. Ajie, M. M. Alvarez, S. J. Anz, R. D. Beck, F. Diederich, K. Fostiropoulos, D. R. Huffman, W. Krätschmer, Y. Rubin, K. E. Schriver, D. Sensharma, R. L. Whetten *J. Phys. Chem.* **1990**, *94*, 8630.
75 T. G. Schmalz, W. A. Seitz, D. J. Klein, G. E. Hite *Chem. Phys. Lett.* **1986**, *130*, 203.
76 H. W. Kroto *Nature* **1987**, *329*, 529.
77 K. Raghavachari, C. M. Rohlfing *J. Phys. Chem.* **1992**, *96*, 2463.
78 H. Schwarz *Angew. Chem.* **1993**, *105*, 1475; *ibid. Int. Ed. Engl.* **1993**, *32*, 1412.
79 G. Meijer, D. S. Bethune *J. Chem. Phys.* **1990**, *93*, 7800.
80 J. M. Hawkins, A. Meyer, S. Loren, R. Nunlist *J. Am. Chem. Soc.* **1991**, *113*, 9394.
81 T. W. Ebbesen, J. Tabuchi, K. Tanigaki *Chem. Phys. Lett.* **1992**, *191*, 336.
82 D. C. Parent, S. W. McElvany *J. Am. Chem. Soc.* **1989**, *111*, 632.
83 S. W. Elvany, B. I. Dunlap, A. O'Keefe *J. Chem. Phys.* **1987**, *86*, 715.
84 G. von Helden, M. T. Hsu, N. G. Gotts, P. R. Kemper, M. T. Bowers *Chem. Phys. Lett.* **1993**, *204*, 15.
85 G. von Helden, M. T. Hsu, N. Gotts, M. T. Bowers *J. Phys. Chem.* **1993**, *97*, 8182.
86 V. Parasuk, J. Almhöf *Chem. Phys. Lett.* **1991**, *184*, 187.
87 M. Feiereisen, M. Gutowski, J. Simmons, J. Almlöf *J. Chem. Phys.* **1992**, *96*, 2926.
88 R. J. Heath, Q. Zhang, S. C. O'Brien, R. F. Curl, H. W. Kroto, R. E. Smalley *J. Am. Chem. Soc.* **1987**, *109*, 359.
89 M. Broyer, A. Goeres, M. Pellarin, E. Sedlmeyer, J. L. Vialle, L. Wöste *Chem. Phys. Lett.* **1992**, *198*, 128.
90 T. Grösser, A. Hirsch *Angew. Chem.* **1993**, *105*, 1390; *ibid Int. Ed. Engl.* **1993**, *32*, 1340.
91 T. M. Chang, A. Naim, S. N. Ahmed, G. Goodloe, P. B. Shevlin *J. Am. Chem. Soc.* **1992**, *114*, 7603.
92 J. R. Heath, S. C. O'Brien, R. F. Curl, H. W. Kroto, R. E. Smalley *Comments Cond. Mater. Phys.* **1987**, *13*, 119.

93 R. E. Smalley *Acc. Chem. Res.* **1992**, *25*, 98.
94 A. J. Stone, D. J. Wales *Chem. Phys. Lett.* **1986**, *128*, 501.
95 G. von Helden, N. G. Gotts, M. T. Bowers *Nature* **1993**, *363*, 60.
96 M. T. Bowers, P. R. Kemper, G. von Helden, P. A. M. von Koppen *Science* **1993**, *260*, 1446.
97 G. von Helden, N. G. Gotts, M. T. Bowers *J. Am. Chem. Soc.* **1993**, *115*, 4363.
98 S. W. McElvany, M. M. Ross, N. S. Goroff, F. Diederich *Science* **1993**, *259*, 1993.
99 D. H. Parker, K. Chatterjee, P. Wurz, K. R. Lykke, M. J. Pellin, L. M. Stock, J. Hemminger *Carbon* **1992**, *30*, 29.
100 S. Iijima *Nature* **1991**, *354*, 56.
101 T. W. Ebbesen, P. M. Ajayan *Nature* **1992**, *358*, 220.
102 C. Yeretzian, J. B. Wiley, K. Holczer, T. Su, S. Nguyen, R. B. Kaner, R. L. Whetten *J. Phys. Chem.* **1993**, *97*, 10097.
103 W. Müller, U. Wirth, H. Mohn, K. Alberti, presented at *Fullerenes '93*, Santa Barbara 1993.
104 R. Taylor, J. P. Hare, A. K. Abdul-Sada, H. W. Kroto *J. Chem. Soc., Chem. Commun.* **1990**, *1423*.
105 R. D. Johnson, G. Meijer, D. S. Bethune *J. Am. Chem. Soc.* **1990**, *112*, 8983.
106 K. Chatterjee, D. H. Parker, P. Wurz, K. Lykke, D. M. Gruen, L. M. Stock *J. Org. Chem.* **1992**, *57*, 3253.
107 K. C. Khemani, M. Prato, F. Wudl *J. Org. Chem.* **1992**, *57*, 3254.
108 A. M. Vassallo, A. Palmisano, L. S. K. Pang, M. A. Wilson *J. Chem. Soc., Chem. Commun.* **1992**, 60.
109 I. N. Kremenskaya, M. A. Nudelman, I. G. Shlyamina, V. I. Shlyamin *Mendelev. Commun.* **1993**, 9.
110 W. A. Scrivens, P. V. Bedworth, J. M. Tour *J. Am. Chem. Soc.* **1992**, *114*, 7917.
111 L. Isaacs, A. Wehrsig, F. Diederich *Helv. Chim. Acta* **1993**, *76*, 1231.
112 R. Taylor, J. P. Parsons, A. G. Avent, S. P. Rannard, T. J. Dennis, J. P. Hare, H. W. Kroto, D. R. M. Walton *Nature* **1991**, *351*, 277.
113 M. S. Meier, J. P. Selegue *J. Org. Chem.* **1992**, *57*, 1924.
114 A. Gügel, M. Becker, D. Hammel, L. Mindach, J. Räder, T. Simon, M. Wagner, K. Müllen *Angew. Chem.* **1992**, *104*, 666; *ibid. Int. Ed. Engl.* **1992**, *31*, 646.
115 A. Gügel, K. Müllen *J. Chromatogr.* **1993**, *628*, 23.
116 A. Mittelbach, W. Hönle, H. G. v. Schnering, J. Carlson, R. Janiak, H. Quast *Angew. Chem.* **1992**, *104*, 1681, *ibid. Int. Ed. Engl.* **1992**, *31*, 1640.
117 R. Ettl, I. Chao, F. Diederich, R. L. Whetten *Nature* **1992**, *353*, 149.
118 F. Diederich, R. L. Whetten, C. Thilgen, R. Ettl, I. Chao, M. M. Alvarez *Science* **1991**, *254*, 1768.
119 J. M. Hawkins, T. A. Lewis, S. D. Loren, A. Meyer, J. R. Heath, Y. Shibato, R. J. Saykally *J. Org. Chem.* **1990**, *55*, 6250.
120 W. H. Pirkle, C. J. Welch *J. Org. Chem.* **1991**, *56*, 6973.
121 C. J. Welch, W. H. Pirkle *J. Chromatogr.* **1992**, *609*, 89.
122 K. Cabrera, G. Wieland, M. Schäfer *J. Chromatogr.* **1993**, *644*, 396.
123 K. Kimata, K. Hosoya, T. Araki, N. Tanaka *J. Org. Chem.* **1993**, *58*, 282.
124 K. Jinno, K. Yamamoto, T. Ueda, H. Nagashima, K. Itoh, J. C. Fetzer, W. R. Biggs *J. Chromatogr.* **1992**, *594*, 105.
125 C. Thilgen, F. Diederich, R. L. Whetten In *Buckminsterfullerenes*; W. E. Billups, M. A. Ciufolini, Eds.; VCH Weinheim, 1993; p 59.
126 A. Hirsch, I. Lamparth, H. R. Karfunkel *Angew. Chem.* **1994**, *106*, 453; *ibid. Int. Ed. Engl.* **1994**, *33*, 437.
127 A. Hirsch, T. Grösser, A. Skiebe, A. Soi, *Chem. Ber.* **1993**, *126*, 1061.
128 G. A. Olah, personal communication.
129 D. E. Manolopoulos, J. C.May, S. E. Down *Chem. Phys. Lett.* **1991**, *181*, 105.
130 P. W. Fowler, D. E. Manolopoulos, R. C. Batten *J. Chem. Soc., Faraday Trans.* **1991**, *87*, 3103.
131 M. Schulman, R. L. Disch, M. A. Miller, R. C. Peck *Chem. Phys. Lett.* **1987**, *141*, 45.
132 H. P. Lüthi, J. Almöf *Chem. Phys. Lett.* **1987**, *135*, 357.
133 D. I. Dunlap *Int. J. Quantum. Chem. Symp.* **1988**, *22*, 257.
134 G. E. Scuseria *Chem. Phys. Lett.* **1991**, *176*, 423.
135 M. Häser, J. Almhöf, G. E. Scuseria *Chem. Phys. Lett.* **1991**, *181*, 497.
136 C. S. Yannoni, P. P. Bernier, D. S. Bethune, G. Meijer, J. R. Salem *J. Am. Chem. Soc.* **1991**, *113*, 3190
137 W. I. F. David, R. M. Ibberson, J. C. Mathewman, K. Prassides, T. J. S. Dennis, J. P. Hare, H. W. Kroto, R. Taylor, D. R. M. Walton *Nature* **1991**, *353*, 147.
138 K. Hedberg, L. Hedberg, D. S. Bethune, C. A. Brown, H. C. Dorn, R. D. Johnson, M. de Vries *Science* **1991**, *254*, 410.
139 S. Liu, Y. J. Lu, M. M. Kappes, J. A. Ibers *Nature* **1991**, *254*, 408.
140 T. G. Schmalz, D. J. Klein In *Buckminsterfullerenes*; W. E. Billups, M. A. Ciufolini, Eds.; VCH Weinheim, 1993; p 83.
141 G. E. Scuseria *Chem. Phys. Lett.* **1991**, *180*, 451.

142 A. L. Balch, V. J. Catalano, J. W. Lee, M. M. Olmstead, S. R. Parkin *J. Am. Chem. Soc.* **1991**, *113*, 8953.
143 H. B. Bürgi, P. Venugopalan, D. Schwarzenbach, F. Diederich, C. Thilgen *Helv. Chim. Acta* **1993**, *76*, 2155.
144 D. E. Manolopoulos *J. Chem. Soc., Faraday Trans.* **1991**, *87*, 2861.
145 D. E. Manolopoulos, P. W. Fowler *Chem. Phys. Lett.* **1991**, *187*, 1.
146 R. Taylor *Tetrahedron. Lett.* **1991**, 3734.
147 R. Taylor *J. Chem. Soc., Perkin Trans. 2* **1992**, 3.
148 K. Balasubramanian *Chem. Phys. Lett.* **1993**, *206*, 210.
149 F. Diederich, R. Ettl, Y. Rubin, R. L. Whetten, R. Beck, M. M. Alvarez, S. Anz, D. Sensharma, F. Wudl, K. C. Khemani, A. Koch *Science* **1991**, *252*, 548.
150 K. Kikuchi, N. Nakahara, T. Wakabayashi, S. Suzuki, H. Shiromaru, Y. Miyake, K. Saito, I. Ikemoto, M. Kainosho, Y. Achiba *Nature* **1992**, *357*, 142.
151 R. Taylor, G. J. Langley, J. S. Dennis, H. W. Kroto, D. R. M. Walton *J. Chem. Soc., Chem. Commun.* **1992**, 1043.
152 R. Taylor, G. J. Langley, A. G. Avent, T. J. S. Dennis, H. W. Kroto, D. R. M. Walton *J. Chem. Soc., Perkin Trans 2* **1993**, 1029.
153 R. Taylor, D. R. M. Walton *Nature* **1993**, *363*, 685.
154 B. L. Zhang, C. H. Xu, C. Z. Wang, C. T. Chan, K. M. Ho *Phys. Rev. B* **1992**, *46*, 7333.
155 J. Tersoff *Phys. Rev. B* **1992**, *46*, 15546.
156 N. Sivaraman, R. Dhamodaran, I. Kaliappan, T. G. Srinivasan, P. R. V. Rao, C. K. Mathews *J. Org. Chem.* **1992**, *57*, 6077.
157 R. S. Ruoff, D. S. Tse, R. Malhorta, D. C. Lorents *J. Phys. Chem.* **1993**, *97*, 3379.
158 W. A. Scrivens, J. M. Tour *J. Chem. Soc., Chem. Commun.* **1993**, 1207.
159 Z. Gasyna, P. N. Schatz, J. P. Hare, T. J. Dennis, H. W. Kroto, R. Taylor, D. R. M. Walton *Chem. Phys. Lett.* **1991**, *183*, 283.
160 S. Leach, M. Vervloet, A. Despres, E. Breheret, J. P. Hare, T. J. Dennis, H. W. Kroto, R. Taylor, D. R. M. Walton *Chem. Phys.* **1992**, *160*, 451.
161 R. D. Johnson, G. Meijer, J. R. Salem, D. S. Bethune *J. Am. Chem. Soc.* **1991**, *113*, 3619.
162 R. M. Flemming, B. Hessen, T. Siegrist, A. R. Kortan, P. March, R. Rycko, G. Dabbagh, R. C. Haddon In *Fullerenes: Synthesis, Properties, and Chemistry of Large Carbon Clusters*; G. S. Hammond, V. J. Kuck, Eds.; p. 25 American Chemical Society Symposium Series 481, 1992.
163 C. S. Yannoni, P. Bernier, D. S. Bethune, G. Meijer, J. R. Salem *J. Am. Chem. Soc.* **1991**, *113*, 3190.
164 C. S. Yannoni, R. D. Johnson, G. Meijer, D. S. Bethune, J. R. Salem *J. Phys. Chem.* **1991**, *95*, 9.
165 R. Tycko, R. C. Haddon, G. Dabbagh, S. H. Göarum, D. C. Douglass, A. M. Mujsce **1991**, *95*, 518.
166 R. D. Johnson, C. S. Yannoni, H. C. Dorn, J. R. Salem, D. S. Bethune *Science* **1992**, *255*, 1235.
167 P. A. Heiney, J. E. Fischer, A. R. McGhie, W. J. Romanow, W. J. Denenstein, J. P. McCauley, A. B. Smith III, D. E. Cox *Phys. Rev. Lett.* **1991**, *66*, 2911.
168 A. Dworkin, H. Swarc, S. Leach, J. P. Hare, T. J. Dennis, H. W. Kroto, R. Taylor, D. R. M. Walton *C. R. Acad. Sci. Paris* **1991**, *312 II*, 979.
169 J. S. Tse, D. D. Klug, D. A. Wislon, Y. P. Handa *Chem. Phys. Lett.* **1991**, *183*, 387.
170 P. A. Heiney *J. Phys. Chem. Solids* **1992**, *53*, 1333.
171 M. F. Meidine, P. B. Hitchcock, H. W. Kroto, R. Taylor, D. R. M. Walton *J. Chem. Soc., Chem. Commun.* **1992**, 1534.
172 A. L. Balch, J. W. Noll, M. M. Olmstead *J. Chem. Soc., Chem. Commun.* **1993**, 56.
173 S. M. Gorun et al. *J. Chem. Soc. Chem. Commun.* **1991**, 1556.
174 J. D. Crane, P. W. Hitchcock, H. W. Kroto, R. Taylor, D. R. M. Walton *J. Chem. Soc., Chem. Commun.* **1992**, 1764.
175 A. Izuoka et al. *J. Chem. Soc., Chem. Commun.* **1992**, 1472.
176 J. D. Crane, P. B. Hitchcock *J. Chem. Soc., Dalton Trans.* **1993**, 2537.
177 P. R. Birkett, C. Christides *J. Chem. Soc., Perkin Trans. 2* **1993**, 1407.
178 O. Ermer *Helv. Chim. Acta* **1991**, *74*, 1339.
179 G. Roth, P. Adelmann *J. Phys. I France* **1992**, *2*, 1541.
180 T. Anderson, K. Nilson, M. Sundahl, G. Westman, O. Wennerström *J. Chem. Soc., Chem. Commun.* **1992**, 604.

Chapter 2 Reduction

2.1 Introduction

2.2 Fulleride Anions

2.3 Reductive Electrosynthesis
2.3.1 Electrocrystallization
2.3.2 Electrophilic Additions to Fulleride Anions

2.4 Reduction with Metals
2.4.1 Alkali Metal Fullerides
2.4.1.1 Generation in Solution and Quenching Experiments
2.4.1.2 Synthesis and Properties of Alkali Metal Fulleride Solids
2.4.2 Alkaline Earth Metal Fullerides
2.4.3 Reduction with Mercury

2.5 Reduction with Organic Donor Molecules

References

2.1 Introduction

The first chemical transformations that have been carried out with C_{60} were reductions. After the pronounced electrophilicity of the fullerenes was recognized, electron transfer reactions with electropositive metals, strong organic donor molecules as well as electrochemical reductions have been used to prepare fulleride salts. Some of these systems exhibit extraordinary solid state properties like superconductivity and molecular ferromagnetism. These phenomena, which so far have not been observed for higher fullerenes, are related to internal properties of the C_{60} molecule. Among all organic molecules, the behavior of C_{60} and its chemically modified forms is unique. Reductive transformations of fullerenes have not only been carried out to prepare fulleride salts. The fulleride ions themselves are reactive species and easily undergo subsequent reactions, for example, with electrophiles. Therefore, the anions provide a valuable synthetic potential for fullerene chemistry.

2.2 Fulleride Anions

Theoretical calculations of the molecular orbital levels of C_{60} show that the lowest unoccupied molecular orbitals (LUMO) exhibit a comparatively low energy and are triply degenerate [Fig. 2.1][1,2,3,4,5,6]. Therefore, C_{60} was predicted to be a fairly electronegative molecule being reducible up to the hexaanion. Indeed, this view was supported by very early investigations that have been carried out with C_{60} in solution, namely cyclic voltammetry studies, which showed its facile and stepwise reduction. In these first investigations, C_{60} was reduced by two[7] and three[8] electrons.

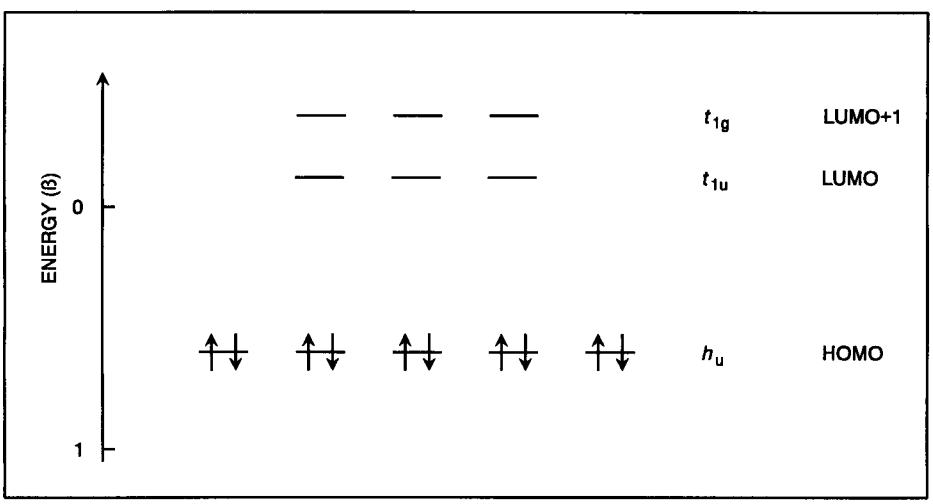

Figure 2.1 Schematic representation of the Hückel molecular orbital diagram for C_{60} (HOMO, LUMO, LUMO+1)^2.

Shortly thereafter, by increasing the expansion of the available potential window, the formation of the tetra-[9], penta-[10] and hexaanion[11,12,13] [Fig. 2.2] could be detected by this technique. The reductions were also found to be reversible at slow scan rates of 100 mV s^{-1}, for example, in a mixture of toluene and acetonitrile as solvent at −10 °C. The different reduction potentials appear almost

equidistant (~Δ 400 mv)[11]. The higher homologue C_{70} exhibits an analogous behavior; six reduction waves at comparable potentials have been observed[11].

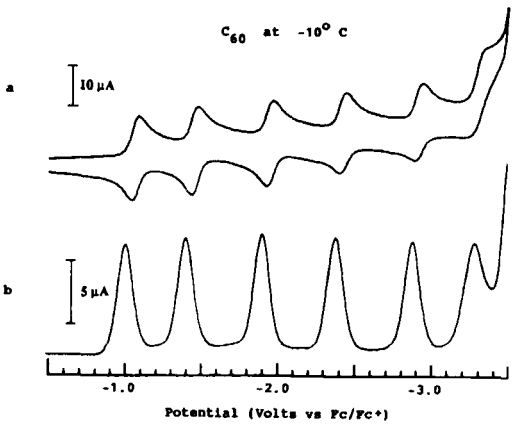

Figure 2.2 Reduction of C_{60} in CH_3CN/toluene at −10 °C using (a) cyclic voltammetry and (b) differential pulse voltammetry[11].

All the reductions are one electron transfer processes. This has been demonstrated, for example for the first four reductions of C_{60} by bulk electrolysis in benzonitrile[9]. The anions are comparatively stable in solution for up to several days, especially at low temperatures. There is a weak dependence of the reduction potentials on the solvent[8] and the electrolyte but a strong dependence on the temperature [Table 2.1]. Differences in the values of the first reductions potentials of up to 600 mV have been observed. The donor-acceptor properties (Gutmann solvent donicity number) of the solvent have a pronounced influence on the first and third reduction potentials[8].

Table 2.1 Reduction potentials (V vs. SCE) of C_{60} reductions for several variations of solvent, electrolyte and temperature[14]

	benzonitrile $TPACIO_4$ RT[15]	CH_2Cl_2 $TBABF_4$ RT[15]	THF $TBACIO_4$ RT[15]	benzene $TBACIO_4$ RT[9]	CH_3CN/toluene $TBAPF_6$ − 10 °C[11]
C_{60}/C_{60}^-	−0.43	−0.44	−0.33	−0.36	−0.98
C_{60}^-/C_{60}^{2-}	−0.85	−0.82	−0.92	-0.83	−1.37
C_{60}^{2-}/C_{60}^{3-}	−1.32	−1.25	−1.49	−1.42	−1.87
C_{60}^{3-}/C_{60}^{4-}	−1.78	−1.72	−1.99	−2.01	−2.35
C_{60}^{4-}/C_{60}^{5-}	-	-	-	−2.60	−2.85
C_{60}^{5-}/C_{60}^{6-}	-	-	-	-	−3.26

Four reversible reductions[16] were found for the chiral higher fullerene D_2-C_{76} and five reversible reductions[17] for C_{84}. The reduction waves of these higher fullerenes seem to appear at somewhat more positive potentials but are comparable to those of C_{60} and C_{70}, showing that they are also electrophilic molecules.

Investigations of the anions C_{60}^{n-} (n = 1-6) and C_{70}^{n-} (n = 1-4) by spectroelectrochemistry have been very valuable for the determination of their individual properties. Each species exhibits a characteristic UV/Vis/NIR and ESR spectrum[9,18,19,20,21,22,23,24]. This knowledge of the spectroscopic properties of the anions allows an unambiguous determination of the oxidation state of reduced C_{60}, obtained by other methods, for example, by chemical reduction. In contrast to C_{60} itself, the anions C_{60}^{n-} (n = 1-6) exhibit strong absorptions in the NIR and the λ_{max} values significantly depend on n. These low energy NIR transitions can be rationalized in terms of the molecular orbital diagram of C_{60} [Fig. 2.1][22]. In the case of the parent C_{60} the t_{1u} orbitals are triply degenerate. Placing one electron into the t_{1u} LUMO results in the observation of an NIR transition at 1078 nm. This low energy absorption is assigned to the symmetry allowed t_{1u}-t_{1g} transition[18,25,26,27] and predicted to be about 1 eV[5,28]. A Jahn-Teller ground state has been suggested[29] for the monoanion, which lowers the energy of the electron in the t_{1u}-orbital. A reduction of the symmetry to D_{5d}, for example, was calculated to lower the energy by about 2 kcal/mol[29]. Such a reduction in symmetry splits the t_{1u} and t_{1g} orbitals into a_{2u} + e_{1u} and a_{2g} + e_{1g} respectively, leaving the possibility of the ground state being either not degenerate or doubly degenerate [Fig 2.3]. A broadening and red-shifting was observed for the 330 nm absorption ("$h_u \rightarrow t_{1g}$") and also for the 255 nm absorption[9], which can be also accounted by a diminution in symmetry[22]. In the visible region, spectral changes produce the colors of the different fulleride anions, which are dark red-purple for C_{60}^-, red-orange for C_{60}^{2-} and for C_{60}^{3-} dark red-brown[14]. The ESR spectra[9,18,21,30] of C_{60}^- show a broad signal for this S = 1/2 system. The g value is remarkably low, lying between 1.997 and 2.000, which additionally supported the conclusion that the electronic ground state of the monoanion is doubly degenerate[21]. The line width is very temperature dependent and decreases with decreasing temperature[21,30].

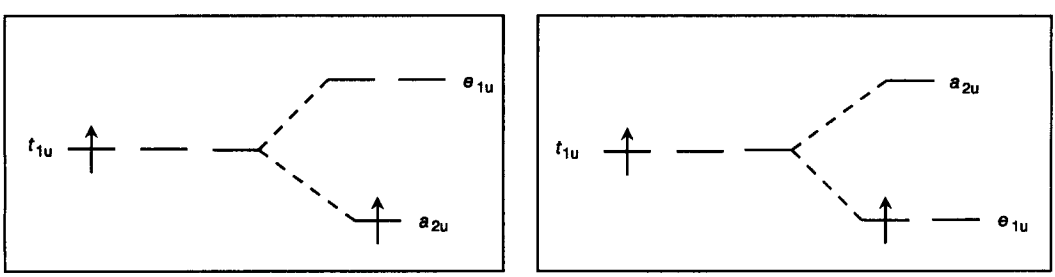

Figure 2.3 The two possibilities of the splitting of the t_{1u} orbitals due to Jahn-Teller distortion in C_{60}^-.

The UV/Vis/NIR spectrum of each anion C_{60}^{n-} dramatically differs from those of the others. This reflects the changes of the orbital energies of the LUMO and LUMO+1 with diminished degeneracy[21]. For the dianion C_{60}^{2-} an ESR spectrum consistent with a triplet ground state (S = 1) was observed [Fig. 2.4][9,21,24], which is the highest spin state for any C_{60}^{n-}.

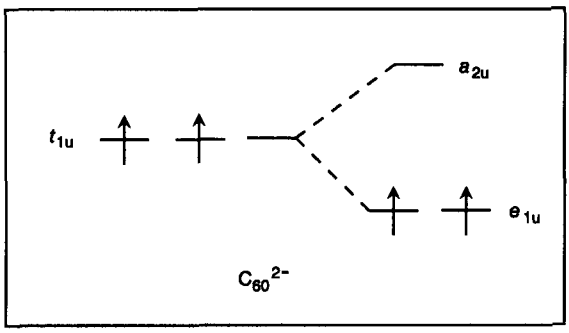

Figure 2.4 Molecular orbital diagram for C_{60}^{2-}.

Additional one-electron reductions lead to a S = 1/2 ground state for the trianion C_{60}^{3-}, to a diamagnetic tetraanion C_{60}^{4-}, a pentaanion C_{60}^{5-} with a spin of 1/2 and finally to the diamagnetic hexaanion C_{60}^{6-}[Fig. 2.5][24].

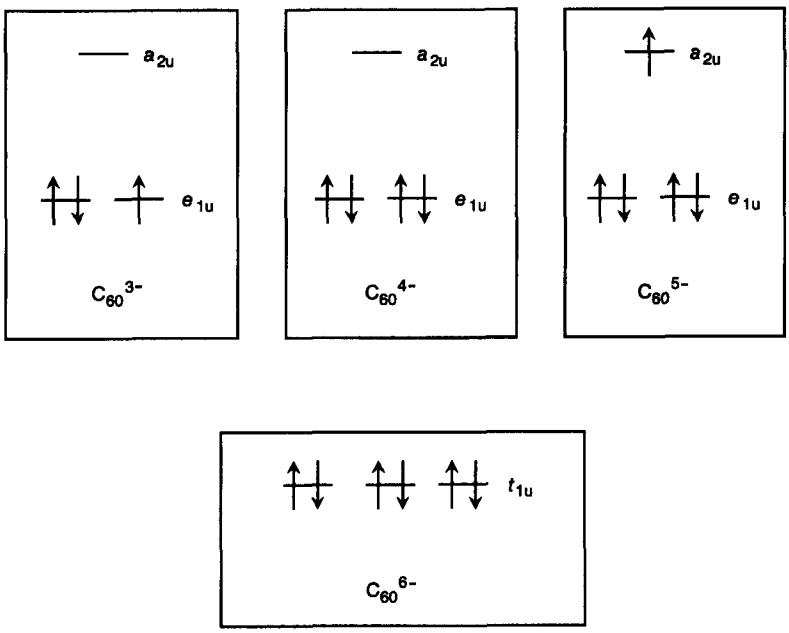

Figure 2.5 Molecular orbital diagrams of C_{60}^{3-}, C_{60}^{4-}, C_{60}^{5-} and C_{60}^{6-}.

2.3 Reductive Electrosynthesis

2.3.1 Electrocrystallization

The possibility of electrochemically producing C_{60} anions in a defined oxidation state by applying a proper potential can be used to synthesize fulleride salts by electrocrystallization[30,31,32,33,34,35,36]. An obvious requirement for this purpose is the insolubility of the salt in the solvent to be used for the electrocrystallization process. This can be achieved by choosing the proper solvent, oxidation state of C_{60} and the counter cation, which usually comes from the supporting electrolyte.

In many cases fulleride anions are more soluble, especially in more polar solvents than the parent fullerenes. For example, in bulk electrolysis experiments with tetra-*n*-butylammonium perchlorate ($TBAClO_4$) as supporting electrolyte, carried out in acetonitrile where C_{60} is completely insoluble, fairly concentrated, dark red-brown solutions of C_{60}^{3-} can be obtained[37]. Upon reoxidation, a quantitative deposition of a neutral C_{60} film on the surface of a gold/quartz crystal working electrode takes place. This C_{60} film can be stepwise reductively doped with TBA^+ leading to $(C_{60}^{-})(TBA^+)$ and $(C_{60}^{2-})(TBA^+)_2$ prior to the redissolution of the C_{60}^{3-} species. This whole process is represented in Scheme 2.1 where (s) and (f) denote "solution" and "film" respectively[37].

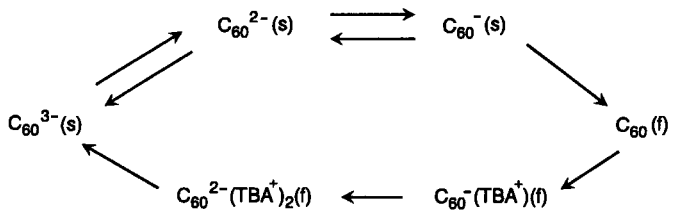

Scheme 2.1

Whereas C_{60} is insoluble and inert in liquid ammonia without any cosolvent, the fulleride anions C_{60}^{n-} (n = 1–4), generated electrochemically with KI as supporting electrolyte dissolve completely in this polar medium[13]. Further reductions lead to the ammonia insoluble potassium salts of the penta- and hexaanions.

The formation of crystalline fulleride salts at the electrode occurs when less polar solvents and bulky cations are used for the electrosynthesis. The first fulleride salt was synthesized by Wudl by bulk electrolysis of C_{60} in *o*-dichlorobenzene with tetraphenylphosphonium chloride as supporting electrolyte[30]. The black crystalline material with the composition $(Ph_4P^+)_3(C_{60}^{-})(Cl^-)_2$ exhibits an ESR line with a g value of 1.9991 and a line width of 45 G at room temperature. With decreasing temperature the ESR line shows an dramatic narrowing. Below 40 K its width is only about 400 mG[31]. An integration of the signal gives 1.5 spins per C_{60}, a value corroborated by static susceptibility measurements[30]. The origin of the extra 0.5 spins per formula unit is not been conclusively clarified. It was suggested that the extra spin is mainly located on the tetraphenylphosphonium[31], which however would require the presence of a so far never observed $Ph_4P\cdot$ moiety. Conductivity measurements of $(Ph_4P^+)_3(C_{60}^{-})(Cl^-)_2$ at room temperature reveal a semiconducting behavior[30].

An analogous single crystalline fulleride salt $(Ph_4P^+)(C_{60}^{-})(I)_x$ was obtained by electrocrystallizing CH_2Cl_2/toluene solutions of C_{60} in the presence of Ph_4PI[34]. The X-ray crystal structure of

$(Ph_4P^+)(C_{60}^-)(I)_x$ [Fig. 2.6] shows, that the C_{60} anions are surrounded by a tetragonally distorted cube of tetraphenylphosphonium cations. There are no short contacts between the C_{60} anions. The shortest center-to-center distance is 12.6 Å. A deficiency of iodine with x between 0.15 and 0.35 was determined. The origin of the resulting extra charge and spin remains to be clarified also in this case. In the NIR spectrum no band due to C_{60}^{2-} has been observed. Both tetraphenylphosphonium salts are stable in air. The electrocrystallization with tetraphenylarsonium halides gives analogous results[36].

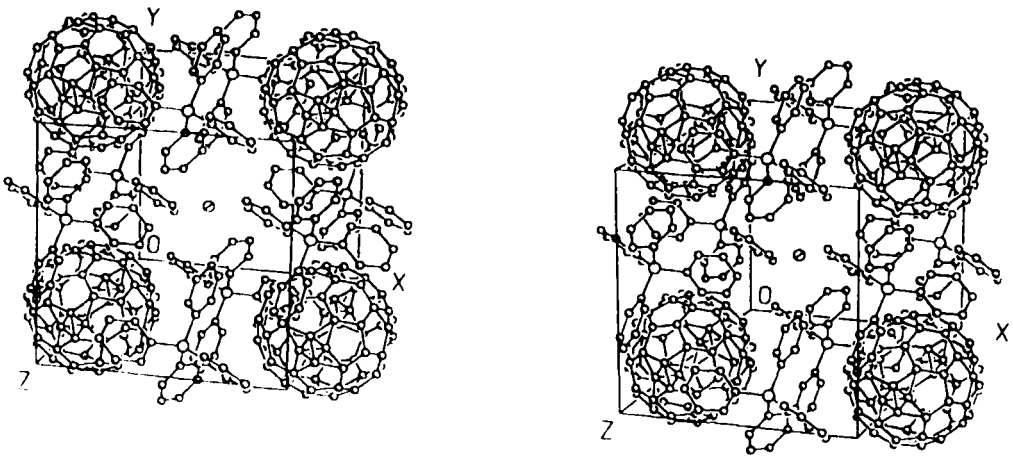

Figure 2.6 Stereoscopic view of the unit cell of $(Ph_4P^+)(C_{60}^-)(I)_x$[34]. The iodide anions at the corners of the unit cell have been omitted for clarity.

The electrocrystallization in the presence of [bis(triphenylphosphoranylidene)]ammonium chloride (PNPCl) leads to the single crystalline salt $(PNP^+)(C_{60}^-)$ which shows no electrical conductivity[33]. The ESR of $(PNP^+)(C_{60}^-)$ changes upon sample ageing. The ESR spectrum of a freshly isolated single crystal exhibits the same features as those of the tetraphenylphosphonium salts. However, after several days a completely new spectrum with a significantly narrower line emerges, as interpreted by a crystal lattice degradation[33].

Another semiconducting fulleride salt, $[Ru(bpy)_3](C_{60})_2$ with bpy = 2,2'-bipyridine, crystallizes on the Pt electrode surface out of dichloromethane solutions saturated with $[Ru(bpy)_3]PF_6$ within a few minutes[35]. The NIR spectra of benzonitrile solutions of this salt demonstrate that the only fulleride anion present is C_{60}^-. The temperature dependence of the conductivity is typical for a semiconductor with the room temperature conductivity being 0.01 S cm^{-1} and the activation energy 0.1 kJ mol^{-1} (0.15 eV). It was postulated that there is an electronic overlap between the two ions of this salt leading to a donation of electron density from the C_{60}^- to the ligand orbitals in the $(Ru(bpy)_3^{2+}$ ($\Delta E° \approx 0.7$)[35].

2.3.2 Electrophilic Additions to Fulleride Anions

The electrochemical generation of fulleride anions can also be used to synthesize covalent organofullerene derivatives, by quenching the anions with electrophiles. This was exemplified in the synthesis of dimethyldihydrofullerene-60, the simplest dialkyl derivative of C_{60}[38]. For this purpose,

benzonitrile solutions of C_{60} and tetra-*tert*-butylammonium perchlorate ($TBAClO_4$) where exhaustively electroreduced in a dry box to yield a dark red solution of C_{60}^{2-}. The treatment of this solution with an excess MeI, after the potential is turned off, leads to the formation of a dark brown solution of $C_{60}(CH_3)_2$ [Scheme 2.2]. This addition reaction proceeds comparatively smoothly. After 40 minutes, still about 50 % of the dianion is present, which subsequently can be reoxidized to C_{60}.

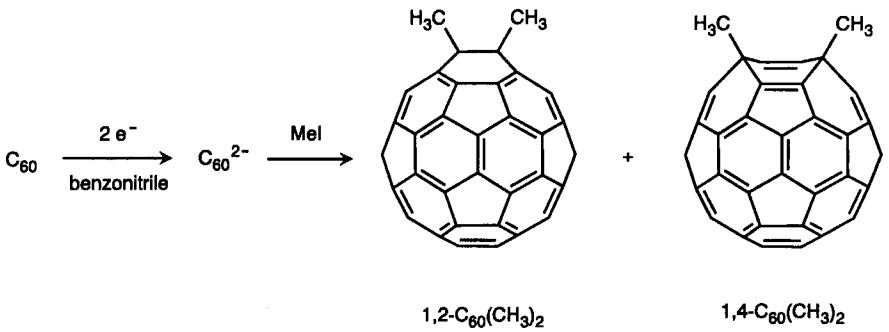

Scheme 2.2

The dimethyldihydrofullerenes-60 isolated are a mixture of the 1,2- and 1,4-isomer [Scheme 2.2] formed in a ratio of 1.4:1. Among the 23 possible regioisomers of $C_{60}(CH_3)_2$ the 1,2- and 1,4- are predicted to be the most stable, with the heat of formation of the 1,4-isomer being a little bit larger than that of the 1,2-isomer[38]. The electron density in the intermediate $C_{60}(CH_3)^-$ is calculated to be largest at C2 (25 %) followed by C4/11 (9 % each). This also suggests that the second electrophilic attack of MeI should be preferred at C2, even if it is taken into account that there are two sites available for a 1,4-addition mode.

2.4 Reduction with Metals

2.4.1 Alkali Metal Fullerides

2.4.1.1 Generation in Solution and Quenching Experiments

A chemical reduction of fullerenes can be easily achieved by the reaction with electropositive metals, for example, alkali- and alkaline earth metals. The anions C_{60}^{n-} (n = 1-5) can be generated in solution by titrating a suspension of C_{60} in liquid ammonia with a solution of Rb in liquid ammonia [Scheme 2.3][39], whereupon the resulting anions dissolve. Monitoring of this titration is possible by detecting the characteristic NIR absorption of each anion by UV/Vis/NIR spectroscopy. The solubility of the alkali metal fullerides in the polar solvent NH_3 demonstrates their salt character.

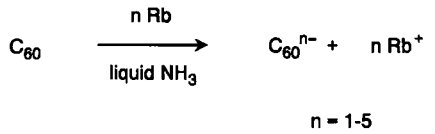

Scheme 2.3

Ultrasound aided reduction of C_{60} and C_{70} with Li metal to anionic species can be carried out in THF as the solvent [Scheme 2.4][40]. In contrast to the parent fullerenes, the anions C_{60}^{n-} and C_{70}^{n-} are very soluble in THF. The solutions generated in this way are deep red-brown. Alkylation of a C_{60} and C_{70} polyanion mixture with excess MeI leads to the formation of polymethylated fullerenes with up to 24 covalently bound methyl groups.

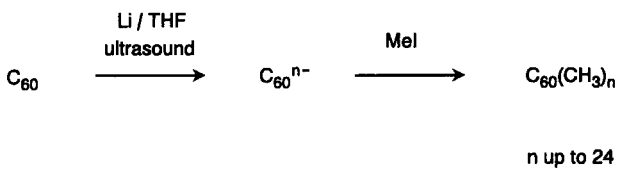

Scheme 2.4

2.4.1.2 Synthesis and Properties of Alkali Metal Fulleride Solids

The discovery of superconductivity[41] in alkali metal doped C_{60} attracted the attention of a broad cross section of the scientific community to this class of compounds. The composition of the first alkali metal doped fullerene was determined to be K_3C_{60}[42,43]. In this compound, the transition to a superconducting state occurs at T_c = 19.3 K[42]. In a short time, a large variety of alkali metal fullerides M_nC_{60} have been synthesized and studied with respect to their solid state properties[42,43,44,45,46,47]. Thereby, the stoichiometries of M_nC_{60} with n, for example, being 2, 3, 4 and 6 as well as the alkali metal with M = Na, K, Rb, Cs have been varied systematically. In addition, mixed alkali compounds $M^1{}_nM^2{}_mC_{60}$ (M^1, M^2 = Li, Na, K, Rb, Cs) can be obtained[46,47]. All of the alkali metals react directly with C_{60}. Since the heavier homologues of the alkali metals have a higher vapor pressure, their direct reaction with the fullerene proceeds more easily. The synthesis of a defined M_nC_{60} can be achieved by allowing stoichiometric amounts of the metal and C_{60} to react at 200 °C in a sealed tube [Scheme 2.5][42]. In most cases additional annealing steps at elevated temperatures are necessary to complete the reaction. The resulting solids are very air sensitive.

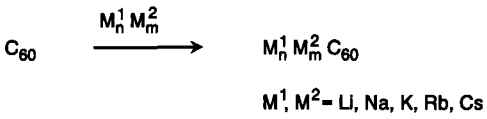

Scheme 2.5

This direct method is a convenient route, especially for saturation doped fullerides M_6C_{60}. A facile control of the alkali metal fulleride stoichiometry of M_nC_{60} (M = K, Rb, Cs) can be obtained using vapor-transport techniques[48]. Thereby, a weighed amount of C_{60} is treated with a large excess of the alkali metal at 225 °C under vacuum. This procedure leads to the saturation-doped products M_6C_{60}. To these fullerides a specific amount of C_{60} is added to give the desired stoichiometry. The process of the formation of $M_{6m/n}C_{60}$ is completed after a subsequent annealing process under vacuum at 350 °C [Scheme 2.6]. Upon heating to 550 °C, K_6C_{60} decomposes to give K_4C_{60}, with the liberated K reacting with the glass [Scheme 2.7][49].

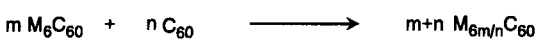

Scheme 2.6

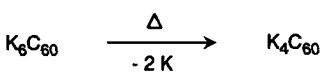

Scheme 2.7

The synthesis of M_nC_{60}(M = Na, n = 2, 3; M = K, n = 3) has been achieved by the reaction of solid C_{60} with solid MH or MBH_4 [Scheme 2.8; Scheme 2.9][49]. The advantage of these reactions is the easier handling of small quantities of MH or MBH_4 compared to that of alkali metals.

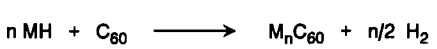

Scheme 2.8

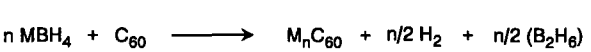

Scheme 2.9

As a source for alkali metals binary alloys of the type CsM (M = Hg, Tl, Bi) can also be used [Scheme 2.10][45]. It was found however that the heavy metals partly co-intercalate into the C_{60} lattice[48,50].

$$C_{60} + n\,MHg_x \xrightarrow[-\,x\,Hg]{} M_nC_{60}$$

Scheme 2.10

Alkali metal doping of C_{60} is also possible by solution-phase techniques[51,52,53]. K_nC_{60} and Rb_nC_{60} containing small fractions of the superconducting M_3C_{60} phases were prepared by allowing toluene solutions of C_{60} to react with the alkali metal[51,52]. During the course of the reaction, the alkali metal fullerides form a black precipitate.

A rapid and easy access to high quality alkali metal fulleride superconductors is obtained by the reaction of stoichiometric amounts of C_{60} and alkali metal in liquid ammonia [Scheme 2.11][53]. After the ammonia is removed from the reaction mixture, the products are annealed in sealed evacuated silica tubes at elevated temperatures (225–350 °C). In this way, large amounts of superconducting fractions M_3C_{60} with $M_3 = K_3$, Rb_3, $CsRb_2$, $RbCs_2$ and KRbCs are available.

$$C_{60} + n\,M\ (\text{in liquid } NH_3) \xrightarrow[-NH_3]{} M_nC_{60}$$

Scheme 2.11

The intercalation of C_{60} with lithium has been achieved by the technique of solid-state electrochemical doping[54]. In this technique, metallic lithium was used as the negative electrode and a polyethylene oxide lithium perchlorate ($P(EO)_8LiClO_4$) polymer film served as electrolyte. The formation of stoichiometric phases Li_nC_{60} (n = 0.5, 2, 3, 4, and 12) has been observed.

The composition of the alkali metal fullerides can be regarded as intercalation compounds of the parent C_{60} FCC (face centered cubic) solid state structure, or of hypothetical BCC (body centered cubic) and BCT (body centered tetragonal) fullerene structures [Fig. 2.7]. In a fulleride phase M_2C_{60}, for example in the sodium salt Na_2C_{60}, the metal occupies the two tetrahedral interstices of a FCC[55]. The fullerides M_3C_{60} also exhibit FCC structures at room temperature[43]. Here, all the available tetrahedral and octahedral interstices are occupied by the alkali metal. The tetrahedral sites with a radius of 1.12 Å are smaller than the octahedral sites having a radius of 2.06 Å. Thus, ions that are occupying tetrahedral sites larger than Na^+ are lattice expanding[47]. On the other hand, all alkali cations are smaller than the octahedral sites, this has a lattice contracting influence. Each alkali metal fulleride superconductor has a M_3C_{60} stoichiometry and the corresponding FCC structure. Significantly, an expansion of the lattice due to bigger cations is accompanied by an enhancement of the T_c of M_3C_{60} [Tab 2.2, Fig. 2.8]. Na_3C_{60} is not superconducting, which is attributed to the fact that below 260 K a reversible structural transition leading to a two phase mixture of Na_2C_{60} and Na_6C_{60} takes place[55].

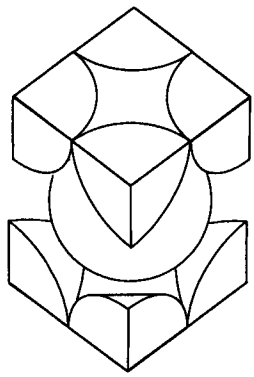

C_{60} (FCC)

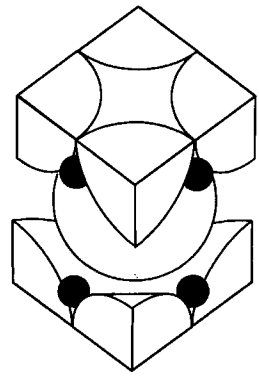

M_2C_{60} (FCC)

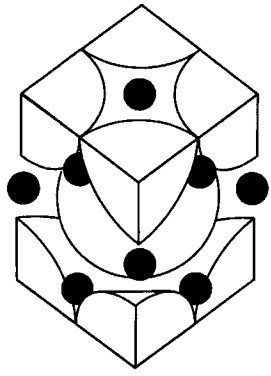

M_3C_{60} (FCC)

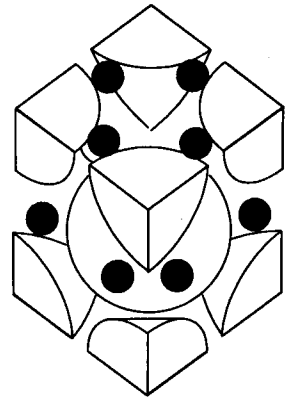

M_4C_{60} (BCT)

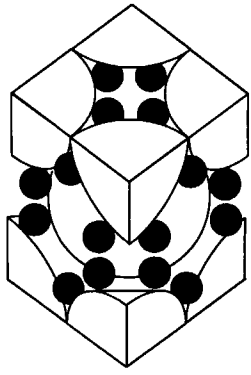

M_6C_{60} (FCC)

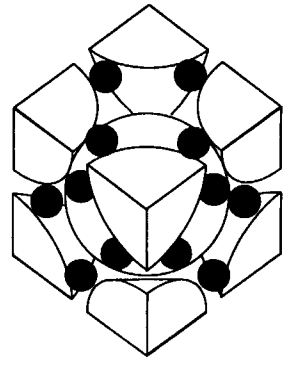

M_6C_{60} (BCC)

Figure 2.7 Schematic representation of C_{60} and M_nC_{60} structures.

Table 2.2 Transition temperatures and lattice parameters of FCC M_3C_{60} superconductors[47]

Material	T_c(K)	a_0 (Å)
$RbCs_2C_{60}$	33	14.555
Rb_2CsC_{60}	31	14.431
Rb_3C_{60}	29	14.384
KRb_2C_{60}	27	14.323
K_2CsC_{60}	24	14.292
K_2RbC_{60}	23	14.243
K_3C_{60}	19	14.240
Na_2CsC_{60}	12	14.134
Li_2CsC_{60}	12	14.120
Na_2RbC_{60}	2.5	14.028
Na_2KC_{60}	2.5	14.025
C_{60}		14.161

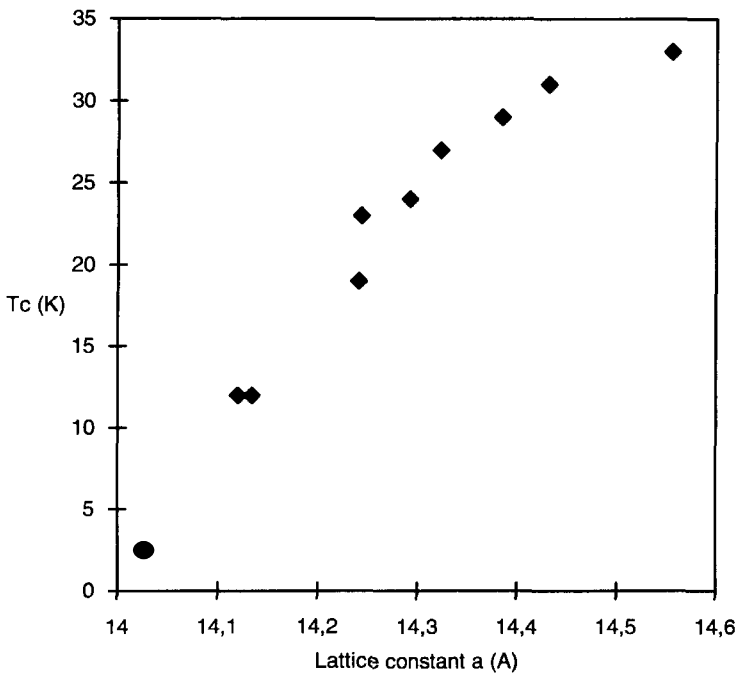

Figure 2.8 The relationship between T_c and a_0 for M_3C_{60} superconductors.

The M_4C_{60} and M_6C_{60} (M = K, Rb, Cs) structures are related to each other. The BCC M_6C_{60} structure is based on the BCC packing of the C_{60} molecules. The metal cations occupy four coordinate

interstices between rotationally ordered C_{60} molecules[44]. The M_4C_{60} structure consists of a BCT packing of the C_{60} molecules[56]. The M_4C_{60} structure can be regarded as a defect M_6C_{60} structure. In M_4C_{60} the six identical sites of a BCC structure are disproportionate into four slightly smaller and two larger ones. The cations M^+ occupy the smaller sites.

The occurrence of superconductivity in alkali metal fullerides always requires the trianionic state of C_{60}. In this case, the band (conduction band) derived from the t_{1u} orbitals is half filled. This gives rise to the maximum conductivity of M_3C_{60}[57]. Superconductivity is absent in Li_nC_{60}, Na_nC_{60} and C_{70} based fullerides. Band structure calculations for K_3C_{60} predict the Fermi-level to be close to the lower maximum of the density of states (DOS) of the conduction band[57]. The higher T_c values for those M_3C_{60}s with enhanced unit cell parameters [Tab. 2.2] can be interpreted with increased densities of states at the Fermi-level. This increase is due to a sharpening of the conduction band caused by a weaker orbital overlap of neighboring C_{60} molecules as the cell volume increases. The DOS in Rb_3C_{60} is about 15 % higher than that of K_3C_{60}[58]. In M_6C_{60}, the bands derived from the t_{1u} orbitals are completely filled, which makes these compounds insulators. Also the fullerides M_2C_{60} and M_4C_{60} are not conducting, although the t_{1u} bands are partly filled. This was interpreted[49] by localized Jahn-Teller distortions on C_{60}^{n-}.

The occurrence of superconductivity in M_3C_{60} can be determined by the disappearance of the resistivity or, more conveniently, by the Meißner-Ochsenfeld-Effect (magnetization measurements). In this method the very air sensitive fullerides are loaded under inert gas conditions into a capillary tube, which is then sealed under vacuum. Upon the transition to the superconducting state, the magnetic susceptibility sharply decreases, since superconductors in their ground state are diamagnetic.

2.4.2 Alkaline Earth Metal Fullerides

Alkaline earth metals can also be intercalated with C_{60}[59]. The preparation of Ca_5C_{60} [Scheme 2.12][60] and Ba_6C_{60} [Scheme 2.13][61,62] has been achieved by the direct reaction of C_{60} with the corresponding alkaline earth metal vapor. Therefore, the alkaline earth metal is mixed with C_{60} in an inert atmosphere and the powder is then placed into a custom designed high-purity tantalum cell, which allows compression into pellets. The pellets are then loaded into quartz tubes, being subsequently sealed under vacuum. Several heat treatments of these samples between 550 and 800 °C for periods ranging from hours to weeks leads to the corresponding fullerides[60,61]. In an alternative preparation method, a Ba layer is placed under a C_{60} layer and the annealing of this sandwich leads to the desired fulleride[62]. In this procedure the amount of Ba in the volume is controlled by photoemmission spectroscopy.

$$C_{60} + 5\,Ca \longrightarrow Ca_5C_{60}$$

Scheme 2.12

$$C_{60} + 6\,Ba \longrightarrow Ba_6C_{60}$$

Scheme 2.13

Upon doping C_{60} with Ca to Ca_5C_{60}, a phase transformation occurs, leading to a simple cubic superconducting phase with T_c of 8.4 K. For Ba_6C_{60}, which is also superconducting (T_c = 7 K), a BBC structure similar to that found in M_6C_{60} (M = K, Rb, Cs) was determined. At low doping levels, an

A15 Ba_3C_{60} structure coexists with the BCC phase[61]. The fact that Ca_5C_{60} as well as Ba_6C_{60} are superconducting without having a FCC structure implies that the superconductivity mechanism is independent of the coordination number, but more related to an integral property of the C_{60} molecule itself. In Ba_3C_{60} the t_{1u} band is completely filled. Higher doping levels are reached in the superconductors Ca_5C_{60} and Ba_6C_{60}. In these compounds, the t_{1g} band is occupied with charge carriers also, as shown by the valence band spectra[60,62]. Therefore, their superconductivity is associated with the t_{1g} band.

2.4.3 Reduction with Mercury

A bulk reduction of C_{60} in solution is also possible with less electropositive metals. This was demonstrated[63] by the reduction of C_{60} with mercury leading to C_{60}^- or C_{60}^{2-}. The addition of a drop of mercury to a 1 mM solution of tetrahexylammonium bromide, (THA)Br, in tetrahydrofuran containing a brownish suspension of C_{60} leads to a rapid disappearance of the suspension and the formation of a clear red solution of the C_{60} monoanion [Scheme 2.14]. The solution is stable in the absence of air. As shown by ESR spectroscopy, the amount of dianion is only about 0.4 % of the total anion concentration.

$$C_{60} \xrightarrow[(THA)Br\,/\,THF]{Hg} C_{60}^- + C_{60}^{2-}$$

Scheme 2.14

These results imply, that the standard potential of the Hg_2Br_2/Hg couple in THF is more negative than in water and sufficiently negative to reduce C_{60} to the mono- and dianion. As predicted by the Nernst law, the formal potential of the Hg_2Br_2/Hg should be shifted to more negative values upon higher (THA)X concentrations. Indeed, a 0.1 M (THA)Br solution increases the concentration of the dianion to 5%.

The reaction behavior of C_{60} towards the Hg_2X_2/Hg couple strongly depends on the solvent. In a solution of 1 mM (THA)I in benzonitrile, for example, no reaction was observed. This is because the formal potential of the Hg_2I_2/Hg couple under these conditions is not sufficiently negative to allow the reduction of C_{60}. An increase of the (THA)I concentration to 0.1 M, however, leads to the reduction of C_{60} to the monoanion and only traces (0.3 %) of the dianion.

2.5 Reduction with Organic Donor Molecules

The synthesis and isolation of fulleride salts is also possible with organic or organometallic donor molecules. Since there exists a large variety of molecular compounds fulfilling the requirement of being a donor of sufficient strength, it can be expected to gain access to materials with tunable solid state properties. The first examples of fullerene based charge-transfer (CT) complexes, containing molecular cationic species already show a remarkable electronic and magnetic behavior[64,65,66,67,68,69,70,71]. The CT-complex formation is straightforward and usually achieved simply by mixing solutions of the

components in a non-polar solvent for example benzene. This leads to the precipitation of air sensitive $(D^+)_nC_{60}^-$ complexes [Scheme 2.15]. The CT-complexes are usually soluble in benzonitrile or THF. If the preparation is carried out in these more polar solvents, the solid CT-complexes can be obtained by precipitation with hexane[70]. In the case of the liquid tetrakis(dimethylamino)ethylene (TDAE) as organic donor, a quantitative transformation to $[TDAE]^+C_{60}^-$ is achieved by allowing the neat TDAE to react with C_{60}[66].

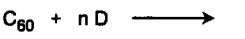

	donor (D)	n
1	(tetraphenylporphinato)chromium(II)	1
2	cobaltocene	1
3	bis(*N*-methylimidazole)(tetraphenylporphinato)tin(II)	1 (D^{2+})
4	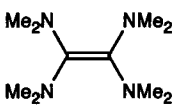 tetrakis(dimethylamino)ethylene (TDAE)	1
5a		1
5b	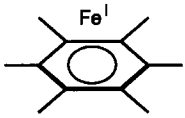 $[Fe^I(C_5H_5)(C_6Me_6)]$	2
5c		3

Scheme 2.15

In the case of the 19-electron complex $[Fe^I(C_5H_5)(C_6Me_6)]$ as donor, the synthesis of **5a-c** can be controlled by choosing the right stoichiometry 1:1, 2:1 or 3:1 respectively[71]. The ease of the reduction of C_{60} depends on the reduction potential of the donor. These reduction potentials themselves however strongly depend on, for example, the polarity of the solvent. Thus, a reliable comparison of the reduction power of the donors in Scheme 2.15 would require the knowledge of their reduction potentials determined under identical conditions.

With the exception of **5b,c**, all the CT-complexes of Scheme 2.15 contain C_{60} as the monoanion. This can be shown by UV/Vis/NIR[70,72] and ESR spectroscopy[68,70]. The characteristic properties of the C_{60} monoanion, such as the 1078 nm NIR absorption or the ESR features, indicating a Jahn-Teller distortion of the t_{1u} orbitals, are found in these chemically prepared systems as well.

This disproportionation is due to both the large electron affinity of C_{60}^- and the low lying second oxidation potential of TDAE. No corresponding disproportionation has been detected[68] for $[TDAE^+]C_{70}^-$.

Under certain conditions the CT-complex formation is reversible. If, for example, solid $[TDAE^+]C_{60}^-$ is treated with toluene in the absence of further TDAE, a quantitative reversion to the parent C_{60} takes place upon the formation of a purple solution [Scheme 2.17][66,72]. An analogous process occurs with $[TDAE^+]C_{60}^-$ under ultra high vacuum at room temperature [Scheme 2.17].

$$C_{60} + TDAE \xleftarrow{\text{ultra high vacuum}} [TDAE^+]C_{60}^- \xrightarrow{\text{toluene}} C_{60} + TDAE$$

Scheme 2.16

Similarly, the treatment of $[Cr^{III}(TPP)^+]C_{60}^-$ in toluene reverses the redox reaction [Scheme 2.18][64]. The addition of a few drops of tetrahydrofuran to the toluene solution promotes the electron transfer again. This is consistent with the lower first reduction potential of C_{60} reported in tetrahydrofuran compared to other solvents[8].

$$Cr^{II}(TPP) + C_{60} \underset{\text{toluene}}{\overset{\text{THF}}{\rightleftharpoons}} [Cr^{III}(TPP)^+C_{60}^-]$$

Scheme 2.17

Among the CT-complexes represented in Scheme 2.15, $[TDAE^+]C_{60}^-$, synthesized by Wudl et. al, exhibits unique solid state properties. This material undergoes a transition to a ferromagnetic state at T_c = 16. 1K[65,73,74,75], a value about 27 times that of previous strictly organic molecular ferromagnets. The ferromagnetic state shows no remanence. This result was interpreted in terms of a soft itinerant ferromagnet[68]. $[TDAE^+]C_{60}^-$ has a *c*-centered monoclinic unit cell[66], with dimensions a = 15. 85 Å, b = 12.99 Å, c = 9.97 Å and β = 93.31 °. The intermolecular contacts along the *c*-axis are only 9.97 Å, a value less than, or comparable to, those of alkali metal doped superconductors M_3C_{60}. This short intermolecular separation suggests a formation of a conduction band, which is partly filled[68]. The pronounced structural anisotropy implies a fairly low-dimensional band structure. The room temperature conductivity of $[TDAE^+]C_{60}^-$ was found to be about 10^{-2} S/cm[65].

References

1 A. D. Haymet *Chem. Phys. Lett.* **1985**, *122*, 421.
2 R. C. Haddon, L. E. Brus, K. Raghavachari *Chem. Phys. Lett.* **1986**, *125*, 459.
3 S. Satpathy *Chem. Phys. Lett.* **1986**, *130*, 545.
4 P. D. Hale *J. Am. Chem. Soc.* **1986**, *108*, 6087.
5 S. Larsson, A. Volosov, A. Rosen *Chem. Phys. Lett.* **1987**, *137*, 501.
6 A. Rosen, B. Wastberg *J. Chem. Phys.* **1989**, *90*, 2525.

7 R. E. Haufler, J. Conceicao, L. P. F. Chibante, Y. Chai, N. E. Byrne, S. Flanagan, M. M. Haley, S. C. O'Brian, C. Pan, Z. Xiao, W. E. Billups, M. A. Ciufolini, R. H. Hauge, J. L. Margrave, L. J. Wilson, R. F. Curl, R. E. Smalley *J. Phys. Chem.* **1990**, *94*, 8634.

8 P.-M. Allemand, A. Koch, F. Wudl, Y. Rubin, F. Diederich, M. M. Alvarez, S. J. Anz, R. L. Whetten *J. Am. Chem. Soc.* **1991**, *113*, 1050.

9 D. Dubois, K. M. Kadish, S. Flanagan, R. E. Haufler, L. P. F. Chibante, L. J. Wilson *J. Am. Chem. Soc.* **1991**, *113*, 4364.

10 D. Dubois, K. M. Kadish, S. Flanagan, L. J. Wilson *J. Am. Chem. Soc.* **1991**, *113*, 7773.

11 Q. Xie, E. Perez-Cordero, L. Echegoyen *J. Am. Chem. Soc.* **1992**, *114*, 3978.

12 Y. Ohsawa, T. Saji *J. Chem. Soc., Chem. Commun.* **1992**, *781*.

13 F. Fhou, C. Jehoulet, A. J. Bard *J. Am. Chem. Soc.* **1992**, *114*, 11004.

14 L. J. Wilson, S. Flanagan, L. P. F. Chibante, J. M. Alford In *Buckminsterfullerenes*; W. E. Billups, M. A. Ciufolini; Eds.; VCH: New York, 1993 p 285.

15 D. Dubois, G. Moninot, W. Kutner, M. T. Jones, K. M. Kadish *J. Phys. Chem.* **1992**, *96*, 7137.

16 Q. Li, F. Wudl, C. Thilgen, R. L. Whetten, F. Diederich *J. Am. Chem. Soc.* **1992**, *114*, 3994.

17 M. S. Meier, T. F. Guarr, J. P. Selegue, V. K. Vance *J. Chem. Soc., Chem. Commun.* **1993**, 63.

18 M. A. Greaney, S. M. Gorun *J. Phys. Chem.* **1991**, *95*, 7142.

19 P. N. Keizer, J. R. Morton, K. F. Preston, A. K. Sugden *Phys. Chem.* **1991**, *95*, 7117.

20 G. A. Heath, J. E. McGrady, R. L. Martin *J. Chem. Soc., Chem. Commun.* **1992**, 1272.

21 D. Dubois, M. T. Jones, K. M. Kadish *J. Am. Chem. Soc.* **1992**, *114*, 6446.

22 D. R. Lawson, D. L. Feldheim, C. A. Foss, P. K. Dorhout, C. M. Elliot, C. R. Martin, B. Parkinson *J. Electrochem. Soc.* **1992**, *139*, L68.

23 D. L. Lawson, D. L. Feldheim, C. A. Foss, P. K. Dorhout, C. M. Elliot, C. M. Martin, B. Parkinson *J. Phys. Chem.* **1992**, *96*, 7176.

24 M. Baumgarten, A. Gügel, L. Gherghel *Adv. Mater.* **1993**, *5*, 458.

25 T. Kato, T. Kodama, M. Oyana, T. Shida, T. Nakagawa, Y. Matsui, S. Suzuki, H. Shiromaru, K. Yamauchi, Y.Achiba *Chem. Phys. Lett.* **1991**, *180*, 446.

26 T. Kato, T. Kodama, M. Oyama, S. Okazaki, T. Shida, T. Nakagawa, Y. Matsui, S. Suzuki, H. Shiromaru, K. Yamauchi, Y. Achiba *Chem. Phys. Lett.* **1991**, *186*, 35.

27 Z. Gasyna, L. Andrews, P. Schatz *J. Phys. Chem.* **1992**, *96*, 7142.

28 F. Negri, G. Orlandi, F. Zerbetto *Chem. Phys. Lett.* **1988**, *144*, 31.

29 N. Koga, K. Morokuma *Chem. Phys. Lett.* **1992**, *196*, 191.

30 P.-M. Allemand, G. Srdanov, A. Koch, K. C. Khemani, F. Wudl, Y. Rubin, F. Diederich, M. M. Alvarez, S. J. Anz, R. L. Whetten *J. Am. Chem. Soc.* **1991**, *113*, 2780.

31 U. Becker, G. Denninger, V. Dyakonov, B. Gotschy, K. Klos, G. Rösler, A. Hirsch, H. Winter *Europhys. Lett.* **1993**, *21*, 267.

32 V. Dyakonov, G. Rösler, H. Klos, B. Gotschy, G. Denninger *Synth. Met.* **1993**, *55-57*, 3214.

33 H. Moriyama, H. Kobayashi, A. Kobayashi, T. Watanabe *J. Am. Chem. Soc.* **1993**, *115*, 1185.

34 A. Penicaud, A. Perez-Benitez, R. Gleason V., E. Munoz, R. Escudero *J. Am. Chem. Soc.* **1993**, *115*, 10392.

35 C. A. Foss, D. L. Feldheim, D. R. Lawson, P. K. Dorhout, C. M. Elliott, C. M. Martin, B. A. Parkinson *J. Electrochem. Soc.* **1993**, *140*, L84-L86.

36 B. Miller, J. M. Rosamilia *J. Chem. Soc., Faraday Trans.* **1993**, *89(2)*, 273.

37 W. Koh, D. Dubois, W. Kutner, M. T. Jones, K. M. Kadish *J. Phys. Chem.* **1992**, *96*, 4163.

38 C. Caron, R. Subramanian, F. D'Souza, J. Kim, W. Kutner, M. T. Jones, K. M. Kadish *J. Am. Chem. Soc.* **1993**, *115*, 8505.

39 W. K. Fullagar, I. R. Gentle, G. A. Heath, J. W. White *J. Chem. Soc., Chem. Commun.* **1993**, 525.

40 J. W. Bausch, G. K. S. Prakash, D. S. Tse, D. C. Lorents, Y. K. Bae, R. Malhorta *J. Am. Chem. Soc.* **1991**, *113*, 3205.

41 A. F. Hebard, M. J. Rosseinsky, R. C. Haddon, D. W. Murphy, S. H. Glarum, T. T. M. Palstra, A. P. Ramirez, A. R. Kortan *Nature* **1991**, *350*, 600.

42 K. Holczer, O. Klein, S.-M. Huang, R. B. Kaner, K.-J. Fu, R. L. Whetten, F. Diederich *Science* **1991**, *252*, 1154.

43 P. W. Stephens, L. Mihaly, P. L. Lee, R. L. Whetten, S.-M. Huang, R. B. Kaner, F. Diederich, K. Holczer *Nature* **1991**, 351.

44 O. Zhou, J. E. Fischer, N. Coustel, S. Kycia, Q. Zhu, A. R. McGhie, W. J. Romanov, J. P. McCauley, A. B. Smith III, D. E. Cox *Nature*, **1991**, *351*, 462.

45 S. P. Kelty, C.-C. Chen, C. M. Lieber *Nature*, **1991**, 223.

46 T. Tanigaki, T. W. Ebbesen *Nature*, **1991**, *352*. 222.

47 K. Tanigaki, I. Hirosawa, T. W. Ebbesen, J. Mizuki, Y. Shimakawa, Y. Kubo, J. S. Tsai, S. Kuroshima *Nature*, **1992**, *356*, 419.

48 J. P. McCauley Jr., Q. Zhu, N. Coustel, O. Zhou, G. Vaughan, S. H. J. Idziak, J. E. Fischer, S. W. Tozer, D. M. Groski, N. Bykovetz, C. L. Lin, A. R. McGhie, B. H. Allen, W. J. Romanow, A. M. Denenstein, A. B. Smith III *J. Am. Chem. Soc.* **1991**, *113*, 8537.

49 D. W. Murphy, M. J. Rosseinsky, R. M. Fleming, R. Tycko, A. P. Ramirez, R. C. Haddon, T. Siegrist, G. Dabbagh, J. C. Tully, R. E. Walstedt *J. Phys.Chem. Solid* **1992**, *53*, 1321.

50 Z. Iqbal, R. H. Baughman, B. L. Ramakrishna, S. Khare, N. S. Murthy, H. J. Bornemann, D. E. Morris *Science* **1991**, *254*, 826.

51 H. H. Wang, A. M. Kini, B. M. Savall, K. D. Carlson, J. M. Williams, K. R. Lykke, P. Wurz, D. H. Parker, M. J. Pellin, D. M. Gruen, U. Welp, W.-K. Kwok, S. Fleshler, G. W. Crabtree *Inorg. Chem.* **1991**, *30*, 2839.

52 H. H. Wang, A. M. Kini, B. M. Savall, K. D. Carlson, J. M. Williams, K. R. Lykke, D. H. Parker, M. J. Pellin, D. M. Gruen, U. Welp, W.-K. Kwok, S. Fleshler, G. W. Crabtree, J. E. Schriber, D. L. Overmyer *Inorg. Chem.* **1991**,

53 D. R. Buffinger, R. P. Ziebarth, V. A. Stenger, C. Recchia, C. H. Pennington *J. Am. Chem. Soc.* **1993**, *115*, 9267.

54 Y. Chabre, D. Djurado, M. Armand, W. J. Romanow, N. Coustel, J. P. McCauley, J. E. Fischer, A. B. Smith III. *J. Am. Chem. Soc.* **1992**, *114*, 764.

55 M. J. Rosseinsky, D. W. Murphy, R. M. Flemming, R. Tycko, A. P. Ramirez, T. Siegrist, G. Dabbagh, S. E. Barrett *Nature* **1992**, *356*, 416.

56 R. M. Fleming, M. J. Rosseinsky, A. P. Ramirez, D. W. Murphy, J. C. Tully, R. C. Haddon, T. Siegrist, R. Tycko, S. H. Glarum, P. Marsh, G. Dabbagh, S. M. Zahurak, A. V. Makhijy, C. Hampton *Nature* **1991**, *352*, 701.

57 J. Fink, E. Sohmen *Phys. Bl.* **1992**, *48*, 11.

58 R. M. Fleming, A. P. Ramirez, M. J. Rosseinsky, D. W. Murphy, R. C. Haddon, S. M. Zahurak, A. V. Makhija *Nature*, **1991**, *352*, 787.

59 Y. Chen, F. Stepniak, J. H. Weaver, L. P. F. Chibante, R. E. Smalley *Phys. Rev. B.* **1992**, *45*, 8845.

60 A. R. Kortan, N. Kopylov, S. Glarum, E. M. Gregory, A. P. Ramirez, R. M. Fleming, F. A. Thiel, R. C. Haddon *Nature* **1992**, *355*, 530.

61 A. R. Kortan, N. Kopylov, S. Glarum, E. M. Gregory, A. P. Ramirez, R. M. Fleming, O. Zhou, F. A. Thiel, P. L. Trevor, R. C. Haddon *Nature*, **1992**, *360*, 566.

62 G. K. Wertheim, D. N. E. Buchanan, L. E. Rowe *Chem. Phys. Lett.* **1993**, *206*, 193.

63 P. Boulas, R. Subramanian, W. Kutner, M. T. Jones, K. M. Kadish *J. Electrochem. Soc.* **1993**, *140*, L130.

64 A. Penicaud, J. Hsu, C. Reed, A. Koch, K. C. Khemani, P. -M. Allemand, F. Wudl *J. Am. Chem. Soc.* **1991**, *113*, 6699.

65 P.-M. Allemand, K. C. Khemani, A. Koch, F. Wudl, K. Holczer, S. Donovan, G. Grüner, J. D. Thompson *Science* **1991**, *253*, 301.

66 P. W. Stephens, D. Cox, J. W. Lauher, L. Mihaly, J. B. Wiley, P.-M. Allemand, A. Hirsch, K. Holczer, Q. Li, J. D. Thompson, F. Wudl *Nature* **1992**, *355*, 331.

67 G. Sparn, J. D. Thompson, P.-M. Allemand, Q. Li, F. Wudl, K. Holczer, P. W. Stephens *Solid State Commun.* **1992**, *82*, 779.

68 F. Wudl, J. D. Thompson *J. Phys. Chem. Solids* **1992**, *53*, 1449 .

69 K. Yoshizawa, T. Sato, K. Tanaka, T. Yamaba, K. Okahara *Chem. Phys. Lett.* **1993**, *213*, 498.

70 J. Stinchcombe, A. Penicaud, P. Bhyrappa, P. D. W. Boyd, C. A. Reed *J. Am. Chem. Soc.* **1993**, *115*, 5212.

71 C. Bossard, S. Rigaut, D. Astruc, M.-H. Delville, G. Felix, A. Fevrier-Bouvier, J. Amiall, S. Flandrois, P. Delhaes *J. Chem. Soc., Chem. Commun.* **1993**, 333.

72 A. Skiebe, T. Kugler, A. Hirsch, H. Klos, B. Gotschy, unpublished results.

73 K. Tanaka, A. A. Zakhidov, K. Yoshizawa, K. Okahara, T. Yamabe, K. Yakushi, K. Kikuchi, S. Susuiki, I. Ikemoto, Y. Achiba *Phys. Lett. A* **1992**, *164*, 221.

74 K. Tanaka, A. A. Zakhidov, K. Yoshizawa, K. Okahara, T. Yamabe, K. Yakushi, K. Kikuchi, S. Susuiki, I. Ikemoto, Y. Achiba *Phys. Rev.* **1993**, *B 47*, 7554.

75 R. Seshadri, A. Rastogi, S. V. Bhat, S. Ramasesha, C. N. R. Rao *Solid. State Commun.* **1993**, *85*, 971.

Chapter 3 Nucleophilic Additions

3.1 Introduction

3.2 Addition of Carbon Nucleophiles
3.2.1 Hydroalkylation and Hydroarylation of C_{60} and C_{70}
3.2.2 Langmuir–Blodgett Films of C_{60}H*t*-Bu
3.2.3 Addition of Macromolecular Carbanions - Fullerene Polymers
3.2.4 Cyclopropanation of C_{60} and C_{70}

3.3 Addition of Amines

3.4 Addition of Hydroxide

References

3.1 Introduction

The reduction experiments performed chemically and electrochemically (Chapter 2) clearly show that C_{60} is a fairly electronegative system. Calculations as well as structure data demonstrate bond alternation with the long bonds at the junctions of five membered and six membered rings (5-6 bonds), and shorter bonds with double bond character at the junctions of two six membered rings (6-6 bonds). These electronic and geometric properties imply that C_{60} behaves like an electron poor conjugated polyolefin, consisting of fused [5]radialene and cyclohexatriene units, rather than a "superarene". A characteristic reaction of an electron poor olefin is the addition of nucleophiles. Indeed, C_{60} undergoes a variety of nucleophilic additions with carbon, nitrogen and oxygen nucleophiles. However, unique for C_{60} and other fullerenes is their spherical polyolefinic structure with the resulting multitude of possible reaction products. One of the major challenges of fullerene chemistry is to control, and at the same time take advantage of, its polyfunctionality by the specific synthesis and isolation of fullerene derivatives as single regioisomers.

3.2 Addition of Carbon Nucleophiles

3.2.1 Hydroalkylation and Hydroarylation of C_{60} and C_{70}

C_{60} readily reacts with organolithium and Grignard compounds to form the anions RC_{60}^- as primary intermediates[1,2,3,4]. This process is very fast. If the reactions are carried out in toluene the corresponding salts $C_{60}R_nM_n$ precipitate instantaneously upon the addition of the organometallic compound. Their protonation yields the hydrofullerene derivatives $C_{60}H_nR_n$. Highly alkylated anions $R_nC_{60}^{n-}$, being soluble in THF, have been also quenched with MeI to form $C_{60}Me_nR_n$[1]. In order to obtain optimum yields of the isomerically pure monoadducts, $C_{60}HR$, which are 1,2-organodihydrofullerenes-60, the addition of the nucleophile was carried out stepwise (titration)[2,3]. After each step, a sample of the homogeneously suspended reaction mixture was protonated for quantitative HPLC analysis. In this way the formation of the products and the consumption of C_{60} could be followed closely from the peak areas. The titration was stopped at the point after which the amount of monoadducts would decrease again, due to the formation of the higher addition products. After titration, the reaction mixture was quenched with 0.01 M hydrogen chloride in methanol [Scheme 3.1; Scheme 3.2].

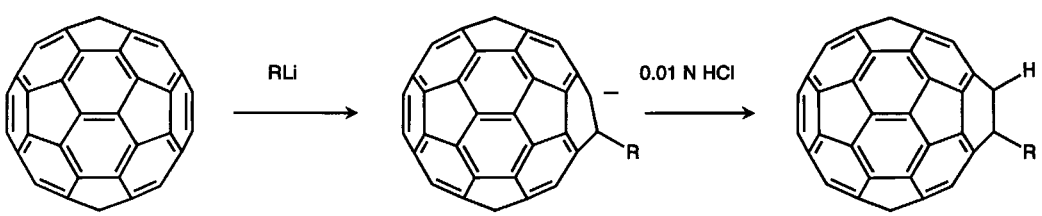

Scheme 3.1

Using organolithium compounds as nucleophiles, 1.2 equiv. were needed to obtain the maximum yield, whereas reactions with the milder Grignard reagents necessitated a 5 to 27-fold excess [Table 3.1]. The purification of the 1,2-organodihydrofullerenes can either be done by preparative HPLC (C_{18}, $CHCl_3$ /CH_3CN, 60:40) or by flash chromatography with mixtures of hexane and toluene.

Scheme 3.2

Table 3.1 Yields of 1-organo-1,2-dihydrofullerenes-60 after titration

R	RM	Equiv. of nucleophiles used	Yield (%)
Me	RLi	1.2	47
t-Bu	RLi	1.2	51
Et	RMgBr	6.8	80
i-Pr	RMgBr	8.1	56
$Me(CH_2)_7$	RMgBr	5.0	67
	RMgBr	26.8	63
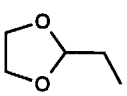	RMgBr	11.9	52
Ph	RMgBr	9.2	74

Fagan et al.[4] isolated the anionic intermediate *t*-$BuC_{60}^-Li^+ \cdot 4CH_3CN$ by allowing stoichiometric amounts of 1.2 M *tert*-butyllithium to react with C_{60} in benzene and recrystallizing the brown crude product from acetonitrile. The ^{13}C-NMR spectrum of the green compound shows the pattern of a C_{60} derivative with C_s-symmetry. Temperature dependent ^1H NMR investigations indicate a hindered rotation of the *tert*-butyl group with $\Delta G^{\ddagger} = 9.3$ kcal/mol. Hindered rotation has also been observed in the radical *t*-BuC_{60}[5]. The NMR experiments are consistent with the calculation of the charge densities in the anions RC_{60}^- (R = H, Me, *t*-Bu) [Fig. 3.1][2]. The negative charge is not delocalized. The highest electron density is found on C-2 next to the sp^3 carbon atom across the 6–6 bond. A significantly lower but still enhanced electron density comes out for C-4 and C-11.

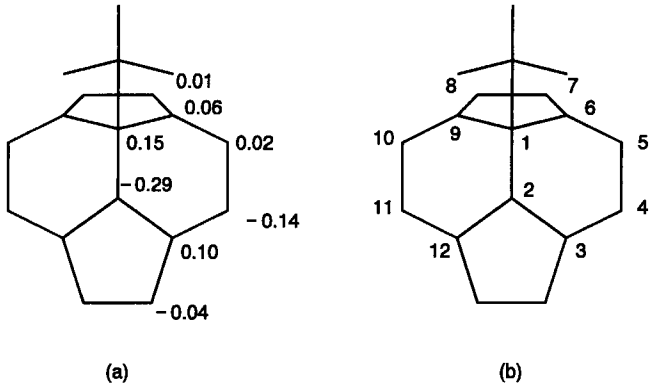

Figure 3.1 Electron densities (Mulliken charges) of the affected pyracylene unit of the intermediate *t*-BuC_{60}^- obtained from AM1 calculations (a) and numbering of the carbon atoms (b).

These electron density considerations imply a preferential proton attack on position 2, which indeed was observed in the experiments. Whereas after the in situ protonation of the intermediates RC_{60}^-, only the 1,2-derivatives could be detected after chromatographic purification[2], the protonation of *t*-BuC_{60}^- Li^+4CH_3CN afforded the 1,2- as well as the 1,4-isomer[4]. The 1,4-isomer, however, is unstable and after ca. 12 h at 25 °C, rearranges to the 1,2-derivative. The anion *t*-BuC_{60}^- can be oxidized with iodine to give the radical *t*-BuC_{60} [Scheme 3.3][4], which was proposed to dimerize at C-4[6]. Out of this radical species, 1,2-$C_{60}H$*t*-Bu can be obtained by treatment with Bu_3SnH upon rearrangement of the initially formed 1,4-$C_{60}H$*t*-Bu[4]. Whereas the anions RC_{60}^- are stable only under inert conditions, solutions of the protonated 1,2-dihydrofullerenes $C_{60}HR$ do not decompose in non-polar solvents in air.

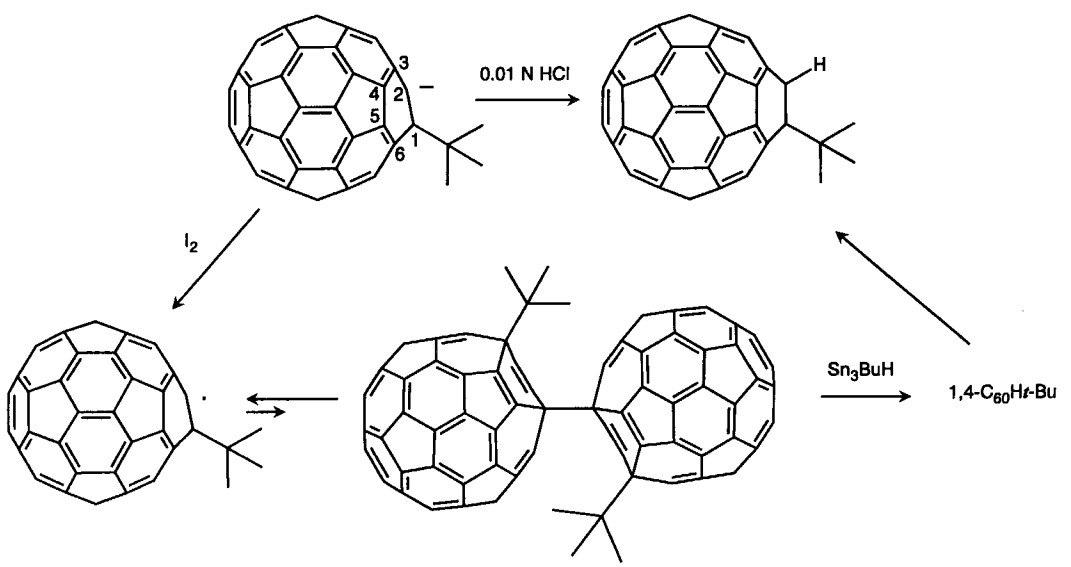

Scheme 3.3

All the expected 32 resonances of the fullerene carbon atoms of the 1-organo-1,2-dihydrofullerenes-60, with four of them half the intensity of the others, were observed in the ^{13}C-NMR spectra, proving the C_s-symmetry[3,4]. This experimental finding is corroborated by AM1 calculations for $C_{60}HR$ (R = H, Me, *t*-Bu) which show the 1,2-isomers as having the lowest heat of formation [Tab 3.2][2]. The formation of other regioisomers, such as the 1,4- or the 1,6-isomers would require the introduction of at least one double bond at the junction of a five membered and six membered ring, which is energetically unfavorable for the fullerene framework[2,7,8]. An enhanced formation of an 1,4-isomer is expected to occur upon an increased steric requirement of the ligands bound to C_{60}, for example, on going from H to *t*-Bu[7,8]. The regioselectivity of these two step additions is closer to that of an electron deficient alkene than to an aromatic system.

Table 3.2 Calculated energies (AM1 heats of formation) in kcal/mol of the 1,6- and 1,2-isomers of $C_{60}H$*t*-Bu, $C_{60}HMe$ and $C_{60}H_2$

	$C_{60}H$*t*-Bu	$C_{60}HMe$	$C_{60}H_2$
1,6-adduct	940.2	947.7	950.0
1,2-adduct	922.1	929.2	931.2

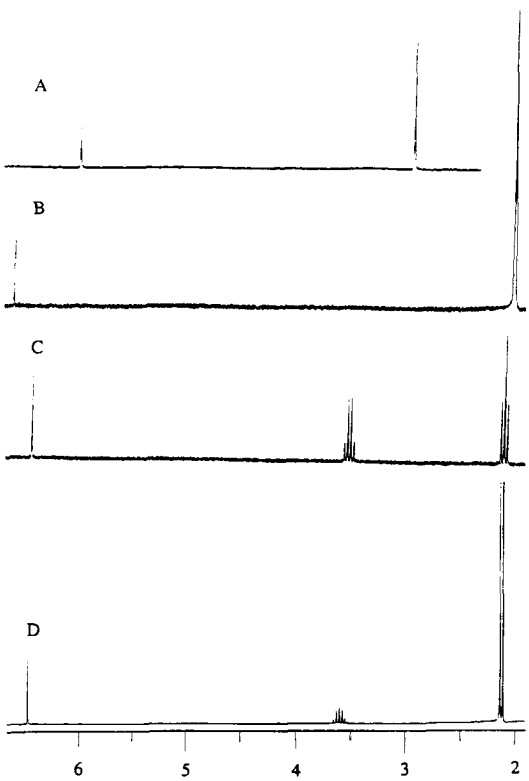

Figure 3.2 ^{1}H NMR spectra of $C_{60}HMe$ (A), $C_{60}H$*t*-Bu (B), $C_{60}HEt$ (C) and $C_{60}H$*i*-Pr (D)[3].

Distinct signals for the fullerenyl protons in the ^1H NMR spectra of $C_{60}HR$ appear at low field between $\delta = 6-7$, which is a further direct proof for the electron withdrawing influence of the fullerene sphere [Fig. 3.2][3]. The chemical shift of the fullerenyl proton also depends on the nature of R. Increased steric requirements, for example, on going from $C_{60}HMe$ to $C_{60}H$*t*-Bu, cause a further down field shift of about 0.7 ppm. These downfield positions already imply a pronounced acidity of the fullerenyl protons. Indeed, the protonation of the *t*-BuC_{60}^- anion, monitored quantitatively by electrochemical methods allowed the determination of the pK_a to be 5.7 (±0.1)[4]. Therefore, $C_{60}H$*t*-Bu is one of the strongest acids consisting exclusively of carbon and hydrogen.

The UV/Vis spectra [Fig. 3.3] of the chestnut brown solutions of the monoadducts $C_{60}HR$, particularly the intensive bands at $\lambda_{max} = 213$, 257 and 326 nm are close to those of C_{60} demonstrating their electronic similarity[3]. The biggest changes in the spectra compared to C_{60} appear in the visible region. The typical features of C_{60} between λ = 400 and 700 nm are lost, and a new and very characteristic band at λ_{max} = 435 nm appears which is independent of the nature of R. Also the electrochemical properties of $C_{60}HR$ are comparable to those of C_{60}[4,9]. The first three reversible reduction waves shift about 100 mV to more negative potentials. Therefore, the fullerene core in these monoadducts still exhibits remarkable electron acceptor properties, which is one reason for almost identical chemical reactivity compared to C_{60}.

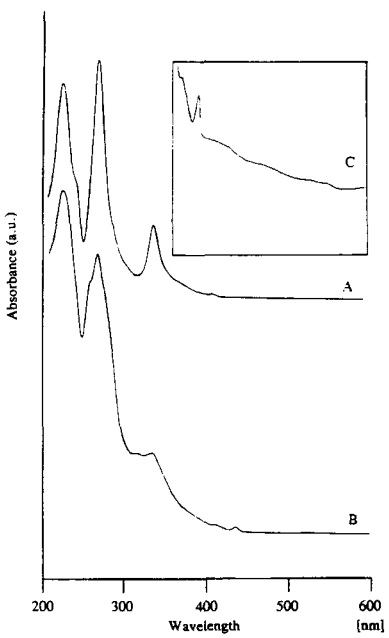

Figure 3.3 Comparative UV/Vis spectra (hexane) of fullerene-60 (A) and $C_{60}H$*t*-Bu (B); the inset is the 400 – 700 nm region of $C_{60}H$*t*-Bu[3].

Product predictions for nucleophilic additions to C_{70}, based on AM1 calculations, show that among the large number of possible isomers a few are energetically favored[10]. Two areas within the molecule can be distinguished, which are the inert belt at the equator and the more reactive C_{60} like double

bonds at the poles [Fig. 3.4]. Experimentally, hydroalkylation and hydroarylation reactions of C_{70} under quantitative HPLC control [Scheme 3.4] yield predominantly one isomer of each $C_{70}HR$[3].

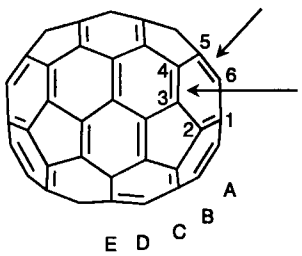

Figure 3.4 Schematic representation of C_{70} with the indication of the two types of reactive double bonds, the numbering and the five different sets of C-atoms.

$$C_{70} + R^- \longrightarrow RC_{70}^- \longrightarrow C_{70}HR \quad (R = Me, Ph)$$

(predominantly 1,2-addition)

Scheme 3.4

The ^{13}C NMR spectra of $C_{70}HR$ exhibit 37 resonances of the fullerene carbons with two of them in the sp^3 region, proving C_s-symmetry for the $C_{70}HR$ adducts. This is consistent with an addition to a double bond of a pole corannulene unit (1,2-addition), leading to 1,2-dihydrofullerene-70 derivatives. These particular 6-6 bonds of C_{70}, being located between the carbons of the sets A and B, have almost the same bond length as the 6-6 bonds in C_{60}[11] and the pole corannulene unit also exhibits bond alternation with longer 5-6 bonds. ^1H NMR data imply that the initial attack of the nucleophile occurred at C-1 and protonation at C-2 [Fig. 3.5].

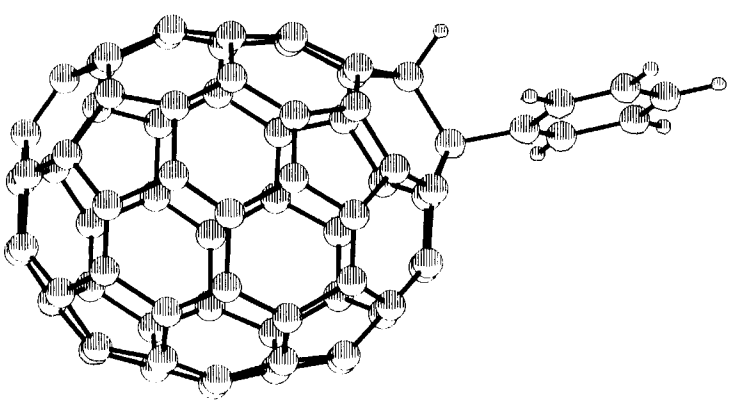

Figure 3.5 Computer model of 1-Phenyl-1,2-dihydrofullerene-70.

3.2.2 Langmuir-Blodgett Films of C_{60}H*t*-Bu

With the dihydrofullerene derivative C_{60}H*t*-Bu the formation of condensed layers at the air/water interface has been achieved by spreading benzene solutions of the fullerene across the expanded water surface area, allowing the benzene to evaporate and compressing the floating film at a speed of $\approx 1.0 \times 10^{-2}$ $nm^2mol^{-1}s^{-1}$ [12,13]. During the latter process, the isotherm of the compression was recorded. High quality Langmuir-Blodgett films can be built up onto a variety of solid substrates, with deposition rates of 0.95 ± 0.05 and a overall film thickness of up to 200 nm [Fig. 3.6].

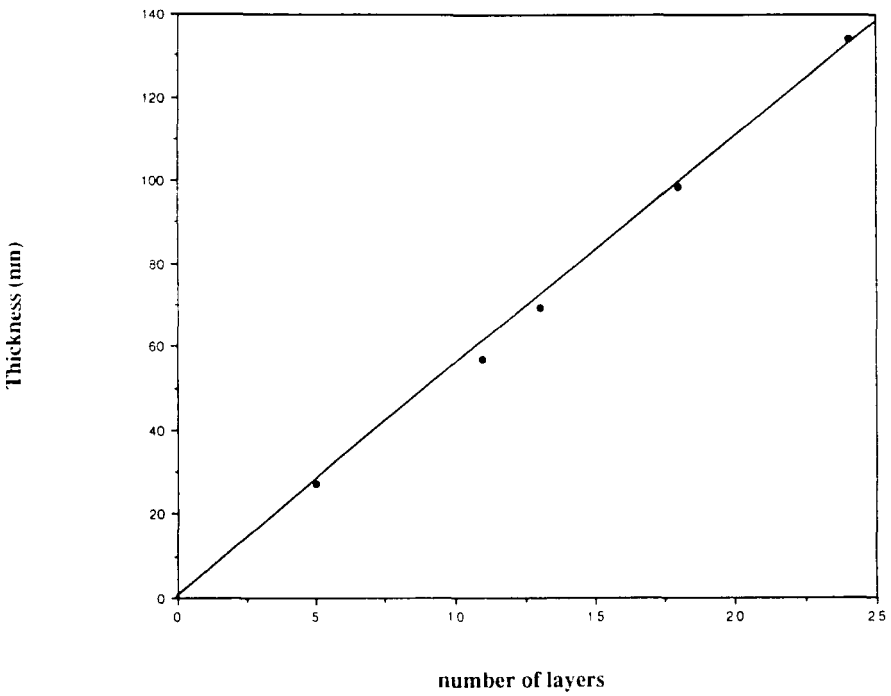

Figure 3.6 *Variation of the LB film thickness of C_{60}H*t*-Bu, monitored periodically during deposition process, vs. the number of LB layers. The average thickness per layer is 5.56 nm*[12].

The film thickness was determined by elipsometry. Electrical measurements, perpendicular to the film plane were made and a d.c. conductivity value of the order of 10^{-10} S cm^{-1} was established for undoped films. LB films of the parent C_{60} exhibit a much poorer quality[14] and the deposition onto substrates often requires a mixing of C_{60} with long-chain fatty acids. Obviously the *tert*-butyl group of C_{60}H*t*-Bu plays an important role in the self assembly and alignment of the fullerene molecules.

Using sufficiently diluted spreading solutions, monolayers of C_{60}H*t*-Bu on the water surface can also be prepared [Fig. 3.7]. Furthermore, these monolayers have been deposited on a variety of substrates including ITO electrodes. The corresponding LB films undergo well defined multistage electrochemical reductions to yield the trianion species. The first two reduction steps are completely reversible.

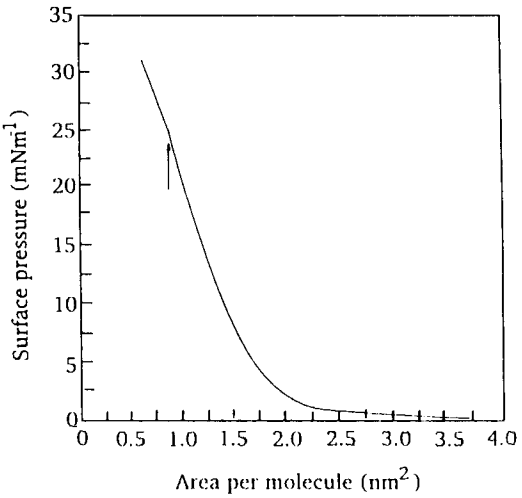

Figure 3.7 Surface area per molecule in nm^2 *vs.* surface pressure for a monomolecular film of C_{60}Ht-Bu on a water surface[12].

3.2.3 Addition of Macromolecular Carbanions - Fullerene Polymers

The affinity of C_{60} towards carbon nucleophiles has been used to synthesize polymer bound C_{60} (flagellenes)[15] as well as surface bound C_{60}[16]. Polymers involving C_{60} are of considerable interest for the following reasons: (i) the fullerene properties can be combined with those of specific polymers, (ii) suitable fullerene polymers should be spin-coatable, solvent-castable or melt-extrudable and (iii) fullerene containing polymers as well as surface-bound C_{60} layers are expected to have remarkable electronic, optical or catalytic properties. Three prototypes of polymers or solids containing the covalently bound C_{60} moiety are possible [Fig. 3.8][17]: fullerene pendant systems **Ia** with C_{60} on the side chain of a polymer ("charm bracelet"[18]) or on the surface of a solid **Ib**, dendritic systems **II** and in-chain polymers **III** ("pearl necklace"[18]) with the fullerene as a part of the main chain. In the latter case, one-, two- and three-dimensional variants can be considered. In addition, combinations of all of these types are possible.

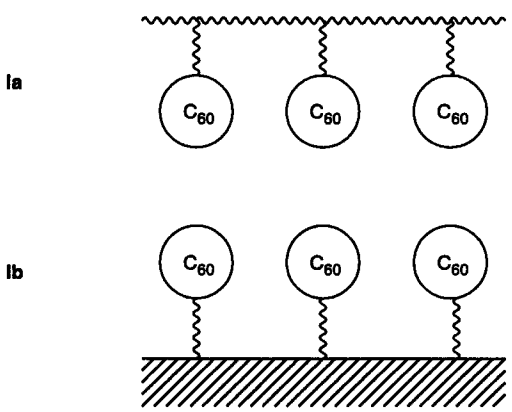

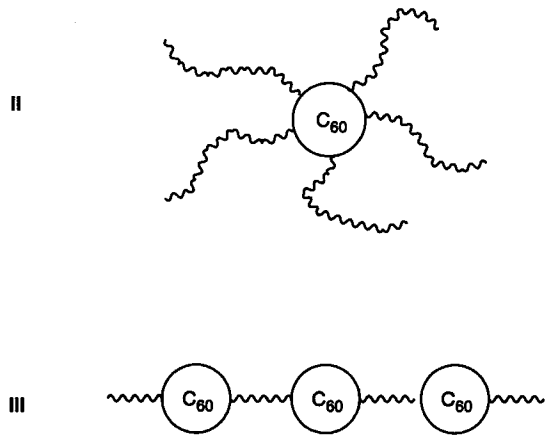

Figure 3.8 The three prototypes of polymers involving the C_{60} moiety. Pendant on-chain (**Ia**), pendant-on surface (**Ib**), dendritic (**II**) and in-chain (**III**)[17].

The addition of living polystyrene to C_{60} leads to the formation of the "flagellanes" which are dendritic systems [Scheme 3.5][15]. These polymers are highly soluble, are melt processable and give rise to nano-phase separated solids.

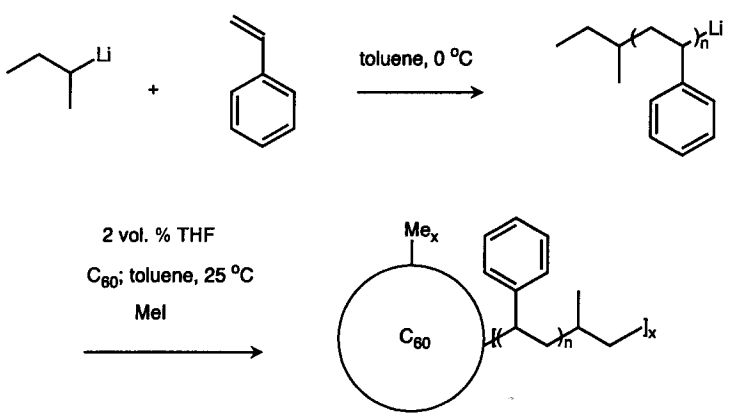

Scheme 3.5

A similar approach was used in grafting C_{60} onto a pregenerated lithiated polyethylene surface [Scheme 3.6][16]. A polyethylene film with terminal diphenylmethyl groups was deprotonated with BuLi to yield an anionic polyethylene surface which was treated with C_{60} and quenched with methanol. The C_{60} incorporation at the polyethylene surface was determined by XPS, UV/Vis and fluorescence spectroscopy.

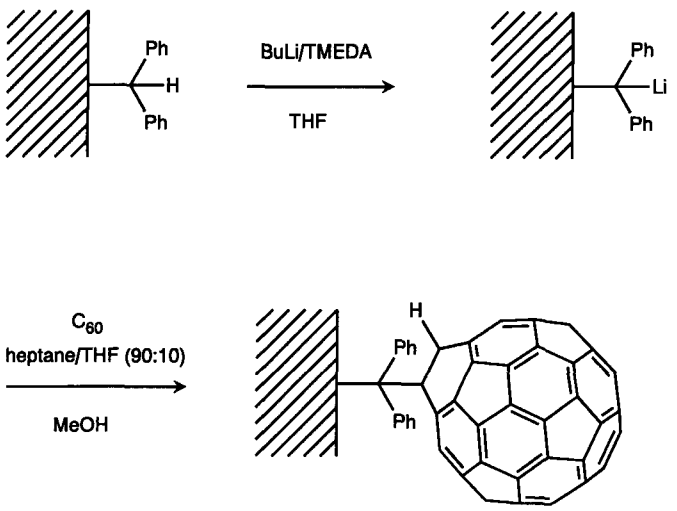

Scheme 3.6

3.2.4 Cyclopropanation of C_{60} and C_{70}

The stabilization of reaction intermediates RC_{60}^- and RC_{70}^- to form dihydrofullerene derivatives can also be achieved by intramolecular nucleophilic substitutions (S_Ni), if R contains a leaving group. As shown by Bingel[19], the generation of a carbon nucleophile by deprotonation of α-halo esters or α-halo ketones leads to a clean cyclopropanation of C_{60}. The cyclopropanation of C_{60} with diethyl bromomalonate in toluene with NaH as auxiliary base proceeds smoothly at room temperature [Scheme 3.7]. By-products are unreacted C_{60} and higher adducts. The monoadduct can be isolated easily from the reaction mixture by column chromatography.

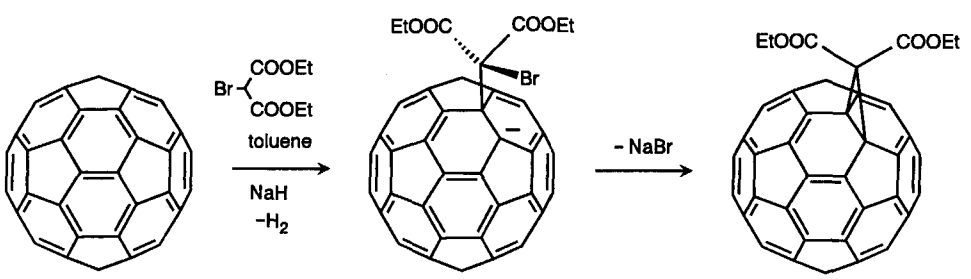

Scheme 3.7

The cyclopropanation of C_{60} with methyl 2-chloroacetylacetate, ω-bromoacetophenone and desyl chloride proceeds similarly[19]. In these cases, the deprotonation to the stabilized carbanions is accomplished with 1,8-diazabicyclo[5.4.0]undec-7-ene (DBU) as auxiliary base.

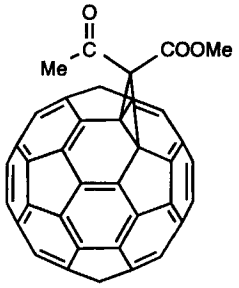

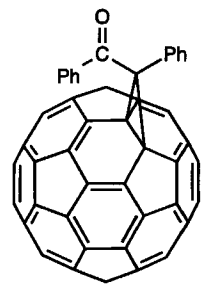

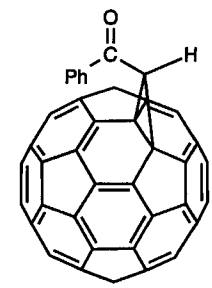

^{1}H- and ^{13}C NMR investigations demonstrate that the nucleophilic additions followed by S_Ni reactions proceed at a 6-6 double bond of the fullerene core. The chemical shifts in the ^{13}C NMR spectra of C-1 and C-2 (66-76 ppm) in all of these methano-1,2-dihydrofullerenes-60 prove the cyclopropane structure. The cyclopropanation of C_{70} with diethyl bromomalonate in the presence of DBU yields predominantly one monoadduct[19] [Scheme 3.8]. As in the case of the acyclic 1-organo-1,2-dihydrofullerenes-70[3], the most C_{60} like 6-6 bond at the pole is attacked by the nucleophile leading to 1,2-[di(ethoxycarbonyl)methano]-1,2-dihydrofullerene-70[19].

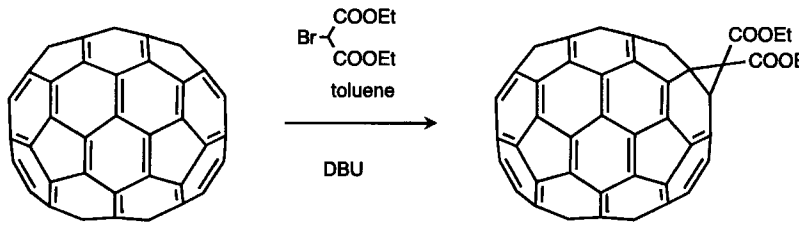

Scheme 3.8

Saponification of such di(ethoxycarbonyl)methylene adducts of C_{60} is achieved by treatment with NaH in toluene at elevated temperatures and subsequent quenching with methanol[20] [Scheme 3.9]. This method provides an easy access to defined water soluble fullerenes and can also be applied for higher di(ethoxycarbonyl)methylene adducts (bis, tris etc.). These malonic acid derivatives of C_{60} are very soluble in polar solvents for example acetone, THF or aqueous base, but insoluble in aqueous acids.

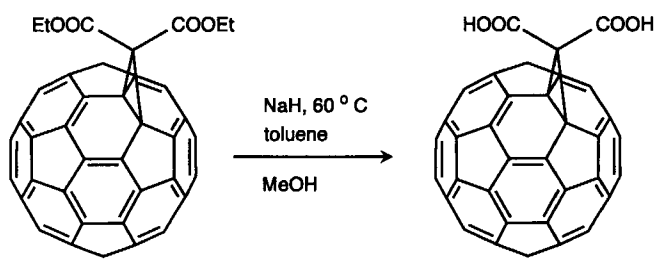

Scheme 3.9

The bis[di(ethoxycarbonyl)methano]tetrahydrofullerenes-60 ($C_{62}(COOEt)_4$) can be synthesized from the monoadducts using identical experimental conditions [Scheme 3.10]. Presuming that the addition takes place exclusively at the 6-6 ring double bonds and the addition to each double bond is symmetrical, 8 regioisomeric bisadducts are possible. This requirement is fulfilled by this cyclopropanation reaction[19], making it an ideal candidate for the investigation of the regiochemistry of C_{60}. The seven stable out of the eight possible regioisomers of $C_{62}(COOEt)_4$ were isolated from the reaction mixture by high performance liquid chromatography (HPLC)[21].

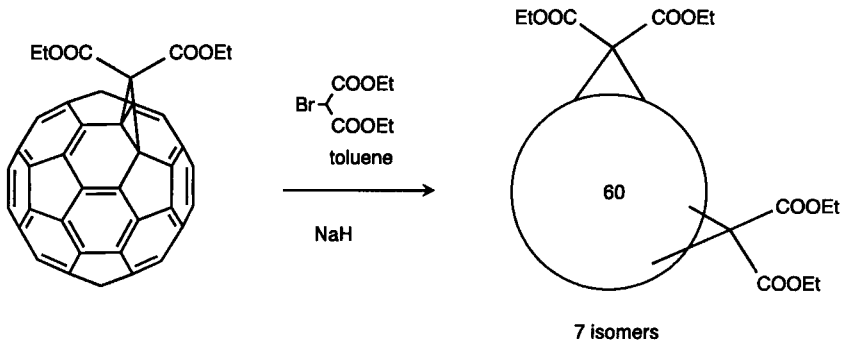

Scheme 3.10

Relative to a given position (6-6 ring bond) in C_{60}, a second addition to a 6-6 ring bond can take place in three areas of the molecule, namely in the same hemisphere (*cis*) at the equator (*e*) or in the opposite hemisphere (*trans*) [Fig. 3.9]. The three-dimensional relationship between two 6-6 bonds can be *cis*, *e* or *trans* and the *cis* and *trans* cases are further subdivided into *cis*-1, *cis*-2, *cis*-3 as well as *trans*-1, *trans*-2, *trans*-3 and *trans*-4. The three bisadducts in which the attacked 6-6 bonds are in *cis*-3, *trans*-2 and *trans*-3 positions [Fig. 3.9] are C_2-symmetric and therefore chiral. These regioisomers of bis[di(ethoxycarbonyl)methano]tetrahydrofullerene-60 ($C_{62}(COOEt)_4$) were isolated as pairs of enantiomers using achiral stationary phases (HPLC)[21]. According to theoretical calculations (AM1), the *cis*-1 isomer is considerably destabilized with respect to the others [Tab. 3.3][21]. This is mainly due to steric repulsion of the methano addents which would be located next to each other. Indeed, this regioisomer was not found in the reaction mixture. The other seven isomers of $C_{62}(COOEt)_4$ could be identified by NMR spectroscopy (symmetry) as well as on the basis of their elution order during HPLC separation (silica gel), which is in line with the calculated AM1-dipole moments of the different regioisomers [Tab. 3.3]. The formation of the bisadducts $C_{62}(COOEt)_4$ shows a remarkable regioselectivity [Tab. 3.3; Fig. 3.10, 3.11]. The *e* as well as the *trans*-3 isomers are significantly preferred. The *cis*- and the *trans*-1 adducts of $C_{62}(COOEt)_4$ in general are less abundant in the reaction mixture compared to the other isomers. It is very likely that not only thermodynamic but also kinetic factors govern the product distribution, since the heats of formation especially of the *e* and *trans* isomers seem to be very similar [Tab. 3.3]. Responsible for the low yield of the D_{2h}-symmetric *trans*-1 isomer is also the reduced statistical probability of its formation.

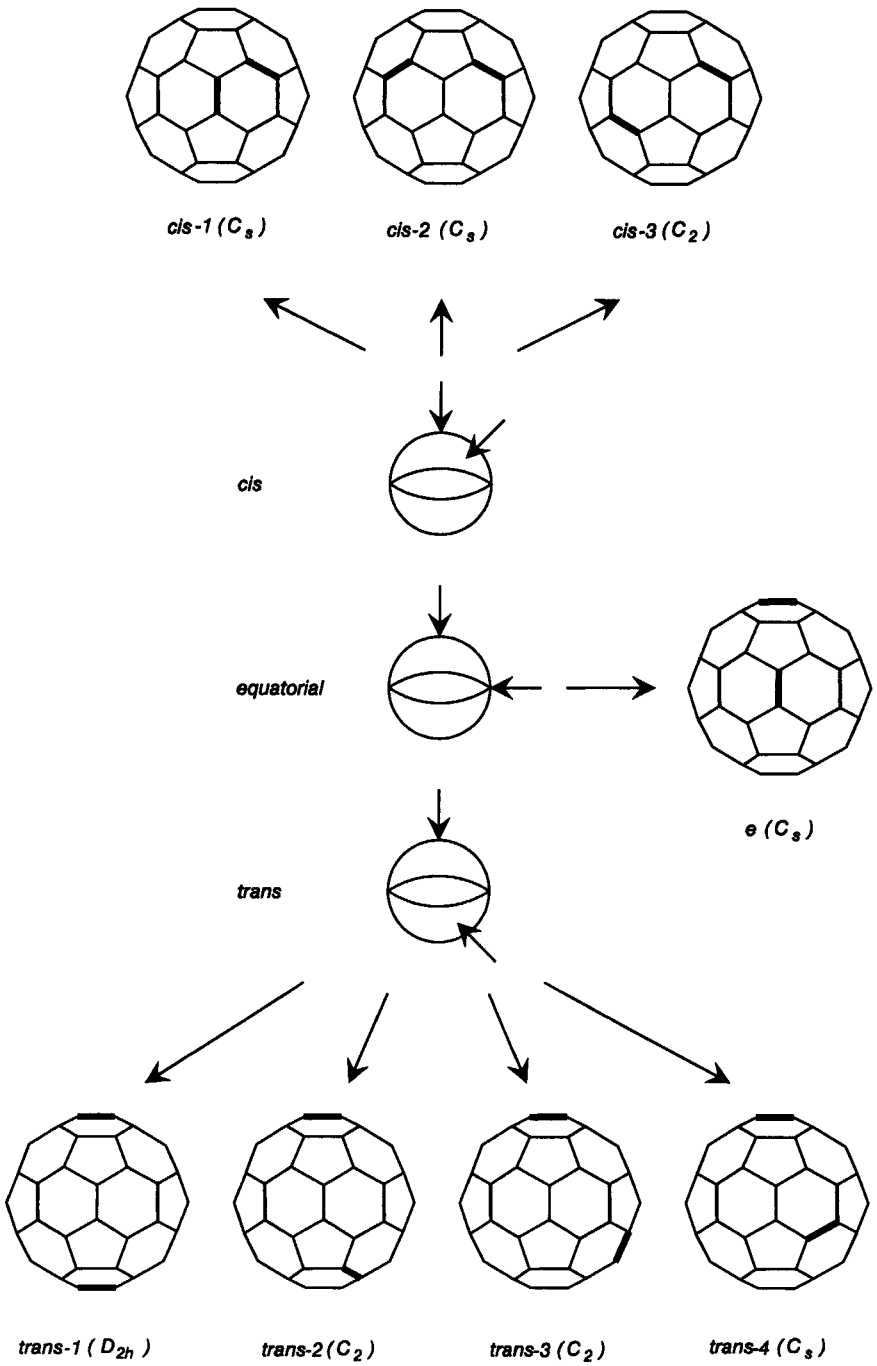

Figure 3.9 Positions of the ligand-carrying bonds in the 8 possible regioisomers of C_{60} with symmetrical additions to 6-6 bonds and symmetry of the corresponding isomers.

Whereas starting from a given monoadduct the attack of only one 6-6 bond leads to a *trans*-1 bisadduct, each of the other regioisomers is formed by attack of any of four bonds. The regioisomers of $C_{62}(COOEt)_4$ have slightly different colors ranging from chestnut brown to red-orange. This is reflected by their electronic absorption spectra. Each regioisomer exhibits a characteristic feature in the visible part with the main absorptions at 430 and 470 nm. The relative intensity, the splitting and the width of these absorptions differ from isomer to isomer. Except for the most symmetrical *trans*-1 isomer, the bisadducts $C_{62}(COOEt)_4$ are very soluble in organic solvents like chloroform or dichloromethane.

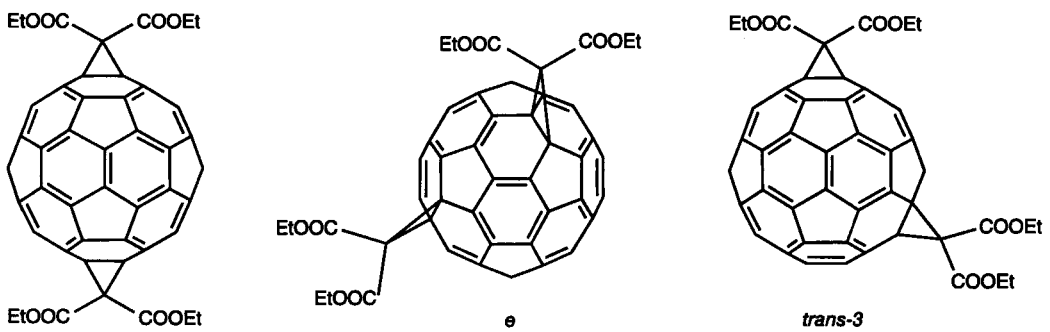

Figure 3.10 Front view representations of the most symmetric and least soluble *trans*-1 isomer as well as of the most abundant *e* and *trans*-3 isomers of $C_{62}(COOEt)_2$ formed by cyclopropanation of $C_{61}(COOEt)_2$

Table. 3.3 Symmetry, order of elution, relative yield, calculated stabilities and dipole moments of the different regioisomers of $C_{62}(COOEt)_2$ formed by cyclopropanation of $C_{61}(COOEt)_2$

Symmetry	Order of Elution	Relative yield (%)	Relative AM1 ΔH_f^0 (kcal/mol)	AM1- Dipole moment (Debye)
trans-1	1	2	0.2	0.1
trans-2	2	13	0.2	1.2
trans-3	3	30	0.1	2.0
trans-4	4	9	0.0	2.3
e	5	38	0.0	2.6
cis-3	6	6	1.3	3.0
cis-2	7	2	1.8	3.5
cis-1	8	0	17.7	3.8

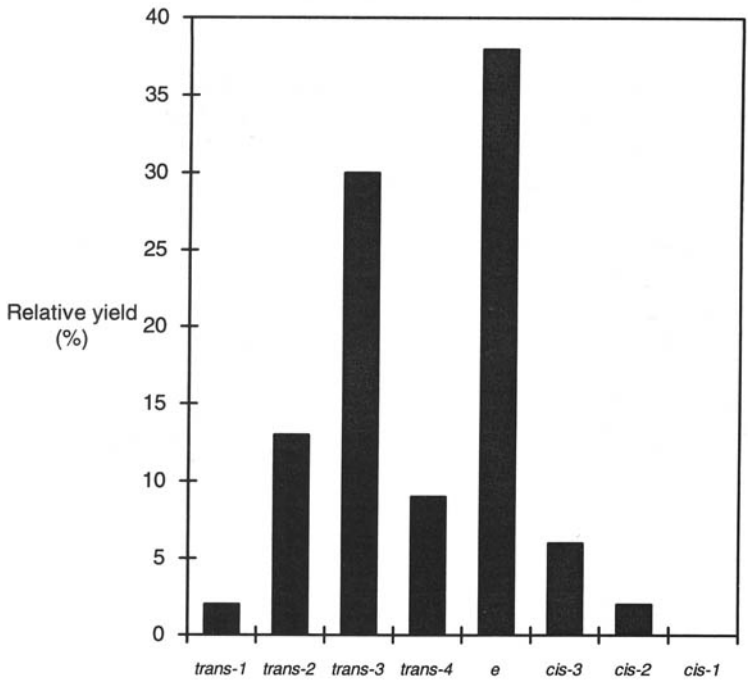

Figure 3.11 Relative yields of the eight regioisomers of $C_{62}(COOEt)_4$ obtained by cyclopropanation of $C_{61}(COOEt)_2$.

To study the regiochemistry of the trisadducts (46 possible isomers) and isolate single isomers in reasonable yields, defined bisadducts of bis[di(ethoxycarbonyl)methano]tetrahydrofullerene-60 have been used as starting materials and treated with diethyl bromomalonate in toluene in the presence of NaH to give tris[di(ethoxycarbonyl)methano]hexahydrofullerenes-60 $(C_{63}(COOEt)_6)$[21]. Some trisadducts, for example the regioisomers with all ligands in the *e* position (trisadduct *e,e,e*) to each other, are only accessible out of one particular bisadduct (bisadduct *e* with the ligands in *e* positions). Others can be formed out of two different bisadducts, such as the trisadduct *trans*-4,*trans*-4,*trans*-2 from the bisadducts *trans*-4 and *trans*-2, or out of three different bisadducts such as *e,trans*-4,*trans*-3 out of *e*, *trans*-4 and *trans*-3. These considerations are useful in identifying the trisadducts by their formation pathway as well as by their symmetry, determined by NMR spectroscopy. All the trisadducts with three identical positional relations, for example *e,e,e,* have a threefold symmetry (D_3, C_3 or C_{3v}), those with two different relations, for example *trans*-4,*trans*-4,*trans*-2, have a twofold symmetry (C_2 or C_s) and those with three different relations, for example *e,trans*-4,*trans*-3, are unsymmetric (C_1). The number of possible regioisomers that can be expected from the cyclopropanation of a certain bisadduct depends on the structure of the bisadduct. For example, 14 regioisomeric trisadducts can in principle be formed if an addition reaction with *e*-$C_{62}(COOEt)_4$ is carried out. However, the number of preferably formed trisadducts can be expected to be much lower, because trisadducts with addents bound in *cis* especially *cis*-1 positions will be considerably destabilized. In the higher adducts (tetra, penta, hexa etc.), the number of preferably formed isomers will further decrease, since many of the possible regioisomers would have the addents bound in *cis* positions. For example, among the 43

possible structures for the hexaadduct $C_{66}(COOEt)_{12}$ without containing unfavorable *cis*-1 positions, one regioisomer with T_h symmetry and all addents in *e* positions ("octahedral sites") is significantly more stable than all the others. The calculated heat of formation of the next most stable isomer is 5 kcal/mol higher[22]. Indeed, the cyclopropanation of $C_{62}(COOEt)_4$ shows a remarkable regioselectivity. The chiral orange-red colored chiral C_3-symmetric *e,e,e*-isomer of $C_{63}(COOEt)_6$ was isolated in 40% yield [Scheme 3.11][21]. In this regioisomer, the addents are bound in "octahedral sites" of the C_{60} molecule and occupy one trigon of the trigonal antiprism (octahedron).

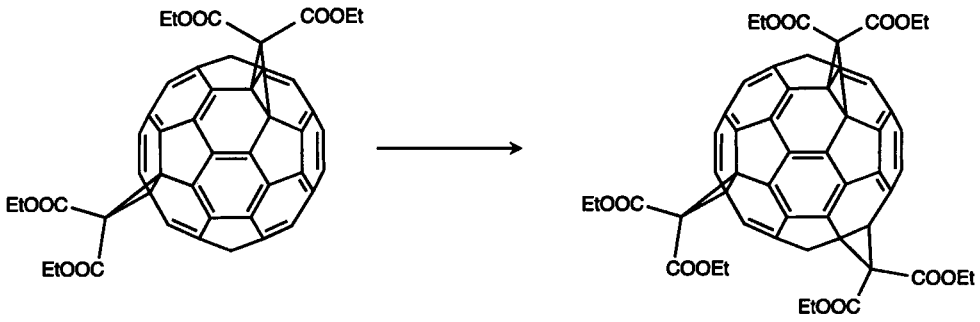

Scheme 3.11

In a similarly pronounced regioselectivity, the D_3-symmetric *trans*-3,*trans*-3,*trans*-3 isomer can be obtained from the corresponding *trans*-3-$C_{62}(COOEt)_4$[21]. In this compound, which is also chiral, the addents are bound in a zigzag fashion at an equatorial belt around the C_3-axis of symmetry. The structural characterization of these highly symmetric adducts can be achieved by NMR spectroscopy. For example, the ^{13}C NMR spectrum of *trans*-3,*trans*-3,*trans*-3- $C_{63}(COOEt)_6$ shows only 10 signals for the fullerene C-atoms[21].

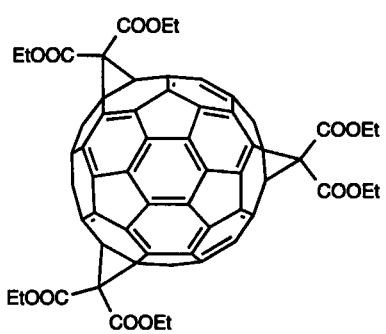

In analogy to the formation of the bisadducts, preferred additions to *e* and *trans-3* positions relative to addents already bound to C_{60} are observed. The addition to other regioisomers of $C_{62}(COOEt)_4$ also proceeds preferably in an *e* or *trans-3* mode. This regioselectivity can be used to systematically synthesize the T_h-symmetric hexaadduct by stepwise additions to "octahedral sites" (*e*-additions) starting from *trans*-1- or *e*-$C_{62}(COOEt)_4$.

3.3 Addition of Amines

Due to their high nucleophilicity, primary and secondary aliphatic amines undergo nucleophilic additions with the electron deficient C_{60}[1,23,24,25]. Treating solid C_{60} with neat amines, for example, with propylamine or ethylenediamine, leads to the formation of green solutions (fast process) which eventually turn chestnut brown (slow process)[1]. Following these reactions by ESR spectroscopy shows increasing signals. The signals of C_{60} radicals as well as multiplets of the ammonium radicals are detectable in the spectra[25]. After several hours the signal intensity decreases again. The brown reaction products are diamagnetic. The green color of the intermediates is typical for anion complexes of C_{60}[4,25]. These observations demonstrate a stepwise mechanism [Scheme 3.12] of these amino additions. First, a single electron transfer from the amine to the C_{60} occurs. The next step is the radical recombination of the positively charged amino radical and the C_{60} monoanion radical which gives rise to the green intermediates. A proton transfer from the nitrogen to C_{60} finally leads to the neutral addition products. The dynamic behavior as well as the position of the proton in these amino adducts is not yet conclusively proven.

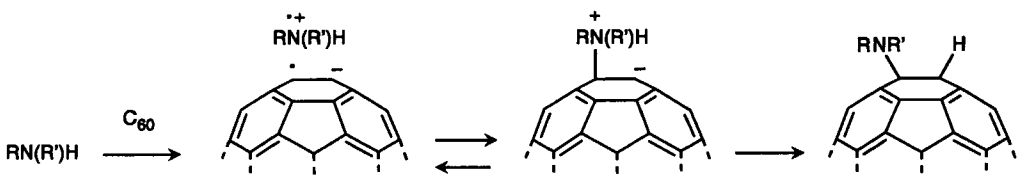

Scheme 3.12

The first step can be frozen out, if a tertiary amine is used which due to steric reasons is unable to add to C_{60} and to transfer protons. This is valid for the tertiary amine tetrakisdimethylaminoethylene (TDAE). Upon electron transfer the C_{60} radical monoanion salt C_{60}[TDAE][26] is formed (Chapter 2). The second step, the formation of the zwitterion, was directly observed by using the less hindered DBU (1,8-diazabicyclo[5.4.0]undec-7-ene) and isolating the green diamagnetic zwitterion complex C_{60}DBU[25] [Scheme 3.13] by precipitation in benzene. In solution, this complex stays in equilibrium with the dissociated C_{60}^- and DBU^+ radicals.

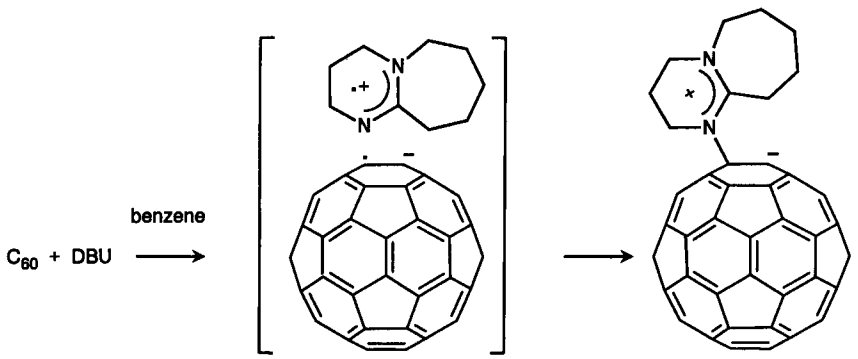

Scheme 3.13

The adducts of primary and secondary amines obtained by this method contain several amino groups attached to the fullerene core. Up to twelve propylamino groups on C_{60} were detected by mass spectrometry for $C_{60}(C_3H_9N)_n$. The product of excess ethylenediamine addition is water soluble. A more uniform adduct was obtained by the reaction of C_{60} with neat morpholine[23]. Whereas most of the amino adducts are soluble in the neat amine, the morpholine adduct precipitates as $C_{60}(morph)_6$. The addition of amines can also be done from benzene or toluene solutions[24,27]. It was reported that the amino groups of amino acids are also able to react with C_{60}, by treating the fullerene, for example, with β-alanine in the presence of sodium hydroxide[28]. The resulting water soluble products however have not been completely characterized.

Clean and isomerically pure monoadducts were obtained by the reaction of secondary diamines, for example, *N,N'*-dimethylethylenediamine, piperazine or homopiperazine with C_{60} between 0 and 100 °C [Scheme 3.14][29]. In dilute solutions of the reactants, mono- and bisadducts are predominantly formed even if a large excess of the diamine is used.

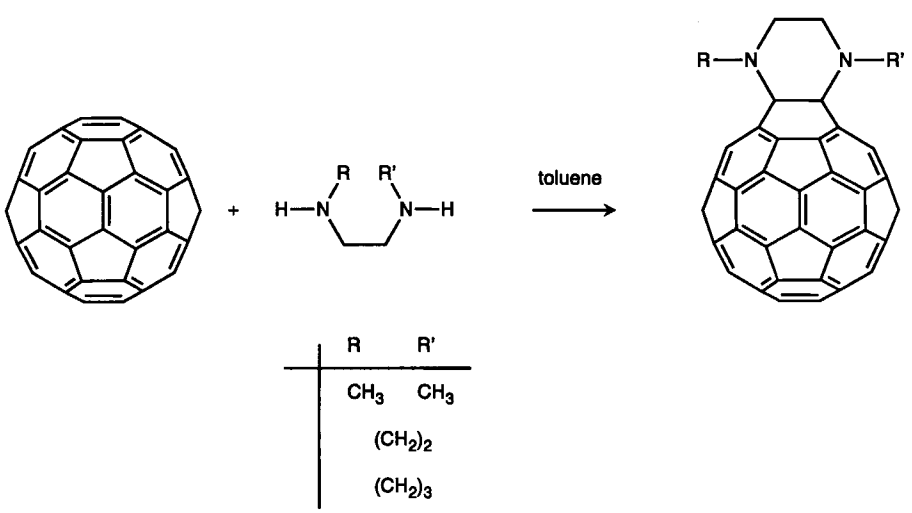

Scheme 3.14

As shown by mass spectrometry and NMR spectroscopy, these amine derivatives of C_{60}, after work-up, are dehydrogenated adducts[29]. After nucleophilic addition, the hydrogens which are brought in by the diamines were oxidatively eliminated. The final adduct formation of the secondary diamines proceeds exclusively at 6-6 bonds. Besides the monoadduct, 6 regioisomeric bisadducts of piperazine and C_{60} were separated by column chromatography.

The facile addition of primary and secondary amines to C_{60} has been used to synthesize polymer bound C_{60} [Scheme 3.15][30,31]. Toluene solutions of precursor polymers containing primary amino groups in the side chain were allowed to react with C_{60} in a "buckyball" fishing process.

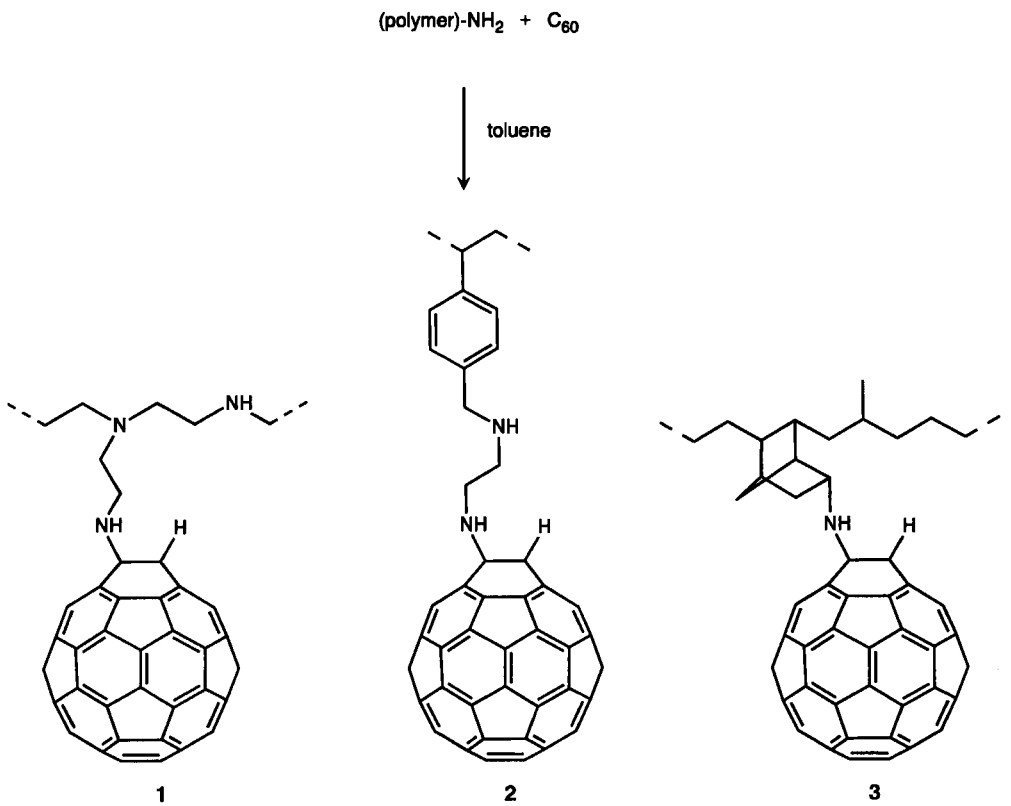

Scheme 3.15

In the polymers **1** and **2** (pendant on-chain, **Ia**, Fig. 3.8) about every twentieth monomer unit of the polymer carries a buckyball as determined by quantitative titration experiments and by thermogravimetric analysis[31]. The formation of **1** proceeds in a fast process via green intermediates upon the precipitation of a light brown gel. The precursor polymer of **3**, the amine functionalized ethylene-propylene terpolymer (EPDM-amine), contains only one amine per polymer chain. Therefore, polymer **3** itself is very soluble in common organic solvents. Viscometric studies on **3** imply that more than one amino group react with the same fullerene molecule, making it a dendritic system **II**[30] [Fig. 3.8].

Self-assembled monolayers (SAMs) of covalently bound C_{60} have been synthesized by the treatment of C_{60} with $(MeO)_3Si(CH_2)_3$ modified indium-tin-oxide (ITO) surfaces [Scheme 3.16][32] as well as cysteamine modified gold surfaces [Scheme 3.17][33]. These cases also take advantage of the

fact that primary amino groups easily add to the fullerene double bonds. The use of ITO treated with $(MeO)_3Si(CH_2)_3NH_2$ and the modified gold substrates allow the electrochemical characterization of the SAMs of C_{60} with cyclic voltammetry as well as quartz crystal microbalance (QCM) measurements. With these investigations it could be shown that monolayers of C_{60} indeed are bound to the surface. The C_{60} surface coverage was determined to be 2.0×10^{-10} mol/cm^2. Although the C_{60} SAMs are stable under ambient conditions, the fullerenes may be desorbed from the surface through electrochemical reduction of the films for extended periods of time (>10 min). The monolayer can be further modified with monomeric amine reagents, which demonstrates the potential of the self-assembly process for growing three-dimensional fullerene structures [Scheme 3.16].

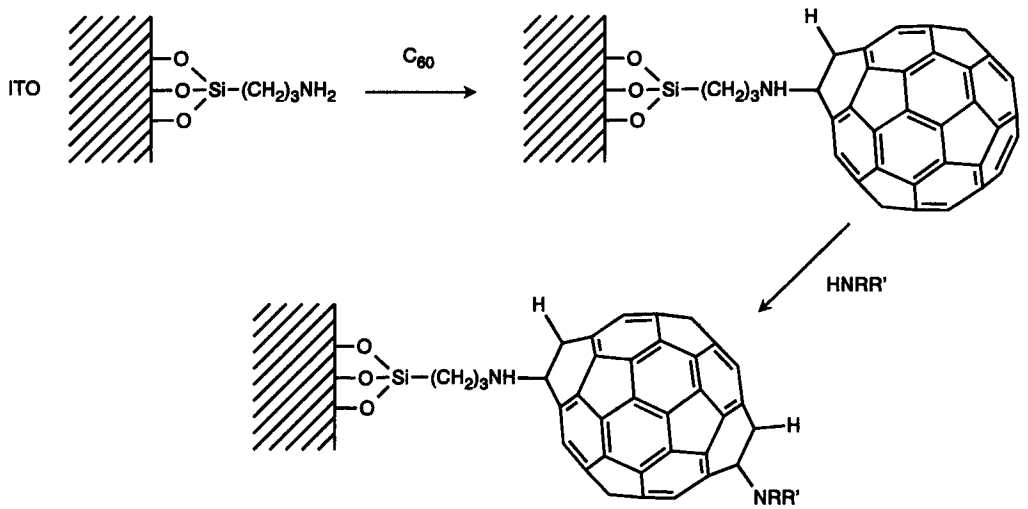

Scheme 3.16

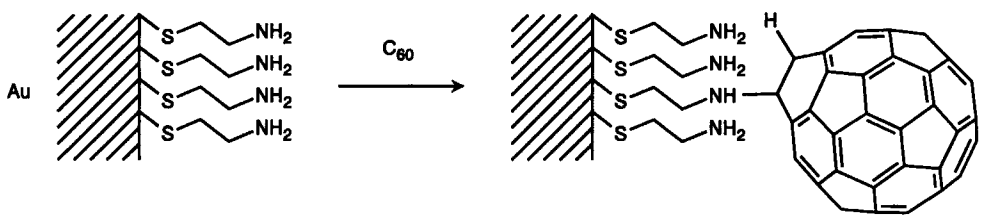

Scheme 3.17

3.4 Addition of Hydroxide

Heating of C_{60}/C_{70} mixtures in toluene in the presence of excess KOH leads to the formation of a precipitate of hydroxylated fullerenes (fullerols), which are soluble in THF but decompose due to the presence of air[34]. The addition of hydroxide to C_{70} proceeds significantly faster than to C_{60}. This was

concluded from time dependent measurements with UV/Vis spectroscopy, as well as by the observation that during the reaction the red color of the C_{60}/C_{70} mixture turns to purple before all the material precipitates. Addition of oxygen to the resultant cooled mixture regenerates the C_{60}/C_{70} mixture in 76 % yield.

The formation of fullerols has also been achieved by the reaction of C_{60} dissolved in benzene with aqueous NaOH in the presence of the phase transfer catalyst tetrabutylammonium hydroxide in air[35]. This reaction proceeds within a few minutes with the precipitation of a brown solid. The addition of hydroxy groups is very slow in the absence of oxygen. About 24 to 26 hydroxy groups can be attached to the fullerene core by this method. It has to be stated however that the exact composition of these compounds is unknown, since so far they have not been completely characterized.

References

1 F. Wudl, A. Hirsch, K.C. Khemani, T. Suzuki, P.-M. Allemand, A. Koch, H. Eckert, H.; G. Srdanov, H. Webb In *Fullerenes: Synthesis, Properties, and Chemistry of Large Carbon Clusters;* G. S. Hammond, V. J. Kuck, Eds.; American Chemical Society Symposium Series 481; 1992; p 161.

2 A. Hirsch, A. Soi, H. R. Karfunkel, *Angew. Chem.* **1992**, *104*, 808; *ibid. Int. Ed. Engl.* **1992**, *31*, 766.

3 A. Hirsch, T. Grösser, A. Skiebe, A. Soi *Chem. Ber.* **1993**, *126*, 1061.

4 P. J. Fagan, P. J. Krusic, D. H. Evans, S. A. Lerke, E. Johnston *J. Am. Chem. Soc.* **1992**, *114*, 9697.

5 P. J. Krusic, D. C. Roe, E. Johnston, J. R. Morton, K. F. Preston *J. Phys.Chem.* **1993**, *97*, 1736.

6 J. R. Morton, K. F. Preston, P.J. Krusic, S.A. Hill, E. Wasserman *J. Am. Chem. Soc.* **1992**, *114*, 5454.

7 D. A. Dixon, N. Matsuzawa, T. Fukunaga, F. N. Tebbe *J. Phys. Chem.* **1992**, *96*, 6107.

8 N. Matsuzawa, D. A. Dixon, T. Fukunaga *ibid.* **1992**, *96*, 7594.

9 A. Hirsch *GIT Fachz. Lab.* **1993**, 764.

10 H. R. Karfunkel, A. Hirsch *Angew.Chem.* **1992**, *104*, 1529; *ibid. Int. Ed. Engl.* **1992**, *31*, 1468.

11 A. L. Balch, V. J. Catalano, J. W. Lee, M. M. Olmstead, S. R. Parkin *J. Am. Chem. Soc.* **1991**, *113*, 8953.

12 G. Williams, A. Soi, A. Hirsch, M. R. Bryce, M. C. Petty *Thin Solid Films* **1993**, *230*, 73.

13 L. M. Goldenberg, G. Williams, M. R. Bryce, A. P. Monkman, M. C. Petty, A. Hirsch, A. Soi *J. Chem. Soc., Chem. Commun.* **1993**, 1310.

14 G. Williams, G. Pearson, M. R. Bryce, M. C. Petty *Thin Solid Films* **1992**, *209*, 150, and references cited herein.

15 E. T. Samulski, J. M. DeSimone, M. O. Hunt Jr., Y. Z. Menceloglu, R. C. Jarnagin, G. A. York, K. B. Labat, H. Wang *Chem. Mater.* **1992**, *4*, 1153.

16 D. E. Bergbreiter, H. N. Gray *J. Chem. Soc., Chem. Commun.* **1993**, 645.

17 A. Hirsch *Adv. Mater.* **1993**, *5*, 859.

18 I. Amato *Science* **1991**, *254*, 30, quoting F. Wudl.

19 C. Bingel *Chem.Ber.* **1993**, *126*, 1957.

20 I. Lamparth *Diplom Disseration,* University of Tübingen, 1993.

21 A. Hirsch, I. Lamparth, H. R. Karfunkel *Angew. Chem.* **1994**, *106*, 453; *ibid. Int. Ed. Engl.* **1994**, *33*, 437.

22 A. Hirsch, H. R. Karfunkel unpublished results.

23 A. Hirsch, Q. Li, F. Wudl *Angew. Chem.* **1991**, *103*, 1339; *ibid. Int. Ed. Engl.* **1991**, *30*, 1309.

24 R. Shedari, A. Govindaraj, R. Nagarajan, T. Pradeep, C. N. R. Rao *Tetrahedron Lett.* **1992**, *23*, 2069.

25 A. Skiebe, A. Hirsch, H. Klos, B. Gotschy *Chem. Phys. Lett.* **1994**, *220*, 138.

26 P.-M. Allemand, K. C. Khemani, A. Koch, F. Wudl, K. Holczer, S. Donovan, G. Grüner, J. D. Thompson *Science* **1991**, *253*, 301.

27 T. Grösser *Diplom Disseration,* Univeristät Tübingen, 1992.

28 L. B. Gan, C. P. Luo, L. B. Xu, D. J. Zhou, C. H. Huang, G. X. Xu presented at the symposium *Fullerenes 1993*, Santa Barbara, June 1993.

29 K.-D. Kampe, N. Egger, M. Vogel *Angew.Chem.* **1993**, *105*, 1203; *ibid. Int. Ed. Engl.* **1993**, *32*, 1174.

30 A. O. Patil, G. W. Schriver, B. Carstensen, R. D. Lundberg *Polym. Bull.* **1993**, 645.
31 K. E. Geckeler, A. Hirsch *J. Am. Chem. Soc.* **1993**, *115*, 3850.
32 K. Chen, W. B. Caldwell, C. A. Mirkin *J. Am. Chem. Soc.* **1993**, *115*, 1193.
33 W. B. Caldwell, K. Chen, C. A. Mirkin, S. J. Babinec *Langmuir*, **1993**, 1324.
34 A. Naim, P. B. Shevlin *Tetrahedron Lett.* **1993**, *33*, 7097.
35 J. Li, A. Takeuchi, M. Ozawa, X. Li, K. Saigo, K. Kitazawa *J. Chem. Soc., Chem. Commun.* **1993**, 1784.

Chapter 4 Cycloadditions

4.1 Introduction

4.2 [4+2] Cycloadditions

4.3 [3+2] Cycloadditions
4.3.1 Addition of Diazomethanes, Diazoacetates and Diazoamides
4.3.2 Addition of Azides
4.3.3 Addition of Trimethylenemethanes
4.3.4 Addition of Azomethine Ylides
4.3.5 Addition of Nitrile Oxides
4.3.6 Addition of Sulfinimides
4.3.7 Addition of Disiliranes

4.4 [2+2] Cycloadditions
4.4.1 Addition of Benzyne
4.4.2 Addition of Enones
4.4.3 Addition of Quadricyclane
4.4.4 Addition of Electron Rich Alkynes
4.4.5 Photopolymerization of C_{60}

4.5 [2+1] Cycloadditions
4.5.1 Addition of Carbenes
4.5.2 Addition of Silylenes

References

4.1 Introduction

In cycloaddition reactions it is always the 6-6 double bonds of C_{60} that act as enes or dienophiles. A large variety of cycloadditions were carried out with C_{60} and the complete characterizations of the products, mainly monoadducts, greatly increased the knowledge of fullerene chemistry. These chemical transformations also provide a very powerful tool for fullerene functionalization. Almost any functional group can be covalently linked to C_{60} by the cycloaddition of suitable addents. Some types of cycloadducts exhibit a remarkable stability; for example, they can be thermally treated up to 400 °C without decomposition. This is an important requirement for further side-chain chemistry as well as for possible applications of the new fullerene derivatives, which may be of interest due to biological properties or as new materials.

4.2 [4+2] Cycloadditions

The 6-6 double bonds in C_{60} are dienophilic[1], which enables the molecule to undergo a variety of Diels-Alder reactions ([4+2] cycloadditions). The conditions for the cycloadduct formation strongly depend on the reactivity of the diene. Whereas equimolar amounts of cyclopentadiene [Scheme 4.1] react with C_{60} at room temperature to give the monoadduct in comparatively high yield[2,3], the formation of a cycloadduct with anthracene [Scheme 4.1] necessitates an excess of the diene in refluxing toluene[1,3,4]. These cycloadducts of C_{60} can be purified by HPLC using gel permeation columns and toluene as eluent[3].

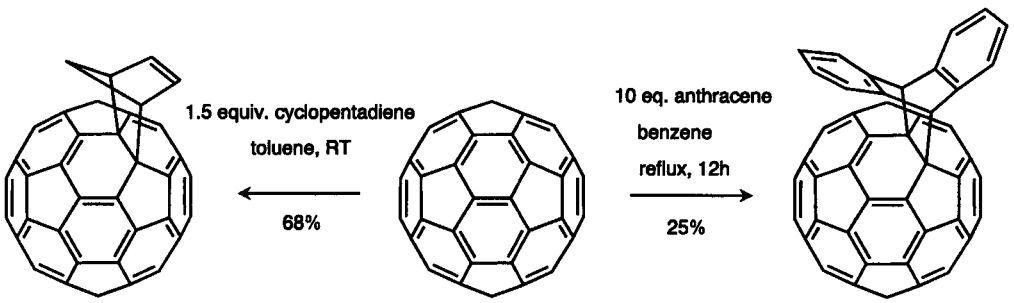

Scheme 4.1

Heating the anthraceno monoadduct in toluene gives the component molecules[1,3], which demonstrates a facile retro-Diels-Alder reaction. A thermal gravimetric analysis (TGA) of solid C_{60}(anthracene) shows a cleavage of the anthracene moiety at an onset temperature of 120 °C[4]. These findings clearly show that there is an equilibrium between addition and elimination of anthracene in toluene under reflux conditions, which also explains the comparatively low yields [Scheme 4.1]. An even more pronounced retro-Diels-Alder reaction occurs by using 1,3-diphenylisobenzofuran (DPIF) or 2,3-dimethylbutadiene (DMBD) as the diene[3]. The corresponding monoadducts cannot be isolated from the reaction mixture. In the case of DPIF the retro-Diels-Alder seems to be facilitated by steric repulsion due to the bulky groups. However, as shown by Wudl et al.[5], the cycloadduct of C_{60} with isobenzofuran [Scheme 4.2] itself, which was generated in situ from 1,4-dihydro-1,4-epoxy-3-phenylisoquinoline, is stable in the solid state as well as in solution and shows no tendency to undergo

cycloreversion. These examples already show that the potential of such reactions for the synthesis of stable fullerene derivatives is restricted by the ease of cycloreversion to the starting materials.

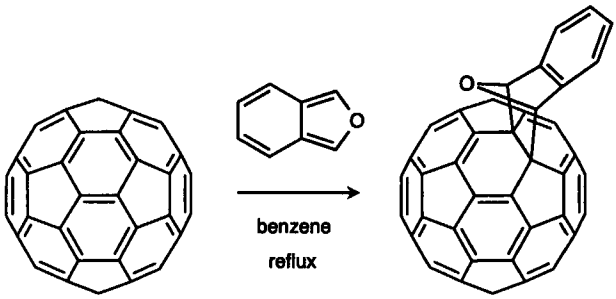

46%

Scheme 4.2

Cyclopentadiene adducts (mono, tetra and hexa) of C_{60} were stabilized against retro-reaction by selective hydrogenation and bromination of the pendant groups[6]. Use of Adam's catalyst and dilute bromine solutions exclusively leads to an addition to the cyclopentene double bonds, because C_{60} itself is inert towards these reagents. The increased stability of the reduced cycloadducts can be demonstrated by mass spectrometry[6].

Another approach to synthesize stable Diels–Alder adducts of C_{60} was introduced by Müllen et al.[7,8,9]. The use of *o*-quinodimethane derivatives as dienes, prepared in situ, leads to thermally stable cycloadducts [Scheme 4.3]. As in the case of the isobenzofuran addition product[5], a cycloreversion of these adducts would need to overcome the stabilization provided by the aromatic system and would also give the unstable *o*-quinodimethane intermediate. A fast ring inversion at elevated temperatures of the cyclohexane moiety causes a C_{2v}-symmetry of the cycloadduct leading to 17 lines for the fullerenyl carbons in the ^{13}C NMR spectra[7].

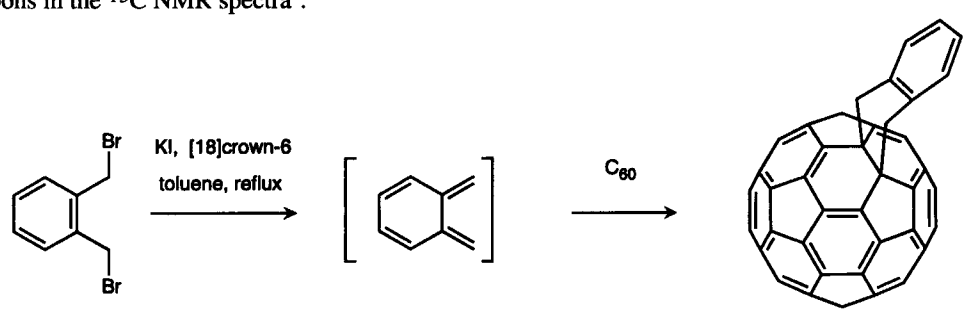

88 %

Scheme 4.3

The analogous reaction of C_{60} with bis-*o*-quinodimethane [Scheme 4.4] leads to a bridged system[7], which can be regarded as a part of a band polymer containing the C_{60} unit and exhibits a significantly decreased solubility. The bis-*o*-quinodimethane was prepared in situ from 1,2,4,5-tetrakis(bromomethyl)benzene. In Scheme 4.4 one possible conformer of the bisadduct is shown.

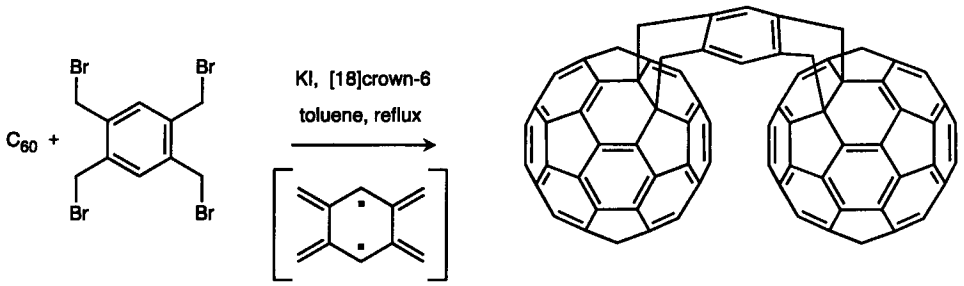

Scheme 4.4

These cycloadditions with *o*-quinodimethanes provide a broad variety of useful fullerene functionalizations, since *o*-quinodimethanes can be prepared using several routes and the resulting cycloadducts are thermally very stable[8]. As an alternative to the iodide induced bromine elimination of 1,2-bis(bromomethyl)benzenes, *o*-quinodimethanes, prepared by thermolysis from 3-isochromanone[9], benzocyclobutenes and isobenzothiophene-2,2-dioxides[8], were added also to C_{60} in good yields [Scheme 4.5]. The ring opening of the benzocyclobutenes or the extrusions of CO_2 and SO_2 require high temperatures. Therefore, the cycloadditions are carried out in refluxing 1,2,4-trichlorobenzene (214 °C).

Information about the electronic structure of the 4,5-dimethoxy-*o*-quinodimethane adduct **1** in the solid state, prepared from 6,7-dimethoxy-3-isochromanone, comes from ESCA measurements[9]. In accord with the crystal structure analysis[9,10], this cycloadduct, which contains the electron rich dimethoxyphenyl moiety, shows an intermolecular donor-acceptor interaction, in particular, of the methoxy oxygen to the C_{60} unit.

A benzo[18]crown-6 adduct **2**, of C_{60} has been synthesized by the addition of the corresponding *o*-quinodimethane in toluene[10]. The solubility of **2** in protic solvents like MeOH strongly increases after the complexation of K^+ ions, as shown by extraction experiments. No complexation-induced shifts have been observed in the electronic absorption spectra of **2**, suggesting that the K^+ ion bound in the crown ether moiety does not interact with the fullerene core. The combination of crown ether and the fullerene moieties in **2** provide a highly amphiphilic character. This behavior allowed the preparation of Langmuir–Blodgett films of monolayers on mica of **2** and its K^+ complex.

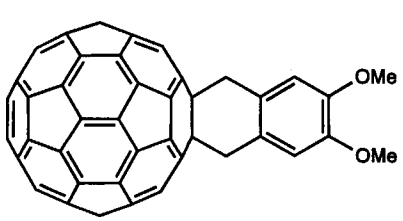

1

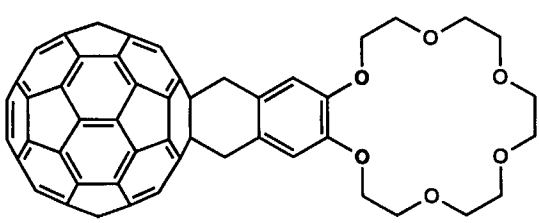

2

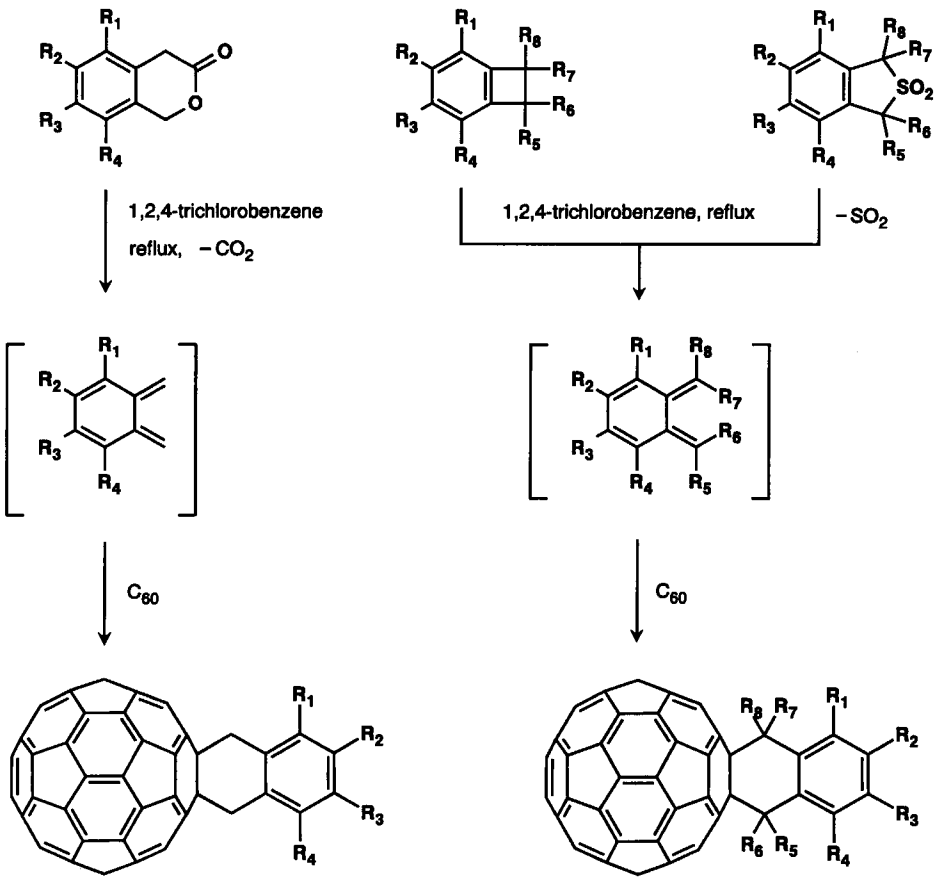

Scheme 4.5

The cycloadduct **3** of C_{60} with 4-(4-fluoro-3-nitrobenzoyl)benzocyclobutene is very stable, loosing the benzocyclobutene moiety above 400 °C[8]. The strong activation of the fluoro-substituted phenyl ring by the nitro- and keto group enables nucleophilic additions to this adduct in very good to quantitative yields [Scheme 4.6]. In this way, C_{60} can be further derivatized and covalently bound to other classes of compounds[8]. With the very nucleophilic aliphatic amines, for example 4,13-diaza-[18]-crown-6 or 1,6-bis(aminomethyl)hexane, the substitution occurs within some minutes, whereas the use of less nucleophilic aromatic amines, for example 4-amino-azobenzene, needs longer reaction times. In the latter case a chromophore is covalently attached to C_{60}. All these cycloadducts are very soluble in chloroform or toluene; therefore, their chromatographic separation can be achieved efficiently by using polystyrene gel as stationary phase[8,9,11,12]. The methods of further functionalization to provide new fullerene derivatives is limited by the electronic properties of C_{60}. For example, treatment of **3** with 1,3-dimercaptobenzene in *N,N*-dimethylacetamide does not yield the expected substitution product but leads to oligophenylene disulfides via oxidative coupling. In this case, the C_{60} derivative acts as a weak oxidizing reagent.

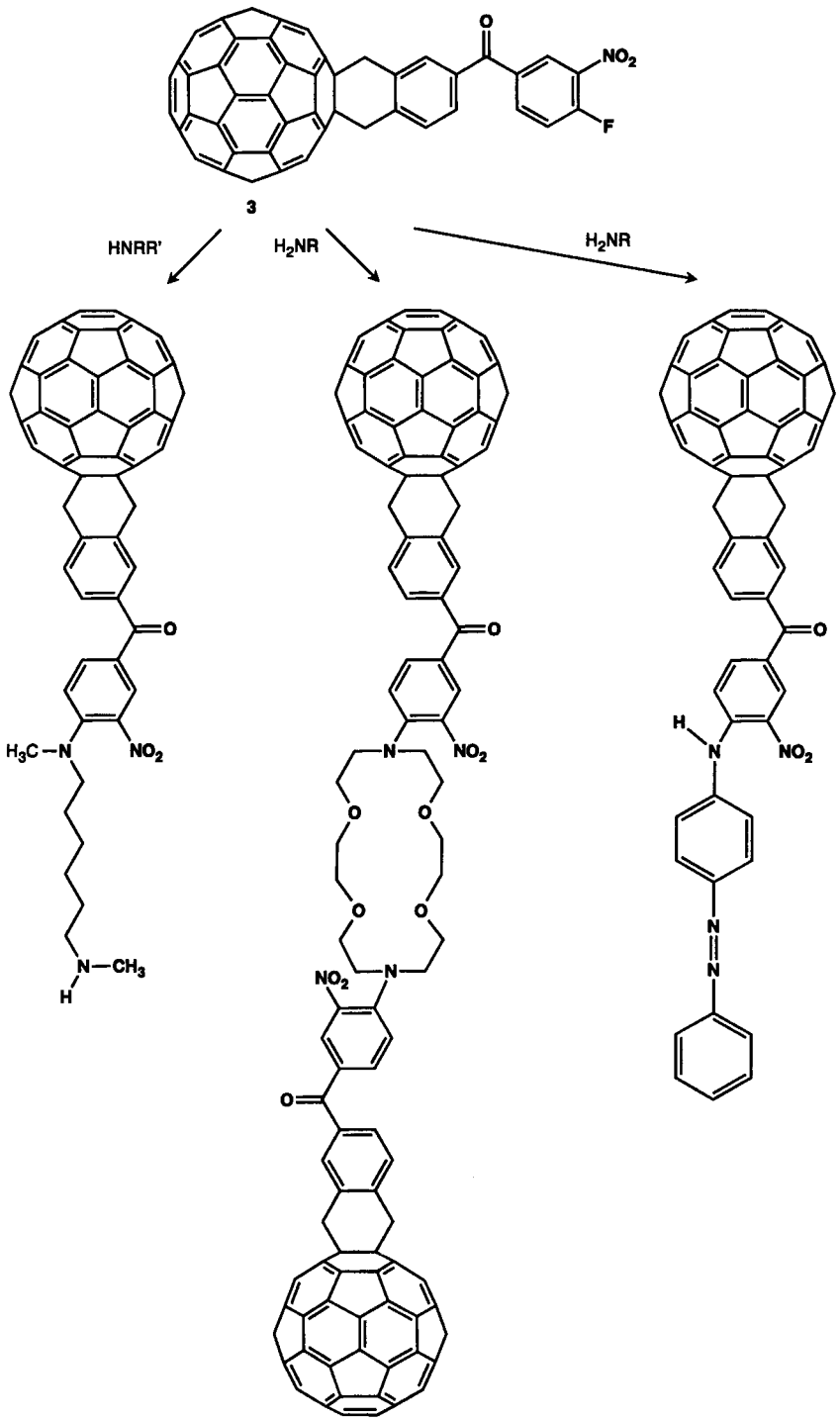
O
NO2
F
3
HNRR'
H2NR
H2NR
H3C–N
NO2
N–CH3
H
O
N
NO2
O
O
O
O
N
NO2
O
H
N
NO2
N
N
O

Scheme 4.6

Similar adducts were obtained by Rubin et al.[13] using 5,6-dimethylene-1,4-dimethyl-2,3-diphenylnorborn-2-en-7-one as diene [Scheme 4.7]. The stabilized adduct is formed after loss of CO. The X-ray crystal structure of black, prismatic single crystals of this cycloadduct confirms the ^1H and ^{13}C NMR investigations, demonstrating additions to 6–6 double bonds of the fullerene framework. Also in this case, the cyclohexene ring undergoes a conformational exchange between the two boat forms of the molecule. Temperature dependent ^1H NMR investigations reveal a coalescence temperature of 35 °C and an activation energy for the boat-to-boat barrier of inversion of $\Delta G^{\ddagger} = 14.6 \pm 0.1$ kcal/mol.

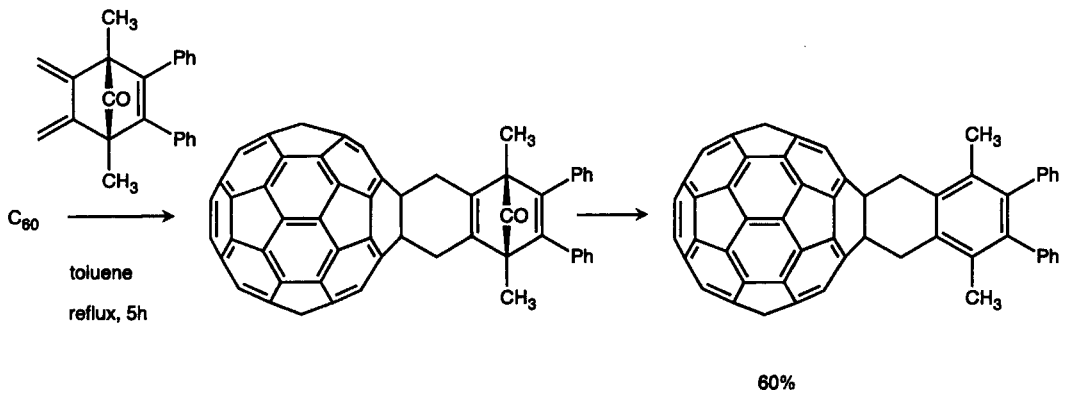

Scheme 4.7

A stable adduct **4** of C_{60} with an electron donor moiety in the side chain [Fig. 4.1][14] was synthesized by the cycloaddition of a rigid diene containing a polynorbornyl-bicyclo[2.2.0]hexyl bridge and a dimethoxybenzene (DMB) unit in toluene at reflux in 63 % yield. The donor-acceptor interaction of the electron rich DMB unit and C_{60} is indicated by the X-ray crystal structure [Fig. 4.1]. The adducts are paired up with the C_{60} unit of one molecule nestling up to the DMB-terminated chain of the other. The cyclohexene ring in **4** adopts an extendend boat conformation in the crystal. Since a folded boat conformation of the cyclohexene ring was predicted to be more stable, it can be anticipated that crystal-packing forces and π-stacking interactions between the C_{60} and the DMB moiety are responsible for the extended conformation in the solid state.

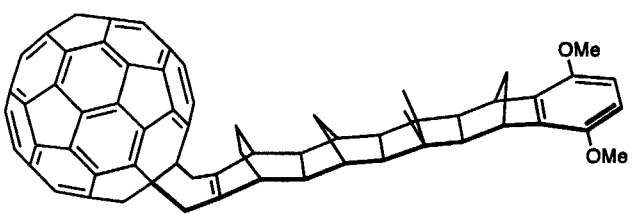

4

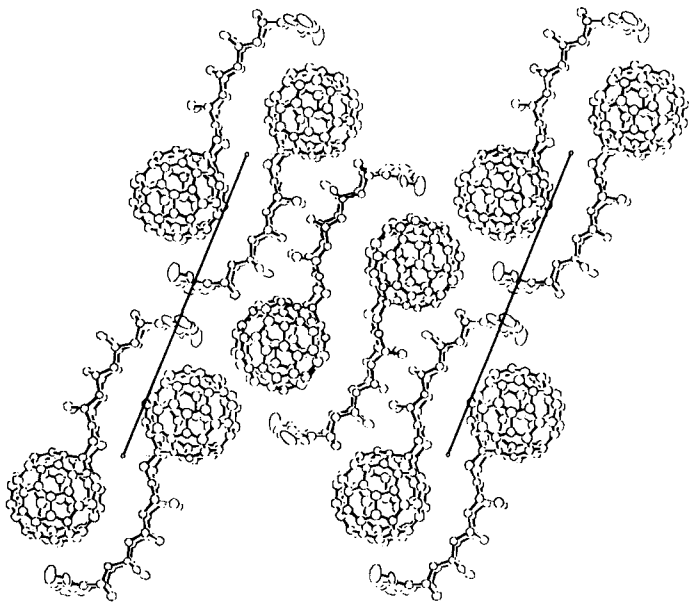

Figure 4.1 View of the crystal packing structure of **4** down the *b*-axis, *a*-axis pointing to the right. Chlorobenzene molecules which are present in the crystal lattice are not shown for clarity[14].

By allowing C_{60} to react with 2-trimethylsilyloxy-1,3-butadiene in toluene at reflux[15], another stable Diels–Alder adduct was obtained [Scheme 4.8]. The ketone **5** is formed after hydrolysis of the uncharacterized intermediate silyl enol ether through flash chromatography.

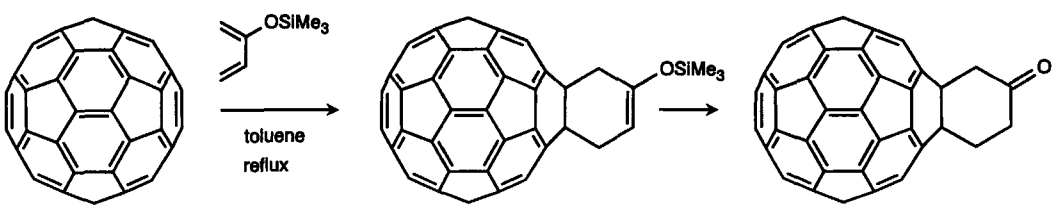

5

Scheme 4.8

This ketone can be reduced with DIBAL-H in toluene at 20 °C to the corresponding racemic alcohol **6** in 93 % yield. With **6**, coupling reactions can be carried out leading to a further functionalization of the fullerene sphere[15]. Esterification with protected amino acids, for example with *N*-(benzyloxycarbonyl)-*L*-alanine or α-benzyl-*N*-(*tert*-butoxycarbonyl)-*L*-glutamate in toluene in the presence of DCC and DMAP at room temperature, provides amino acid derivatives of C_{60} as mixtures of diastereomers in high yields [Scheme 4.9]. Photolysis experiments carried out in the presence of the alcohol adduct **6** show that $^1O_2$ is formed efficiently (Φ = 0.84 at 532 nm and 0.72 at 355 nm in C_6D_6), which raises the possibility of using these systems for photodynamic therapy[15].

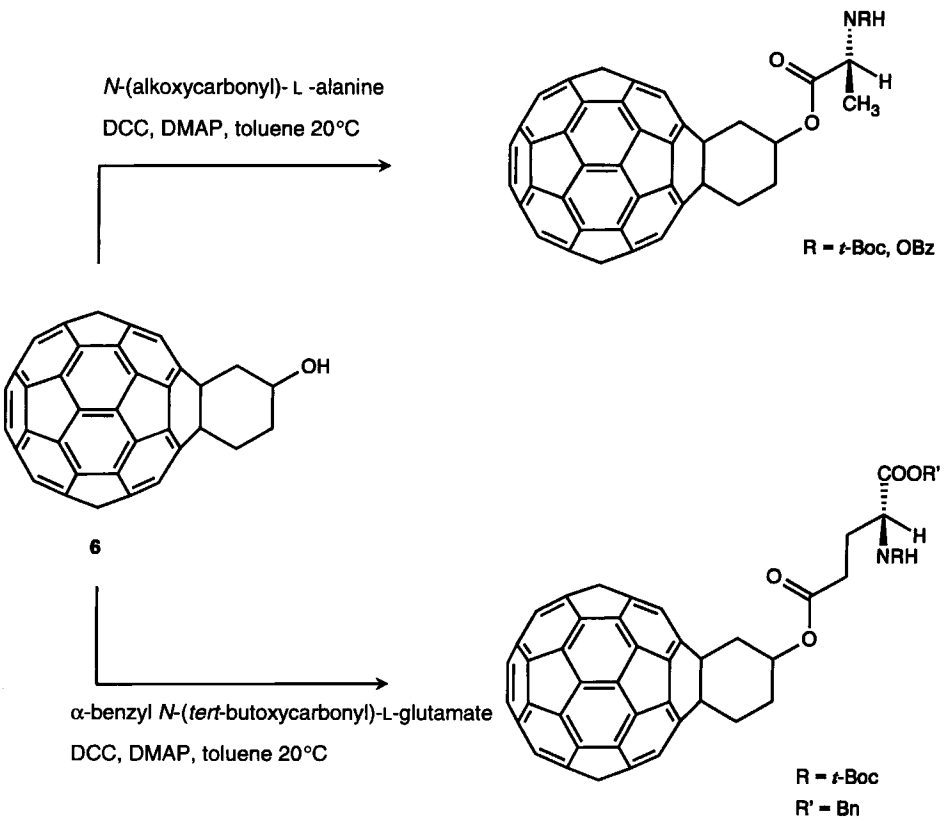

Scheme 4.9

Regioselective [4+2] cycloadditions to C_{60} were found to be possible also with 2,3-dimethylbuta-1,3-diene and with the monoterpene 7-methyl-3-methylideneocta-1,6-diene (myrcene)[16]. These monoadduct formations proceed under mild and controlled conditions.

4.3 [3+2] Cycloadditions

4.3.1 Addition of Diazomethanes, Diazoacetates and Diazoamides

A broad variety of methano-bridged fullerenes are accessible by the reaction of C_{60} with different diazomethanes[17,18,19,20,21,22,23,24,25,26,27], diazoacetates[18,28] and diazoamides[29]. These chemical transformations of C_{60} were discovered by Wudl and are based on the finding [1,17,18] that C_{60} behaves as an 1,3-dipolarophile. In the case of the synthesis of the parent methano-fullerene $C_{61}H_2$, by treating C_{60} with diazomethane in toluene, the pyrazoline intermediate **7** could be isolated and

characterized[20,22]. It has been shown that the first step of this reaction, the [3+2] cycloaddition of the diazomethane, occurs at a 6-6 double bond [Scheme 4.10]. The extrusion of N_2 out of **7** can be achieved photochemically or thermally by refluxing of **7** in toluene. By these procedures, two different methano-bridged fullerenes are formed, namely the ring closed system **8a**, where the bridging occurs in 1,2-position[22], as well as the 1,6-bridged isomer with the ring opened structure **8b** (fulleroid)[20] [Scheme 4.10]. Whereas the photolysis of **7** gives a mixture of **8a** and **8b** the thermolysis leads almost only to **8b** with only traces of **8a** detectable by ^1H NMR spectroscopy. Importantly, individual photolysis of **8a** and **8b** did not lead to their interconversion and thermolysis of **8b** failed to generate **8a**[22]. Calculations at the semi-empirical MNDO and the HF (3-21G) levels show that these experimentally isolated isomers, **8a** and **8b**, are indeed the two low-energy isomers of $C_{61}H_2$[30]. The two isomers, **8a** and **8b**, are quite close in energy. At the HF/3-21G level **8a** is 6 kcal/mole more stable than the ring opened form **8b**.

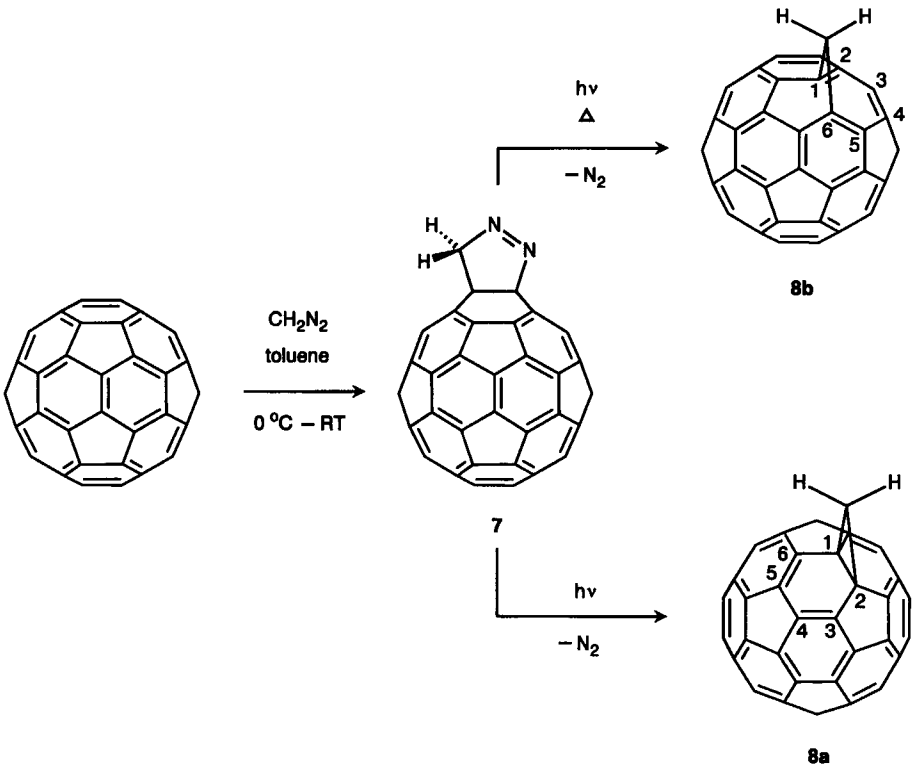

Scheme 4.10

The additions of other diazo compounds, for example substituted diphenyldiazomethanes[24] or alkyl diazoacetates[28], also lead to mixtures of different isomers. Four different isomers **A**-**D** (R = R') obtained from single additions of symmetric diazo compounds can in principle be considered. These are the corresponding ring closed and ring opened structures with the methylene bridges in 1,2- (**A, B**) and in 1,6-positions (**C, D**). In the case of 1,6-bridges with asymmetrical methylene groups (R ≠ R'), two isomers of each **C** and **D** must be distinguished with R above a pentagon and R' above a hexagon and vice versa. Based on calculations on the MNDO level[24] with several R and R' the isomers **A** and **C**

are the most stable. Indeed, the isomers that are found in the reaction mixtures are in all cases the closed 1,2-bridged structures **A** and the open 1,6-bridged structures **C**. These findings together with calculations of the stabilities of different regioisomeric addition products $C_{60}R_n$[31,32,33,34,35] with R being a segregated group lead to the formulation of the simple *rule* stating that *for C_{60} as well as for C_{60} derivatives it is energetically unfavorable to introduce double bonds at 5-6 ring junctions or to reduce the greatest possible number of [5]radialene rings.* As will be shown in Chapter 6 and 8, this is always valid as long as additional strain introduced by sterical demanding addents (eclipsing interactions) does not prevail. In the case of methano bridges, however those steric arguments do not have to be considered. Whereas in the structures **A** and **C** only 6-6 double bonds are present, structures **B** and **D** require the formal introduction of two 5-6 double bonds.

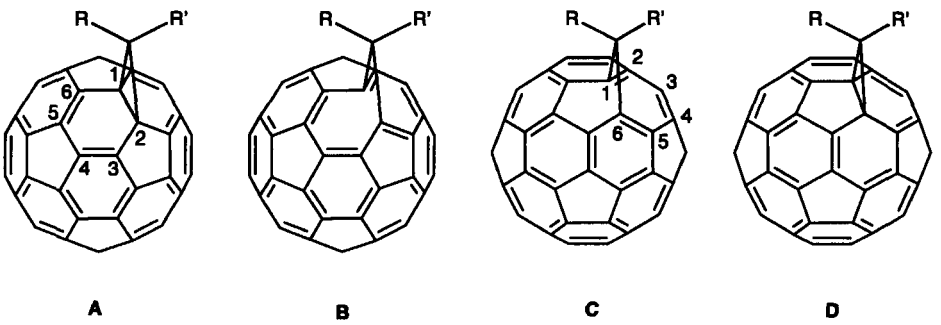

The structural assignment of the different methano-bridged isomers is based on NMR criteria [Fig. 4.2]. From the NMR spectra the symmetry of the isomers, for example C_s or C_{2v} can be determined. More importantly in analogy to the methanoannulenes[36], which can also exhibit ring opened or ring closed structures, the ^{13}C NMR chemical shifts of the bridgehead C-atoms and the coupling constants ^1J(C,H) of the methano bridge C-atom, which depend very strongly on the structure under consideration, can be used to distinguish between the different isomers[20,22,24,28]. The bridgehead carbons of **A** resonate between δ 70-90, whereas the bridgehead carbons of **C** appear between δ 130-150. Typical coupling constants ^1J(C,H) for the methano bridge C-atoms of **A** lie in the range of 165-170 Hz, whereas those of **C** lie between 140 and 145 Hz. In addition, the ^1H NMR chemical shift of a proton, which is in close proximity to the fullerene sphere, strongly depends on whether it is located above a five membered or a six membered ring. A proton located above a pentagon resonates up to 3.5 ppm more downfield than a proton above a hexagon. These results were interpreted in terms of local and ring-current anisotropy effects. Calculations of local ring-currents in C_{60} further corroborate these findings[37]. The existence of two types of ring currents is predicted. These are the strong paramagnetic ring currents in the pentagons and the mild diamagnetic currents supported by the hexagons. As a consequence, the strong paramagnetic ring currents are expected to deshield protons located above pentagons, and the mild diamagnetic ring currents should weakly shield the protons being closely located above the center of the hexagons. Although this ring-current model was predicted for the parent C_{60}, it may be operative within the homo-rings of the ring opened structures **C**.

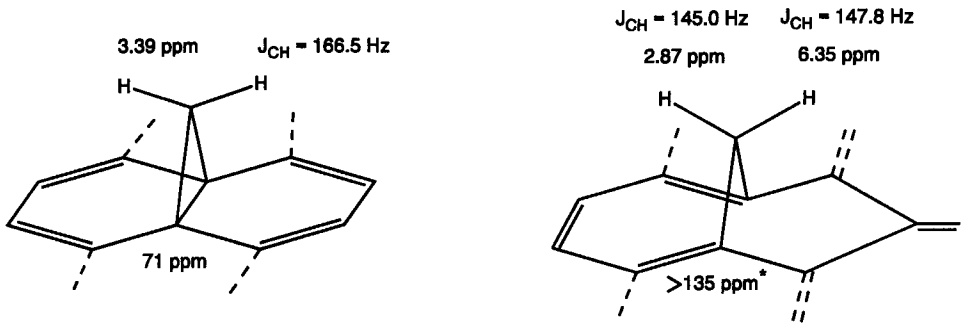

Figure 4.2 Chemical shifts for the bridgehead C-atoms and the methylene H-atoms and coupling constants ^1J(C,H) for the methano bridge C-atoms in $C_{61}H_2$ for isomers **8a** and **8b**. * The exact peak position for the bridgehead carbons in **8b** is not identified. The corresponding C-atoms resonate in the region between 130 and 150 ppm together with all the other sp^2-carbons of the fullerene sphere. In the case of the 1,6-addition adduct of C_{60} with (*p*-methoxyphenyl)diazomethane, the exact peak position of the bridgehead C-atoms was found by HETCOR analysis to be 138.65 ppm[24].

The ratio of the different isomers **A** or **C** in the reaction mixtures after loss of N_2 depends on the diazomethane or the alkyl diazoacetate used for the cycloaddition. For example, whereas the cycloaddition of (*p*-methoxyphenyl)diazoethane leads predominantly to the 6-6-ring bridged cycloadduct **A**[24], the addition of alkyl diazoacetates [Scheme 4.11] reproducibly yields the three isomers **9**–**11** in the ratio of 1:1:3, as determined by ^{1}H NMR spectroscopy[28]. In the latter case, the cycloaddition proceeds sluggishly at room temperature and is therefore carried out in refluxing toluene. Under these conditions the formation of the open structures **C** are kinetically favored. The predominance of isomer **11** over **10** by a ratio of 3:1 represents a remarkable diastereoselectivity. Since there is no obvious steric effect present, an electronic effect was taken into consideration. Although unambiguous evidence is given for [3+2] cycloadditions of diazomethanes[20] and diphenyldiazomethanes[38] at room temperature followed by the thermal or photochemical extrusion of N_2, a pyrazoline intermediate could not be detected in the synthesis of **9**–**11** by the addition of alkyl diazoacetates in boiling toluene[28]. However, also in this case, it is very likely that the first step is a [3+2] cycloaddition since the 5-6-ring bridged as well as the 6-6- ring bridged isomers are formed simultaneously. In the case of a [2+1] cycloaddition of carbenes, exclusively the 6-6- ring bridged isomers are formed (see Chapter 4.5.1).

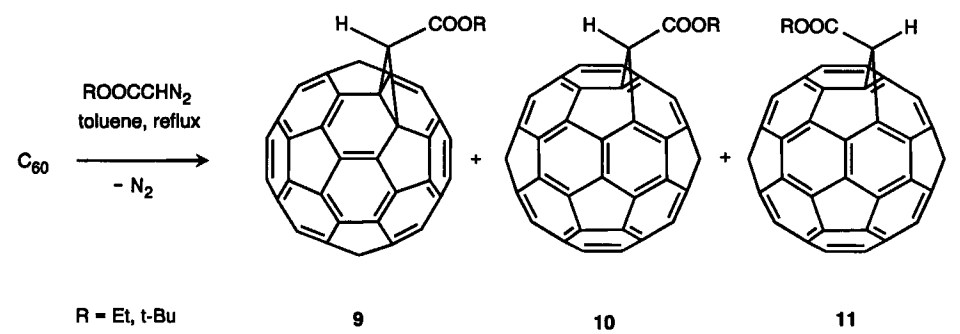

Scheme 4.11

Significantly, purified mixtures of isomers of **A** and **C** equilibrate, in most cases, quantitatively to the ring closed 6-6-ring bridged cycloadducts **A** after refluxing in toluene for several hours [Scheme 4.12]. This implies that cycloadducts **C** are the thermodynamically most stable isomers[24,28]. As a mechanism for the isomerization to the thermodynamically stable isomers, a [1,5] shift of the methano bridge as well as *retro*-carbene additions coupled to additions leading to the stable isomer have been suggested[20,24,28]. That intermolecular reactions may be important for the isomerization is supported by the finding that only the purified mixture of **9–11** undergoes a quantitative isomerization to **9**, whereas refluxing the original reaction mixture in toluene for 31 h reproducibly leads to a mixture of isomers in the ratio of ca. 4:1:4[28].

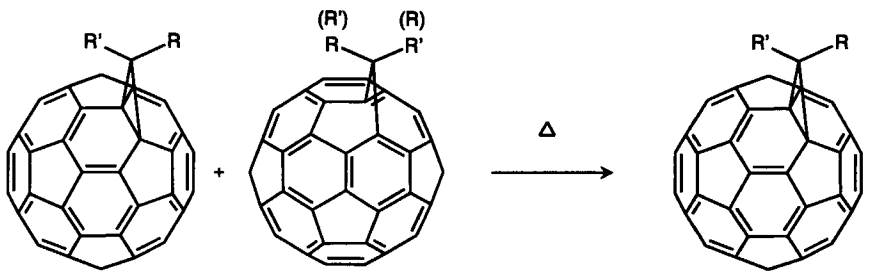

Scheme 4.12

The redox properties of C_{60} are retained to a large extent in the methano-bridged fullerenes[17,19,20]. The reduction waves undergo a small shift of about 100 mV to more negative potentials [Fig. 4.3]. No significant difference between 5-6- and 6-6-ring-bridged cycloadducts is observed[20]. That the acceptor properties of fullerene derivatives are retained is an important requirement for further transformations (*n*-doping) to charge-transfer complexes with interesting properties as materials.

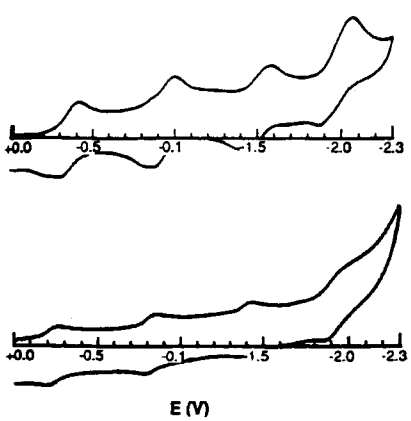

Figure 4.3 Comparative cyclic voltammograms of C_{60} (A) and $C_{61}Ph_2$ (B) versus Ag/Ag^+ as a reference in tetrahydrofuran with tetrabutylammonium fluoroborate as supporting electrolyte[17].

The electronic absorption spectra of C_{60} and 1,6- and 1,2-methano-bridged cycloadducts (monoadducts) exhibit almost the same features in the UV region, consisting of three dominant bands at 325, 259 and 219 nm[17,20,22,28]. In the visible region, however, the spectra of the ring-closed 1,2-bridged adducts differ significantly from those of C_{60} and the open 1,6-bridged isomers [Fig 4.4][28]. Very characteristic for the spectra of all the 1,2-bridged cycloadducts is a new sharp band with λ_{max} near 430 nm. This band is also always observed in the spectra of other adducts, such as the Diels–Alder adducts of C_{60} (Chapter 4.2) or the 1,2-dihydrofullerenes-60 (Chapter 3.2), which of course also have closed transannular 6–6 bonds. The origin of this interesting electronic transition remains to be clarified. In contrast, the spectra of the open 1,6-bridged isomers resemble much more the spectrum of C_{60} [Fig 4.4]. These findings independently prove that in the open 1,6-bridged isomers, the spherical chromophore of the pure fullerene is less perturbed than in the closed 1,2-bridged isomers. Whereas the purple color of solutions of 1,6-bridged isomers are almost the same as that of C_{60}, the color of monoadducts of C_{60} with the addents at the closed 6–6 bonds is chestnut brown to wine red.

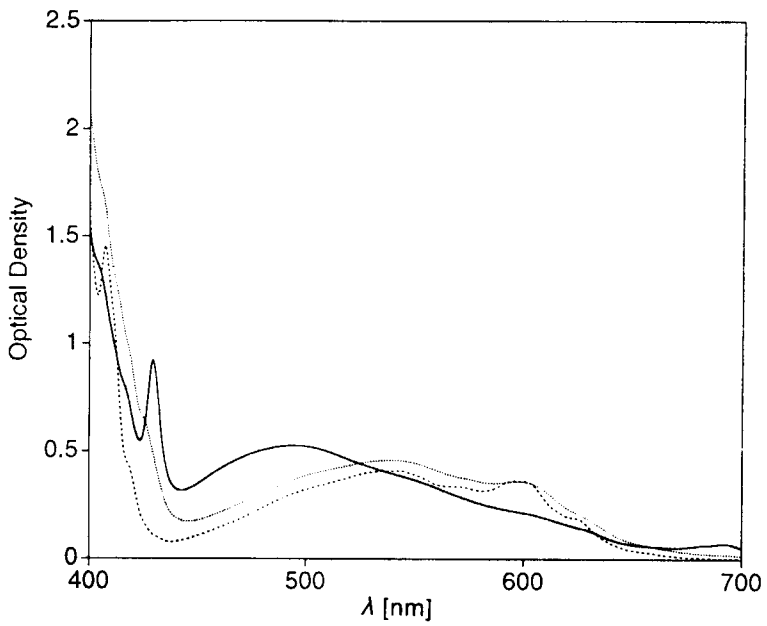

Figure 4.4 Electronic-absorption spectra recorded in toluene of the mixture of (ethoxycarbonyl)-methylene-bridged fullerenes **9**–**11** with the relative ratio (1:1:3) (·····), of pure isomer **9** (——), and of C_{60} (- - - -)[28].

The cycloadditions of substituted phenyldiazomethanes provide access to a broad variety of fullerene compounds bearing functional groups which are important for further chemical modifications and applications of these materials. These reactions were creatively exploited by Wudl[5,17,18,19,21,24,25,26] and others[39]. Substituents on the phenyl ring include amino, hydroxy, alkoxy, alkoxycarbonyl and nitro groups, as well as halogens and crown ethers[18]. In particular, *p,p'*-disubstituted diphenylmethano-bridged fullerenes[40] are easily prepared from readily available substituted

benzophenones, which are converted to diazomethanes via the hydrazones[41]. Also, bis(diazo) compounds react specifically with C_{60}. The cycloaddition of phenylene-bis(diazomethane), for example [Scheme 4.13], leads to the phenyl bridged fullerene dimer **12**, which can be regarded as a "two-pearl section" of the "pearl necklace polymer" with C_{60} as a part of the main chain[19]. The electronic properties of these dimers, such as the electronic absorption spectra and cyclic voltammetry, are indistinguishable from those of other methano-bridged fullerenes.

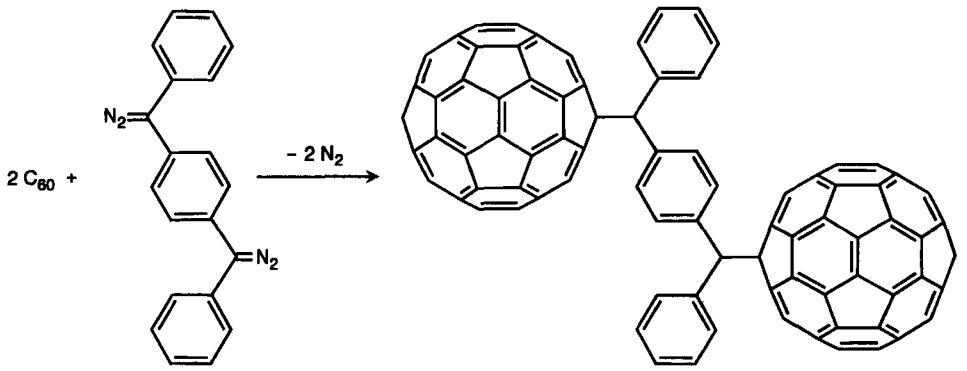

12

Scheme 4.13

As an example of the synthesis of a diphenylmethano-bridged fullerene derivative with reactive functional groups on the phenyl rings, the preparation of the diphenol derivative **13** is given in Scheme 4.14. It can be obtained from the corresponding methyl ether by treatment with BBr_3 in *o*-dichlorobenzene at 0 °C to room temperature in 94 % yield. In contrast to the nonpolar diphenylmethano bridged fullerenes, **13** is soluble and stable in pyridine but only very sparingly soluble in benzene or toluene.

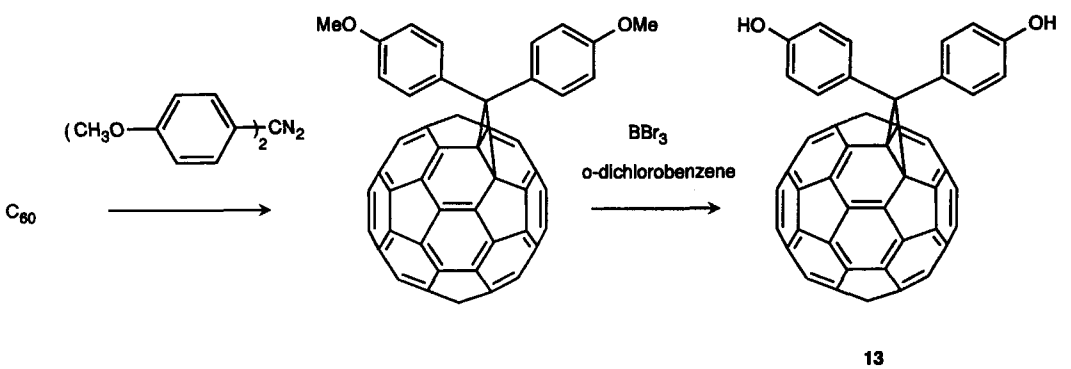

13

Scheme 4.14

Copolymerization of **13** and sebacoyl chloride leads to a polymer with C_{60} pending on the side chain [Scheme 4.15][21]. Poly(ester) **14** is more soluble than the dimer **12**[19] for example in nitrobenzene or benzonitrile. Solution cyclic voltammetry of polymer **14** in THF shows that the electronic properties

of the diphenylmethano-bridged fullerenes are retained. In a similar fashion, **13** can be copolymerized with hexamethylene diisocyanate to give the poly(urethane) **15** as an insoluble brown powder [Scheme 4.15][21]. The structure of **15** was assigned on the basis that its IR spectrum, which is essentially superimposable with that of poly(bisphenol A hexamethyleneurethane) (PBAU).

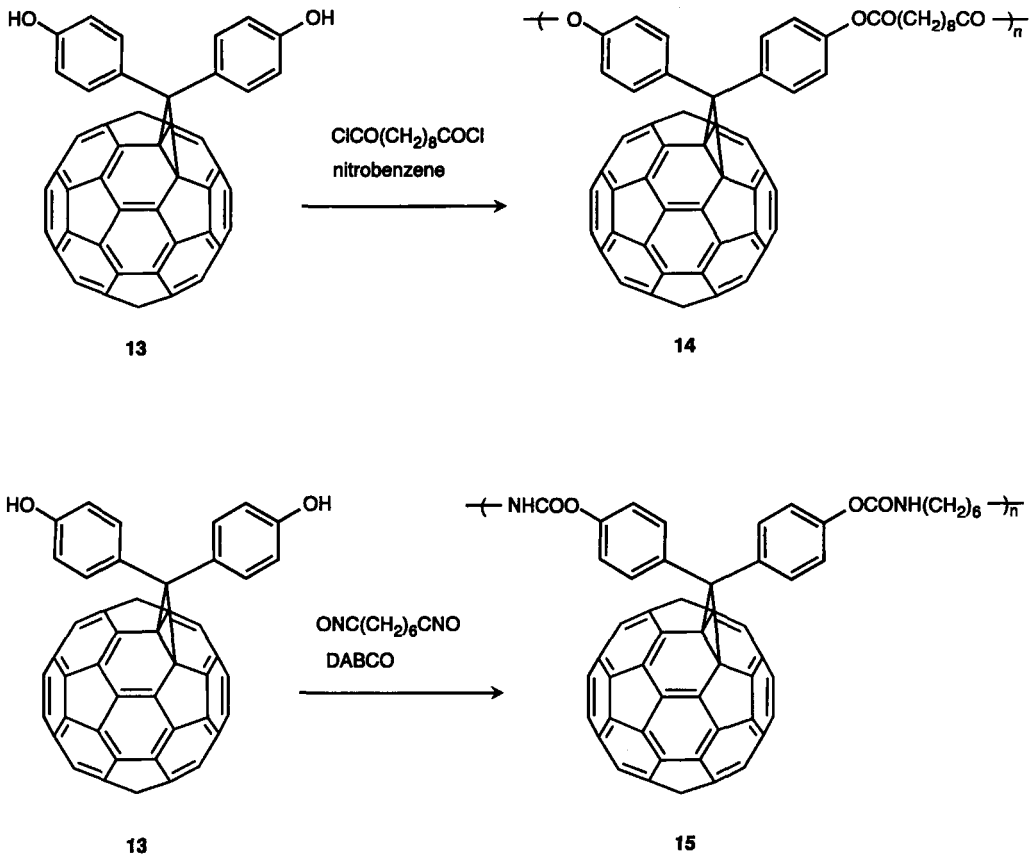

Scheme 4.15

The diphenol derivative **13** has also been used to synthesize fullerene-bound dendrimers by treatment with the fourth-generation dendrimer [G-4]-Br **16** in the presence of K_2CO_3 [Scheme 4.16][26]. The reaction was monitored by size-exclusion chromatography (SEC). Under optimized reaction conditions the dendritic system was obtained in 79 % yield after work up as a light brown-colored glass. The dendritic macromolecules dramatically improve the solubility of the fullerene in organic solvents.

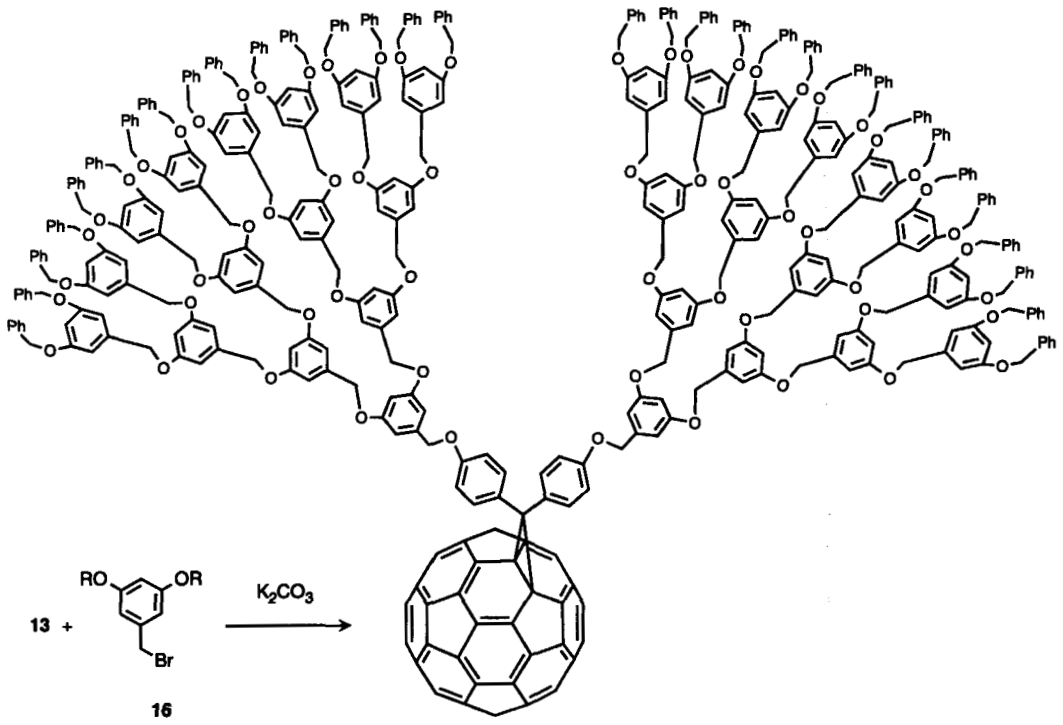

Scheme 4.16

The synthesis of a water-soluble diphenylmethano-bridged fullerene **18** was achieved by hydrolyzing the bis(acetamide) **17** with acetic acid/aqueous hydrochloric acid and then converting it to the bis(succinamide) **18** by treatment with succinic anhydride [Scheme 4.17][42]. Compound **18** is soluble in water at pH ≥ 7. This is an important requirement for the investigation of the biological activity of fullerenes. Remarkably, it has been shown that **18** is an inhibitor for the HIV enzymes protease (HIVP) and reverse transcriptase (HIVRT)[43]. As suggested by molecular modelling, specific C_{60} derivatives fit exactly in the active sites of the enzymes due to their steric and chemical complementarity. In particular, the design considerations require that an "active" C_{60} derivative should have polar functional groups at one end of the carbon cluster, which is fulfilled for **18**. In addition, the compound was also found to be nontoxic to three different lines of test cells. This first example of a biological active fullerene is already impressive and it is obvious that more specific tailor-made derivatives, for example a C_{60} moiety attached as a target on certain oligopeptides, can be expected to show even more potent and selective activity.

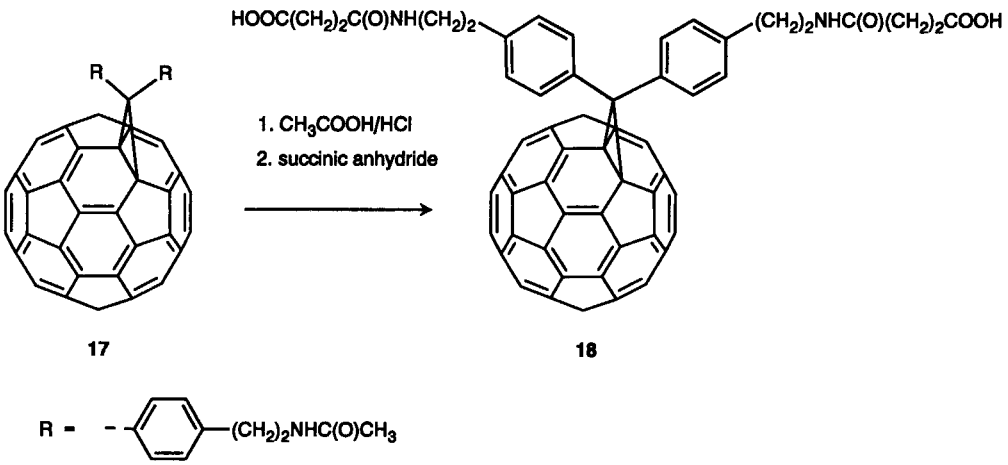

Scheme 4.17

Another versatile synthon for the preparation of fullerene derivatives with polar groups on the side chain is the 1,2-dihydro-1,2-(carboxymethano)fullerene-60 (**19**), which can be obtained either from the corresponding ethoxycarbonylmethyl carboxylate **20** or *tert*-butyl carboxylate **21**, which themselves are accessible by the reaction of the corresponding diazoacetate with C_{60} [Scheme 4.18][27].

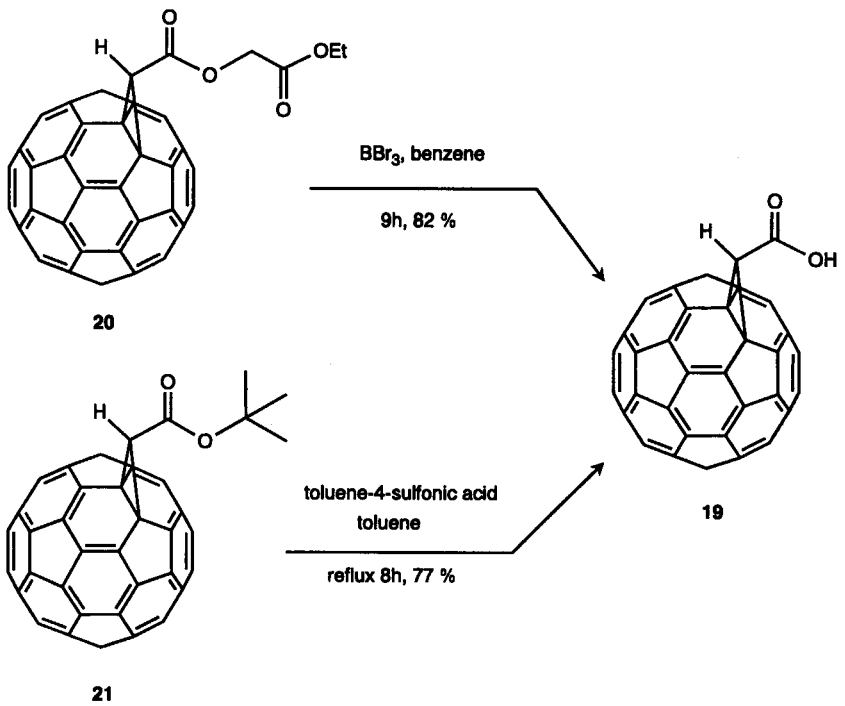

Scheme 4.18

With the carboxylic acid **19**, dicyclohexylcarbodiimide (DCC) mediated esterification and amidation reactions can be carried out [Scheme 4.19][27]. For example, the reaction of **19** with EtOH in the presence of DCC and 1*H*-benzotriazol-1-ol (BtOH) in bromobenzene with a catalytic amount of 4-(dimethylamino)pyridine (DMAP) affords the ester **22** in 68 % yield. Similar to such esterifications the *N*-[(methanofullerene)-carbonyl]-substituted amino acid esters, **23** and **24**, are formed in good yields. Whereas the glycine derivative **23** is poorly soluble in most organic solvents, the phenylalanine derivative **24** is sufficiently soluble in $CDCl_3$ to record ^{13}C NMR spectra.

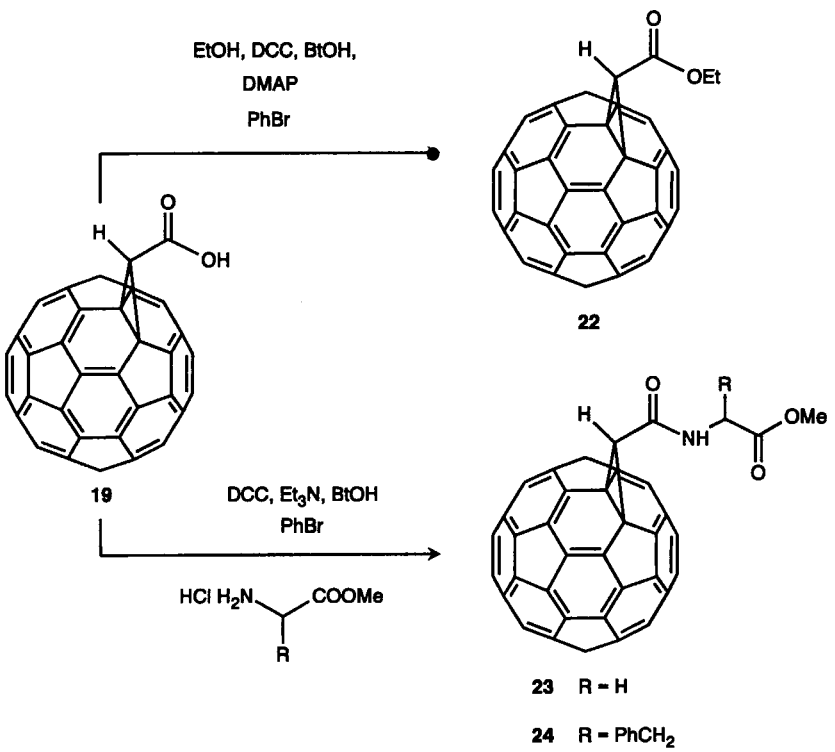

Scheme 4.19

Even an oligopeptide has been attached to C_{60} [Scheme 4.20][25]. This was achieved by coupling to a carboxylic group in the side chain of the cyclopropane ring as well. First, the *tert*-butyl carboxylate **25** was synthesized by the reaction of the corresponding diazomethylbenzoate with C_{60}. After the hydrolysis with trifluoromethanesulfonic acid, the acyl chloride was generated by treatment with oxalyl chloride. Finally, in a one step procedure the fullerene peptide **26** was obtained by the reaction with the N-deprotected pentapeptide H-(*L*-Ala-Aib)$_2$-*L*-Ala-OMe. On the basis of CD and IR spectroscopy, as well as of solvent titration experiments monitored by NMR spectroscopy, it was concluded that the ordered secondary structure predominantly adopted in solution by **26** is the 3_{10}-helix rather than the α-helix.

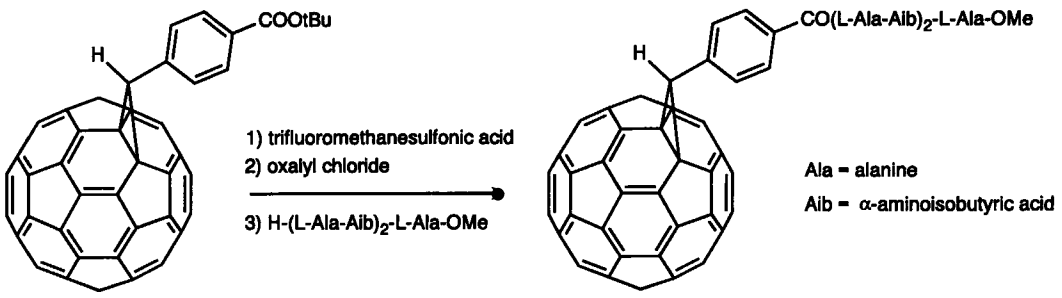

25 **26**

Scheme 4.20

Besides diazomethanes and diazoacetates, cycloaddition of C_{60} with diazoamides have been successfully carried out[29]. A large variety of diazoamides are easily accessible in high yields by direct diazoacetylation with succinimidyl diazoacetate[44] of primary and secondary amino groups in amino compounds including protected amino acids. As in the case of the addition of diazoacetates the synthesis of the amido-, lysine- and phenylalanine derivatives **27–30** [Scheme 4.21] requires elevated temperatures and is carried out in refluxing toluene. In contrast to the different isomers of the addition products of C_{60} with diazomethanes or diazoacetates, which have identical R_f values, the 1,2-methano-bridged and two 1,6-methano-bridged isomers of cycloadduct **27** can be isolated by chromatography on silica gel with toluene as eluent. The 1,2-methano-bridged isomer is the most retentive. The different regioisomers of **28–30** elute simultaneously and are less retentive on silica gel columns. Compared to the morpholenide moiety in **27,** the more extended substituents in **28–30** increase the solubility and at the same time reduce the difference in retention behavior of the regioisomers. This one step synthesis of amide derivatives of C_{60} provides a facile access to fullerene derivatives with biological importance.

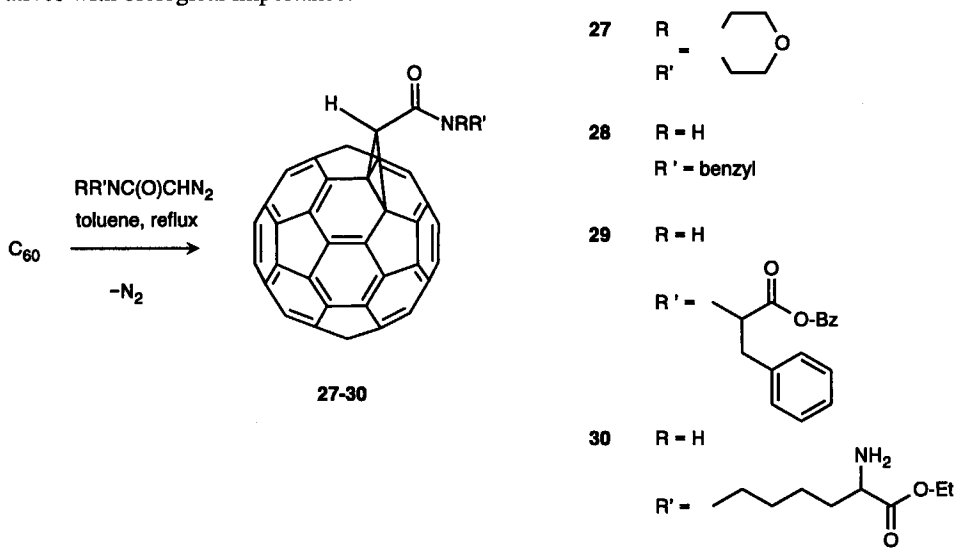

Scheme 4.21

4.3.2 Addition of Azides

Organic azides can also serve as 1,3-dipoles and undergo [3+2] cycloadditions to C_{60}, leading to aza-bridged fullerenes[45]. The azide addition is carried out by refluxing equimolar amounts of C_{60} and the azide in chlorobenzene for several hours [Scheme 4.22]. Thereby, two major products are formed, one of which (**31**) can be converted into the other (**32**) by additional heating in chlorobenzene or in the solid state at 180 °C. As shown by the combination of ^{13}C- and ^{15}N NMR spectroscopy, the thermodynamically most stable isomers **32** have a 1,6-aza-bridged ring-opened structure. The aza-bridged fullerenes are more electronegative than their carbon analogs but not as electronegative as unsubstituted C_{60}, as determined by cyclic voltammetry[45].

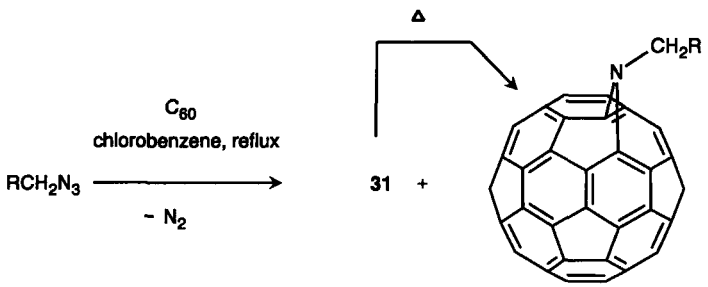

32

Scheme 4.22

4.3.3 Addition of Trimethylenemethanes

Stable five membered ring adducts of C_{60} can be synthesized by [3+2] cycloadditions of trimethylenemethanes (TMM)[5]. The TMM intermediates are prepared in situ by thermolysis from 7-alkylidene-2,3-diazabicycloheptene (nonpolar TMM) and from methylenecyclopropanone ketals (polar TMM). In the case of the methylenecyclopropanone ketal addition [Scheme 4.23], the two compounds, **33** and **34a**, were isolated after chromatography on silica gel.

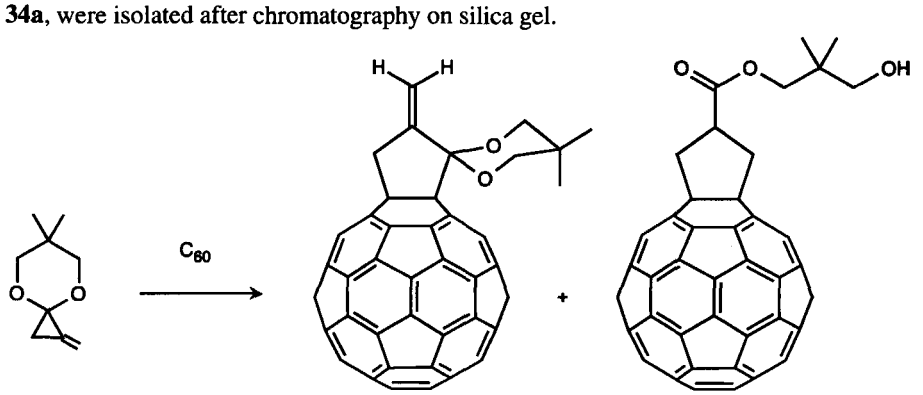

33a **34a**

Scheme 4.23

The structure of the α-methylenecyclopropanone ketal **33** is reminiscent of the addition mode of the corresponding TMM to C=O[46]. The ester **34a** is probably the product of silica gel catalyzed hydrolysis of the ketene acetal **33b**, which is the expected product in the reaction of TMM with electron deficient olefins[47]. NMR spectroscopic investigations of these adducts reveal that the cycloadditions occur at 6–6 double bonds.

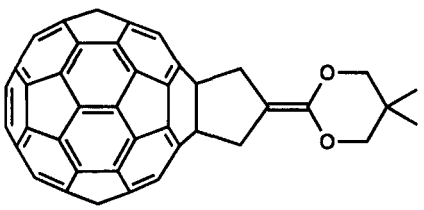

33b

A variety of chemical transformations in the side chain have been carried out with the alcohol **34** as starting material[48]. These valuable investigations are important for the following reasons: (i) The side-chain chemistry provides access to new fullerene derivatives including those with sugar and amino acid moieties which may be important for possible applications, for example investigations of their biological activity; (ii) information becomes available on the scope of reactions which allow side-chain chemistry and at the same time do not affect the fullerene core. In general, it was found that C_{60} survives acidic to weakly basic conditions as well as several oxidations and reductions required to carry out a range of C–O and C–C bond forming reactions [Scheme 4.24, 4.25, 4.26].

In particular the benzoate **34b** can be obtained by the treatment of **34a** with benzoyl chloride and pyridine in toluene or alternatively and more conveniently by condensation with benzoic acid, dicyclohexylcarbodiimide (DCC) and 4-(dimethylamino)pyridine (DMAP) in CH_2Cl_2 [Scheme 4.24]. Similar procedures lead to the methacrylic ester **34c** in quantitative yield as well as to the amino acid derivatives **34d** and **34e**. For the full conversion of **34a** to the corresponding derivatives, an excess of reagents is necessary. The C–O bond formation can also be achieved under acidic conditions. The tetrahydropyranyl ether **34f** was synthesized by the treatment of **34a** with dihydropyran and pyridinium-*p*-toluenesulfonate in quantitative yields. Furthermore the sugar derivative **34g** was obtained by acidic etherification with tri-*O*-acetylglycal in the presence of *p*-toluenesulfonic acid.

The oxidation of the hydroxyl group in **34a** with pyridinium chlorochromate (PCC) in CH_2Cl_2 affords the aldehyde **34h** [Scheme 4.25]. The reduction of **34h** back to **34a** is possible with Et_3SiH in the presence of $TiCl_4$, whereas upon treatment of **34h** with diisobutylaluminium hydride a competitive reaction with the fullerene core was observed.

The aldehyde group in **34h** itself bears a potential for C–C bond elongation reactions. For example, **34i** was obtained in 89 % yield by the reaction with a stabilized ylide as an *E*-isomer (>95:5) [Scheme 4.26]. Also Lewis-acid mediated reactions are possible. The reaction of the aldehyde **34h** with allyltributyltin and $TiCl_4$ gave the homoallylic alcohol **34j** in 86 % yield.

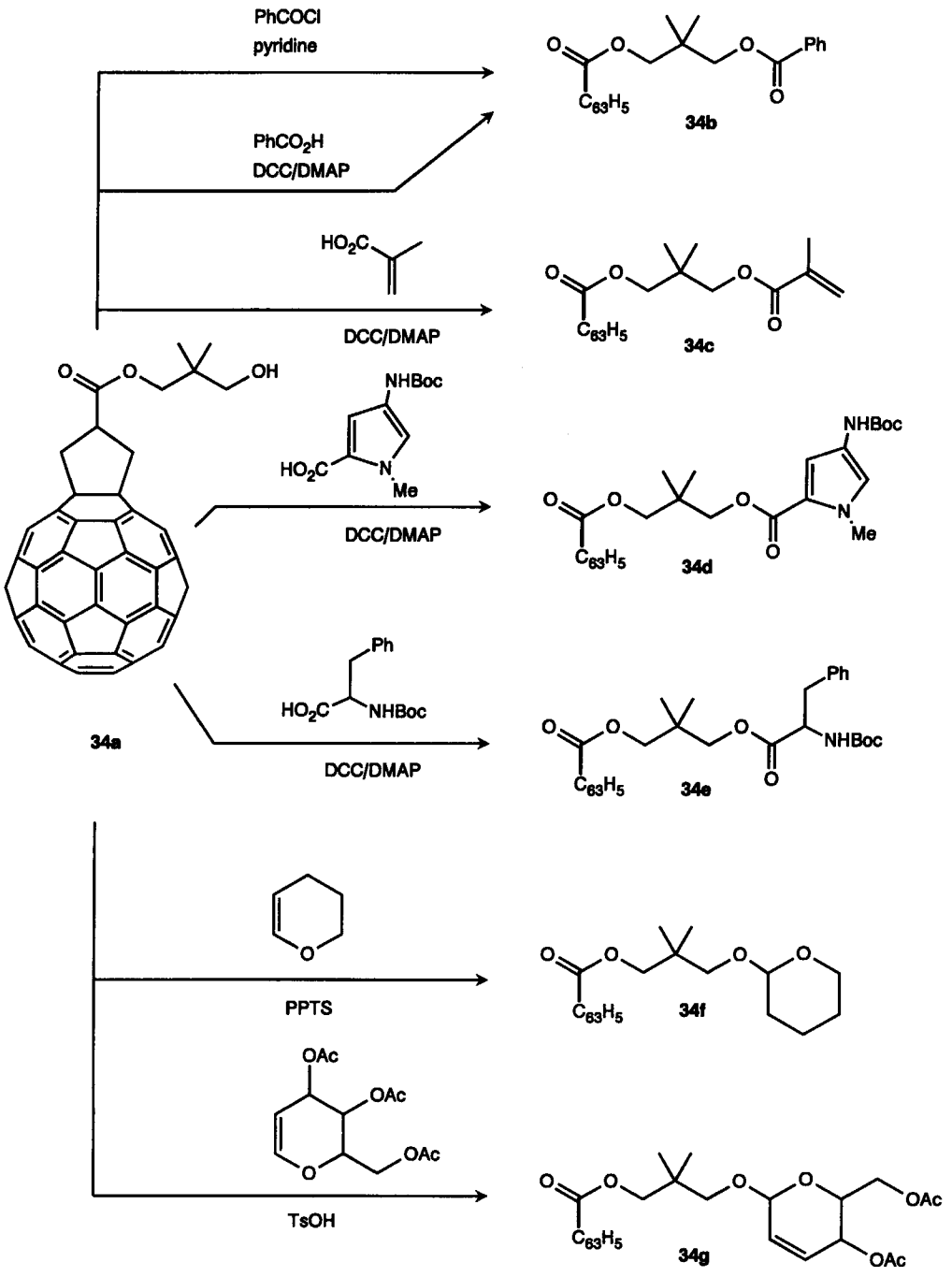
PhCOCl
pyridine
PhCO2H
DCC/DMAP
HO2C
DCC/DMAP
OH
NHBoc
HO2C
N
Me
DCC/DMAP
34a
Ph
HO2C
NHBoc
DCC/DMAP
PPTS
OAc
OAc
OAc
TsOH
C63H5
34b
34c
34d
34e
34f
34g

Scheme 4.24

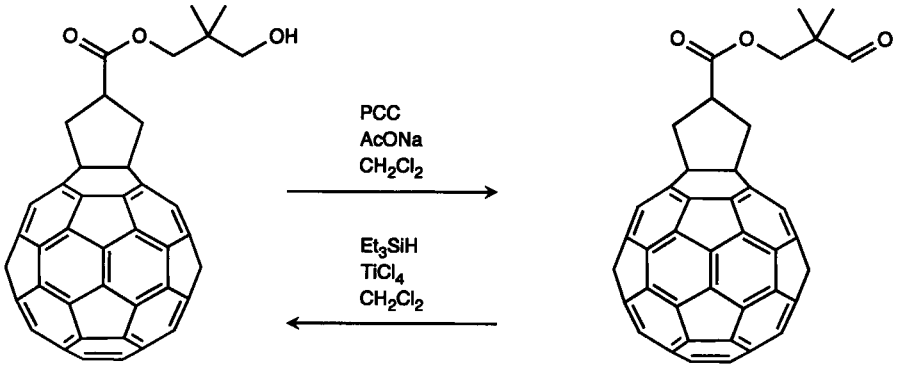

34a **34h**

Scheme 4.25

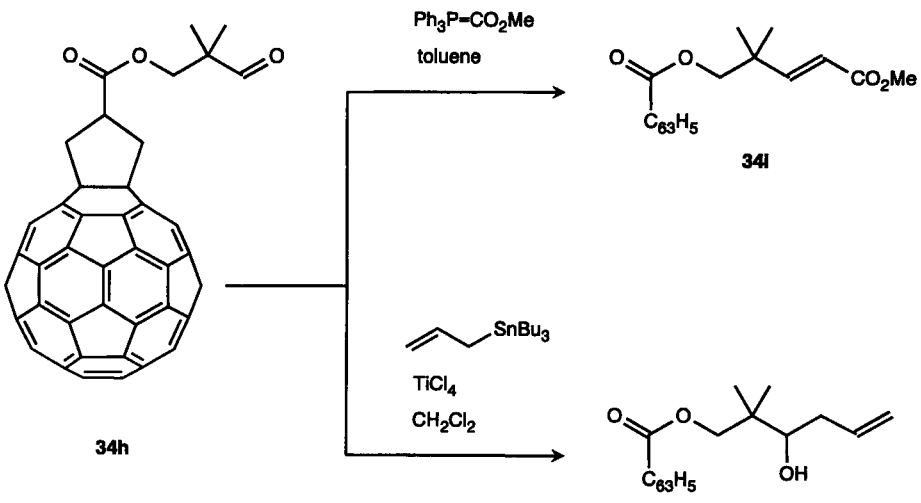

34h **34l** **34j**

Scheme 4.26

Some of these fullerene derivatives **34** have been investigated with respect to their biological activity[49]. To obtain water solubility, a requirement to study the biological activity, alcohol **34a** was transform into the carboxylic acid **34k** by reaction with succinic anhydride in the presence of DMAP. The in vitro cytotoxicity of **34k** against the HeLa S3 cell line was evaluated by the study of the inhibition of growth rate. Compound **34k** kills the cells when the culture is exposed to low-power visible light. The cyctotoxicity of **34k** is mediated by its ability to cleave DNA upon the formation of single strand breaks. It was suggested that this activity is due to the efficient conversion of triplet oxygen into highly reactive singlet oxygen by the photoexcited C_{60} moiety in its triplet state[50].

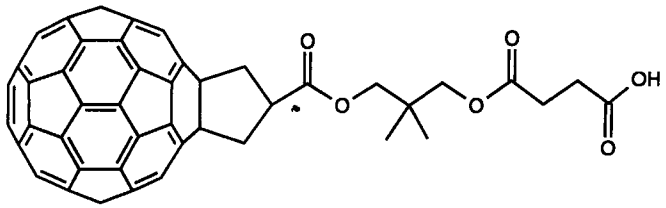

34k

4.3.4 Addition of Azomethine Ylides

Azomethine ylides, planar species of the general formula (R^1R^2)-C=N$^+$$(R^3)$-C-$(R^4R^5)$, which are very reactive 1,3-dipoles, have also been added to C_{60}[51]. These species can be generated in situ from a wide variety of readily accessible starting materials. For example, the azomethine ylide **36**, obtained by decarboxylating *N*-methylglycine in the presence of paraformaldehyde in refluxing toluene, subsequently adds to C_{60} to give the *N*-methylpyrrolidine derivative **37** in 41 % yield [Scheme 4. 27].

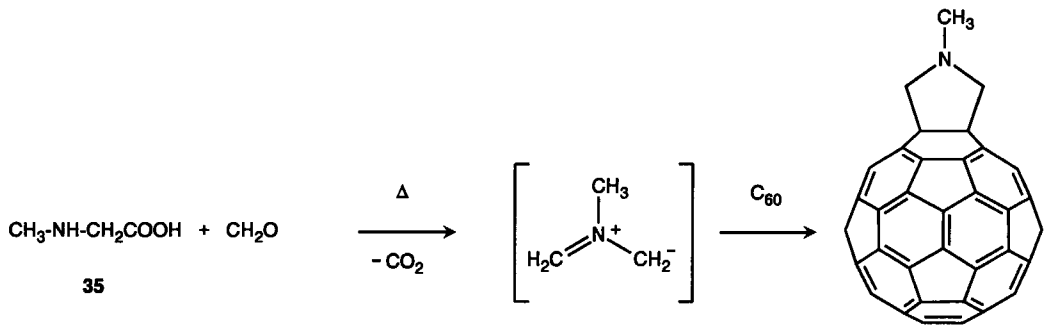

Scheme 4.27

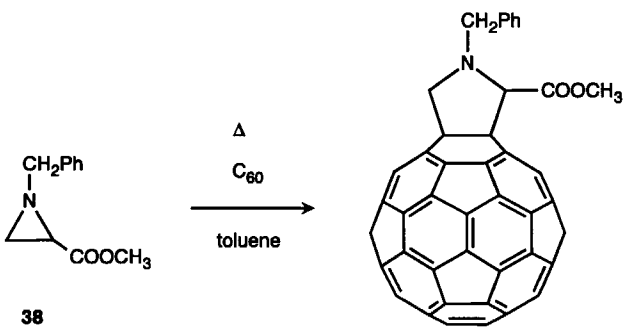

Scheme 4.28

The pyrrolidine derivative **39** has been synthesized by the addition of the corresponding azomethine ylide generated by the thermal ring opening of the aziridine **38** as shown in Scheme 4.28.

Additions of azomethine ylides to C_{60} provide another versatile method for the derivatization of fullerenes, since these reactions tolerate a large variety of functional groups. In addition, further side chain chemistry can be carried out. For example, upon heating the 3-triphenylmethyl-5-oxazolidinone (**40**) at reflux for 16 h with C_{60} in equimolar amounts, compound **41** can be isolated in 39 % yield. The subsequent treatment of **41** with trifluoromethanesulfonic acid, then pyridine and dansyl chloride (DnsCl) yields the dansyl pyrrolidine derivative **43** in 76 % yield [Scheme 4.29]. During this reaction pathway, the amine **42** is involved as intermediate.

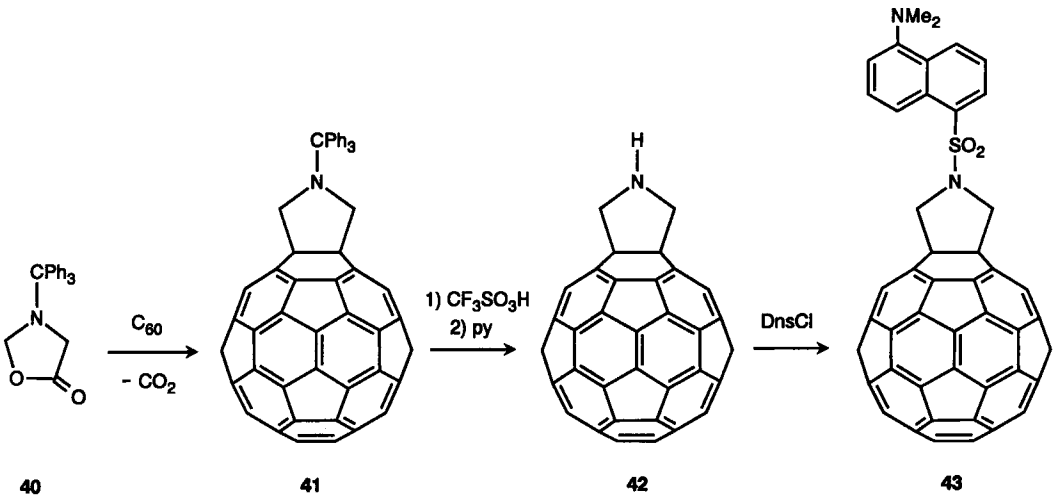

40 **41** **42** **43**

Scheme 4.29

The combination of two electroactive species, C_{60} as well as ferrocene, is realized in compound **44** which was synthesized by heating a mixture of ferrocene aldehyde, *N*-methylglycine and C_{60} in toluene at reflux. The cyclic voltammetry of **44** shows both the reduction pattern of the C_{60} moiety and the oxidation pattern of the ferrocene moiety.

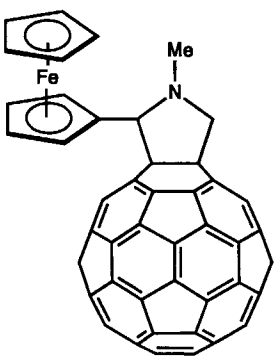

44

4.3.5 Addition of Nitrile Oxides

Isoxazoline derivatives **45** of C_{60} are accessible by 1,3-dipolar cycloadditions of nitrile oxides to 6-6 double bonds of the fullerene [Scheme 4.30][52,53] . The nitrile oxides with R = methyl, ethyl, ethoxycarbonyl and anthryl are generated *in situ* from the corresponding nitroalkane, phenylisocyanate and triethylamine. The isoxazoline derivative of C_{60} with R = anthryl (**45d**) crystallizes in black prisms out of a solvent mixture of CS_2 and acetone (3:2)[53]. The X-ray crystal structure analysis of **45d** [Fig. 4.5] confirms the NMR spectroscopic results which show that the addition of the nitrile oxide occurs on a 6-6 double bond of the fullerene framework. In these crystals, the fullerene derivative **45d** forms a CS_2 inclusion compound in the ratio 1:1.

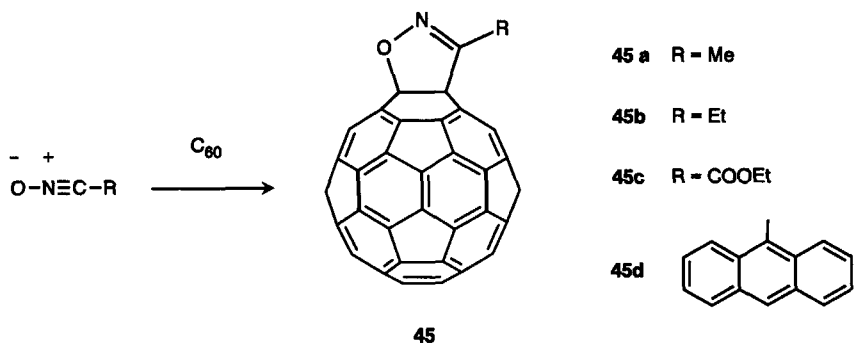

Scheme 4.30

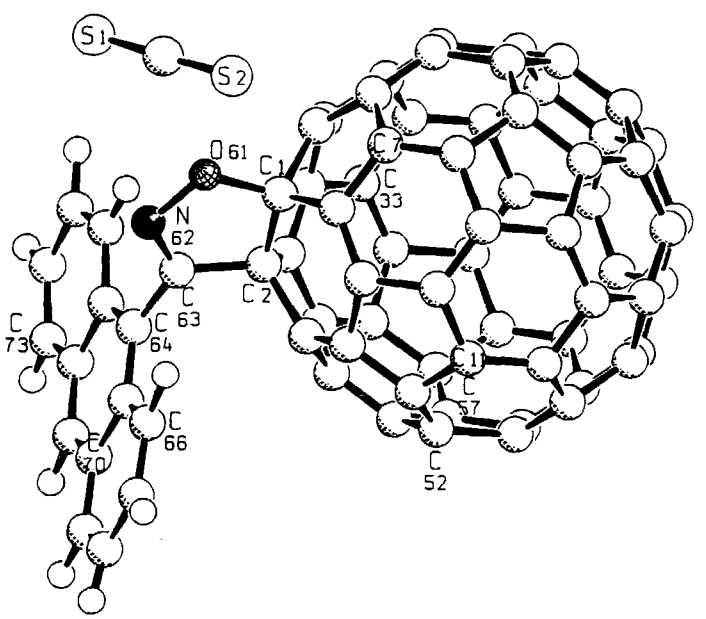

Figure 4.5 Molecular structure of **45d** in the single crystal[53].

4.3.6 Addition of Sulfinimides

A sulfur-containing heterocyclic fullerene derivative **46** has been synthesized by the reaction of C_{60} with *N*-(1-adamantyl)bis(trifluoromethyl)sulfinimide [Scheme 4.31][54]. The sulfinimide can be prepared from the corresponding sulfenamide by 1,3-dehydrohalogenation. High yields of **46** with only a small amount of higher adducts can be obtained if an excess of C_{60} is allowed to react with the sulfinimide. Compound **46** is stable up to 300 °C. The ^{19}F NMR spectrum of **46** exhibits one singlet, which is in contrast to that of the starting material. This provides evidence that the addition of the sulfinimide occurs at the 6-6 bond. Only in this structure is the magnetic equivalence of the two trifluoromethyl groups given. The reaction of C_{60} with a large excess of the sulfinimide results in the formation of the hexaadduct within one week.

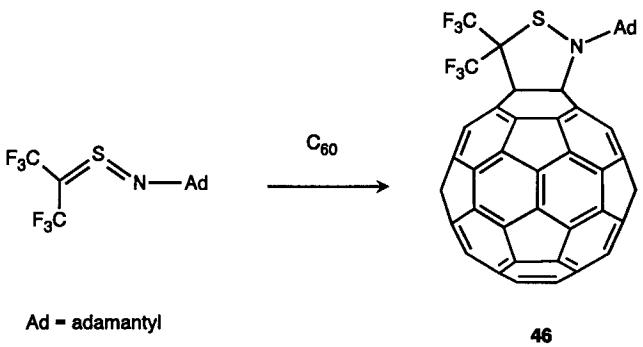

Ad = adamantyl

46

Scheme 4.31

4.3.7 Addition of Disiliranes

Photoexcited C_{60} is a stronger electron acceptor than C_{60} in the ground state[55,56,57]. Since strained Si-Si σ bonds can act as electron donors, a photochemical cycloaddition of disiliranes to C_{60} is possible. The irradiation of a toluene solution of 1,1,2,2-tetramesityl-1,2-disilirane and C_{60} with a high pressure mercury-arc lamp results in the formation of the 1,1,3,3-tetramesityl-1,3-disilolane **47** in 82 % yield with complete consumption of C_{60} [Scheme 4.32][58]. A similar photochemical cycloaddition was obtained with 1,1,2,2-tetrakis(2,6-dimethylphenyl)-1,2-disilirane. The disiliranes are thermally unreactive toward C_{60} at 90 °C. NMR investigations as well as theoretical calculations at the AM1 level reveal a 6-6 ring bridged structure for **47**. The rate of disappearance of C_{60} during the photoreaction was suppressed by the addition of diazabicyclo[2.2.2]octane and by tetramethoxybenzene, each of which has a lower oxidation potential and is unreactive to photoreaction of C_{60}. The reaction was completely suppressed by the addition of rubrene as triplet quencher. These observations were interpreted by the presence of photochemically generated exciplex intermediates derived from the disilirane and a triplet state of C_{60}.

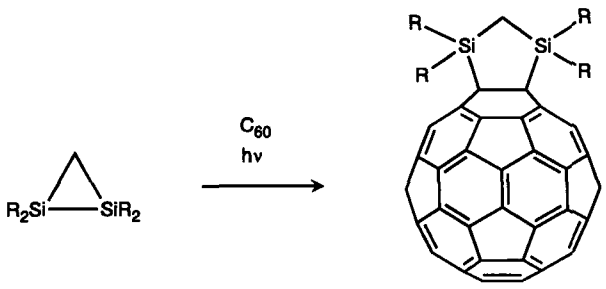

Scheme 4.32

4.4 [2+2] Cycloadditions

4.4.1 Addition of Benzyne

The addition of benzyne to C_{60} leads to [2+2] cycloadducts[59,60,61]. An alternative [4+2] cycloaddition was not observed. The in situ generation of benzyne can be achieved by diazotization of anthranilic acid at room temperature with isoamyl nitrite, by diazotization of the potassium salt of anthranilic acid in the presence of 18-crown-6 and by the oxidation of 1-aminobenzotriazole with lead tetraacetate [Scheme 4.33]. The adduct formation occurs in the 1,2-position leading to the corresponding ring-closed structure.

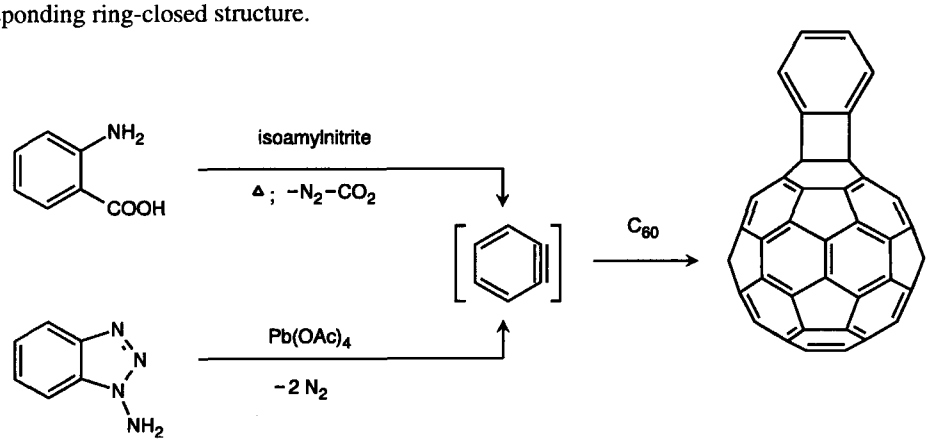

Scheme 4.33

4.4.2 Addition of Enones

The photochemical [2+2] cycloaddition of enones to C_{60} is possible by irradiation of benzene solutions of the components with a high pressure mercury lamp or with a XeCl excimer laser[62] [Scheme 4.34]. Analysis of the reaction products by ^1N NMR, IR and "Buckyclutcher"-HPLC[63] shows

that the isolated monoadducts **48** are a mixture of two isomers, which are the *cis* and *trans*-fused stereoisomers arising from the [2+2] cycloaddition to a 6–6 bond of C_{60}. Significantly, the IR carbonyl stretching frequencies of these two isomers differ remarkably by about 20 cm^{-1}. The *cis* and *trans* isomers of **48** are chiral (C_1 symmetry). The corresponding enantiomers of each diastereomer for R = Me have been resolved and isolated by HPLC using chiral stationary phases[64]. Chiroptical investigations indicate that the fullerene moiety in the strained *trans* cycloadducts has a skewed π-system with local C_2 symmetry. The enantiomers of the *trans* adducts show a much greater polarometric response than those of the *cis* adducts. These [2+2] cycloadditions cannot be achieved by irradiation at 532 nm where C_{60} is the only light absorbing component. This indicates that fullerene triplets, being efficiently produced from fullerene singlets[65], do not undergo addition to ground state enones. It was suggested that the photochemical [2+2] cycloadditions of enones to C_{60} proceeds by stepwise addition of enone triplet excited states to the fullerene via an intermediate triplet 1,4-biradical, which is consistent with the observation that alkenes, such as cyclopentene or cyclohexene, do not photochemically cycloadd to C_{60}[62].

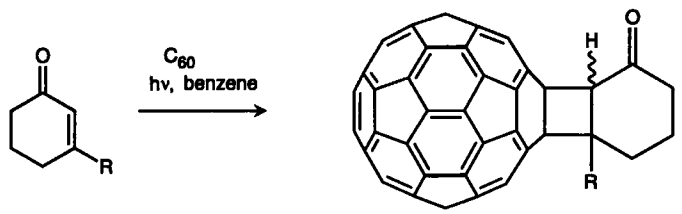

48

Scheme 4.34

4.4.3 Addition of Quadricyclane

A thermal [2+2] cycloaddition of quadricyclane can be achieved by allowing a 10-fold excess to react with C_{60} in toluene at 80 °C[66] [Scheme 4.35].

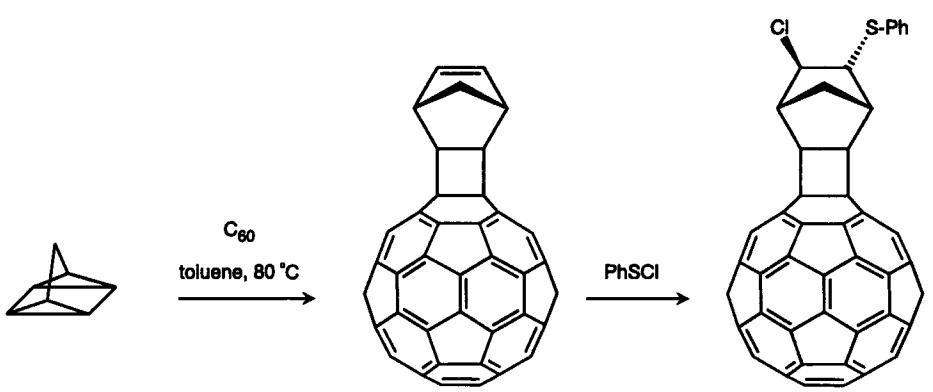

49

Scheme 4.35

The reaction proceeds smoothly and gives **49** in 43 % yield. The stereochemistry of the addition is *exo* with respect to the norbornene moiety and in line with the usual cycloaddition behavior of quadricyclane[67]. The norbornene double bond in **49** is unhindered and reacts readily with electrophiles. For example, the *anti*-addition of benzenesulfenyl chloride proceeds quantitatively at room temperature [Scheme 4.35].

4.4.4 Addition of Electron Rich Alkynes

The ease of the photoreaction of C_{60} with electron rich organic molecules has been used to cycloadd *N,N*-diethylpropynylamine to C_{60} upon irradiation of oxygen-free toluene solutions of the components for 20 minutes at room temperature [Scheme 4.36][68].

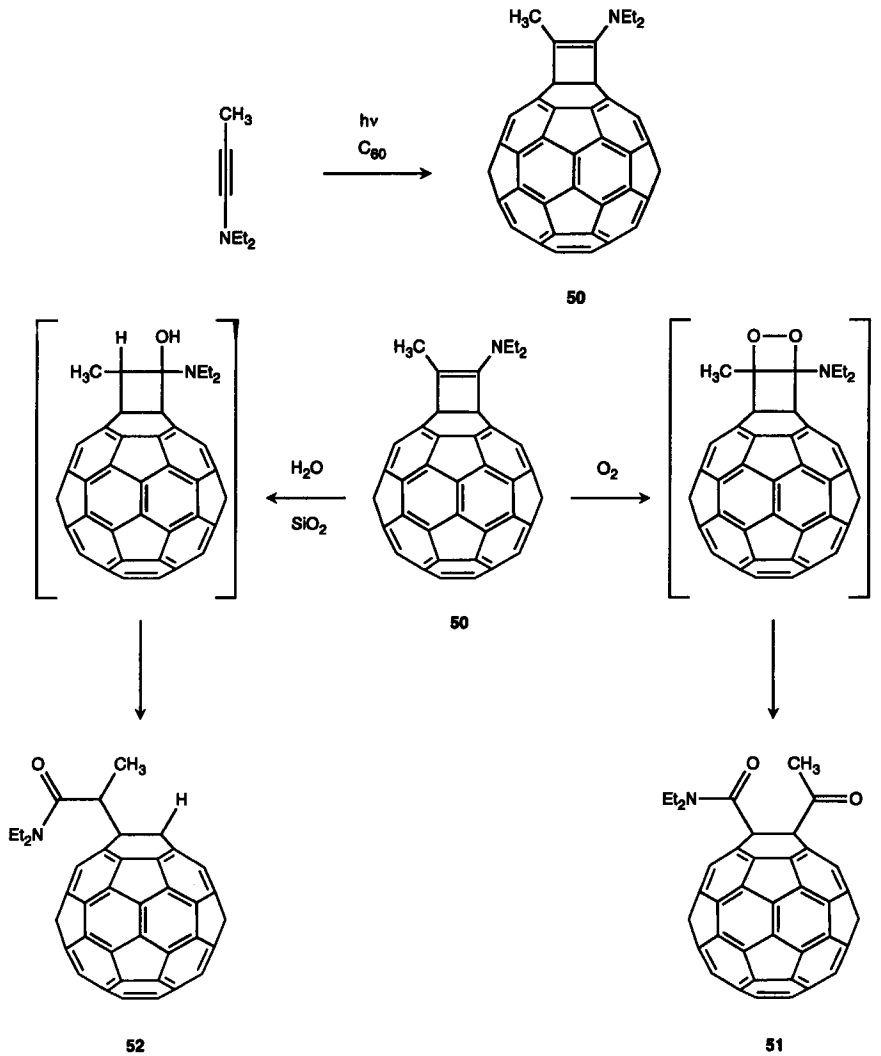

Scheme 4.36

The formation of the cycloadduct **50** by thermal treatment of C_{60} with the alkyne was shown to be very slow. The cycloadduct **50** is not very stable and upon exposure to air and room light for 2 hours cleanly produces the oxoamide **51** via a 1,2-dioxetane intermediate [Scheme 4.36]. The SiO_2 catalyzed hydrolysis of **50** leads to the amide **52** and not the cyclobutanone and diethylamine [Scheme 4.36]. Apparently the dihydrofullerene core is such a strong electron acceptor that it is a better leaving group than diethylamine.

4.4.5 Photopolymerization of C_{60}

If oxygen-free C_{60} films are irradiated with visible or ultraviolet light, a phototransformation into a polymer occurs[69,70,71,72,73]. After phototransformation, the films are no longer soluble in toluene. The optical absorption spectra show that the electronic absorptions of C_{60} are broadened but appear at the same positions. It was concluded from IR and Raman spectroscopy that the fullerenes are linked together by carbon-carbon bonds. In the laser desorption mass spectra of the polymers, peaks of up to 20 crosslinked C_{60} molecules $(C_{60})_n$ were observed. A photochemical [2+2] reaction was proposed which drives the photopolymerization of solid C_{60} [Fig. 4.6]. The mechanism proceeds via the long-lived triplet T_1 state and exhibits a temperature threshold near 250 K. This mechanism is active in molecular solids when two carbon double or triple bonds on adjacent molecules are oriented parallel to one another and are separated by less that ≈ 4.2 Å[74]. This requirement is fulfilled in solid C_{60}, where the molecules are separated by as little as 3.5 Å.

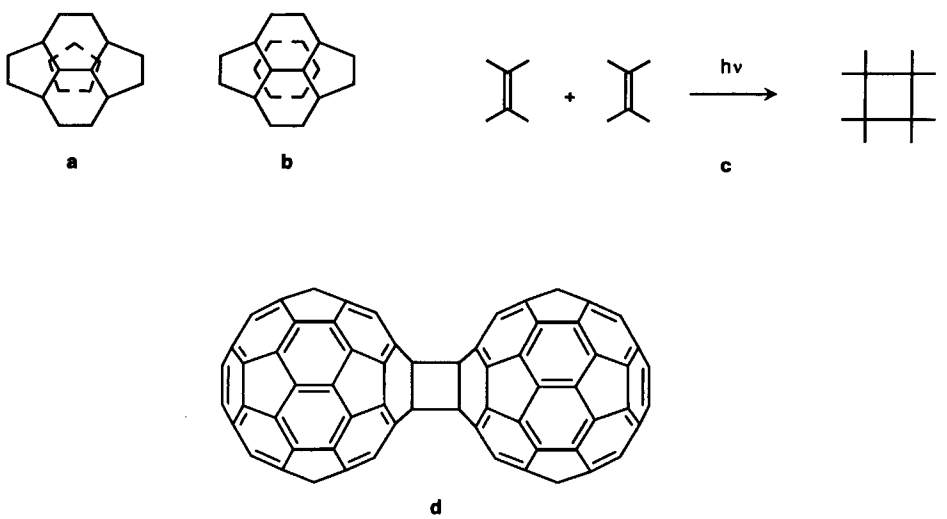

Figure 4.6 Two possible conformations (**a**) and (**b**) of adjacent C_{60} molecules in the solid state. Schematic [2+2] cycloaddition reaction between parallel carbon double bonds on adjacent molecules (**c**). A C_{60} dimer produced by a photoinduced [2+2] cycloaddition reaction.

4.5 [2+1] Cycloadditions

4.5.1 Addition of Carbenes

Thermal extrusion of N_2 from *O*-benzyl- and *O*-pivaloyl-protected diazirin produces carbenes which react with C_{60} in toluene to give the fullerene sugars **53**[75] [Scheme 4.37]. These [2+1] carbene additions cleanly lead to 1,2-methano-bridged sugar monoadducts. The fullerene derivatives **53** are chiral and enantiomerically pure.

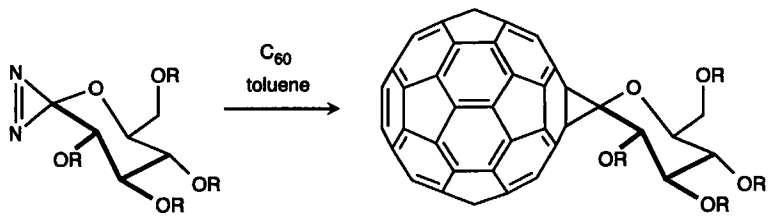

53 R = Bn, Piv

Scheme 4.37

The dimethoxymethanofullerene **54** has been synthesized via the corresponding carbene, which was prepared in situ upon the thermolysis of the oxadiazole **55** in 32 % yield [Scheme 4.38][27].

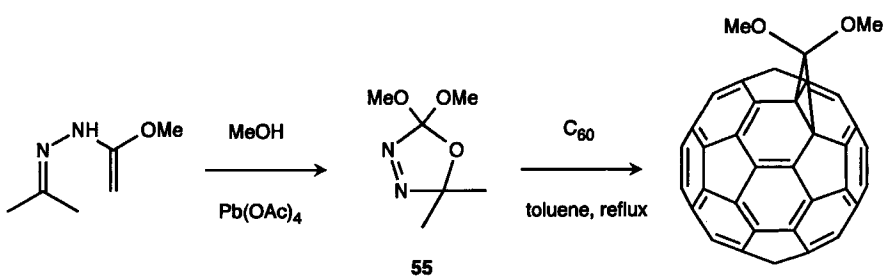

55 **54**

Scheme 4.38

4.5.2 Addition of Silylenes

The addition of bis(2,6-diisopropylphenyl)silylene as a reactive divalent species to C_{60} [Scheme 4.39] yields the [2+1] cycloadduct **56** as the ring-closed 1,2-bridged isomer[76]. The silylene was prepared in situ from the trisilane **57** by photolysis with a low-pressure lamp in toluene solution.

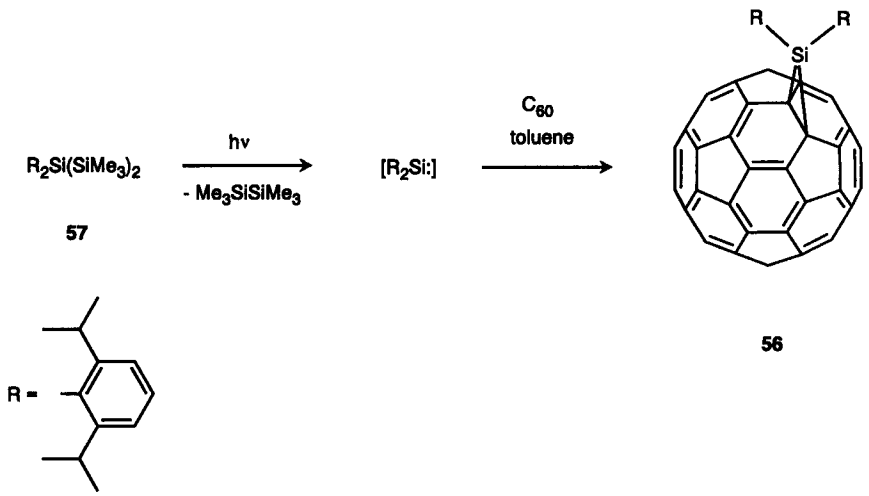

Scheme 4.39

References

1 F. Wudl, A. Hirsch, K. C. Khemani, T. Suzuki, P.-M. Allemand, A. Koch, H. Eckert, H.; G. Srdanov, H. Webb In *Fullerenes: Synthesis, Properties, and Chemistry of Large Carbon Clusters;* G. S. Hammond, V. J. Kuck, Eds.; p 161 American Chemical Society Symposium Series 481, 1992.

2 V. M. Rotello, J. B. Howard, T. Yadev, M. M. Conn, E. Viani, L. M. Giovane, A. L. Lafleur *Tetrahedron Lett.* **1993**, *34*, 1561.

3 M. Tsuda, T. Ishida, T. Nogami, S. Kurono, M. Ohashi *J. Chem. Soc., Chem. Commun.* **1993**, 1296.

4 J. A. Schlueter, J. M. Seaman, S. Taha, H. Cohen, K. R. Lykke, H. H. Wang, J. M. Williams *J. Chem. Soc., Chem. Commun.* **1993**, 972.

5 M. Prato, T. Suzuki, H. Foroudian, Q. Li, K. Khemani, F. Wudl, J. Leonetti, R. D. Little T. White, B. Rickborn, S. Yamago, E. Nakamura *J. Am. Chem. Soc.* **1993**, *115*, 1594.

6 M. F. Meidine, R. Roers, G. J. Langley, A. G. Avent, A. D. Darwish, S. Firth, H. W. Kroto, R. Taylor, D. R. M. Walton *J. Chem. Soc., Chem. Commun.* **1993**, 1342.

7 P. Belik, A. Gügel, J. Spikermann, K. Müllen *Angew. Chem.* **1993**, *105*, 95, *ibid. Int. Ed. Engl.* **1993**, *32*, 78.

8 A. Gügel, A. Kraus, J. Spikermann, P. Belik, K. Müllen *Angew. Chem.* **1994**, *106*, 601; *ibid. Int. Ed. Engl.* **1994**, *33*, 559.

9 P. Belik, A. Gügel, A. Kraus, J. Spikermann, V. Enkelmann, G. Frank, K. Müllen *Adv.Mater.* **1993**, *5*, 854.

10 F. Diederich, U. Jonas, V. Gramlich, A. Hermann, H. Ringsdorf, C. Thilgen *Helv. Chim. Acta* **1993**, *76*, 2445.

11 A. Gügel, M. Becker, D. Hammel, L. Mindach, J. Räder, T. Simon, M. Wagner, K. Müllen *Angew. Chem.* **1992**, *104*, 666; *ibid. Int. Ed. Engl.* **1992**, *31*, 644.

12 A. Gügel, K. Müllen *J. Chromatogr.* **1993**, 23.

13 Y. Rubin, S. Khan, D. I. Freedberg, C. Yeretzian *J. Am. Chem. Soc.* **1993**, *115*, 344.

14 S. I. Khan, A. M. Oliver, M. N. Paddon-Row, Y. Rubin *J. Am. Chem. Soc.* **1993**, *115*, 4919.

15 Y.-Z. An, J. L. Anderson, Y. Rubin *J. Org. Chem.* **1993**, *58*, 4799.

16 B. Kräutler, M. Puchberger *Helv. Chim. Acta* **1993**, *76*, 1626.

17 T. Suzuki, Q. Li, K.C. Khemani, F. Wudl, Ö. Almarsson *Science* **1991**, *254*, 1186.

18 F. Wudl *Acc. Chem. Res.* **1992**, *25*, 157.

19 T. Suzuki, Q. Li, K. C. Khemani, F. Wudl *J. Am. Chem. Soc.* **1992**, *114*, 7300.

20 T. Suzuki, Q. Li, K.C. Khemani, F. Wudl *J. Am. Chem. Soc.* **1991**, *114*, 7301.

21 S. Shi, K. C. Khemani, Q. Li, F. Wudl *J. Am. Chem. Soc.* **1992**, *114*, 10656.

22 A. B. Smith III, R. M. Strongin, L. Brard, G. T. Furst, W. J. Romanow, K. G. Owens, R. C. King *J. Am. Chem. Soc.* **1993**, *115*, 5829.

23 M. Prato, T. Suzuki, F. Wudl, V. Lucchini, M. Maggini *J. Am. Chem. Soc.* **1993**, *115*, 7876.
24 M. Prato, V. Lucchini, M. Maggini, E. Stimpfl, G. Scorrano, M. Eiermann, T. Suzuki, F. Wudl *J. Am. Chem. Soc.* **1993**, *115*, 8479.
25 M. Prato, A. Bianco, M. Maggini, G. Scorrano, C. Toniolo, F. Wudl *J. Org. Chem.* **1993**, *58*, 5578.
26 L. Wooley, C. J. Hawker, J. M. J. Frechet, F. Wudl, G. Srdanov, S. Shi, Q. Li, M. Kao *J. Am. Chem. Soc.* **1993**, *115*, 9836.
27 L. Isaacs, F. Diederich *Helv. Chem. Acta* **1993**, *76*, 2454.
28 L. Isaacs, A. Wehrsig, F. Diederich *Helv. Chim. Acta* **1993**, *76*, 1231.
29 A. Skiebe, A. Hirsch *J. Chem. Soc., Chem. Commun.* **1994**, 335.
30 K. Raghavachari, C. Sosa *Chem. Phys. Lett.* **1993**, *209*, 223.
31 D. A. Dixon, N. Matsuzawa, T. Fukunaga, F. N. Tebbe *J. Phys. Chem.* **1992**, *96*, 6107.
32 N. Matsuzawa, D.A. Dixon, T. Fukunaga *ibid.* **1992**, *96*, 7594
33 N. Matsuzawa, T. Fukunaga, D. A. Dixon *ibid.* **1992**, *96*, 10747.
34 A. Hirsch, A. Soi, H.R. Karfunkel *Angew. Chem.* **1992**, *104*, 808; *ibid. Int. Ed. Engl.* **1992**, *31*, 766.
35 C. C. Henderson, C. M. Rohlfing, P. A. Cahill *Chem. Phys. Lett.* **1993**, *213*, 383.
36 a) E. Vogel *Pure Appl. Chem.* **1969**, *20*, 237; b) E. Vogel *ibid.* **1982**, *54*, 1015; c) E. Vogel *ibid.* **1993**, *65*, 143.
37 A. Pasquarello, M. Schlüter, R. C. Haddon *Science* **1992**, *257*, 1660.
38 S. R. Wilson, Y. Wu *J. Chem. Soc., Chem. Commun.* **1993**, 784.
39 J. Osterodt, M. Nieger, P.-M. Windscheif, F. Vögtle *Chem. Ber.* **1993**, *126*, 2331.
40 F. Wudl In *Buckminsterfullerenes;* W. E. Billups, M. A. Ciufolini Eds; VCH: Weinheim, 1993; pp 317-335.
41 J. March *Advanced Organic Chemistry*, 3 rd Edition; Wiley: New York, 1985; p 1062.
42 R. Sijbesma, G. Srdanov, F. Wudl, J. A. Castoro, C. Wilkins, S. H. Friedman, D. L. DeCamp, G. L. Kenyon *J. Am. Chem. Soc.* **1993**, *115*, 6510.
43 S. M. Friedman, D. L. DeCamp, R. P. Sijbesma, G. Srdanov, F. Wudl, G. L. Kenyon *J. Am. Chem. Soc.* **1993**, *115*, 6506.
44 A. Quihia, L. Rene, J. Guilhem, C. Pascard, B. Badet *J. Org. Chem.* **1993**, *58*, 1641.
45 M. Prato, Q. Li, F. Wudl, V. Lucchini *J. Am. Chem. Soc.* **1993**, *115*, 1148.
46 S. Yamago, E. Nakamura *J. Org. Chem.* **1990**, *55*, 5553.
47 S. Yamago, E. Nakamura *J. Am. Chem. Soc.* **1989**, *111*, 7285.
48 S. Yamago, H. Tokuyama, E. Nakamura, M. Prato, F. Wudl *J. Org. Chem. 1993*, *58*, 4796.
49 H. Tokuyama, S. Yamago, E. Nakamura, T. Shiraki, Y. Sugiura *J. Am. Chem. Soc.* **1993**, *115*, 7918.
50 J. W. Arbogast, C. S. Foote *J. Am. Chem. Soc.* **1991**, *113*, 8886.
51 M. Maggini, G. Scorrano, M. Prato *J. Am. Chem. Soc.* **1993**, *115*, 9798.
52 M. S. Meier, M. Poplawska *J. Org. Chem.* **1993**, *58*, 4524
53 H. Irngartinger, C. M. Köhler, U. Huber-Patz, W. Krätschmer *Chem Ber.* **1994**, *127*, 581.
54 D. Brizzolara, J. T. Ahlemann, H. W. Roesky, K. Keller *Bull. Chim. Fr.* **1993**, *130*, 745.
55 J. W. Arbogast, C. S. Foote, M. Kao *J. Am. Chem. Soc.* **1992**, *114*, 2277.
56 J. W. Arbogast, A. P. Darmanyan, C. S. Foote, Y. Rubin, F. Diederich, M. M. Alvarez, S. J. Anz, R. L. Whetten *J. Phys. Chem.* **1991**, *95*, 11.
57 R. J. Sension, A. Z. Szarka, G. R. Smith, R. M. Hochstrasser *Chem. Phys. Lett.* **1991**, *185*, 179.
58 T. Akasaka, W. Ando, K. Kobayashi, S. Nagasa *J. Am. Chem. Soc.* **1993**, *115*, 10366.
59 A. Gügel, *Doctoral Thesis*, Max-Plank Institut Mainz, 1993.
60 M. Tsuda, T. Ishida, T. Nogami, S. Kurono, M. Ohashi *Chem. Lett.* **1992**, 2333.
61 S. H. Hoke II, J. Molstad, D. Dilattato, M. J. Jay, D. Carlson, B. Kahr, R. G. Cooks *J. Org. Chem.* **1992**, *57*, 5069.
62 S. R. Wilson, N. Kaprinidis, Y. Wu, D. I. Schuster *J. Am. Chem. Soc.* **1993**, *115*, 8495.
63 C. J. Welch, W. H. Pirkle *J. Chromatgr.* **1992**, *609*, 89.
64 S. R. Wilson, Y. Wu, N. A. Kaprinidis, D. I. Schuster *J. Org. Chem.* **1993**, *58*, 6548.
65 J. W. Arbogast, C. S. Foote, M. Kao *J. Am. Chem. Soc.* **1992**, *114*, 2277.
66 M. Prato, M. Maggini, G. Scorrano, V. Lucchini *J. Org. Chem.* **1993**, *58*, 3613.
67 T. L. Gilchrist, R. C. Storr *Organic Reactions and Orbital Symmetry;* Cambridge University Press: Cambridge, 1979; p 163.
68 X. Zhang, A. Romero, C. S. Foote *J. Am. Chem. Soc.* **1993**, *115*, 11024.
69 A. M. Rao, P. Zhou, K.-A. Wang, G. T. Hager, J. M. Holden, Y. Wang, W. T. Lee, X. X. Bi, P. C. Eklund, D. S. Cornett, M. A. Duncan, I. J. Amster *Science* **1993**, *259*, 955.
70 D. S. Cornett, I. J. Amster, M. A. Duncan, A. M. Rao, P. C. Eklund *J. Phys. Chem.* **1993**, *97*, 5036.
71 P. Zhou, Z. H. Dong, A. M. Rao, P. C. Eklund *Chem. Phys. Lett.* **1993**, *211*, 337.

72 Y. Wang, J. M. Holden, Z. H. Dong, X. X. Bi, P. C. Eklund *Chem. Phys. Lett.* **1993**, *211*, 341.
73 A. Ito, T. Morikawa, T. Takahashi *Chem. Phys. Lett.* **1993**, *211*, 333.
74 K. Venkatesan, V. Ramamurthy In *Bimolecular Photoreactions in Crystals*, V. Ramamurthy, Ed; VCH: Weinheim, 1991; Chap. 4; 133.
75 A. Vasella, P. Uhlmann, C. A. A. Waldraff, F. Diederich, C. Thilgen *Angew. Chem.* **1992**, *104*, 1383; *ibid. Int. Ed. Engl.* **1992**, *31*, 1388.
76 T. Akasaka, W. Ando, K. Kobayashi, S. Nagase *J. Am. Chem. Soc.* **1993**, *115*, 1605.

Chapter 5 Hydrogenation

5.1 Introduction

5.2 Oligohydrofullerenes $C_{60}H_{2n}$ and $C_{70}H_{2n}$ (n = 1–6)
5.2.1 Hydrogenation via Hydroboration, Hydrozirconation and Zinc/Acid Reduction
5.2.2 Theoretical Investigations

5.3 Polyhydrofullerenes $C_{60}H_{2n}$ and $C_{70}H_{2n}$(n = 7–30)
5.3.1 Birch–Hückel Reduction
5.3.2 Transfer Hydrogenation of C_{60} and C_{70}
5.3.3 Catalytic Hydrogenation
5.3.4 Theoretical Investigations

References

5.1 Introduction

From the beginning of the "fullerene era", one of the obvious challenges for the chemists, having these new fascinating unsaturated molecules in their hands, was the hydrogenation to "fulleranes". Indeed, hydrogenations of C_{60} were among the first reported attempts to chemically modify fullerenes. However, reaching this goal has been shown to be very difficult. No complete structural characterization of any polyhydrofullerene has so far successfully been carried out. Also, the completely hydrogenated $C_{60}H_{60}$ has not been synthesized up to now. The reason is the instability of the polyhydrofullerenes. Why are the polyhydrofullerenes, even those which are not completely saturated such as $C_{60}H_{36}$, unstable? This question has been answered, at least partly, on the basis of brilliant theoretical investigations, systematically carried out on several $C_{60}H_{2n}$'s. An increasing degree of hydrogenation introduces considerable strain into the framework of the spheres. It turns out that this instability is one of the characteristic and unique properties of fullerene chemistry. On the other hand, hydrides of fullerenes with a very low degree of hydrogenation, such as $C_{60}H_2$, $C_{60}H_4$ and $C_{70}H_2$, have been specifically synthesized and completely characterized. Since organic fullerene chemistry is still a young discipline, this field is being intensively researched and it is only a question of time until characterizable polyhydrofullerenes, at least those with a moderate degree of hydrogenation, will become available.

5.2 Oligohydrofullerenes $C_{60}H_{2n}$ and $C_{70}H_{2n}$ (n = 1–6)

5.2.1 Hydrogenation via Hydroboration and Hydrozirconation

One approach to the synthesis of hydrofullerenes is defined stoichiometrically controlled additions to only one or a few reactive 6–6 double bonds of C_{60} and C_{70}. Presuming that the addition patterns are similar to those of nucleophilic additions and cycloadditions (Chapters 3 and 4), then a limited number of energetically favored isomers can be expected in the reaction mixtures. This would allow the chromatographic isolation and also the systematic characterization of isomerically pure hydrofullerenes with a low degree of hydrogenation. Especially in the case of the simplest hydrocarbon derivatives $C_{60}H_2$ and $C_{70}H_2$, the number of thermodynamically and kinetically favored isomers is very low. The high regioselectivtity of nucleophilic additions to C_{60} and C_{70} in which two-step mechanisms are involved imply that similar two-step procedures, for example, a hydrometalation followed by hydrolysis, should be promising methods to synthesize oligohydrofullerenes. This was demonstrated by the synthesis of $C_{60}H_2$ via hydroboration and hydrozirconation [Scheme 5.1][1,2]. This simplest of the hydrocarbon derivatives of C_{60} has also been prepared by a defined zinc/acid reduction[3]. In each case, only a single regioisomer of dihydrofullerene-60 ($C_{60}H_2$) is formed, which can be isolated from the reaction mixture by HPLC. The analysis of the ^1H NMR spectra of $C_{60}H_2$ and the deuterated $C_{60}HD$ prepared by hydrolysis of the reaction intermediate $C_{60}HBH_2$ with D_2O, demonstrates complete accordance with the results of the hydroalkylation reactions[4,5] (Chapter 3). This regioisomer is the 1,2-addition product. As in the case of the 1-organo-1,2-dihydrofullerenes, the fullerenyl protons in the parent 1,2-dihydrofullerene $C_{60}H_2$ resonate at low field, ca. δ = 5.9 in toluene-d_8[1]. Another fingerprint, the UV/Vis spectra[1,2] of the chestnut-brown solutions of $C_{60}H_2$, especially the sharp band at 430 nm, independently reveal a characteristic property of the 1,2-monoadduct of C_{60}[4].

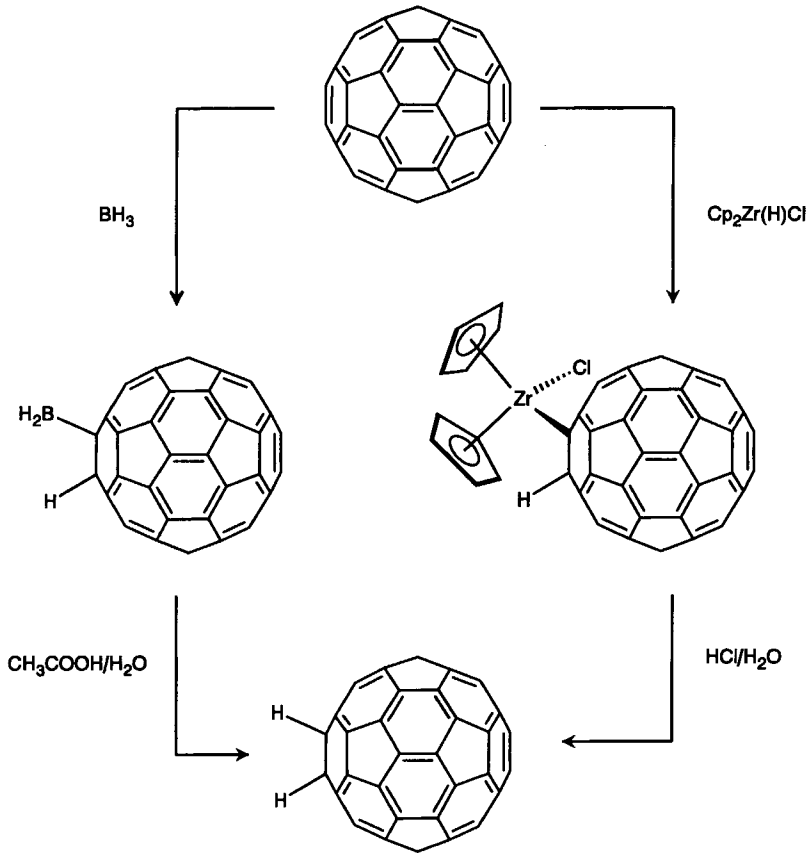

Scheme 5.1

The electrochemical behavior of C_{60} determined by cyclic voltammetry[3] is very similar to that of $C_{60}HR$ (R = alkyl)[6]. The reduction waves are slightly shifted to more negative potentials compared to C_{60}. Interestingly, the reduction of $C_{60}H_2$ at slower scan rates is accompanied by the appearance of a new set of reoxidation waves at potentials which closely match the anodic peak potentials of the corresponding parent C_{60} species. The formation of C_{60} out of $C_{60}H_2$ during cyclic voltammetry was confirmed by HPLC analysis. The experiments indicate the instability of anionic hydrofullerenes.

The very soluble intermediate $(\eta^5\text{-}C_5H_5)_2ZrClC_{60}H$ [Scheme 5.1] is accessible to further hydrozirconations[2]. Therefore, by using a two-fold excess of $(\eta^5\text{-}C_5H_5)_2Zr(H)Cl$, the higher adducts $[(\eta^5\text{-}C_5H_5)_2ZrCl]_nC_{60}H_n$ (n = 2,3) are formed as by-products. Their hydrolysis leads to $C_{60}H_4$ and $C_{60}H_6$ as a mixture of different regioisomers. The defined regioisomer 1,2,3,4-$C_{60}H_4$ of tetrahydrofullerene-60 was obtained as major product by the hydroboration and subsequent hydrolysis of $C_{60}H_2$ in 10-15 % yield [Scheme 5.2][7]. This most polar *cis*-1 regioisomer makes up approximately 50 % of the total amount of $C_{60}H_4$. It was observed that a mixture of $C_{60}H_4$ isomers partially isomerizes on a Pt contaminated Buckyclutcher I column to 1,2,3,4-$C_{60}H_4$, which also indicates that this regioisomer is the major kinetic and apparent thermodynamic product.

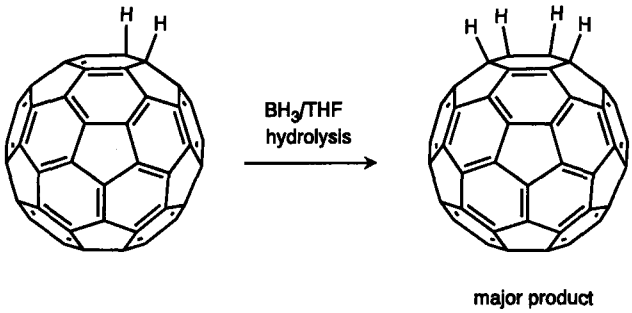

Scheme 5.2

Upon hydroboration of C_{70} followed by hydrolysis of the presumed intermediates $C_{70}HBH_2$, two isomers of $C_{70}H_2$ are obtained. These are the 1,2-dihydrofullerene-70 (**1**) as the major and the 3,4-dihydrofullerene-70 (**2**) as the minor reaction product [Scheme 5.3][8,9].

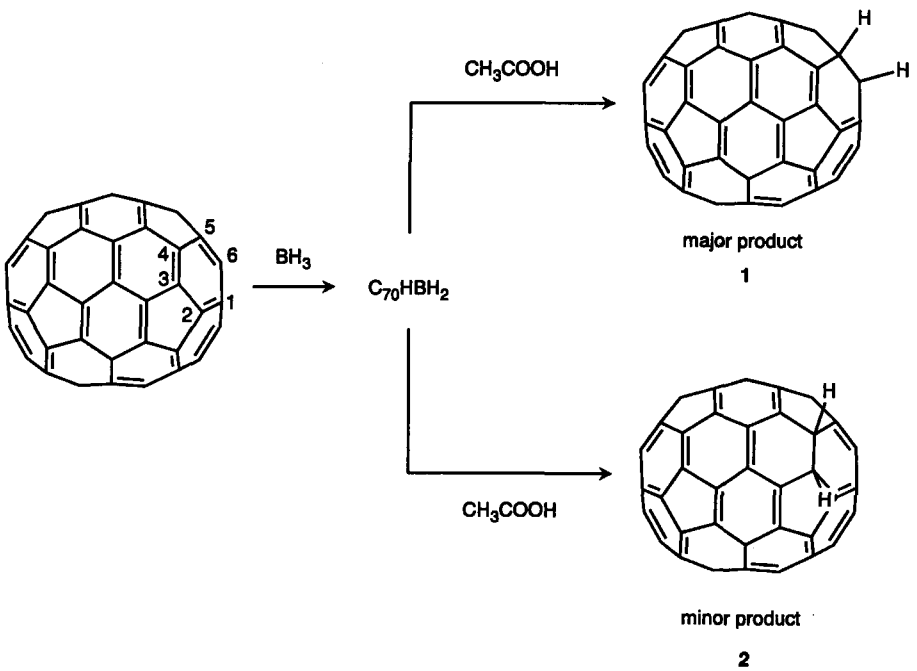

Scheme 5.3

In hydroalkylation or -arylation reactions of C_{70}, only the thermodynamically most stable 1,2-isomers of alkylated or arylated $C_{70}HR$ were isolated from the reaction mixture[4]. Both isomers **1** (1,2-adduct) and **2** (3,4-adduct) of $C_{70}H_2$ are kinetic products of the two-step hydrogenation reaction. An isomerization in pure solution at room temperature for several weeks or at 100 °C for one hour is not observed[8,9]. The 3,4-product is less stable toward decomposition than the 1,2-isomer, but both isomers are indefinitely stable in toluene/hexane solution at -20 °C. A conversion of pure isomer **2** to a mixture of **1** and **2** (isomerization), and C_{70} (decomposition) over a platinum on silica catalyst was

observed at room temperature. The energy difference ΔG_{295} of these isomers was experimentally determined to be 1.4 ± 0.2 kcal/mol with 1,2-$C_{70}H_2$ being lower in energy.

5.2.2 Theoretical Investigations

For the dihydrofullerene $C_{60}H_2$, 23 different regioisomers are in principle possible. The formal addition of an A-B molecule, for example H_2, to the externally C_{60} sphere could proceed in three ways[10]: (1) The addition to one double bond of the low-energy Kekulé structure [Fig. 5.1], which would leave all the other bonds unchanged (6-6 double bonds and 5-6 single bonds); (2) the conjugate addition of two atoms, which requires the formal introduction of 5-6 double bonds in order to retain a closed-shell Kekulé structure [Fig 5.1]; and (3) the hydrogenolysis that accompanies cleavage of a bond in C_{60}. A variety of calculations of different isomers of $C_{60}H_2$ and $C_{70}H_2$ were carried out at the MNDO level[4,8,10,11]. The results of the MNDO calculations[10] for all 23 regioisomers of $C_{60}H_2$ are listed in Table 5.1. The most stable isomer of $C_{60}H_2$ is indeed the 1,2-addition product, which was exclusively found in the experiments. The next three most stable isomers are the 1,4-, the 1,16- and the 1,6-adducts respectively. In the former one and in the latter two 5-6 double bonds have to be introduced into the canonical Kekulé structure. For the closed-shell isomers an additional introduction of a 5-6 double bond costs about 8.5 kcal/mol [Tab. 5.1, Fig. 5.2].

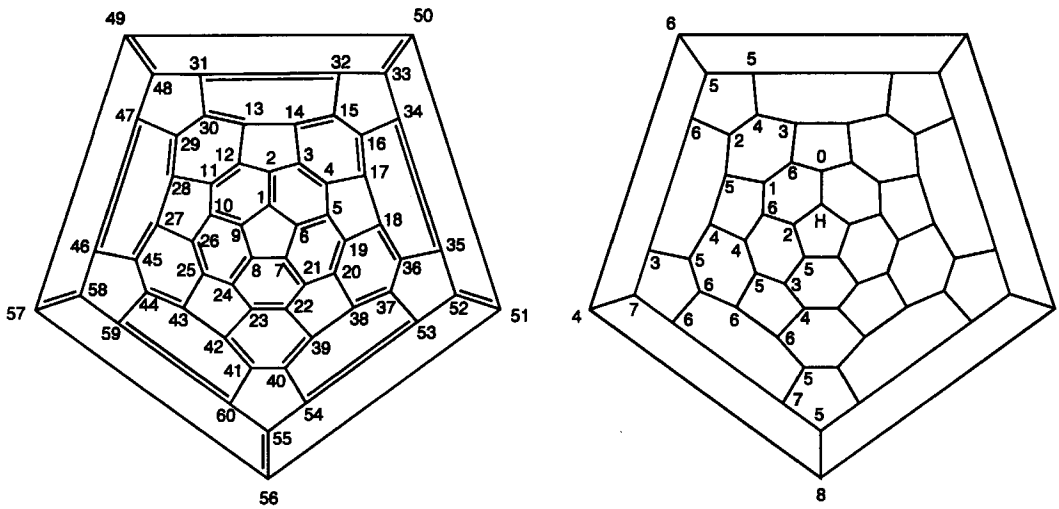

Figure 5.1 (A) Numbering system and lowest energy canonical Kekulé structure of C_{60}. (B) Topologically counted minimum number of 5-6 double bonds which have to be introduced by the addition of two hydrogens[10].

The 1,2- and the 1,4-isomers differ only by about 4 kcal/mol. In the 1,2-isomer, other than removing one π-bond, the bonding of the framework does not change. However, there is an eclipsing interaction present between the two hydrogen atoms in the neighboring 1 and 2 positions, which was estimated to be 3-5 kcal/mol. In the 1,4-isomer one 5-6 double is introduced, which costs 8.5 kcal/mol but there are no eclipsing interactions present. Thus, the 1,2-isomer should be about 4-6 kcal/mol more stable than the 1,4- isomer which is in agreement with the calculated energy difference [Tab. 5.1].

Table 5.1 Symmetry, spin states, calculated MNDO heats of formation ($\Delta H_f°$) and number of 5–6 double bonds for $C_{60}H_2$[10]

isomer[a]	symmetry	spin state	$\Delta H_f°$ kcal/mol	bond alterations[b]
C_{60}	I_h	singlet	811.7	
$C_{60}H_2$-6	C_s	singlet	794.5	2
	C_s	triplet	815.8	
$C_{60}H_2$-7	C_s	singlet	822.1	5
	C_s	triplet	815.8	
$C_{60}H_2$-10	C_1	singlet	821.6	6
$C_{60}H_2$-4	C_s	singlet	780.0	1
	C_s	triplet	815.2	
$C_{60}H_2$-2	C_{2v}	singlet	776.1	0
	C_s	triplet	828.1	
$C_{60}H_2$-19	C_2	singlet	807.9	4
$C_{60}H_2$-20	C_1	singlet	817.1	5
$C_{60}H_2$-21	C_1	singlet	800.1	3
	C_1	triplet	814.1	
$C_{60}H_2$-22	C_1	singlet	809.6	4
	C_1	triplet	812.8	
$C_{60}H_2$-16	C_1	singlet	791.6	2
$C_{60}H_2$-15	C_s	singlet	808.2	4
	C_s	triplet	809.7	
$C_{60}H_2$-36	C_1	singlet	816.5	5
$C_{60}H_2$-37	C_1	singlet	824.8	6
$C_{60}H_2$-38	C_s	singlet	825.2	6
$C_{60}H_2$-39	C_1	singlet	826.5	6
	C_2	OS	813.5	
	C_2	triplet	812.9	
$C_{60}H_2$-40	C_1	singlet	819.1	5
	C_1	OS	813.3	
	C_1	triplet	812.8	
$C_{60}H_2$-35	C_1	singlet	801.5	3
$C_{60}H_2$-52	C_1	singlet	831.8	c
	C_1	OS	831.9	
	C_1	triplet	812.8	
$C_{60}H_2$-53	C_1	singlet	826.8	6
$C_{60}H_2$-55	C_s	singlet	820.1	5
	C_{2v}	OS	811.3	
	C_{2v}	triplet	813.4	
$C_{60}H_2$-51	C_2	singlet	811.6	4
$C_{60}H_2$-49	C_1	singlet	824.6	6
$C_{60}H_2$-56	C_s	singlet	835.9	c
	C_{2h}	OS	813.4	
	C_{2h}	triplet	812.8	

[a] the number indicates the carbon carrying the second H-atom.
[b] number of newly formed double bonds in five-membered rings.
[c] for $C_{60}H_2$-52 and $C_{60}H_2$-56 an alternating structure of the C-C single bonds and double bonds is not obtained. In this case the number of bond alterations is not defined.

Enhancing the eclipsing interaction in the 1,2-position by introducing more steric requiring addents will, therefore, lead to a further destabilization and the 1,4-isomer will eventually become the most stable structure. An eclipsing interaction is also present in the 1,6-isomer, which has two 5-6 double bonds and should, therefore, be about 2 x 8.5 kcal/mol less stable than the 1,2-isomer, which is in good agreement with the calculated value of 18.4 kcal/mol [Tab. 5.1]. On the other hand, the 1,16-isomer having no eclipsing interactions and also two 5-6 double bonds is about 3 kcal/mol more stable than the 1,6-isomer.

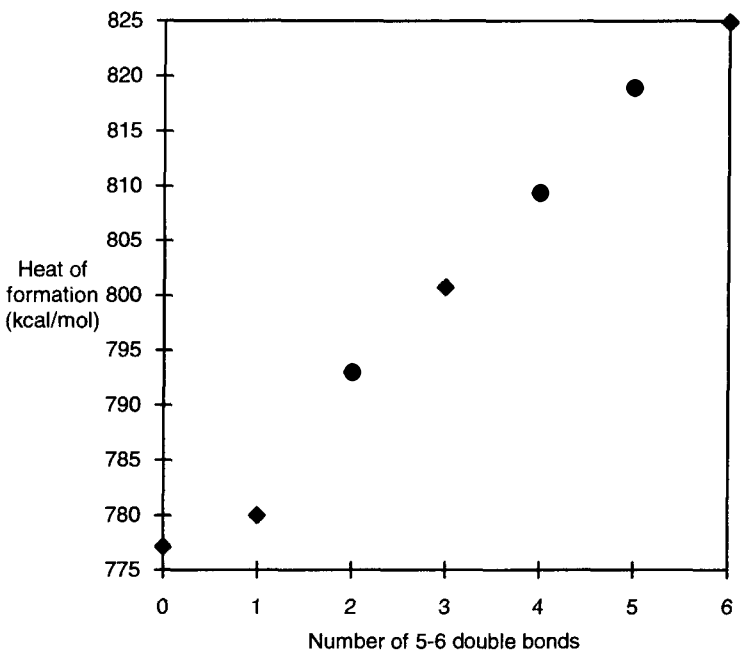

Figure 5.2 Dependence of the MNDO heats of formations ($\Delta H_f°$) of the $C_{60}H_2$ isomers on the number of 5-6 double bonds introduced by the hydrogen addition[10]. The heats of formation are average values of the different structures from Table 5.1 with the same number of 5-6 double bonds.

These four most stable isomers of $C_{60}H_2$ have also been calculated using ab initio methods at the HF/3-21G and HF/6-31G* levels[8]. The investigations show that the energy ordering obtained by semiempirical calculations is preserved [Tab. 5.2]. The energy difference between the isomers, however, becomes more pronounced using ab initio methods. For $C_{70}H_2$, 143 regioisomers are in principle possible. The four most stable isomers calculated by the semiempirical AM1 and MNDO methods[8,11] are represented in Figure 5.3. Additions to the "C_{60} like" double bonds in C_{70} at the pole in the 1,2-position and in the 3,4-position are the most favorable. Whereas at the AM1 and MNDO level the 3,4-isomer is slightly favored over the 1,2-isomer, this order is reversed at both ab initio levels[8,9]. The predictions from the ab initio calculations are consistent with the experimental results. In

the synthesis of $C_{70}H_2$ from C_{70} and BH_3, the 1,2-isomer is the most abundant in the reaction mixture, which contains the 3,4-isomer as the minor product[8]. The calculated energy difference of 1,2-$C_{70}H_2$ (**A**) and 3,4-$C_{70}H_2$ (**B**) at the HF/6-31G* level is in excellent agreement with the experimentally observed value of $\Delta G_{295} = 1.4 \pm 0.2$ kcal/mol[9].

Table 5.2 Relative energies of the most stable isomers of $C_{60}H_2$ and $C_{70}H_2$[8]

	MNDO/PM-3	HF/3-21G	HF/6-31G*
$C_{60}H_2$-2	0.0	0.0	0.0
$C_{60}H_2$-4	3.8	7.8	7.6
$C_{60}H_2$-16	15.5	23.1	20.9
$C_{60}H_2$-6	18.4	26.4	24.0
$C_{70}H_2$ **A**	0.0	0.0	0.0
$C_{70}H_2$ **B**	-1.1	0.2	1.3
$C_{70}H_2$ **C**	0.3	2.1	4.5
$C_{70}H_2$ **D**	1.4	5.8	6.4

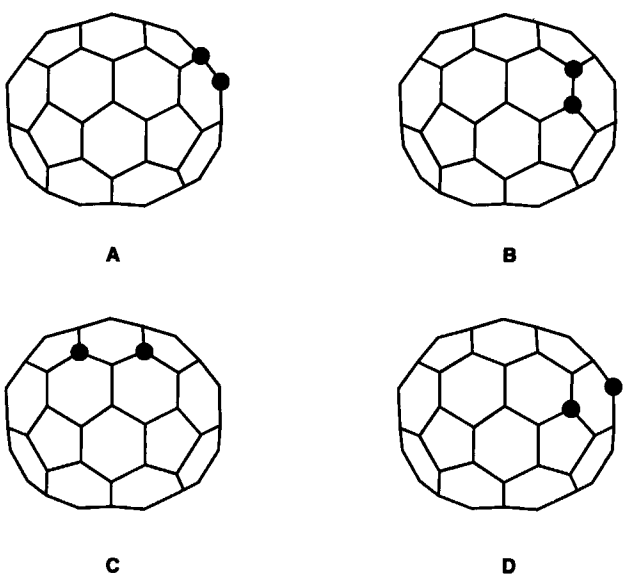

Figure 5.3 The four most stable regioisomers of $C_{70}H_2$[8,11]. The dots represent C-H units.

If the formation of tetrahydrofullerene-60 ($C_{60}H_4$) occurs by additions to two 6-6 double bonds, which are two 1,2-additions with respect to the cyclohexatriene units in C_{60}, then eight regioisomers are possible[12,13]. This very plausible assumption is corroborated by the theoretical investigations of multiple additions to C_{60} in a 1,2- and a 1,4-mode. These investigations predict 1,2-additions to be favorable over 1,4-additions up to the formation of $C_{60}H_{12}$[13] (see also Table 5.5 in Chapter 5.3.4).

Table 5.3 Relative energies in kcal/mol of the eight regioisomers of $C_{60}H_4$ formed by two 1,2-addition to 6-6 double bonds of C_{60}.

	MNDO/AM1	HF/3-21G
cis-1	3.3	0
cis-2	3.5	25
cis-3	2.4	24
e	0	13
trans-4	0.2	17
trans-3	0.4	15
trans-2	0.6	16
trans-1	0.5	16

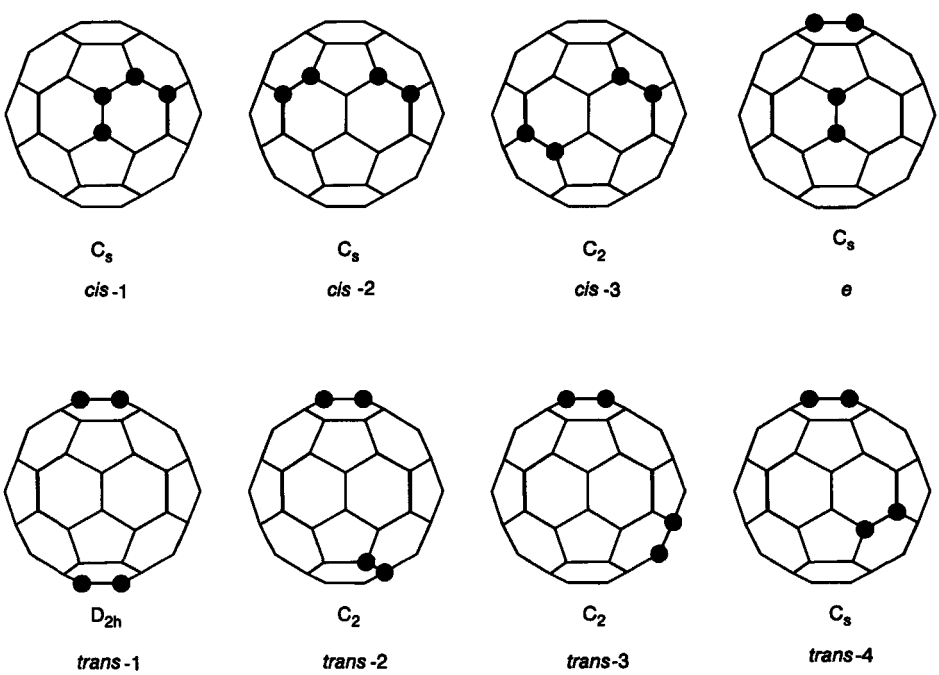

Figure 5.4 The eight regioisomers of $C_{60}H_4$ formed by "1,2-additions". The dots represent C-H units[12,13].

The eight different isomers of $C_{60}H_4$ exhibit a similar AM1 heat of formation with the *cis* isomers being slightly energetically disfavored [Tab. 5.3]. However, according to ab initio calculations the *cis*-1 isomer exhibits a significantly lower energy than the other seven isomers[7]. In addition, the energy spread is more pronounced. Indeed, the *cis*-1 isomer (1,2,3,4-$C_{60}H_4$) of the tetrahydrofullerenes-60 is the major product found in the reaction mixture[9]. On the other hand, upon cyclopropanation reactions of C_{60} (Chapter 3) the corresponding *cis*-1 isomer of $C_{62}(COOEt)_4$ does not form at all, which is mainly due to the much higher steric requirement of the bulky bis(diethoxycarbonyl)methylene groups[14]. Interestingly the *e*-isomer is the second most stable isomer of $C_{60}H_4$ [Tab. 5.3]. The *e*-isomer of $C_{62}(COOEt)_4$ is the major product formed by the biscyclopropanation of C_{60}.

For $C_{60}H_6$, 46 regioisomers are possible assuming that only 1,2-additions to the cyclohexatriene units in C_{60} take place[12]. The four most stable and the four least stable isomers are represented in Figure 5.5. Significantly, in the most stable regioisomer the hydrogens are bound to 6-6 double bonds, which are all in *e*-positions to each other. In this way, one benzenoid hexagon perpendicular to the three-fold axis of this C_3-symmetrical chiral isomer is formed, which may be one reason for the extra stability. The significant bond length alternation between 6-6 and 5-6 bonds in the parent C_{60} is remarkably reduced in this particular hexagon. In the case of the nucleophilic cyclopropanation of C_{60} (Chapter 3) the corresponding *e,e,e*-isomer was formed out of the *e*-isomeric bisadduct as the major product[14]. The least stable isomers of $C_{60}H_6$ are those with the hydrogens bound in *cis* especially in *cis*-1 positions [Fig. 5.5].

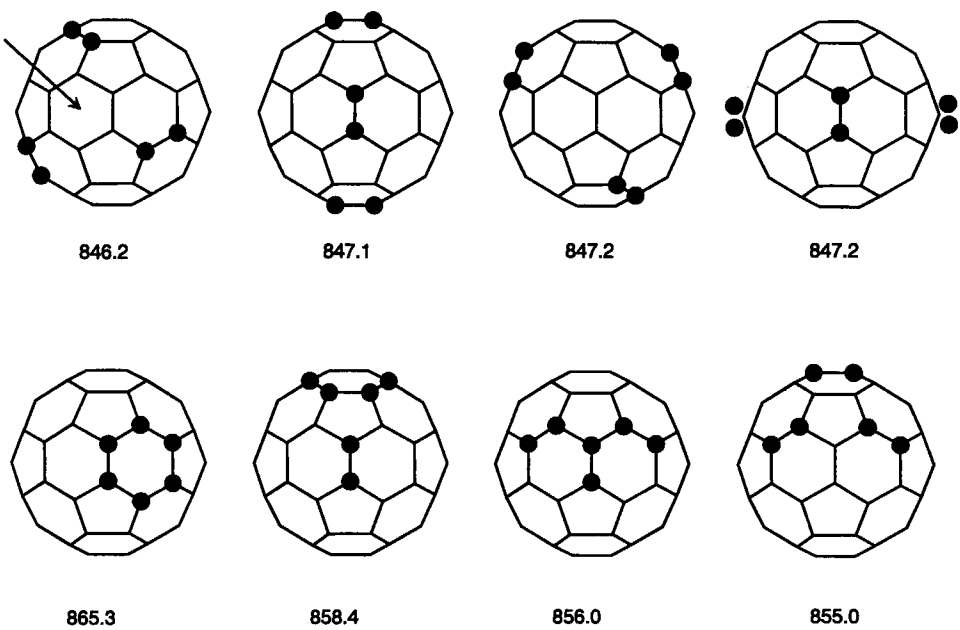

Figure 5.5 The four most stable and the four least stable regioisomers of $C_{60}H_6$ formed by "1,2"-additions" and their AM1-heats of formation[12]. The arrow points to the benzenoid hexagon in the *e,e,e* isomer. The dots represent C-H units.

Among the possible regioisiomers of $C_{60}H_{12}$ formed by "1,2-additions", the T_h-symmetrical regioisomer in which the additions occur in octahedral sites of C_{60} (complete *e*-addition mode) is by far the most stable [Fig. 5.6][12]. In this regioisomer, eight independent benzenoid subunits with a decreased bond length alternation are formed.

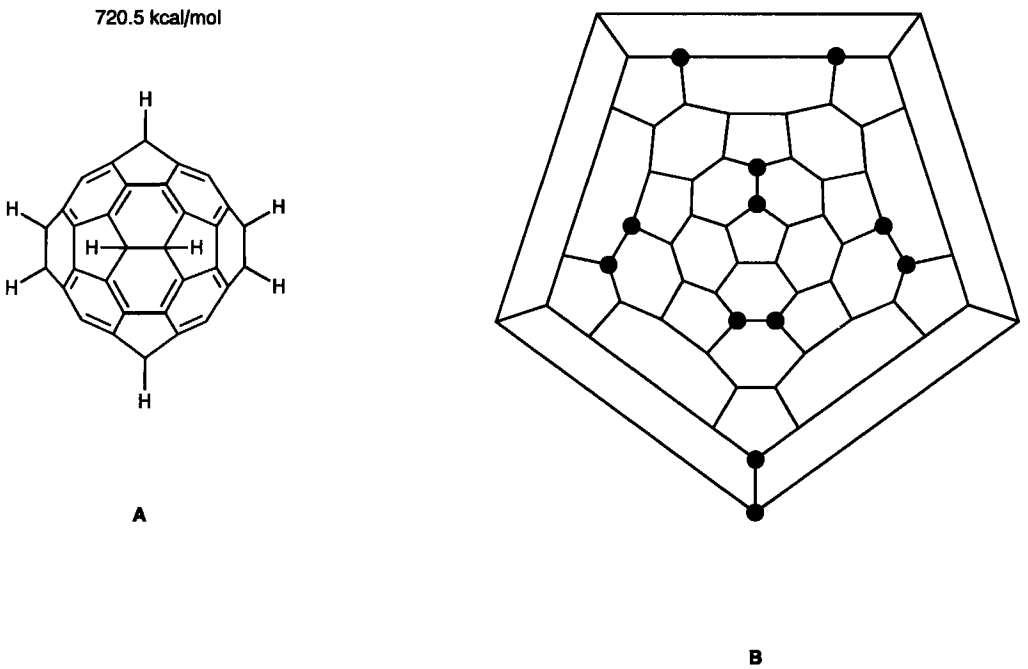

Figure 5.6 The most stable regioisomer of $C_{60}H_{12}$ with T_h-symmetry and its AM1 heat of formation[12]. (A) Front view (B) Schlegel diagram.

5.3 Polyhydrofullerenes $C_{60}H_{2n}$ and $C_{70}H_{2n}$ (n = 7-30)

5.3.1 Birch-Hückel Reduction

The hydrogenation of fullerenes by standard methods, for example by the catalytic hydrogenation, has been shown to be unsuccessful in many cases. Using the Birch-Hückel reduction with Li in liquid NH_3 in the presence of *t*-BuOH, however, the formation of polyhydrofullerenes can be achieved [Scheme 5.4][15,16]. Thereby, the purple C_{60} is converted to a light cream to off white substance.

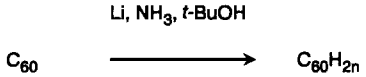

Scheme 5.4

The careful investigation of the initial reaction products with a variety of mild mass spectrometric methods[16], for example with laser desorption-laser photoionization time-of-flight (L^2TOF), laser desorption Fourier transform ion cyclotron resonance (FTICR) and liquid secondary ion mass spectrometry (LSIMS) [Fig. 5.7], show that a mixture of polyhydrofullerenes is formed upon Birch-Hückel reduction. The maximum of the mass distribution is centered on the mass of $C_{60}H_{32}$.

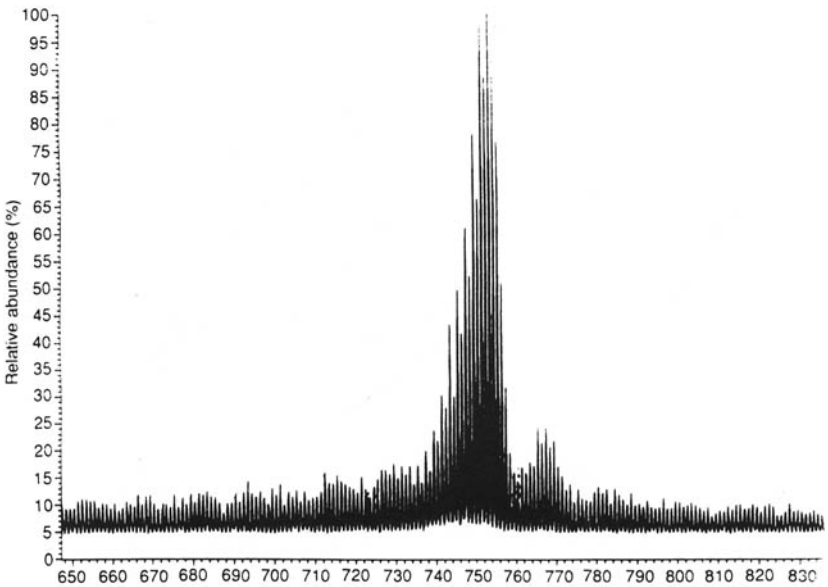

Figure 5.7 Positive ion liquid ion secondary ion mass spectrum of polyhydrofullerenes $C_{60}H_{2n}$, formed by Birch-Hückel reduction of C_{60}, in 3-NOBA matrix[16].

Table 5.4 Experimental and Monte Carlo simulated product distribution from Birch-Hückel reduction of C_{60}[16]

Polyhydrofullerene composition	Experimental distribution[a] (% of base peak)	Monte Carlo distribution[b] (% of base peak)
$C_{60}H_{24}$	39 (24)	0.2
$C_{60}H_{26}$	53 (35)	3
$C_{60}H_{28}$	72 (57)	19
$C_{60}H_{30}$	96 (89)	53
$C_{60}H_{32}$	100 (100)	100
$C_{60}H_{34}$	71 (62)	98
$C_{60}H_{36}$	11 (10)	55
$C_{60}H_{38}$	-- (--)	14
$C_{60}H_{40}$	-- (--)	0.3

[a] Derived from LSIMS data of Fig. 5.7 and FTICRMS data (in parentheses). [b] Based on reduction of 20000 molecules of C_{60}.

This experimentally determined mass distribution of the polyhydrofullerenes is in good agreement with the numerically simulated product distribution using Monte Carlo methods which are based on the assumption, that a 1,4-addition mode to the cyclohexatriene units of C_{60} is valid in Birch-Hückel reductions [Tab. 5.4][16].

Significantly, the mass spectrometric investigation of these polyhydrofullerenes $C_{60}H_{2n}$ by electron impact (EI) mass spectrometry[16], where the sample is heated to 400 °C, show a base peak at 756 u corresponding to $C_{60}H_{36}$ and also a secondary maximum at 738 u corresponding to $C_{60}H_{18}$ together with a strong peak at 720 u due to C_{60}^+. This points to a thermal decomposition of the polyhydrofullerenes leading inter alia to the compounds $C_{60}H_{36}$ and $C_{60}H_{18}$, which have an enhanced stability. By chromatography on silica gel these products can be obtained as major components eluting with mixtures of CH_2Cl_2 and hexanes as mobile phase[15]. However, the broad peaks in the ^1H NMR spectra show that there are not two single compounds present, but a mixture of polyhydrofullerenes. Therefore, the structures of $C_{60}H_{36}$ and $C_{60}H_{18}$ were not conclusively determined by spectroscopic methods. The kinetic instability of the polyhydrofullerenes is also shown by the reaction with 2,3-dichloro-5,6-dicyanobenzoquinone (DDQ) in refluxing toluene. Thereby, the Birch-Hückel products completely convert to C_{60}, which shows that the hydrogenation is completely reversible [Scheme 5.5][15].

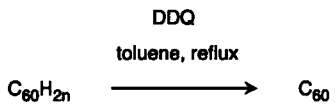

Scheme 5.5

5.3.2 Transfer Hydrogenation of C_{60} and C_{70}

The hydrogenation to polyhydrofullerenes is also possible by transfer hydrogenation[17] using 9,10-dihydroanthracene as a hydrogen source[18,19,20]. The treatment of C_{60} in a sealed glass tube in a melt of 9,10-dihydroanthracene at 350 °C under N_2 leads to a color change of the dissolved fullerene in 30 minutes from brown, rubin-red, orange and yellow to colorless [Scheme 5.6].

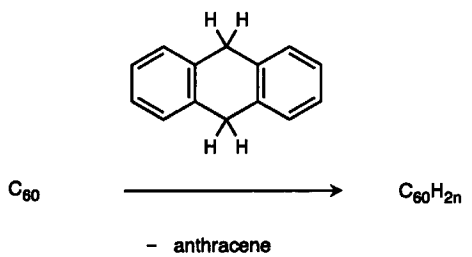

Scheme 5.6

The resulting product also shows a base peak in the mass spectra (EI, FAB, FD) centered on 756 u, corresponding to $C_{60}H_{36}$[18]. An enhancement of the reaction time to 24 h recolorizes the reaction mixture and the isolated reaction product shows a mass distribution determined by the same techniques centered at 738 u, corresponding to $C_{60}H_{18}$. This behavior was explained by a dehydrogenation of the initially formed products by anthracene, which is a coproduct in this reaction[18]. Thereby, the hydrogenation of anthracene inter alia leads to the inert 1,2,3,4-tetrahydroanthracene. Polydeuterated fullerenes $C_{60}D_{2n}$ can be obtained analogously using 9,10-dideuteroanthracene as a deuterium source. The clear solutions of the polyhydrofullerenes in a variety of organic solvents become inhomogeneous upon the formation of a precipitate. This, together with the broad peaks in the ^1H NMR spectra shows the instability of these $C_{60}H_{2n}$'s. The thermal treatment of $C_{60}H_{2n}$ in the solid state at 550 °C leads to a complete reversion to C_{60} [Scheme 5.7].

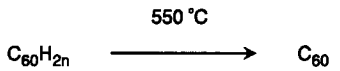

Scheme 5.7

The reaction temperature of the transfer hydrogenation can be lowered to 250 °C by addition of 7*H*-benz[*de*]anthracene as a catalyst[19]. In this way, higher degrees of hydrogenation (n up to 22) are obtained for C_{60}. Also, the less reactive C_{70} can be hydrogenated and deuterated in this way [Scheme 5.8] [19]. Interestingly, the base peak in the EI mass spectra of $C_{70}H_{2n}$ at 876 u shows that in this case a polyhydrofullerene with 36 hydrogens also exhibits an enhanced stability.

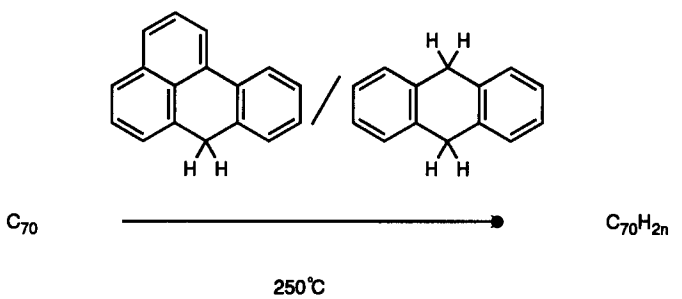

Scheme 5.8

The peaks in the ^1H NMR spectra of $C_{70}H_{2n}$ are also broad since decomposition takes place, which makes the structural determination impossible. The C-H bonds of $C_{60}H_{2n}$ and $C_{70}H_{2n}$ can be cleaved by UV photons (248 nm, 5 eV), which was shown by laser desorption mass spectrometry (LDMS), where compared to EI always smaller masses of $C_{60}H_{2n}$ and $C_{70}H_{2n}$ are detected[20]. Velocity distribution measurements of $C_{60}H_x^+$ carried out at different laser fluences and wave lengths show mass distributions always peaking at $C_{60}H_{25}^+$. This points to an extra stability of $C_{60}H_{24}$[20].

5.3.3 Catalytic Hydrogenation

A radical-induced hydrogenation of C_{60} and C_{70} can be obtained with iodoethane as the hydrogen radical promoter [Scheme 5.9][21,22,23]. In this method the fullerenes are placed in a glass vessel inside an autoclave with an excess of iodoethane and are pressurized with hydrogen to 6.9 MPa. The hydrogenation is carried out at 400 °C for 1h. The polyhydrofullerenes are obtained as a light brown solid. No hydrogenation of the fullerenes takes place if the experiment is carried out in the absence of iodoethane.

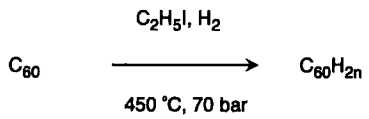

Scheme 5.9

In contrast to the material obtained by the Birch-Hückel reduction[15] and transfer hydrogenation[18,19,20], these polyhydrofullerenes are insoluble in many organic solvents and are only slightly soluble in nitrobenzene. The analysis by fast atom-bombardment (FAB) mass spectrometry revealed a mixture of hydrofullerenes comprised mainly of $C_{60}H_{36}$ and $C_{70}H_{36}$. Reactions at higher temperatures and pressures result in a lower degree of hydrogenation. The solid-state ^{13}C NMR spectrum of the polyhydrogenated fullerenes excludes the presence of single highly symmetric compounds. Thermogravimetric analysis and infrared emission spectroscopy show that the hydrogenated products begin to decompose at ~ 350 °C[21].

Catalytic hydrogenation of C_{60} is also possible on activated carbon with Ru as catalyst in refluxing toluene [Scheme 5.10][24,25]. Thereby, comparatively high degrees of hydrogenation (up to $C_{60}H_{50}$) are obtained. The degree of hydrogenation of C_{60} increases with increasing hydrogen gas pressure and by elevating the reaction temperature. A complete reversion to C_{60} takes place upon the treatment of $C_{60}H_{2n}$ with DDQ in refluxing toluene. Also C_{70} was hydrogenated in this way leading to polyhydrofullerenes-70 consisting mainly of $C_{70}H_{36}$. Dehydrogenation of $C_{70}H_{2n}$ to C_{70} with DDQ proceeds quantitatively.

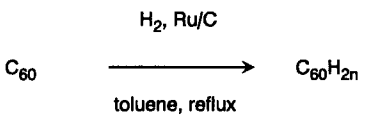

Scheme 5.10

5.3.4 Theoretical Investigations

Several systematic calculations on a variety of structures of the polyhydrofullerenes $C_{60}H_{2n}$ have been carried out at different theoretical levels[4,8,10,11,12,13,26,27,28,29,30,31]. Since the number of the theoretically possible regioisomers of the several $C_{60}H_{2n}$ adducts is very high, not every single structure has been calculated. The situation becomes even more complicated, if not only isomers with externally but also with hydrogens added internally to the C_{60} cage are considered. However, based on

the results available so far, some trends of the stability of different polyhydrofullerenes, depending on the addition mode and the degree of hydrogenation of C_{60} and of C_{70}, can be seen.

As pointed out in Chapter 5.2.2, the addition of hydrogen to C_{60} leading to hydrofullerenes $C_{60}H_{2n}$ with a low degree of hydrogenation ($n \leq 6$) is energetically favored if it proceeds in a 1,2-mode to the 6–6 bonds of the cyclohexatriene units of the C_{60}-framework[13]. This mode avoids the energetically unfavorable introduction of 5–6 double bonds. On the other hand, the eclipsing interaction of the hydrogens resulting from one 1,2-addition costs about 3–5 kcal/mol. Thus, it can be expected that the strain energy, due to eclipsing interactions of the hydrogens, will become increasingly important upon increasing the degree of hydrogenation. Therefore, the polyhydrofullerenes will eventually be unstable. Indeed, calculations of several $C_{60}H_{2n}$ isomers formed by a 1,2- or a 1,4-addition mode with the semiempirical MNDO method would predict 1,4-additions to be more favorable than 1,2-additions starting for $n > 6$ [Tab. 5.5][13]. But only up to $n = 12$ are exclusive 1,4-additions possible. Higher degrees of hydrogenation also require formal 1,2-additions. The comparatively stable polyhydrofullerene formed by the complete and exclusive 1,4-addition mode is T_h-$C_{60}H_{24}$ [Fig. 5.8].

Table 5.5 Calculated MNDO heats of formation of $C_{60}H_{2n}$ formed by 1,2- and 1,4-addition[13]

n	$\Delta H_f°$ (kcal/mol) 1,2-addition	1,4-addition
0[a]	973.3	973.3
1	931.2	935.6
2	889.4	899.0
4	805.3	814.0
6	720.5	720.9
8	653.9	652.2
10	587.2	576.9
12	518.1	504.3
18	354.2	-
24	242.2	-
30	335.0	-

[a] n = 0 corresponds to C_{60}

The most stable isomer of $C_{60}H_{12}$ has T_h-symmetry[12,13]. Here all the additions occurred in a 1,2-mode in *e* positions (octahedral sites) of C_{60} [Fig. 5.6]. A further 1,2-addition of hydrogen to this regioisomer requires the addition to a neighboring cyclohexatriene double bond (*cis*-1 position), which costs energy due to eclipsing interactions. This is consistent with non-zero H-C-C-H torsion angles of $C_{60}H_{2n}$ ($n > 8$)[13].

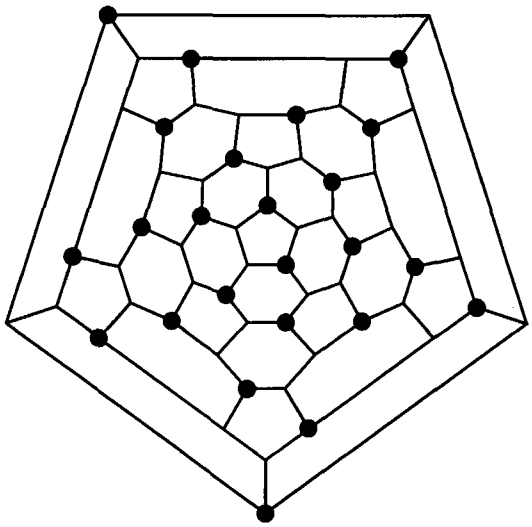

Figure 5.8 Schlegel diagram of T_h-$C_{60}H_{24}$.

To obtain a measure for the dependence of n on the stability of $C_{60}H_{2n}$, the normalized[13] calculated heats of formation $\Delta H_f°$ were introduced:

$$\Delta(\Delta H_f°)_n = (\Delta H_f°(C_{60}H_{2n}) - \Delta H_f°(C_{60}H_2))/n$$

Whereas for 1,2-additions, a destabilization begins for n > 6 with $\Delta(\Delta H_f°)$ becoming endothermic the opposite is observed for 1,4-additions, where the values become more exothermic. Even for larger values (n up to 12) the normalized values are more exothermic than for n = 1 in this addition mode[13]. The large destabilization for $C_{60}H_{60}$ (n = 30) of $\Delta(\Delta H_f°)$ = 20.8 kcal/mol significantly shows the accumulating influence on continuing 1,2-additions to C_{60}.The polyhydrofullerenes $C_{60}H_{36}$ and $C_{60}H_{48}$ are the most stable molecules in the $C_{60}H_{12n}$ (n = 1,2,3,4,5) series of *exo*-hydrogenated C_{60}, ab initio calculated at the Hartree-Fock level[30].

These theoretical investigations support the experimental findings[15,16,18,21,24,25] that (1) a complete hydrogenation of C_{60} is difficult to obtain and has not been observed so far and that (2) even polyhydrogenated fullerenes with a lower degree of hydrogenation, such as $C_{60}H_{36}$ are not stable and will slowly decompose. The reasons for the instabilities of polyhydrofullerenes in terms of simple topological arguments are inter alia (1) enhanced eclipsing interactions of the H-atoms as in the case of *cis*-1 additions in the 1,2-mode; (2) strain within the C-network of polyhydrofullerenes, especially due to the deviation from the tetrahedral angle of sp^3-C-atoms and (3) introduction of 5-6 double bonds. Initially formed reaction mixtures may rearrange to form more stable compounds. This can be responsible for a predominant occurrence of the species $C_{60}H_{36}$, $C_{70}H_{36}$ and $C_{60}H_{18}$ after thermal treatment of polyhydrofullerenes, which were obtained, for example, from Birch-Hückel reductions. These reactions lead to a mass distribution centered on the degree of hydrogenation of about 32 using mild mass spectrometric techniques.

For $C_{60}H_{36}$, among others, the two structures represented in the Schlegel diagrams of Fig. 5.19 have been suggested[15,32,33]. Whereas in structure **A**[15] all double bonds are located in pentagons, which may be unfavorable, in the structure **B**[32] with *T*-symmetry only 6-6 double bonds and pentagons constructed with single bond edges are present. In addition, similar to T_h-$C_{60}H_{12}$, four benzenoid rings are formed in **B**, which may provide further stabilization. The MM2 heat of formation of **B** is significantly lower, about 89 kcal/mol, than that of **A**[34]. Also solid state ^{13}C NMR spectra, which show five major peaks that are expected for the five sets of different C-atoms favor structure **B**[23,34]. For **A**, five equivalent T_h- structures are possible. Putting any of the 36 hydrogens of **A** inside the fullerene leads to conformers with higher energies[26]. The addition of two hydrogens to $C_{60}H_{34}$ to complete the structure of **A** is a more exothermic reaction than further additions, which lead to higher degrees of hydrogenation. This indicates that structure **A** also exhibits an enhanced stability compared to similar polyhydrofullerenes.

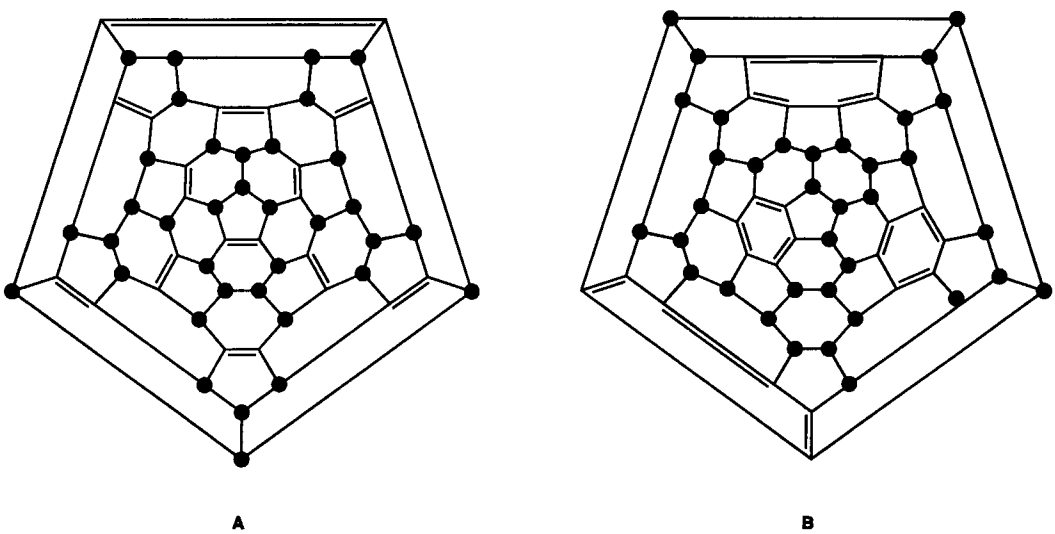

Figure 5.9 Schlegel diagram representations of two possible isomers of $C_{60}H_{36}$.

A stucture proposal for $C_{70}H_{36}$ from molecular mechanics calculations (MM3) is based on the expectation that only less reactive nonconjugated or aromatic like double bonds are present after the hydrogenation process [Fig. 5.10][19]. This is in line with observed and calculated reactivities[4,8,11] of C_{70}. The double bonds in the pole pentagons in this structure of $C_{70}H_{36}$, however, seem to be unfavorable. The heat of formation of this regioisomer is calculated to be 490.2 kcal/mol. A further hydrogenation of two double bonds is predicted to lead to a destabilization with an increase of ΔH_f° of about 45 kcal/mol[19]. Alternatively, a structure with 6-6 double bonds at the poles instead could be postulated.

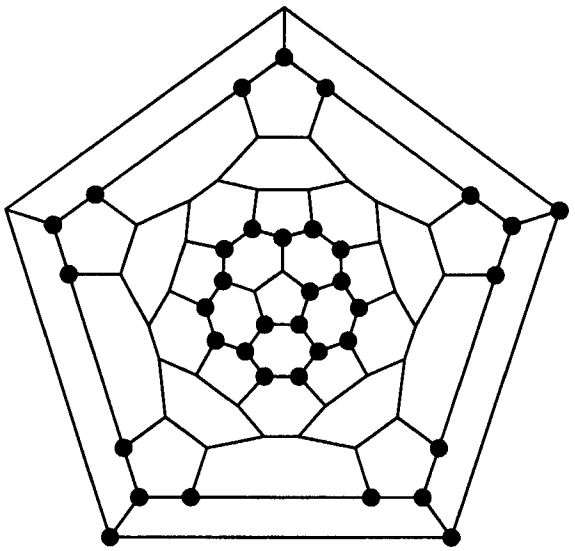

Figure 5.10 Postulated structure for $C_{70}H_{36}$[19].

The icosahedral $C_{60}H_{60}$ [Fig 5.11] is neither the only nor the most stable conformer of the completely hydrogenated C_{60}. Molecular mechanics calculations (MM3) on $C_{60}H_{60}$ show that moving just one hydrogen inside the cage and forming a new conformer is an exothermic process and decreases the energy by 53 kcal/mol[27].

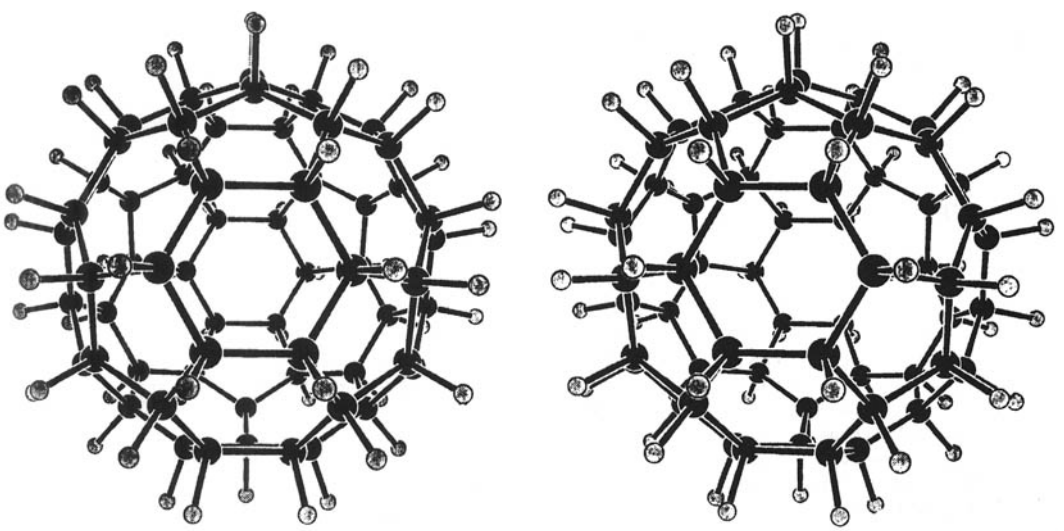

Figure 5.11 All-outside isomer of $C_{60}H_{60}$[27].

A conformer of $C_{60}H_{60}$ with 10 hydrogens added inside the cage is the lowest energy isomer [Fig. 5.12]. This minimum energy isomer with C_1-symmetry is predicted to have a heat of formation being 400 kcal/mol lower than that for the all-outside isomer[27]. The all-outside isomer is highly strained due to eclipsing hydrogen-hydrogen interactions and due to the 120° angles of the sp^3-carbons (20 planar cyclohexane rings). Putting hydrogens inside leads to fewer eclipsing interactions and also to a decrease of many CCC bond angles. In another study the comparison on the basis of ab initio calculations of the stabilities of totally *exo*-hydrogenated $C_{60}H_{60}$ and T_h-$C_{60}H_{60}$, with 12 hydrogens added inside the cage, predicts the latter conformer to be the more stable[30]. The calculated energy barrier for the hydrogen penetration from outside to inside the C_{60} cage, however, is very high (at least 2.7 eV/atom).

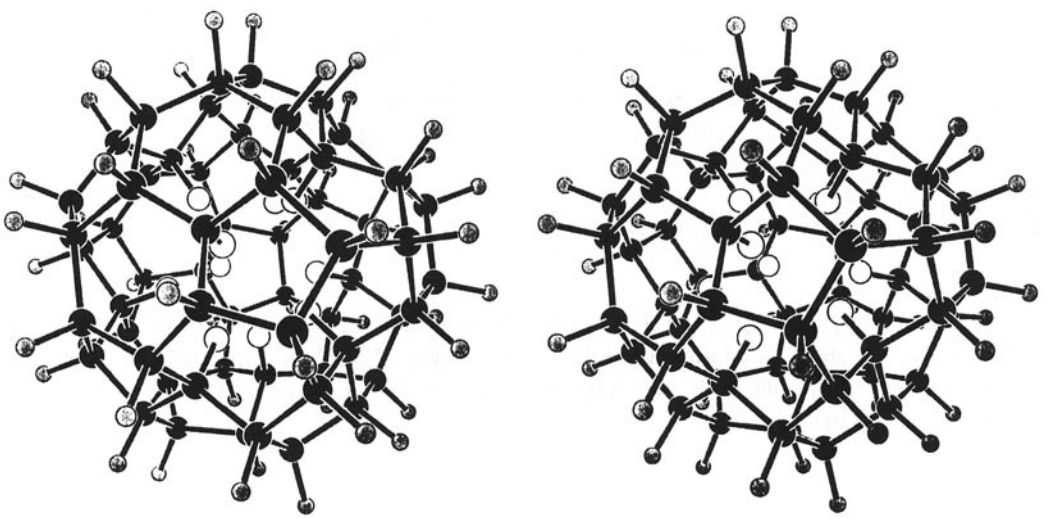

Figure 5.12 Most stable isomer of $C_{60}H_{60}$ with ten hydrogens inside[27].

References

1 C. C. Henderson, P. A. Cahill *Science* **1993**, *259*, 1885.
2 S. Ballenweg, R. Gleiter, W. Krätschmer *Tetrahedron Lett.* **1993**, *34*, 3737.
3 T. F. Guarr, M. S. Meier, V. K. Vance, M. Clayton *J. Am. Chem. Soc.* **1993**, *115*, 9862.
4 A. Hirsch, A. Soi, H.R. Karfunkel *Angew. Chem.* **1992**, *104*, 808; *ibid. Int. Ed. Engl.* **1992**, *31*, 766.
5 A. Hirsch, T. Grösser, A. Skiebe, A. Soi *Chem. Ber.* **1993**, *126*, 1061.
6 P. J. Fagan, P. J. Krusic, D. H. Evans, S. A. Lerke, E. Johnston *J. Am. Chem. Soc.* **1992**, *114*, 9697.
7 C. C. Henderson, R. A. Assink, P. A. Cahill *Angew. Chem.* **1994**, 106, 803; *ibid. Int. Ed. Engl.* **1994**, *33*, 786.
8 C. C. Henderson, C. M. Rohlfing, P. A. Cahill *Chem. Phys. Lett.* **1993**, *213*, 383.
9 C. C. Henderson, C. M. Rohlfing, K. T. Gillen, P. A. Cahill *Science* **1994** in press.
10 N. Matsuzawa, D. A. Dixon, T. Fukunaga *J. Phys. Chem.* **1992**, *96*, 7594.
11 H. R. Karfunkel, A. Hirsch, *Angew.Chem.* **1992**, *104*, 1529; *ibid. Int. Ed. Engl.* **1992**, *31*, 1468.
12 H. R. Karfunkel, A. Hirsch, *unpublished results.*

13 N. Matsuzawa, T. Fukunaga, D. A. Dixon *J. Phys. Chem.* **1992**, *96*, 10747.
14 A. Hirsch, I. Lamparth, H. R. Karfunkel *Angew. Chem.* **1994**, *106*, 453; *ibid. Int. Ed. Engl.* **1994**, *33*, 437.
15 R. E. Haufler, J. Conceicao, L. P. F. Chibante, Y. Chai, N. E. Byrne, S. Flanagan, M. M. Haley, S.C. O'Brian, C. Pan, Z. Xiao, W. E. Billups, M. A. Ciufolini, R. H. Hauge, J. L. Margrave, L. J. Wilson, R. F. Curl, R. E. Smalley *J. Phys. Chem.* **1990**, *94*, 8634.
16 M. R. Banks, M. J. Dale, I. Gosney, P. K. G. Hodgson, R. C. K. Jennings, A. C. Jones, J. Lecoultre, P. R. R. Langridge-Smith, J. P. Maier, J. H. Scrivens, M. J. C. Smith, C. J. Smyth, A. T. Taylor, P. Thorburn, A. S. Webster *J. Chem. Soc., Chem. Commun.* **1993**, 1149.
17 C. Rüchardt, M. Gerst, M. Nölke *Angew. Chem.* **1992**, *104*, 1516; *ibid. Int. Ed. Engl.* **1992**, *31*, 1523.
18 C. Rüchhardt, M. Gerst, J. Ebenhoch, H. -D. Beckhaus, E. E. B. Campbell, R. Tellgmann, H. Schwarz, T. Weiske, S. Pitter *Angew. Chem.* **1993**, *105*, 609; *ibid. Int. Ed. Engl.* **1993**, *32*, 584.
19 H. -D. Beckhaus, C. Rüchardt, E. E. B. Campbell, R. Tellgmann *submitted.*
20 E. E. B. Campbell, R. Tellgmann, C. Rüchardt, M. Gerst, J. Ebenhoch, H. -D. Beckhaus, *submitted.*
21 A, M. Vassallo, M. A. Wilson, M. I. Attalla *Energy Fuels* **1988**, *2*, 539.
22 M. I. Attalla, M. A. Wilson, R. A. Quezada, A. M. Vassallo *Energy Fuels* **1989**, *3*, 59.
23 M. I. Attalla, A. M. Vassallo, B. N. Tattam, J. V. Hanna *J. Phys. Chem.* **1993**, *97*, 6329.
24 K. Shigematsu, K. Abe, M. Mitani, K. Tanaka *Chem. Express* **1993**, *8*, 37.
25 K. Shigematsu, K. Abe, M. Mitani, K. Tanaka *Chem. Express* **1992**, *7*, 957.
26 B. I. Dunlap, D. W. Brenner, J. W. Mintmire, R. C. Mowrey, C. T. White *J. Phys. Chem.* **1991**, *95*, 5763.
27 M. Saunders *Science* **1991**, *253*, 330.
28 D.A. Dixon, N. Matsuzawa, T. Fukunaga, F. N. Tebbe *J. Phys. Chem.* **1992**, *96*, 6107.
29 D. Bakowies, W. Thiel *Chem. Phys. Lett.* **1992**, *193*, 236.
30 T. Guo, G. E. Scuseria *Chem. Phys. Lett.* **1992**, *191*, 427.
31 J. Cioslowski *Chem. Phys. Lett.* **1991**, *181*, 68.
32 R. Taylor In *The Fullerenes. New Horizons for the Chemistry, Physics and Astrophysics of Carbon;* H. W. Kroto, D. R. M. Walton Eds; Cambridge University Press: Cambridge, 1993; p 87.
33 S. J. Austin, R. C. Batten, P. W. Fowler, D. B. Redmond, R. Taylor *J. Chem. Soc., Perkin Trans. 2* **1993**, 1383.
34 C. Rüchardt, *personal communication.*

Chapter 6 Radical Additions

6.1 Introduction

6.2 ESR Investigations of Radical Additions
6.2.1 Addition of Single Radicals
6.2.2 Multiple Radical Additions

6.3 Metalation of C_{60} with Pentacarbonylrhenium Radicals

6.4 Hydrostannylation of C_{60}

6.5 Addition of Bis(trifluoromethyl)nitroxide

6.6 Radical Copolymerization of C_{60} and Paracyclophane

References

6.1 Introduction

Similar to nucleophiles (Chapter 3), a large variety of radicals easily add to C_{60} and C_{70}, forming diamagnetic or paramagnetic adducts. The fullerenes behave like a radical sponge. Defined radical species, such as $R_nC_{60}^{\cdot}$ (n = 1,3,5), were intensively investigated by ESR spectroscopy, which revealed a variety of interesting phenomena of these adducts. One of them is the formation of fullerene dimers. In addition to such spectroscopic in situ investigations, the addition of radicals to C_{60} has been used to synthesize new materials including polymers and perfluoroalkylated fullerenes, which may have importance for technological applications.

6.2 ESR Investigations of Radical Additions

6.2.1 Addition of Single Radicals

ESR studies of a large variety of monoradical adducts $RC_{60}^{\cdot}$ and $RC_{70}^{\cdot}$ have provided a valuable insight into the electronic situation on the fullerene surface and other physical phenomena of these species[1,2,3,4,5,6,7,8]. The organic radical species R$^{\cdot}$, which is to be added to the fullerene, can be generated in situ either photochemically or thermally by established free radical reactions from suitable precursor molecules. The photochemical generation of the radicals R$^{\cdot}$ can be achieved by the direct UV irradiation in the ESR cavity of saturated benzene or *tert*-butylbenzene solutions of C_{60} containing a small molar excess of a radical precursor, such as alkyl bromides, carbon tetrachloride, dialkylmercury compounds, hydrocarbons RH and di-*tert*-butylperoxide. Thereby, the radicals R$^{\cdot}$ are either generated directly from the halides RX, for example with *tert*-butyl bromide, or indirectly using *tert*-butoxy radicals as intermediates [Scheme 6.1].

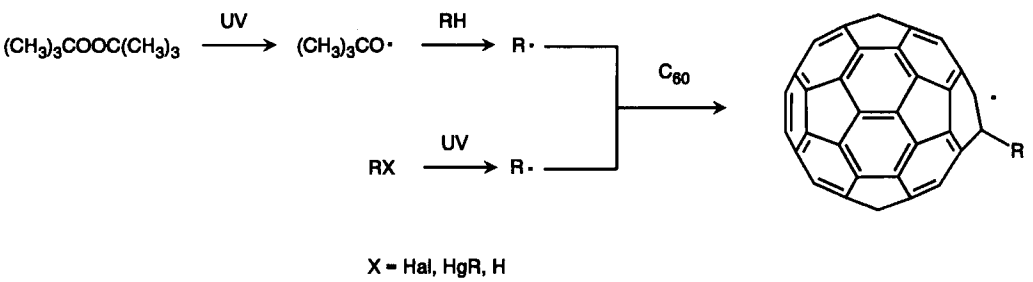

Scheme 6.1

The stability of the radical species $RC_{60}^{\cdot}$ strongly depends on the nature of R. Sterically demanding groups, such as the *tert*-butyl group, give rise to rather persistent radicals $RC_{60}^{\cdot}$[1,2,3]. But also the less stable $HC_{60}^{\cdot}$ can be studied in situ[5]. At low temperatures the ESR spectrum of *t*-$BuC_{60}^{\cdot}$ [Fig. 6.1] consists of ten narrow lines appropriate for a hyperfine interaction of the unpaired electron with nine equivalent protons of the *tert*-butyl group[1]. Besides *t*-$BuC_{60}^{\cdot}$, a series of other monoalkyl radical adducts have been similarly investigated[1,2,3,4]. In all cases, the observed hyperfine structures are those expected for the corresponding group R. From the ^{13}C satellites in the ESR spectra the symmetry of the radicals as well as information about the localization of the unpaired electron in $RC_{60}^{\cdot}$ can be obtained [Fig. 6.2].

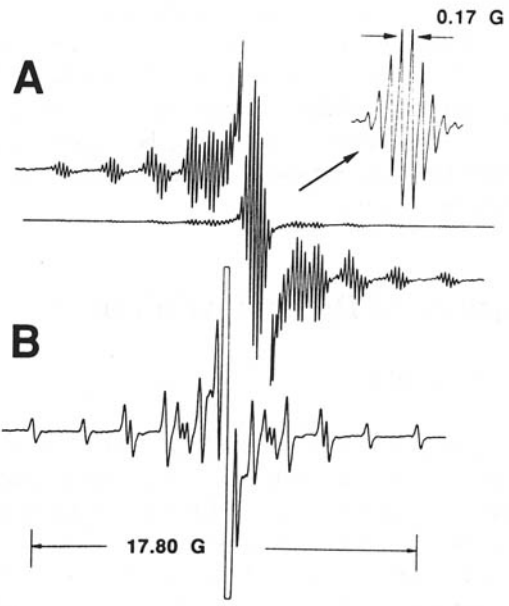

Figure 6.1 ESR spectra of *t*-Bu$C_{60}^{\cdot}$ in benzene at 80 °C: (A) $(CH_3)_3CC_{60}^{\cdot}$ shows the ^{13}C hyperfine satellites and the 0.17G hyperfine splitting due to the 9 methyl protons. (B) $(CD_3)_3CC_{60}^{\cdot}$ shows the ^{13}C satellites[1].

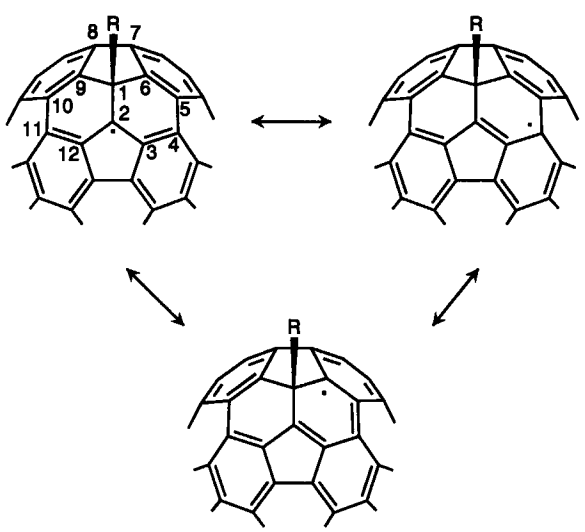

Figure 6.2 The five major canonical resonance structures of $RC_{60}^{\cdot}$.

In *t*-Bu$C_{60}$$^{\cdot}$, for example, ten pairs of ^{13}C satellites are clearly resolved. A C_s-symmetry can be deduced from their relative intensities and splittings[1]. The unpaired electron is mostly located on two fused six-membered rings of the C_{60} surface, which rules out an extensive delocalization on the C_{60} framework. The highest spin densities are located on the carbons 2, (4,11) and (6,9) and were estimated to be ~0.33, ~0.17 and ~0.17 respectively[1]. This leads to the formulation of the major canonical resonance forms represented in Figure 6.2. The analogous investigations with other radicals R$C_{60}$$^{\cdot}$, for example with $CCl_3C_{60}$$^{\cdot}$ or $C_{60}H^{\cdot}$, the simplest hydrogenated fullerene radical, lead qualitatively to the same results[3,5].

$C_{60}H^{\cdot}$ was generated in situ by the irradiation of saturated degassed benzene solutions of C_{60} in the presence of tri-*n*-butyltin hydride, 1,4-cyclohexadiene or thiophenol with the focussed light of a high pressure Hg/Xe arc [Scheme 6.2]. Alternatively, ESR spectra were also recorded in solid neon[5]. The proton hyperfine splitting of $C_{60}H^{\cdot}$ was determined to be 33.07 G[5].

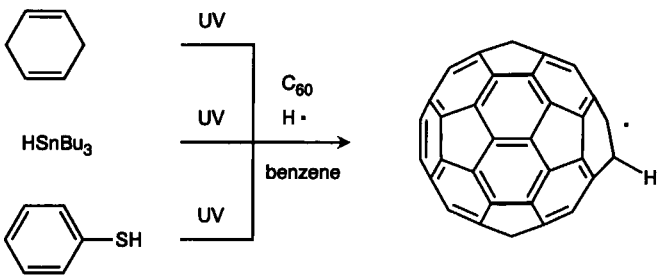

Scheme 6.2

In the monoalkyl radical adducts, R$C_{60}$$^{\cdot}$ exhibits a substantial amount of hindered rotation about the C_{60}–R bond. This was concluded inter alia from the temperature-dependent line-shape changes in the ESR spectra and from the observation of distinct rotamers for $(^{13}CH_3)(CH_3)_2CC_{60}$$^{\cdot}$ with staggered conformations at low temperatures[4] [Fig. 6.3]. Simulations[9,10,11] of the temperature dependent spectral line shapes led to an activation energy for the internal rotation in *t*-Bu$C_{60}$$^{\cdot}$ of 8.2 kcal/mol. A similar value (9.3 kcal/mol) was found[12] in the anion *t*-BuC_{60}^-, whereas for R$C_{60}$$^{\cdot}$ (R = ethyl, isopropyl) the internal rotations are also hindered with similar values for the activation energy barrier and the alkyl groups adopt a preferred conformation on the C_{60} surface even at elevated temperatures; the methyl group in $CH_3C_{60}$$^{\cdot}$ above 270 K undergoes a fast rotation on the ESR time scale[4]. In $CH_3CH_2C_{60}$$^{\cdot}$, the preferred equilibrium conformation is asymmetrical. The terminal methyl group prefers the position directly above a hexagon [Fig. 6.3][4].

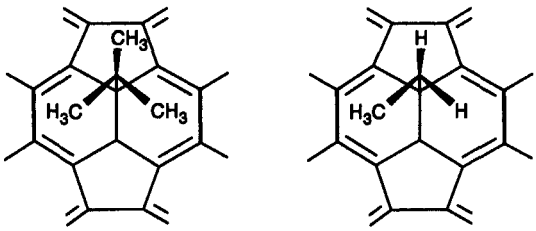

Figure 6.3 Preferred conformations in the radicals t-Bu$C_{60}^{\bullet}$ and $CH_3CH_2C_{60}^{\bullet}$.

The addition of alkylthio and alkoxy radicals to C_{60} is also possible [Scheme 6.3 and 6.4][7]. Radical precursors, such as alkyl-disulfides (RSSR), bis(alkylthio)mercury compounds (RSHgSR) or dialkyl peroxides (ROOR), can be used from which the radicals are generated in situ upon irradiation. The radicals $RSC_{60}^{\bullet}$ are not persistent. Their ESR spectra are only observable as long as light is shining through the sample. The intensities of the signals in the spectra of $RSC_{60}^{\bullet}$ also decrease when the temperature is increased above room temperature. This behavior points to a reversal of the alkylthio radical addition due to the weak fullerene-sulfur bond[7]. This became especially evident upon the gradual change of color from amber for phenylthiyl radical adducts to the original purple of C_{60}[13]. In some cases, the cleavage of the carbon-sulfur bond of RSSR (R = benzyl, *tert*-butyl) was observed, which leads exclusively or partly to the radicals $RC_{60}^{\bullet}$. This is particularly the case when the light is not filtered through a Ni/Co sulfate solution[7].

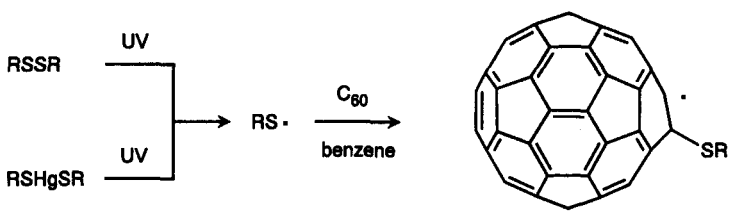

Scheme 6.3

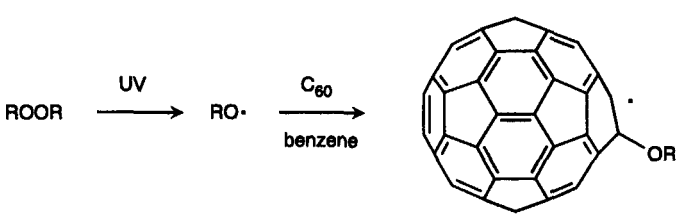

Scheme 6.4

For $CH_3SC_{60}^{\cdot}$ four local conformational minima are obtained by molecular mechanics calculations using the MMX force field [Fig. 6.4][7]. Thereby, the asymmetric conformation **B** for this radical is preferred.

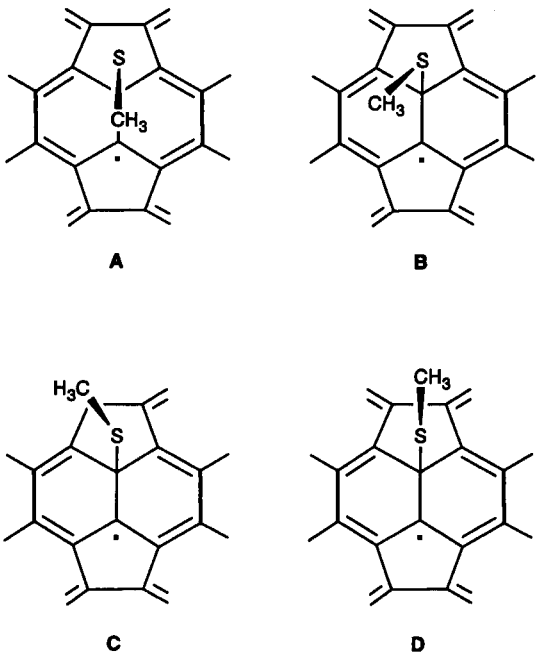

Figure 6.4 The structures of the local conformational minima of the radical $CH_3SC_{60}^{\cdot}$ obtained by molecular mechanics calculations[7].

A characteristic feature in the ESR spectra of alkyl radical adducts $RC_{60}^{\cdot}$ (R = alkyl) is the temperature dependence of the signal intensities. For t-$BuC_{60}^{\cdot}$, for example, the intensity significantly increases as the temperature is raised from 30 to 130 °C and decreases again upon cooling to room temperature and disappears at ca. 10 °C[2,3]. Such a cycle can be repeated several times without significant radical decay. This behavior, similar to that of the classical Gomberg radical $Ph_3C^{\cdot}$[14], was interpreted in terms of an equilibrium of the radicals $RC_{60}^{\cdot}$ with their diamagnetic dimers $RC_{60}C_{60}R$[·2,3] [Scheme 6.5]. A comparison of the temperature behavior of a variety of $RC_{60}^{\cdot}$ radicals shows that the dimer bond strength depends on the size of the entering radical [Tab 6.1]. A measure for the dimer bond stengths are the enthalpies of the dimerization [Scheme 6.5], obtained from the plots of ln (T x Intensity) against $1000/T$[2,3].

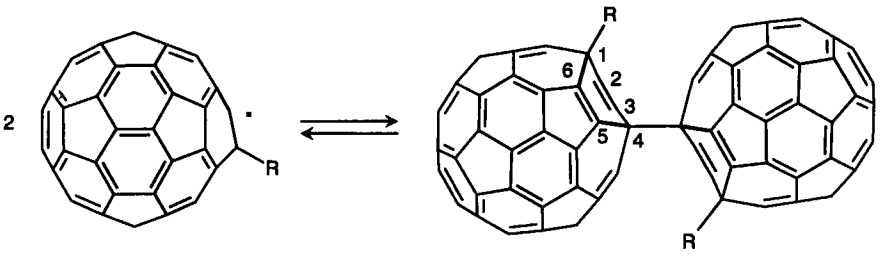

Scheme 6.5

Table 6.1 Enthalpies of dimerization (kcal mol^{-1}) for $RC_{60}^{\cdot}$ radicals[3].

R	ΔH	T/K
iso-propyl	35.5	420-450
$C_6D_5CH_2$	17.1	250-310
CBr_3	17.0	300-380
tert-butyl	22.0	300-400
adamantyl	21.6	300-400

The dependence of the dimer bond strength on the size of R suggests that bond formation occurs in close proximity to the C-atom carrying R. This is also in line with the observed predominant localization of the unpaired electron in the positions 2, (4,11) and (6,9) [Fig. 6.2]. Dimerization at C-4 or C-11 seems to be most likely because of sterical reasons[2,3].

The addition of a bulky radical to C_{70} gives rise to three different regioisomeric radical adducts of $RC_{70}^{\cdot}$ [Scheme 6.6][6]. Radicals such as $(CH_3)C^{\cdot}$, $CCl_3^{\cdot}$ or $(MeO)_2PO^{\cdot}$ have been used. The latter can be generated in situ upon photolysis of di-*tert*-butyl peroxide in benzene containing dimethyl phosphite.

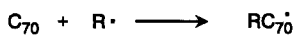

Scheme 6.6

Since C_{70} contains five types of C-atoms, five different radicals should in principle be possible [Fig. 6.5]. The ESR signals of one radical species of $RC_{70}^{\cdot}$ can be attributed to structure A in Figure 6.5. This is the most "C_{60}-like" structure and produces a similar *g* value (2.0021) and comparable hyperfine interactions as observed in $RC_{60}^{\cdot}$ (R = *tert*-butyl). The temperature dependence of the ESR-signal intensity of this radical adduct $RC_{70}^{\cdot}$ (structure **A**) is also characteristic of the dissociation of a dimer (ΔH = ca. 11 kcal/mol)[6]. The attribution of the other two radical adducts of $RC_{70}^{\cdot}$ to two of the structures **B**-**E** in Figure 6.5 remains to be addressed.

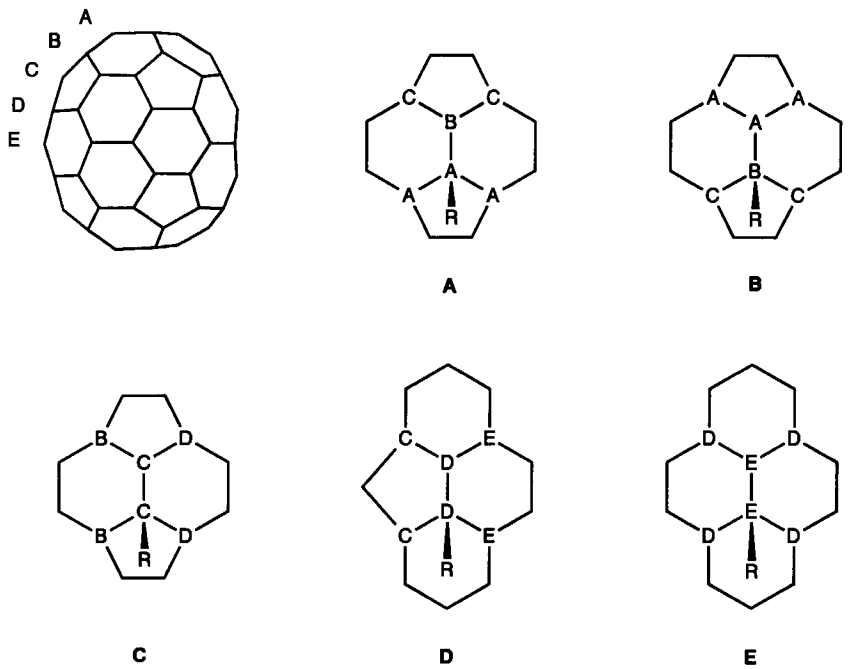

Fig 6.5 The five possible structures of $RC_{70}^{\cdot}$.

6.2.2 Multiple Radical Additions

A prolonged irradiation of C_{60} solutions in the presence of excess radical precursors leads to multiple radical additions[13,15], giving rise to broad and featureless ESR spectra. Some of these multiple radical species are rather persistent. Furthermore, radicals with higher spin multiplicities have been observed[13]. Valuable insight of such multiple radical additions came from the ESR spectrocopic investigations of benzyl radicals, ^{13}C-labelled at the benzylic positions[15]. These radicals can be prepared in situ by photolysis of saturated solutions of C_{60} in labelled toluene containing about 5% di-*tert*-butyl peroxide[16]. Thereby, the photochemically generated *tert*-butoxy radicals readily abstract a benzylic hydrogen atom from the toluene. Two radical species with a different microwave power saturation behavior can be observed[15]. The ESR absorptions of these species do not decay when the light is distinguished. The spectrum of each species can be recorded without being superimposed by the other simply by changing the microwave power level. One radical species can be attributed to an allylic radical **3** and the other to a cyclopentadienyl radical **5** formed by the addition to three and five adjacent [5]radialene double bonds, respectively [Scheme 6.7]. In **3** a coupling occurs to three nuclei (two identical and one different) and in **5** to five equivalent ^{13}C nuclei. In these experiments no evidence for the radical **1** is found, which is very likely a short-lived species[15].

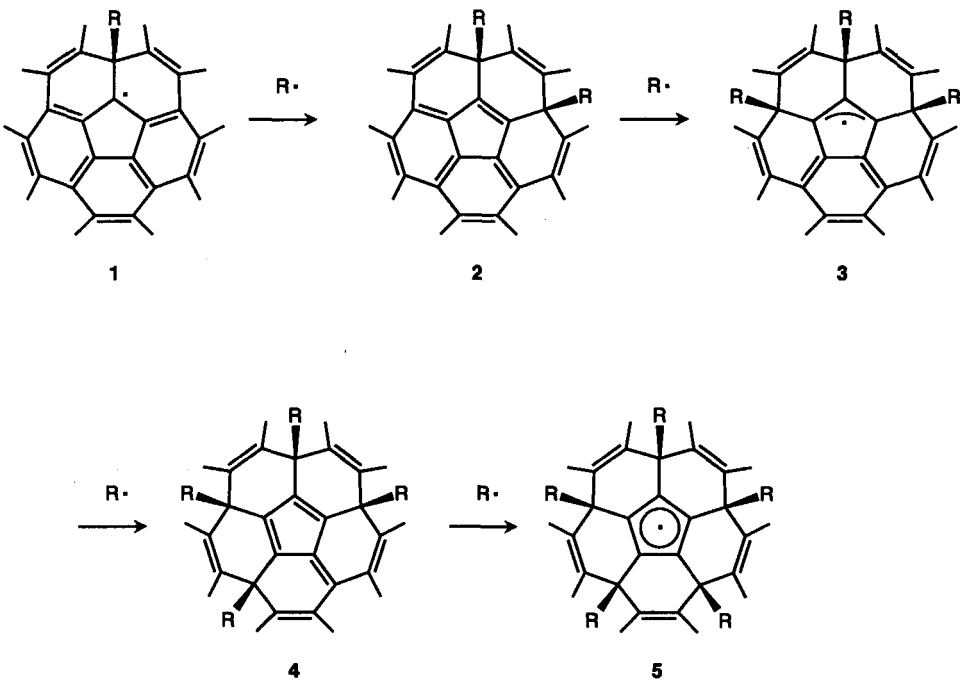

Scheme 6.7

The ESR spectra of **3** and **5** do not provide information on whether or not the corresponding radical species carry an even number of benzyl groups attached elsewhere on the surface of the C_{60} molecule. Looking at the high reactivity of radicals towards C_{60}, it is very unlikely that only single radical adducts, such as $R_3C_{60}^{\bullet}$ or $R_5C_{60}^{\bullet}$, are responsible for the observed ESR spectra. But very important information about the electronic and chemical properties of a certain area of the fullerene surface namely a corannulene substructure are extractable from these experiments. The orbitals with a spin density in radical species containing a moiety **5** are highly degenerate due to the local five-fold symmetry. Such radicals have an efficient spin-relaxation behavior and do not power saturate very readily[8]. The formation of species **3** and **5** from C_{60} proceeds by initial addition of one benzyl radical leading to the monoadduct **1**. The unpaired spin in this radical is mostly localized on carbon 2, (4,11) and (6,9) [Fig. 6.2]. This electronic localization as well as the steric requirement of the benzyl group will direct a second attack accompanied with a radical recombination to position 4 or 11. A third attack to the diamagnetic **2** can occur anywhere on the fullerene surface. However, upon the formation of **3** the unfavorable 5-6 double bond[17] in **2** disappeared and a resonance stabilized allyl radical is formed. Indeed, semiempirical calculations on two different adducts $H_3C_{60}^{\bullet}$, **6** and **7**, show that **6**, in which the three groups are all added in adjacent 1,4-positions, is about 8.5 kcal/mol lower in energy than **7**, where the groups are added in non adjacent positions[8]. A radical $R_3C_{60}^{\bullet}$, in which a third attack occurred far away from the groups already attached in $C_{60}R_2$ (**2**), would be very unstable due to a facile formation of a diamagnetic $C_{60}R_4$, which is not detectable in the ESR spectra. Another reason for the stability of **3** is the steric protection provided by the three attached benzyl groups. The radical recombination of **3** with a benzyl radical leads to **4** for the same reasons for which **2** is formed from **1**. The stability of **4** is restricted due to the two unfavorable 5-6 double bonds, which directs another attack to form the resonance stabilized **5**. In addition, sterical arguments are responsible for the

remarkable stability of **5**. In the case of methyl radical additions, this steric hindrance is by far less important. This may be the reason why the corresponding species **3** and **5** of methyl adducts of C_{60} are not observable by ESR spectroscopy[15].

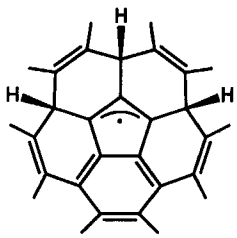

6

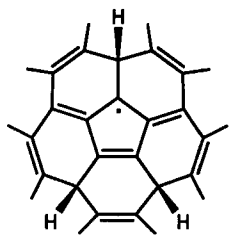

7

Mass spectrometric investigations of reaction products obtained by multiple radical additions show that up to eight benzyl groups are added to C_{60}. The addition of methyl radicals leads to products with up to 34 methyl groups attached to C_{60}[15].

Additions of perfluoroalkyl groups generated from fluoroalkyl iodides R_fI and fluoroacyl peroxides $R_fC(O)OO(O)CR_f$ have also been carried out[18]. As in the case of the alkyl radical additions, ESR-spectroscopic investigations of fluoroalkyl monoadducts show a hindered rotation about the R_f–C_{60} bond and the tendency to dimerization. The production of perfluoralkylated fullerenes **8** [Scheme 6.8] can be achieved by the treatment of C_{60} with the radical precursors R_fI or $R_fC(O)OO(O)CR_f$ in a sealed glass tube at 200 °C for 24h and fluorocarbons or halofluorocarbons as solvents[18]. This leads to a substantial coverage of the C_{60} surface with up to 16 covalently bound fluoroalkyl groups. Due to sterical crowding a coverage of the C_{60} surface with more than 24 perfluoroalkyl groups seems to be unrealistic[18]. Whereas C_{60} itself is rather insoluble in fluorocarbons or halofluorocarbons, **8** shows a remarkable solubility in these solvents. Using other solvents to synthesize perfluoroalkylated fullerenes, such as 1,2,4-trichlorobenzene, leads to polyadducts also having hydrogen bound to C_{60}. The solid perfluoroalkylated fullerenes **8** are amorphous glassy materials, being more volatile than the parent C_{60}[18]. Under high vacuum, the perfluorohexylated **8** can be sublimed quantitatively to deposit a thin film on a glass substrate. Another characteristic property is the remarkable stability of these materials, which do not decompose until 270 °C and resist the treatment with aqueous sulfuric acid and sodium hydroxide.

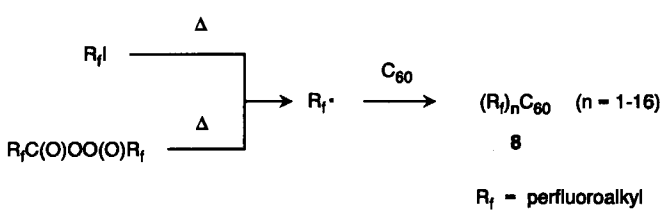

Scheme 6.8

6.3 Metalation of C_{60} with Pentacarbonylrhenium Radicals

The photodissociation of the Re-Re bond of $Re_2(CO)_{10}$ has been used to generate the rhenium carbonyl radicals $\cdot Re(CO)_5$, which add to C_{60} in benzene to form $C_{60}[Re(CO)_5]_2$ (**9**) [Scheme 6.9][19]. This reaction was followed quantitatively by IR spectroscopy, which allows the determination of the stoichiometry of this complex. The IR spectrum of **9** is characteristic of a species with the local structure $X-Re(CO)_5$[20]. Alternatively, $C_{60}[Re(CO)_5]_2$ (**9**) can be synthesized by the reaction of $(\eta^3-Ph_3C)Re(CO)_4$ with C_{60} in the presence of carbon monoxide [Scheme 6.9][19]. Thereby, $\cdot Re(CO)_5$ radicals are generated in situ via homolysis of the weak Re-C bond in the $Ph_3CRe(CO)_5$ intermediate. Molecular modelling investigations on **9** suggest that a 1,4-addition mode takes place[19].

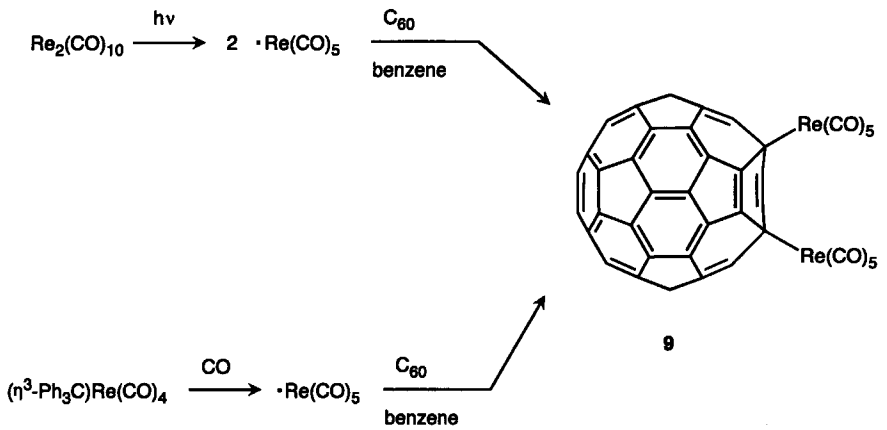

Scheme 6.9

The formation of the adduct **9** is reversible. Although the photochemical preparation of **9** proceeds in yields greater than 90 %, solutions containing this complex decompose over a period of one day to regenerate C_{60} and $Re_2(CO)_{10}$[19]. When CCl_4 is added to a solution of $C_{60}[Re(CO)_5]_2$ (**9**), $Re(CO)_5Cl$ and C_{60} are the only products formed. This together with the first order kinetics of the decay, obtained from the time-dependent IR spectra, led to the formulation of the mechanism for the decomposition represented in Scheme 6.10.

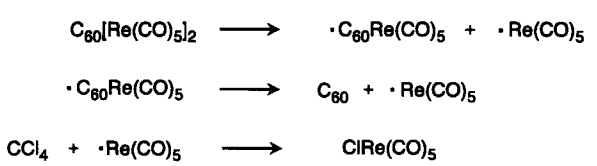

Scheme 6.10

6.4 Hydrostannylation of C_{60}

Refluxing benzene solutions of C_{60} in the presence of a 20-fold excess of Bu_3SnH leads to the hydrostannylation [Scheme 6.11][21]. Multiple additions can also take place. In order to maximize the yield of the monoadduct $C_{60}HSnBu_3$ (**10**), the time dependence of the reaction was followed quantitatively by HPLC. After about 4 hours, the concentration of the monoadduct **10** reaches its maximum. The isolation of **10** can be achieved by preparative HPLC on a C_{18}-reversed-phase stationary phase with $CHCl_3/CH_3CN$ (60:40, v/v) as eluent. The structural determination of $C_{60}HSnBu_3$ (**10**) was done by ^1H NMR spectroscopy and other methods, showing that a 1,2-addition takes place regioselectively [Scheme 6.11][21].

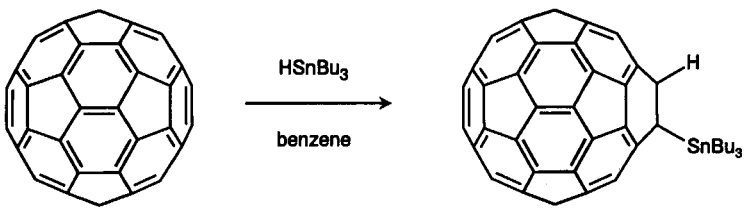

10

Scheme 6.11

6.5 Addition of Bis(trifluoromethyl)nitroxide

The treatment of C_{60} with an excess of bis(trifluoromethyl)nitroxide ($(CF_3)_2NO\cdot$ radicals) leads to multiple additions with an average of 18 $(CF_3)_2NO$ groups bound to the fullerene sphere [Scheme 6.12][22]. The reaction has been carried out in a glass tube equipped with a teflon valve. The resulting light brown solid decomposes at temperatures above 158 °C.

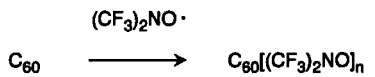

n = 18

Scheme 6.12

6.6 Radical Copolymerization of C_{60} and Paracyclophane

Simple radical chemistry can be used to generate fullerene polymers. A polymer with fullerenes as part of the main chain has been synthesized by the free radical copolymerization of C_{60} and paracyclophane [Scheme 6.13][23]. In this case xylylene, the diradical analogue of the benzyl radical, was first generated from paracyclophane in a tube furnace at 650 °C. The xylyene was then swept into a reaction vessel containing C_{60} dissolved in toluene. The addition of xylylene to the C_{60} solution leads to an immediate change of the color from purple to olive-green. A brown precipitate of the C_{60}-

p-xylylene copolymer forms by allowing the reaction mixture to warm to room temperature. Due to cross-linking through multiple benzylations of the C_{60} molecules, this C_{60}-*p*-xylylene copolymer is insoluble in organic solvents. The solid material was characterized by solid state ^{13}C NMR, IR as well as by thermal gravimetric analysis. Elemental analysis was used to calculate the composition of the copolymer. On the basis of the carbon:hydrogen ratio, the ratio of xylylene to C_{60} was determined to be 3.4:1.0.

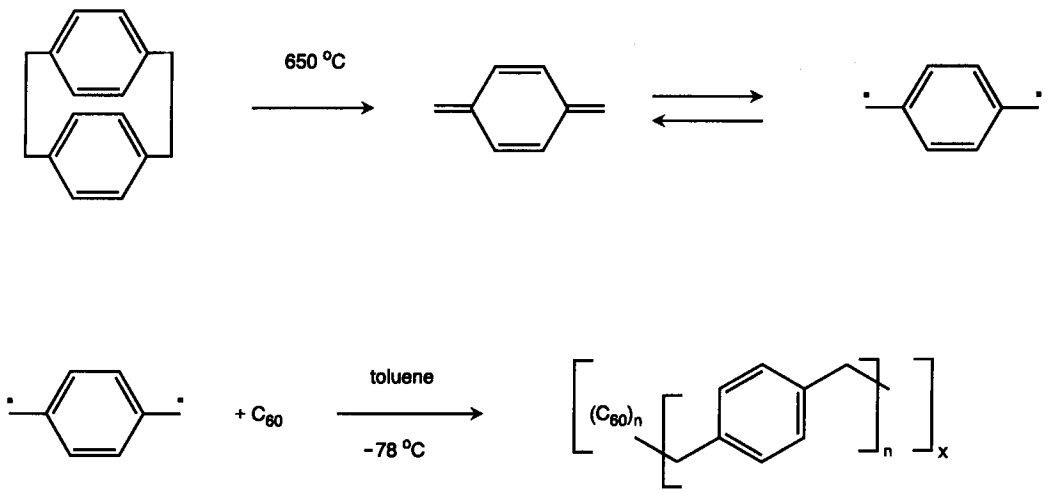

Scheme 6.13

References

1 J. R. Morton, K.F. Preston, P.J. Krusic, S.A. Hill, E. Wasserman *J. Phys. Chem.* **1992**, *96*, 3576.
2 J. R. Morton, K.F. Preston, P.J. Krusic, S.A. Hill, E. Wasserman *J. Am. Chem. Soc.* **1992**, *114*, 5454.
3 J. R. Morton, K. F. Preston, P. J. Krusic, E. Wasserman *J. Chem. Soc., Perk. Trans. 2* **1992**, 1425.
4 P. J. Krusic, D.C. Roe, E. Johnston, J.R. Morton, K.F. Preston *J. Phys. Chem.* **1993**, *97*, 1736.
5 J. R. Morton, K. F. Preston, P. J. Krusic, L. B. Knight Jr. *Chem. Phys. Lett.* **1993**, *204*, 481.
6 P. N. Keizer, J. R. Morton, K.F. Preston *J. Chem. Soc., Chem. Commun.* **1992**, 1259.
7 M. A. Cremonini, L. Lunazzi, G. Placucci, P. J. Krusic *J. Org. Chem.* **1993**, *58*, 4735.
8 P. J. Fagan, B. Chase, J. C. Calabrese, D. A. Dixon, R. Harlow, P. J. Krusic, N. Matsuzawa, F. N. Tebbe, D. L. Thorn, E. Wasserman *Carbon* **1992**, *30*, 1213.
9 C. S. Johnson Jr. *Adv. Magn. Reson.* **1965**, *1*, 33.
10 C. S. Johnson Jr. *J. Chem. Phys.* **1964**, *41*, 3277.
11 P. Krusic, P. Meakin, J. P. Jesson *J. Phys. Chem.* **1971**, *75*, 3438.
12 P. J. Fagan, P.J. Krusic, D.H. Evans, S.A. Lerke, E. Johnston *J. Am. Chem. Soc.* **1992**, *114*, 9697.
13 P. J. Krusic, E. Wasserman, B. A. Parkinson, B.Malone, E. R. Holler Jr., P. N. Keizer, J. R. Morton, K. F. Preston *J. Am. Chem. Soc.* **1991**, *113*, 6274.
14 J. M. McBridge *Tetrahedron* **1974**, *30*, 2009.
15 P. J. Krusic, E. Wasserman, P. N. Keizer, J. M.Morton, K. F. Preston *Science* **1991**, *254*, 1183.
16 P. J. Krusic, J. K. Kochi *J. Am. Chem. Soc.* **1968**, *90*, 7155.
17 N. Matsuzawa, D. A. Dixon, T. Fukunaga *J. Phys. Chem.* **1992**, *96*, 7594.

18 P. J. Fagan, P. J. Krusic, C. N. McEven, L. Lazar, D. Holmes Parker, N. Herron, E. Wasserman *Science* **1993**, *262*, 404.
19 S. Zhang, T. L. Brown, Y. Du, J. R. Shapley *J. Am. Chem. Soc.* **1993**, *115*, 6705.
20 K. Raab, W. Beck *Chem. Ber.* **1985**, *118*, 3830.
21 A. Hirsch, T. Grösser, A. Skiebe, A. Soi *Chem. Ber.* **1993**, *126*, 1061
22 D. Brizzolara, J. T. Ahlemann, H. W. Roesky, K. Keller *Bull. Soc. Chim. Fr.* **1993**, *130*, 745.
23 D. A. Loy, R. Assink *J. Am. Chem. Soc.* **1992**, *114*, 3977.

Chapter 7 Transition Metal Complex Formation

7.1 Introduction

7.2 (η^2-C_{60}) Transition Metal Complexes

7.3 Hydrometalation Reactions

7.4 Organopalladium Polymers of C_{60}

References

7.1 Introduction

The electron deficiency of the fullerenes C_{60} and C_{70}, established by calculations, electrochemistry as well as the reaction behavior towards nucleophiles, was independently demonstrated by the investigations of fullerene transition metal complexes. A variety of single crystal structures and spectroscopic studies show that the complexation of transition metals to the fullerene core proceeds similarly to well established reactions of electron deficient olefins in a dihapto manner or as hydrometalation reactions. Some of these complexation reactions are more or less reversible. The resulting thermodynamic control explains the remarkable regioselectivity observed at the formation of higher addition products, for example bisadducts or hexaadducts. Packing effects in the solid-state structure can also play an important role for the exclusive formation of a specific regioisomer. One driving force for the formation of a certain solid-state structure of fullerene derivatives could be due to π-π interactions of ligand-bound electron-rich arene moieties and the electron-poor fullerene core itself. This is demonstrated by impressive examples for supramolecular arrangements in single crystals of fullerene transition metal complexes.

7.2 (η^2-C_{60}) Transition Metal Complexes

The question whether C_{60} behaves like an aromatic or an electron deficient alkene was answered elegantly by Fagan[1,2,3]. The complex $[Cp^*Ru(CH_3CN)_3]^+ O_3SCF_3^-$ [$Cp^* = \eta^5$-$C_5(CH_3)_5$] is known to react with electron-rich planar arenes upon displacement of the three coordinated acetonitrile ligands resulting in a strong η^6-binding of ruthenium to the six-membered rings of the arenes[4]. On the other hand, the reaction of this ruthenium complex with an electron-deficient alkene leads to the displacement of one acetonitrile ligand and the formation of a η^2-olefin complex. By the reaction with a ligand containing both an alkene functionality as well as an arene ring, the ruthenium exclusively binds to the arene ring[4]. This remarkable selectivity makes the ruthenium complex a good candidate for testing the transition metal complex formation behavior of C_{60}. Allowing C_{60} to react with a 10-fold excess of $[Cp^*Ru(CH_3CN)_3]^+ O_3SCF_3^-$ in CH_2Cl_2 at 25 °C for a period of five days leads to the formation of a brown precipitate of $[Cp^*Ru(CH_3CN)_2]_3(C_{60})^{3+}$ $(O_3SCF_3^-)_3$, in which two acetonitrile ligands are retained on each ruthenium [Scheme 7.1][2]. This finding suggests that each ruthenium is bound to one double bond of the C_{60} sphere. Therefore the reactivity of C_{60} is also shown from this point of view to be that of an electron-deficient olefin.

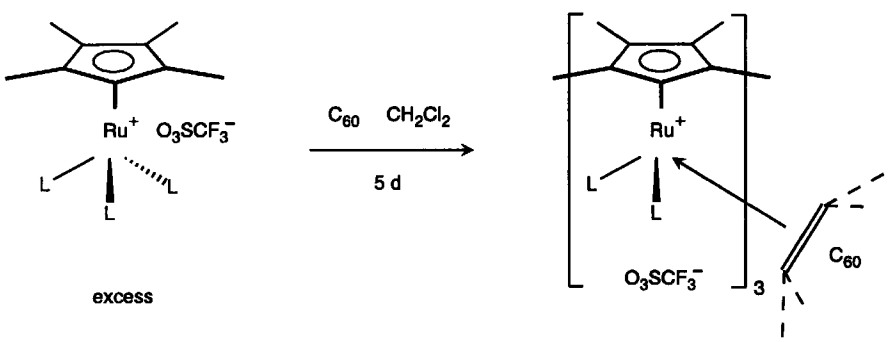

Scheme 7.1

Considering the geometry of the p-orbitals within a hexagon of the C_{60} framework, which are tilted away from the center of the ring, it is already obvious that a binding of C_{60} to a metal in a hexahapto-fashion is not favorable because the orbital overlap will be weakened.

The binding of C_{60} to transition metals in a η^2-fashion becomes clearly evident by the formation of platinum, palladium and nickel complexes[1,2,3,5,6,7]. Low-valent complexes of these metals easily undergo complexation with electron-deficient olefins[8,9]. A typical structural aspect is the loss of planarity of the olefin coordinated to the transition metal, because the four groups bound to the olefin bend back away from the metal [Fig. 7.1]. In substituted ethylenes, C_2X_4, this deformation increases upon increasing electronegativity of X. In C_{60}, the arrangement around 6-6 double bonds is already preorganized. Therefore, the combination of both strain and electron deficiency of the 6-6 double bonds is an important driving force of η^2-binding of C_{60} with low-valent transition metals. The reaction of equimolar amounts of $(Ph_3P)_2Pt(\eta^2\text{-}C_2H_4)$ with C_{60} leads to a dark emerald green solution of $(Ph_3P)_2Pt(\eta^2\text{-}C_{60})$ [Scheme 7.2]. Single crystal X-ray structure analysis confirmed the η^2-binding of the platinum to a 6-6 fullerene double bond[1].

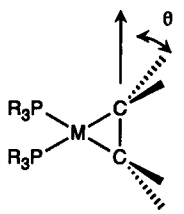

Figure 7.1 The coordination of an olefin to the transition metal fragment $M(PPh_3)_2$ (M = e.g. Ni, Pd, Pt) leads to a deviation from planarity of the olefin system. The angle θ is a measure of the deformation of the groups attached to the carbon-carbon double bonds from planarity.

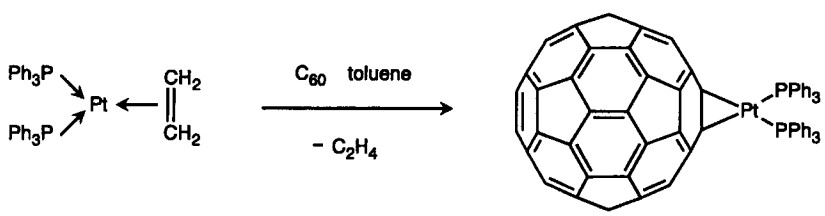

Scheme 7.2

Similar complex formation reactions are also possible with the metal reagents $M(PEt_3)_4$ (M = Ni, Pd) [Scheme 7.3][3]. All these metal derivatives exhibit almost identical properties as $(Ph_3P)_2Pt(\eta^2\text{-}C_{60})$. The same compounds can also be synthesized by the reaction with the complexes $(Et_3P)_2Pd(\eta^2\text{-}CH_2{=}CHCO_2CH_3)$[7]. Using stoichiometric amounts of reagents, these reactions are very selective in forming only monoadducts in a high yield rather than a mixture polyadducts and unreacted C_{60}.

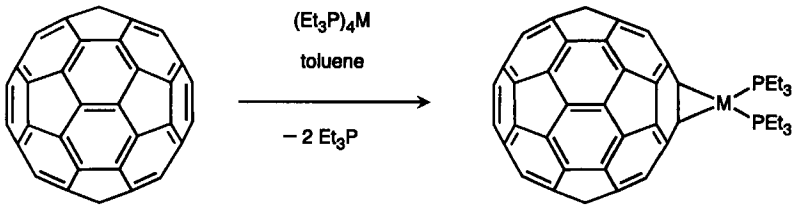

Scheme 7.3

However, the reactions can be driven to the formation of air sensitive hexaadducts $[(Et_3P)_2M]_6C_{60}$ by using a 10-fold excess of the metal reagent $M(PEt_3)_4$ (M = Ni, Pd, Pt)[2,3,5]. Each compound exists as a single structural isomer. The X-ray crystal structure of $[(Et_3P)_2Pt]_6C_{60}$, for example, shows that the molecule has a C_{60} core octahedrally coordinated with 6 $(Et_3P)_2Pt$ groups [Fig. 7.2]. This results in an overall T_h point group symmetry, ignoring the ethyl groups. Each platinum is bound across a 6-6 double bond. It is very interesting to note that excluding the carbons bound to the platinum leads to a network of eight 1,3,5-linked benzene like rings [Fig. 7.2]. Indeed, the crystal structure of $[(Et_3P)_2Pt]_6C_{60}$ shows that the bond alternation within the six octahedrally arranged "benzene rings" (bonds C and E) is reduced to 0.037 Å, half the value in C_{60}. Both bonds approach the typical value for arenes (ca. 1.395 Å). As a consequence, the remaining π-system in the C_{60} core becomes more delocalized, which is corroborated by Hückel calculations[10].

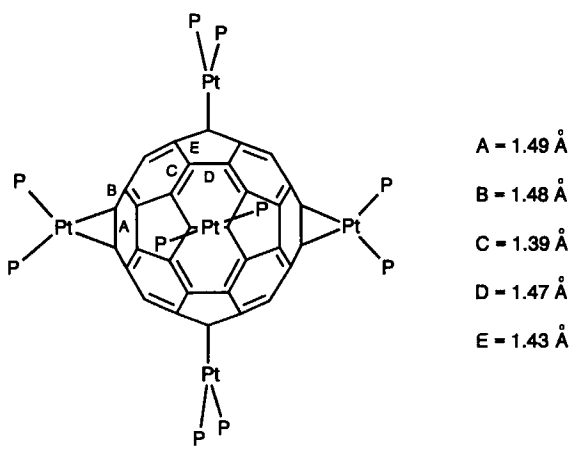

A

A = 1.49 Å
B = 1.48 Å
C = 1.39 Å
D = 1.47 Å
E = 1.43 Å

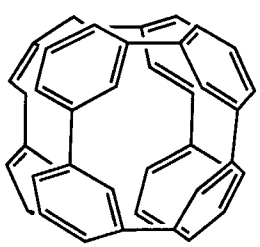

B

Figure 7.2 **A**: Bond lengths for the five different sets of C-C bonds and favored electronic resonance structure of $[(Et_3P)_2Pt]_6C_{60}$ determined by X-ray crystal structure analysis. The ethyl groups on the P-atoms are omitted for clarity. **B**: 48-electron π system produced by the saturation of six double bonds in the octahedral sites of C_{60}, leaving eight linked benzenoid hexagons.

This electronic argument, the formation of a more delocalized aromatic system (8 benzene-like rings) out of the more bond-localized non-aromatic C_{60} system, may be an additional driving force for the octahedral arrangement of 6 metal units on the fullerene sphere. But steric factors must also be considered, because there is no room for a seventh $(Et_3P)_2Pt$ ligand and the octahedral array of metal fragments in $[(Et_3P)_2M]_6C_{60}$ is sterically the optimum situation.

An important requirement for the exclusive formation of octahedrally coordinated $[(Et_3P)_2M]_6C_{60}$ in these high yields is a certain degree of reversibility of the $(Et_3P)_2M$ addition, because not only the octahedral sites in C_{60} are available for complex formation. The complexation of the metal fragments in $[(Et_3P)_2Pt]_2C_{60}$ in non-octahedral sites was confirmed by ^{31}P NMR spectroscopy. The reversibility of the adduct formation was confirmed by substitution experiments as well as by electrochemistry studies[7]. The addition of 1 equiv. of diphenylacetylene to a solution of $[(Et_3P)_2Pt]_6C_{60}$ in benzene leads to an instantaneous reaction to produce the complexes $(Et_3P)_2Pt(\eta^2\text{-}C_2\text{-}Et_2)$ and $[(Et_3P)_2Pt]_5C_{60}$ as major components [Scheme 7.4][5]. Because of the steric inaccessibility of the C_{60} bonds in the hexaadduct, it is unlikely that this is an associative reaction. Therefore it was concluded that $[(Et_3P)_2Pt]_6C_{60}$ is in an equilibrium with a small amount of the metal fragment $(Et_3P)_2Pt$ even in non polar solvents.

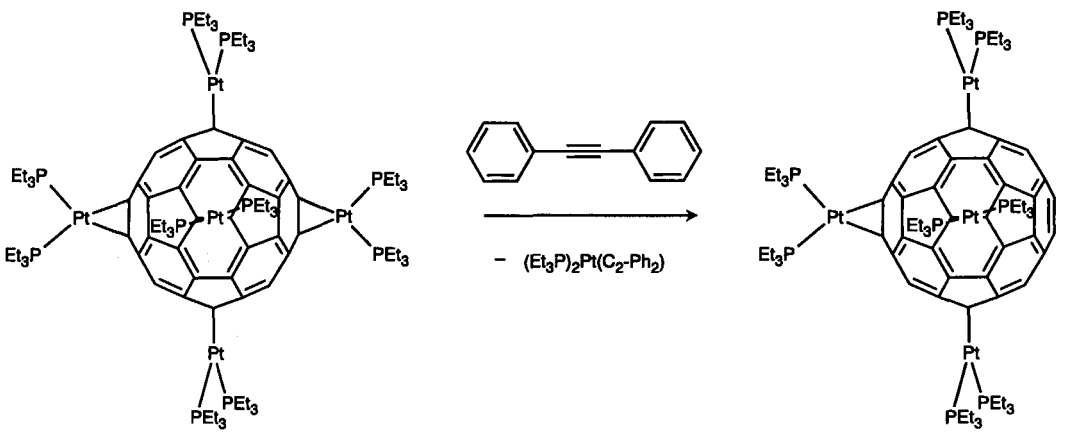

Scheme 7.4

The first reduction potentials of $(Et_3P)_2MC_{60}$ (M = Ni, Pd, Pt) are shifted by about 0.23–0.34 V to more negative potentials as compared to C_{60}[7]. Therefore, these organometallic complexes are about 0.10–0.2 V harder to reduce than organic monoadducts of the type $C_{60}RR'$ (R,R' = organic group or H). The additional shift in the metal complexes relative to the organic derivatives was attributed to a higher inductive donation of electron density into the C_{60} moiety, which further lowers the electron affinity. This also explains the high selectivity for the monoadduct formation with these low-valent transition metal reagents. The tendency of a second metal fragment to add to a monoadduct is significantly reduced. Bisadducts $[(Et_3P)_2M]_2C_{60}$ react with C_{60} in solution and form the corresponding monoaddition products. With increasing amounts of metal complexation, the adducts become increasingly harder to reduce. This is in agreement with a decreasing tendency of further complexation of electron-rich metal fragments. The addents begin to equilibrate on and off the C_{60} framework most readily in the hexaadducts $[(Et_3P)_2M]_6C_{60}$, which allows the T_h symmetry to be achieved in these complexes.

There are several effects which can influence the electronic structure of C_{60} upon metal complex formation. One effect is the removal of one double bond from the remaining 29 fullerene double bonds. As in any polyene system, this decreased conjugation is expected to raise the energy of the LUMO and therefore decreases the electron affinity of the system. On the other hand, the d-orbital backbonding transfers electron density from the metal into π^* orbitals of the remaining double bonds, which also decreases the electron affinity.

Coordination of C_{60} with the (η^5-C_9H_7)Ir(CO) fragment lowers the first reduction potential only by 0.08 V relative to C_{60}[11], indicating a weaker backbonding capability. The corresponding complex (η^5-C_9H_7)Ir(CO)(η^2-C_{60}) can be obtained by refluxing equimolar amounts of (η^5-C_9H_7)Ir(CO)(η^2-C_8H_{14}) and C_{60} in CH_2Cl_2 [Scheme 7.5]. The coordinated C_{60} molecule in this complex can be substituted upon treatment with strongly coordinating ligands, for example with CO, $P(OMe)_3$ or PPh_3 [Scheme 7.5]. Thereby, the color of the solutions changes from green to the characteristic purple of C_{60}. These reactions can be monitored quantitatively by UV/Vis and IR spectroscopy. Significantly, the substitution of C_{60} in (η^5-C_9H_7)Ir(CO)(η^2-C_{60}) by weaker coordinating ligands, such as C_2H_4 or C_2H_2, is more than 100 times slower than the reaction with carbon monoxide. This implies an associative pathway for the substitution reaction. The air-stable solutions of (η^5-C_9H_7)Ir(CO)(η^2-C_{60}) show an additional well defined absorption band at 436 nm. This band is also observed in the monoadducts $C_{60}RR'$ (R,R' = organic group or H), discussed in the preceding chapters, and can, therefore, not be attributed to Ir-to-C_{60} charge-transfer transitions. It arises instead from a transition largely centered on the C_{60} ligand[12].

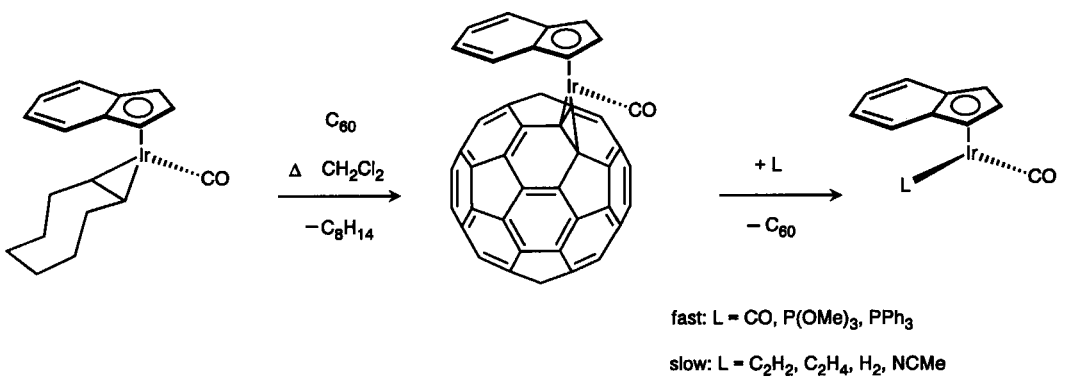

Scheme 7.5

An adduct formation that is more reversible occurs upon addition of Vaska's complex $Ir(CO)Cl(PPh_3)_2$ [Scheme 7.6][13]. This complex is known to react with electron-deficient olefins, such as tetracyanoethylene, to form stable η^2 adducts[14]. The carbon monoxide stretching frequency in these complexes can be used as a measure of the electron-withdrawing influence of the ligands. In the tetracyanoethylene adduct of $Ir(CO)Cl(PPh_3)_2$, for example, the carbonyl stretching frequency is considerably stronger than in the C_{60} adduct (η^2-C_{60})Ir(CO)Cl(PPh_3)$_2$, demonstrating that C_{60} is less effective in electron withdrawing than tetracyanoethylene. The electron-withdrawing influence of C_{60} is similar to that observed for O_2 in $O_2Ir(CO)Cl(PPh_3)_2$. There was a correlation found between the reversibility of adduct formation and the magnitude of the carbonyl stretching frequency. Therefore, both the C_{60} and the dioxygen complex fall into the category of "easily reversible". Single crystals of (η^2-C_{60})Ir(CO)Cl(PPh_3)$_2$ containing five molecules of benzene per formula unit can be obtained by

mixing equimolar benzene solutions of the components. The reversible process takes place upon redissolving these crystals in CH_2Cl_2.

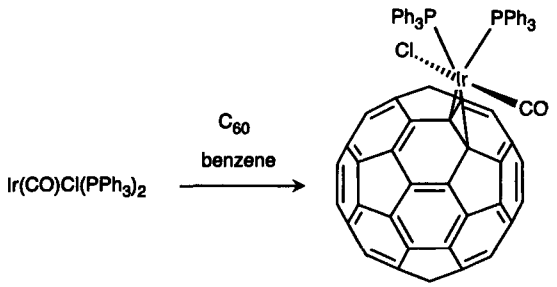

Scheme 7.6

In addition to $Ir(CO)Cl(PPh_3)_2$, other Vaska-type iridium compounds were added to C_{60}[15,16]. By using a complex $Ir(CO)Cl(bobPPh_2)_2$ (bob = 4-$(PhCH_2O)C_6H_4CH_2$) containing two phenyl rings in each side chain, a supramolecular architecture is formed in the single crystals of $(\eta^2\text{-}C_{60})Ir(CO)Cl(bobPPh_2)_2$ [Fig. 7.3]. The C_{60} spheres of one molecule are chelated by the phenyl rings in the two side arms of another molecule, which is a further example for a π-π interaction between an electron-rich moiety in the side chain of the addent and the electron-poor C_{60}. This attractive interaction is also reflected by the decrease in the P-Ir-P bond angle as compared to that in $(\eta^2\text{-}C_{60})Ir(CO)Cl(PPh_3)_2$.

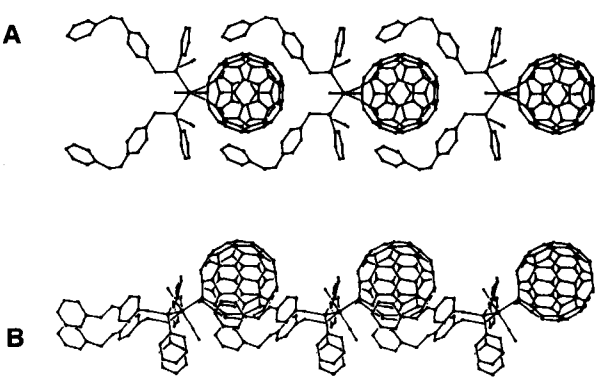

Figure 7.3 X-ray crystal structure of $(\eta^2\text{-}C_{60})Ir(CO)Cl(bobPPh_2)_2$ (bob = 4-$(PhCH_2O)C_6H_4CH_2$)[15]. The two views A and B show the supramolecular chelation architecture of this system.

The addition of $Ir(CO)Cl(PMe_2Ph)_2$ to C_{60} in benzene in different molar ratios leads to the formation of air sensitive crystals of the bisadducts, which were identified by X-ray crystallography [Scheme 7.7][16]. Two different conformational isomers were observed. In each case the Ir-moieties are bound at the opposite ends of the C_{60} molecules in *trans*-1 positions. Both electronically and sterically, the formation of the *trans*-1 isomers is not expected to be favored over the *trans*-2, *trans*-3, *trans*-4

and *e* isomers to the extent that the formation of the latter is completely supressed. Since the additions of the iridium complexes to C_{60} are reversible, the low solubility of this bisadduct, which is characteristic for *trans*-1 isomers, as well as packing effects in the solid, can play a major role in the exclusive formation of this regioisomer.

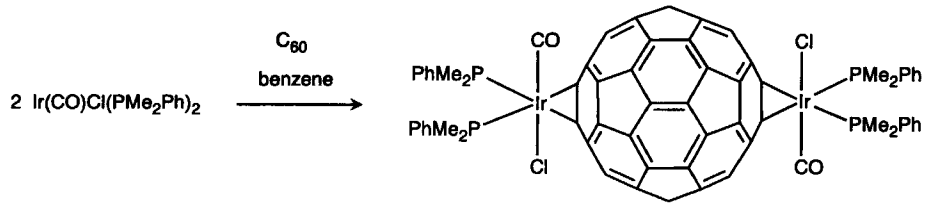

Scheme 7.7

Upon treatment of C_{70} with Vaska's complex in benzene one regioisomer of (η^2-C_{60})Ir(CO)Cl(PPh_3)$_2$ is selectively formed, which was characterized by IR spectroscopy as well as by X-ray crystallography [Scheme 7.8][17]. As in the case of the organodihydrofullerenes, the addition of the Ir-complex occurs in the 1,2-position at the poles. As in the case of the C_{60} analogues, such as (η^2-C_{70})Ir(CO)Cl(PPh_3)$_2$, the two C-atoms of the fullerene involved in the metal binding are pulled out from the surface. Therefore, the *exo*-double bonds of the pole pentagons are the most accessible for this type of coordination because the other 6-6 bonds in C_{70} have a more flattened local structure. The bond lengths of the [5]radialene subunits of C_{70} at the poles are almost the same as those in C_{60}.

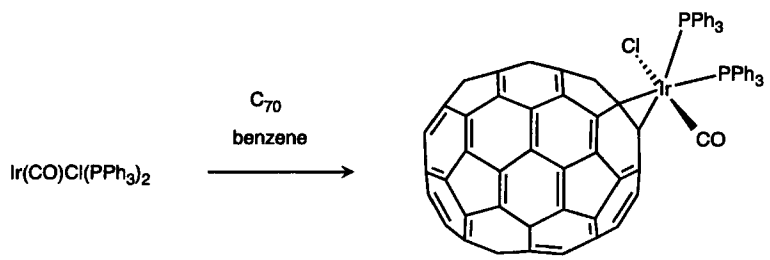

Scheme 7.8

The complex Ir(CO)Cl($PPhMe_2$)$_2$ is more reactive in oxidative addition reactions than Vaska's complex itself[18]. This allows the synthesis of a bisadduct of C_{70} by treatment with a six- to twelve-fold excess of Ir(CO)Cl($PPhMe_2$)$_2$ in benzene [Scheme 7.9][19]. Whereas in solution several isomers exist in equilibrium, which can be shown by $^{31}P\{^1H\}$ NMR spectroscopy, the uniform and characteristic morphology of the single crystals of {(η^2-C_{70})[Ir(CO)Cl($PPhMe_2$)$_2$]$_2$} indicate that there is a single regioisomer present in the solid state. The molecule has a C_2-symmetry and the Ir-atoms are bound on the *exo*-double bonds of the opposite pole pentagons, which electronically as well as sterically is the most favorable situation. Three isomers of "pole-opposite pole" bound bisadducts are in principle possible. The fact that this C_2-symmetrical isomer is formed exclusively was explained by packing effects of the solid state structure [Fig. 7.4][19]. Arene/fullerene π-π interactions play an important role thereby. The phenyl rings of the phosphine ligand of one fullerene lie close over the surface of another C_{70} portion.

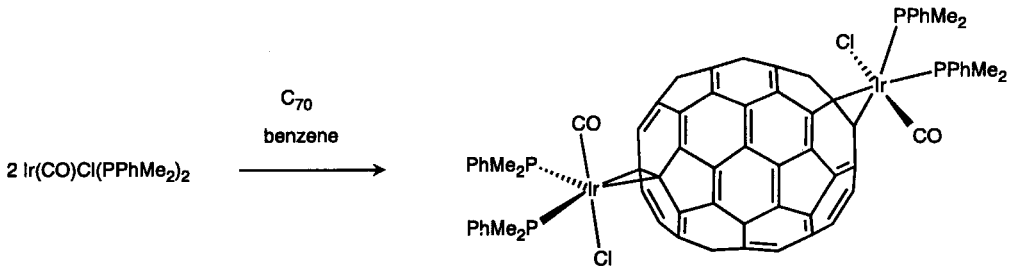

Scheme 7.9

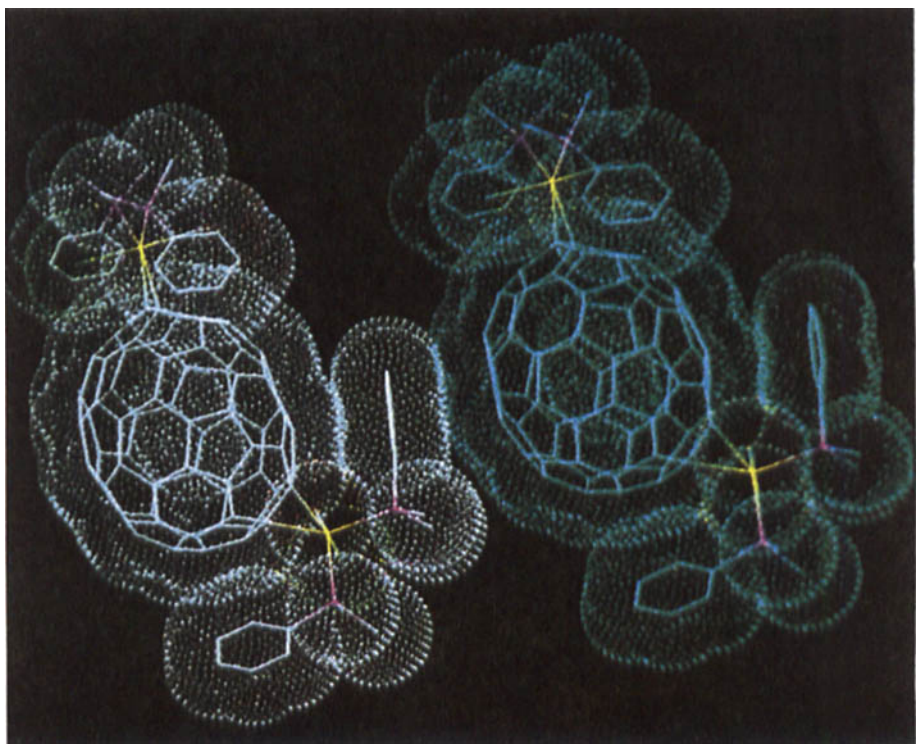

Figure 7.4 Representation of the close contact by van der Waals dot clouds of two molecules of $\{(\eta^2\text{-}C_{70})[Ir(CO)Cl(PPhMe_2)_2]_2\}$ in the solid state[19].

A binuclear addition product of C_{60} has been synthesized by the addition of two molecules of $Ir_2Cl_2(1,5\text{-COD})_2$ [Scheme 7.10][20]. Single crystals of the air-stable complex $C_{60}[Ir_2Cl_2(1,5\text{-COD})_2]_2 \cdot 2\ C_6H_6$ were grown by slow diffusion of benzene solutions of the components. The complexation of $Ir_2Cl_2(1,5\text{-COD})_2$ takes place without any leaving groups. In this complex, two molecules of $Ir_2Cl_2(1,5\text{-COD})_2$ bind to the opposite ends of the same C_{60} framework and the two Ir atoms of each $Ir_2Cl_2(1,5\text{-COD})_2$ are bound *cis*-1 to the same hexagon of C_{60}, leading to a C_{2h} symmetry. Each 1,5-COD ligand is bound to the Ir with two η^2-bonds.

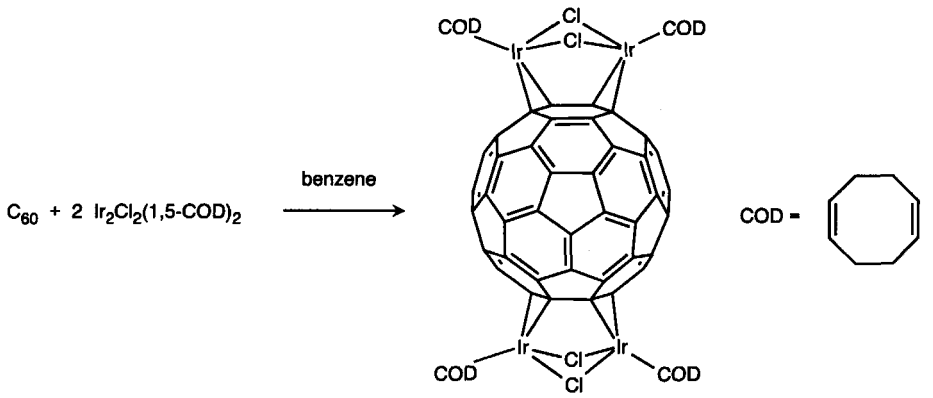

Scheme 7.10

The hydrogenation catalyst $RhH(CO)(PPh_3)_3$ is known to undergo hydrometalation reactions with electron deficient olefins[21]. In the case of the reaction with C_{60}, however, a complexation in a dihapto manner leading to (η^2-C_{60})[$RhH(CO)(PPh_3)_3$] rather than a hydrometalation takes place [Scheme 7.11], which was shown by X-ray structure analysis and NMR spectroscopy[22]. The green black crystals of this complex are formed in 75 % yield. Unlike (η^2-C_{60})$Ir(CO)Cl(PPh_3)_2$ which dissociates into C_{60} and $Ir(CO)Cl(PPh_3)_2$ the green solutions of (η^2-C_{60})[$RhH(CO)(PPh_3)_3$] are stable.

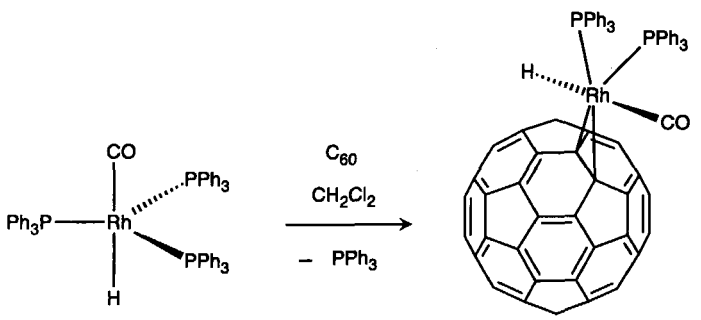

Scheme 7.11

7.3 Hydrometalation Reactions

Whereas the reaction of C_{60} with $RhH(CO)(PPh_3)_3$ results in complex formation in a dihapto fashion, a hydrometalation is possible with the stronger nucleophilic reagent $Cp_2Zr(H)Cl$ (Cp = η^5-C_5H_5[23] [Scheme 7.12][24]. Upon treatment of C_{60} with this Zr-complex, a red solution forms that is different from η^2 transition metal complexes of C_{60} exhibiting a green color in solution. The structure of the air sensitive $Cp_2ZrClC_{60}H$ was confirmed by ^1H NMR spectroscopy. The hydrogen transferred from the Zr to C_{60} resonates at δ = 6.09, a typical value for fullerenyl protons[25]. The hydrolysis of $Cp_2ZrClC_{60}H$ with aqueous HCl provides access to the simplest C_{60} hydrocarbon $C_{60}H_2$ [Scheme 7.12]. The spectroscopic characterization of $C_{60}H_2$ shows that the compound is the isomerically pure 1,2-addition product.

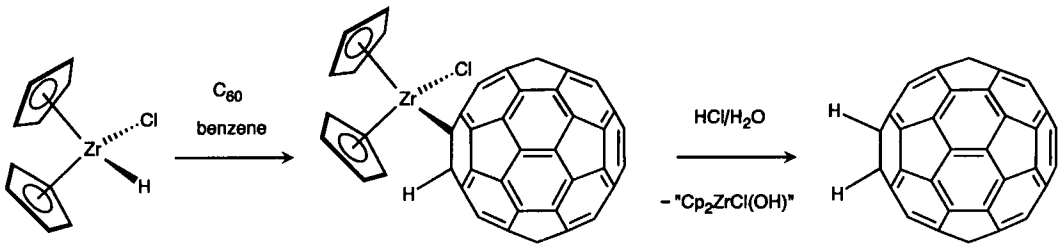

Scheme 7.12

7.4 Organopalladium Polymers of C_{60}

Organometallic polymers of C_{60} can be obtained by the reaction of C_{60} solutions with the palladium complex $Pd_2(dba)_3 \cdot CHCl_3$ (dba = dibenzylideneacetone)[26]. The resulting replacement of the dba ligands leads to a dark brown precipitate of $C_{60}Pd_n$. Depending on the C_{60}:Pd ratio it is believed that these polymers form linear "pearl necklace" or two- and three-dimensional arrangements. The Pd:C_{60} ratio can be changed form 1:1 to 3:1 upon heating a suspension of the initially formed polymer in toluene under reflux with regeneration of free C_{60}. The mode of the binding of the palladium to the fullerene core has not been conclusively proven. These materials exhibit catalytic activity in the hydrogenation of olefins and acetylenes at room temperature[27].

References

1 P. J. Fagan, J. C. Calabrese, B. Malone *Science* **1991**, *252*, 1160.
2 P. J. Fagan, J. C. Calabrese, B. Malone In *Fullerenes: Synthesis, Properties, and Chemistry of Large Carbon Clusters;* G. S. Hammond, V. J. Kuck, Eds.; p 177, American Chemical Society Symposium Series 481, 1992.
3 P. J. Fagan, J. C. Calabrese, B. Malone *Acc. Chem. Res.* **1992**, *25*, 134.
4 P. J. Fagan, M. D. Ward, J. C. Calabrese *J. Am. Chem. Soc.* **1989**, *111*, 1698 .
5 P. J. Fagan, J. C. Calabrese, B. Malone *J. Am. Chem. Soc.* **1991**, *113*, 9408.
6 B. Chase, P. J. Fagan *J. Am. Chem. Soc.* **1992**, *114*, 2252.
7 S. A. Lerke, B. A. Parkinson, D. H. Evans, P. J. Fagan *J. Am. Chem. Soc.* **1992**, *114*, 7807.
8 S. D. Ittel, J. A. Ibers *Adv. Organomet. Chem.* **1976**, *14*, 33.
9 T. Yoshida, T. Matsuda, S. Otsuka *Inorg. Synth.* **1990**, *28*, 122.
10 P. W. Fowler, D. J. Collins, S. J. Austin *J. Chem. Soc., Perkin. Trans. 2* **1993**, 275.
11 R. S. Koefod, M. F. Hudgens, J. R. Shapley *J. Am. Chem. Soc.* **1991**, *113*, 8957.
12 Y. Zhu, R. S. Koefod, C. Devadoss, J. R. Shapley, G. B. Schuster *Inorg. Chem.* **1992**, *31*, 3505.
13 A. L. Balch, V. J. Catalano, J. W. Lee *Inorg. Chem.* **1991**. *30*, 3990.
14 L. Vaska *Acc. Chem. Res.* **1968**, *1*, 335.
15 A. L. Balch, V. J. Catalano, J. W. Lee, M. M. Olmstead *J. Am. Chem. Soc.* **1992**, *114*, 5455.
16 A. L. Balch, J. W. Lee, B. C. Noll, M. M. Olmstead *J. Am. Chem. Soc.* **1992**, *114*, 10984.
17 A. L. Balch, V. J. Catalano, J. W. Lee, M. M. Olmstead, S. R. Parkin *J. Am. Chem. Soc.* **1991**, *113*, 8953.
18 A. J. Deeming, B. L. Shaw *J. Chem. Soc. A* **1969**, 1802.
19 A. L. Balch, J. W. Lee, M. M. Olmstead *Angew. Chem.* **1992**, *104*, 1400; *ibid. Int. Ed. Engl.* **1992**, *31*, 1356.
20 M. Rasinkangas, T. T. Pakkanen, T. A. Pakkanen, M. Ahlgren, J. Rouvinen *J. Am. Chem. Soc.* **1993**, *115*, 4901.
21 G. Yagupsky, C. K. Brown, G. J. Wilkinson *J. Chem. Soc. A* **1970**, 1392.
22 A. L. Balch, J. W. Lee, C. Noll, M. M. Olmstead *Inorg. Chem.* **1993**, *32*, 3577.

23 J. Schwartz *Pure Appl. Chem.* **1980**, *52*, 733.
24 S. Ballenweg, R. Gleiter, W. Krätschmer *Tetrahedron Lett.* **1993**, *34*, 3737.
25 A. Hirsch, T. Grösser, A. Skiebe, A. Soi *Chem.Ber.* **1993**, *126*, 1061.
26 H. Nagashima, A. Nakaoka, Y. Saito, M. Kato, T. Kawanishi, K. Itoh *J. Chem. Soc., Chem. Commun.* **1992**, 377.
27 H. Nagashima, A. Nakaoka, S. Tajima, Y. Saito, K. Itoh *Chem. Lett.* **1992**, 1361.

Chapter 8 Oxidation and Reactions with Electrophiles

8.1 Introduction

8.2 Electrochemical Oxidation of C_{60} and C_{70}

8.3 Oxygenation

8.4 Osmylation

8.5 Halogenation
8.5.1 Fluorination
8.5.2 Chlorination
8.5.3 Bromination
8.5.4 Reaction with Iodine

8.6 Reactions with Strong Oxidizing Reagents and Acids

8.7 Reaction with Lewis Acids and Fullerenation of Aromatics

References

8.1 Introduction

Although the reduction of the fullerenes is by far more facile than their oxidation, there is a large variety of oxidative functionalizations as well as electrophilic additions that have been carried out. Controlled oxygenations and halogenations lead to defined adducts. Valuable information about the regiochemistry of C_{60} can be obtained from chlorinations and brominations, as well as osmylations. Both mono- and polyadducts of halogenated and osmylated fullerenes have been completely characterized by X-ray crystallography and NMR spectroscopy. Another interesting phenomenon that accompanies some oxygenations and fluorinations is the ring opening and rupture of the fullerene framework itself. Positively charged C_{60} can be stabilized in very acidic media and the hydrolysis of these species with water provides access to the polar and water soluble fullerols. The interaction of fullerenes with Lewis acids has been used to separate C_{60} from C_{70} as well as to carry out fullerenations of aromatics.

8.2 Electrochemical Oxidation of C_{60} and C_{70}

Whereas C_{60} and C_{70} are easy to reduce, their oxidation occurs at comparatively high anodic potentials. Theoretical investigations predict the first oxidation potential of C_{60} to be comparable to that of naphthalene[1]. Anodic electrochemistry with fullerenes has been carried out with C_{60} films[2] as well as in solution[3,4,5]. The cyclic voltammetry of C_{60} in a 0.1 M solution of Bu_4NPF_6 in trichloroethylene at room temperature exhibits a chemically reversible, one-electron oxidation wave at +1.26 V vs Fc/Fc^+ [5]. Under identical conditions, a one-electron, chemically reversible oxidation is also observed for C_{70}. The oxidation of C_{70} occurs 60 mV more negative than that of C_{60}, at + 1.20V vs Fc/Fc^+. The energy difference between the first oxidation and reduction potentials is a measure for the energy difference between the HOMO and the LUMO in solution and was determined to be 2.32 V for C_{60} and 2.22 V for C_{70}. The cationic radical species generated electrochemically are relatively long-lived at room temperature. The life-time of the radicals was estimated to be >0.5 min. For C_{70} a second one-electron oxidation ($C_{70}^{\cdot+} \rightarrow C_{70}^{2+}$) was observed at a potential of 1.75 V. Oxidized solutions of C_{60} and C_{70} in benzonitrile at potentials of + 1.90 V are orange in color, air stable and ESR silent at -150 °C[3]. It was suggested that under these conditions an overall four-electron transfer followed or accompanied by one or more chemical reactions takes place.

8.3 Oxygenation

Oxygenated fullerenes $C_{60}O_n$ and $C_{70}O_n$ can be found in the fullerene mixture generated by graphite vaporization[6,7]. The formation of these oxides is due to a small amount of molecular oxygen present in the fullerene reactor. The $C_{70}O$ was isolated from the fullerene extract by preparative HPLC[6]. Mixtures of $C_{60}O_n$ (n up to 5) can also be generated by electrochemical oxidation of C_{60}[8] or by photolysis of the crude fullerene extract[7]. More drastic conditions, such as UV irradiation in hexane[9] or heating in the presence of oxygen[10,11], lead to an extensive oxidation or fragmentation of C_{60}. Upon photooxygenation of C_{60} by irradiating an oxygenated benzene solution for 18h at room temperature and subsequent purification by flash chromatography followed by semipreparative HPLC, $C_{60}O$ (**1**) can be obtained in 7% yield [Scheme 8.1][10].

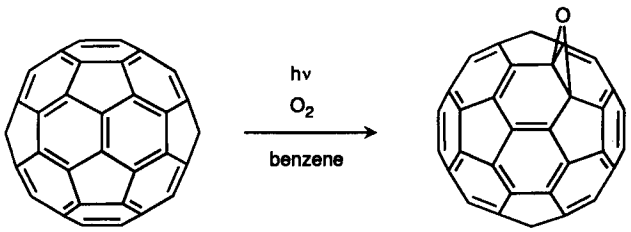

1

Scheme 8.1

The spectroscopic analysis of **1** demonstrates that it exhibits the 1,2-bridged epoxide structure as shown in Scheme 8.1. This becomes especially evident by the appearance of a peak at $\delta = 90.18$ in the ^{13}C NMR spectrum[10], which is due to the sp^3 bridgehead carbons of the C_{60} cage. Another possible isomer of $C_{60}O$ could be the ring-opened 1,6-bridged structure **2**. Interestingly, ab initio calculations[12,13] of **1** and **2** at the LSD/DZP level predict **2** to be more stable, although its formation has not been observed experimentally.

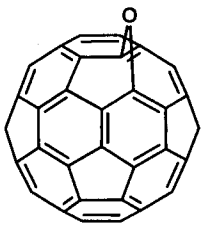

2

Chromatography of $C_{60}O$ (**1**) on neutral alumina leads to an efficient conversion to C_{60} in 91 % yield[10]. $C_{60}O$ (**1**) can also be prepared by allowing toluene solutions of C_{60} to react with dimethyldioxirane[14] [Scheme 8.2]. The product obtained in this way is identical to that prepared by photochemical epoxidation[10]. Upon the treatment of C_{60} with dimethyldioxirane, a second product forms simultaneously [Scheme 8.2] which was identified to be the 1,3-dioxolane **3**. It is surprising that the O–O bond of the dimethyldioxirane breaks to form **3** and it is not clear whether **1** is formed directly or via cleavage of acetone from **3**. Upon heating **3** in toluene for 24 h at 110 °C, no decomposition could be observed by HPLC, which implies that **1** and **3** are formed in different pathways.

Studies on crystalline $C_{60}O$[15] using calorimetry and high resolution X-ray powder diffraction show a face centered cubic lattice, $a = 14.185$ Å with an orientational disorder at room temperature. An orientational ordering transition occurs at 278 K upon which a simple cubic phase develops. At 19 K this phase, which is similar to the orientational ordered phase of C_{60} itself, shows additional randomness due to a distribution of orientation of the oxygens in $C_{60}O$.

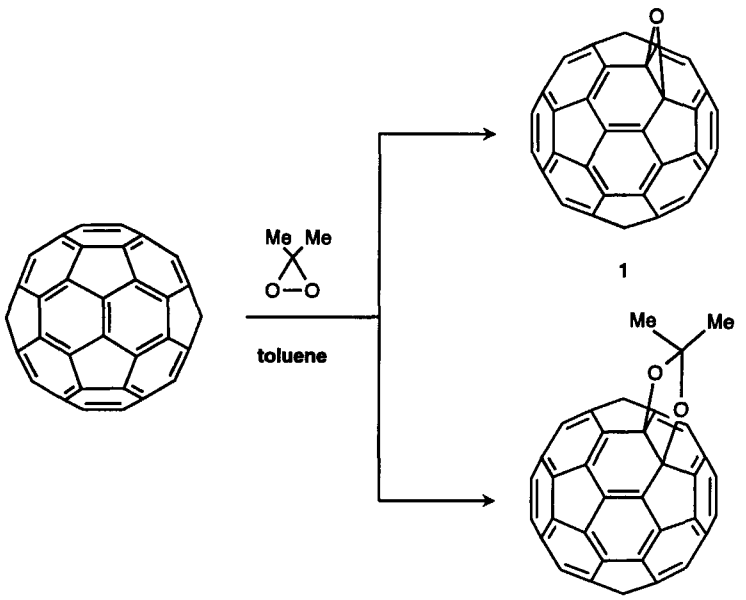

Scheme 8.2

A light-induced oxygen incision of C_{60} results in an opening of the fullerene cage [Scheme 8.3][16]. These reactions were carried out with solid C_{60} sublimed onto KBr crystals. The samples were irradiated with an Ar^+ laser in a chamber filled with O_2. The reaction of C_{60} with oxygen was monitored by IR spectroscopy. The electronic excitation of C_{60} in the presence of oxygen produces singlet oxygen ($^1O_2$) very efficiently[17]. This highly reactive form of oxygen reacts with C_{60} in a second step to cleave a C=C bond, which leads to a dioxetane intermediate that converts into the dicarbonyl compound $C_{60}O_2$ (**4**) [Scheme 8.3]. During the experiment, the IR bands of C_{60} decrease in intensity and at the same time C=O stretch bands due to the formation of $C_{60}O_2$ appear. A calculated IR spectrum of $C_{60}O_2$ fits well to the experimentally observed spectrum. If the time of irradiation of the C_{60} is increased, the formation of $C_{60}O_4$ in addition to that of **4** can be detected by mass spectrometry. This ring-opening reaction of C_{60} could be used for the inclusion of small atoms or ions into the cage[16].

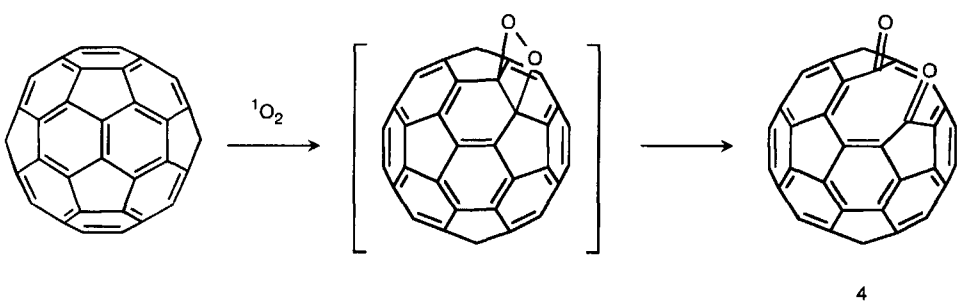

Scheme 8.3

8.4 Osmylation

The addition of the strong and selective oxidizing reagent osmium tetroxide carried out by Hawkins provided the first fully characterized C_{60} derivatives [Scheme 8.4][18,19,20,21,22]. The pyridine accelerated addition of two equiv. of OsO_4 in toluene leads predominantly to the precipitation of the bisadduct **5** as mixtures of regioisomers. The monoadduct **6** can be obtained in high yield by osmylation in the absence of pyridine followed by the addition of pyridine or by using a stoichiometric amount of OsO_4 in the presence of pyridine [Scheme 8.4][19]. It was observed that the osmylation product fully reverted back to C_{60} when heated under vacuum[18].

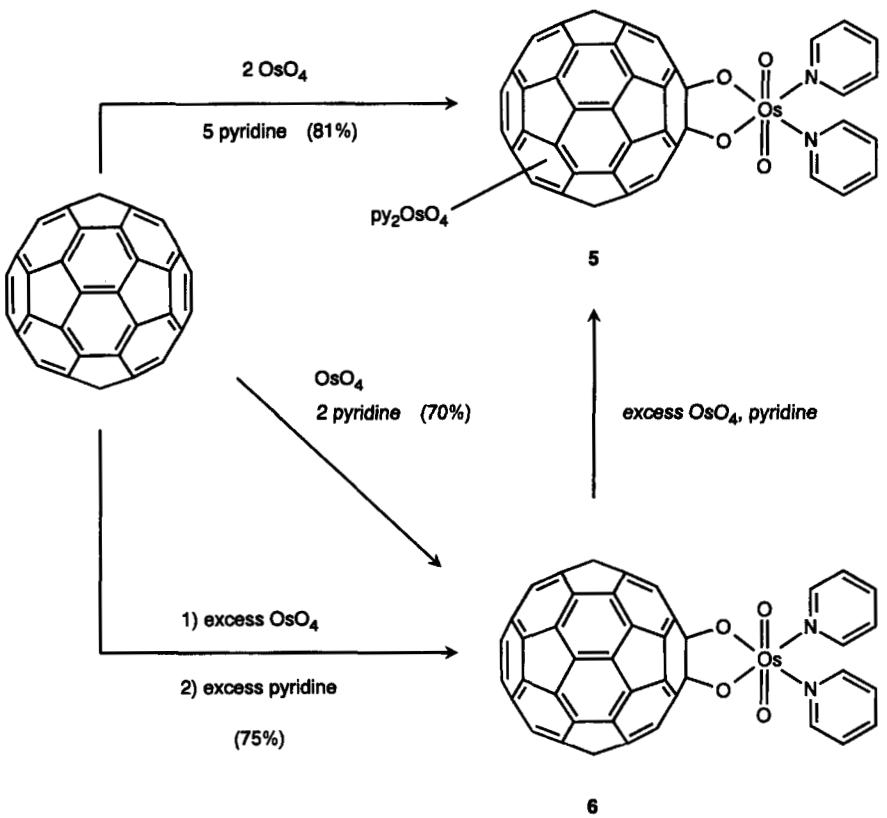

Scheme 8.4

The pyridine molecules in **5** or **6** can be exchanged for other coordinating ligands, such as 4-*tert*-butylpyridine [Scheme 8.5][19]. This ligand-exchange reaction has been used to increase the solubility of the osmylated fullerenes, which allows their spectroscopic characterization as well as the growth of high quality single crystals[19].

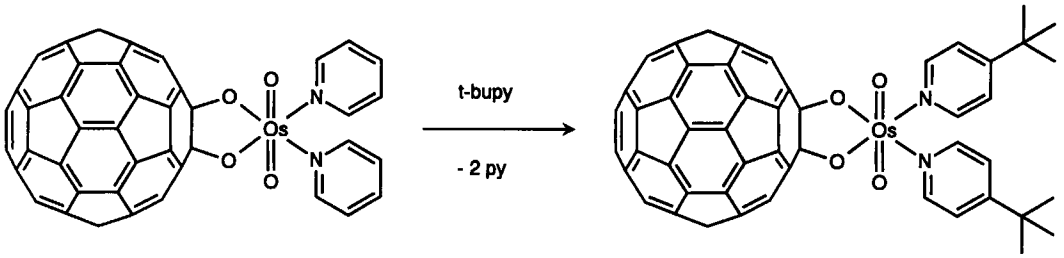

6 **7**

Scheme 8.5

The soccer ball shaped framework of C_{60} was confirmed for the first time by the X-ray crystal structure of **7**[19]. The bridging of the OsO_4-unit occurs in the characteristic 1,2-mode to a 6-6 double bond of the fullerene core. The 17 sets of carbons in the C_{2v}-symmetric **7** were assigned using the 2D NMR INADEQUATE technique on the basis of their connectivities[20]. In these experiments ^{13}C-enriched material was used. The coupling constants $^1J_{CC}$ fall into three categories, 48 Hz, 54-57 Hz and 65-71 Hz. These values can be attributed to the three types of C-C bonds present in **7**, namely the $C(sp^2)$-$C(sp^3)$ bonds, the longer 5-6 bonds and the shorter 6-6 bonds, respectively[20].

In a detailed investigation of the regiochemistry of the bisosmylation of C_{60}, five regioisomers of $C_{60}[OsO_4(t\text{-bupy})_2]_2$ (**8**) have been isolated by preparative HPLC[22]. After their isolation, these regioisomers were converted to their 4-*tert*-butylamine analogues and analyzed by NMR spectroscopy.

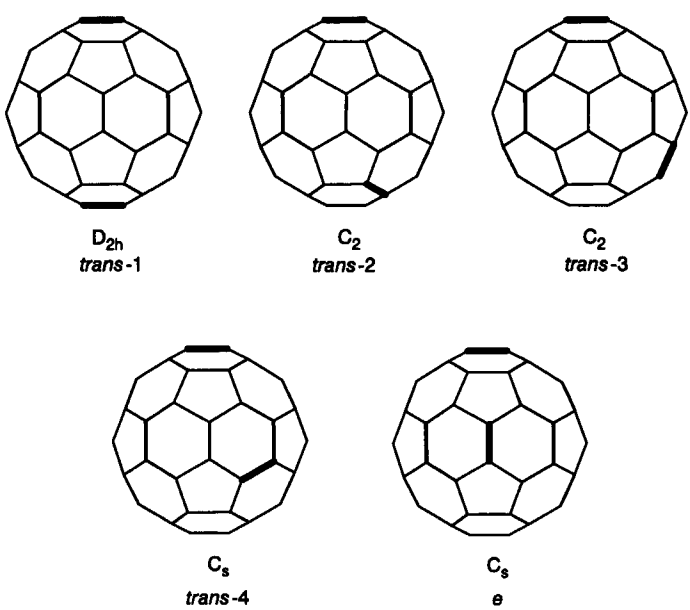

As in the case of the regioisomers of $C_{62}(COOEt)_4$ (Chapter 3)[23], the least polar *trans*-1 regioisomer is much less soluble than the other isomers. In the case of **8**[22] the solubility of the least retentive regioisomer is so low that it could not be analyzed. The symmetry and the elution order of the

other 4 regioisomers of **8** allow a tentative assignment of the *trans*-2, *trans*-3, *trans*-4 isomers and an unambigous assignment of the *e*-isomer [Table 8.1][22]. Three sets of peaks for the bridgehead fullerene C-atoms as well as for the 4-*tert*-butylpyridine protons are found in the *e* isomer, which is consistent with the positioning of one of the osmyl groups across the mirror plane.

Table 8.1 Elution order, symmetry and assignment of regioisomers of **8**[22]

order of elution	^{13}C peaks for the C_{60} moiety	symmetry[a]	assignment[b]
2	30(equal intensity)	C_2	*trans*-2
3	30(equal intensity)	C_2	*trans*-3
4	32(4 half intensity)	C_s	*trans*-4
5	32(4 half intensity)	C_s	*e*

[a] obtained from the NMR spectra.
[b] based on the symmetry and the order of elution.

The same order of elution and symmetry was observed in the regioisomers of the bisadducts $C_{62}(COOEt)_4$[23], which further corroborated the assignment in Table 8.1. The fact that no *cis* isomers have been found demonstrates the pronounced steric requirement of the osmyl group, which makes this hemisphere inaccessible to a second attack.

The C_2-symmetric *trans*-2 and *trans*-3 isomers are chiral. The bisosmylation in the presence of chiral *N*-donor ligands L* provides an asymmetric induction for the formation of enantiomerically enriched *trans*-2 and *trans*-3 isomers of **5** with optical rotations up to 3700° [Scheme 8.6, Table 8.2][24].

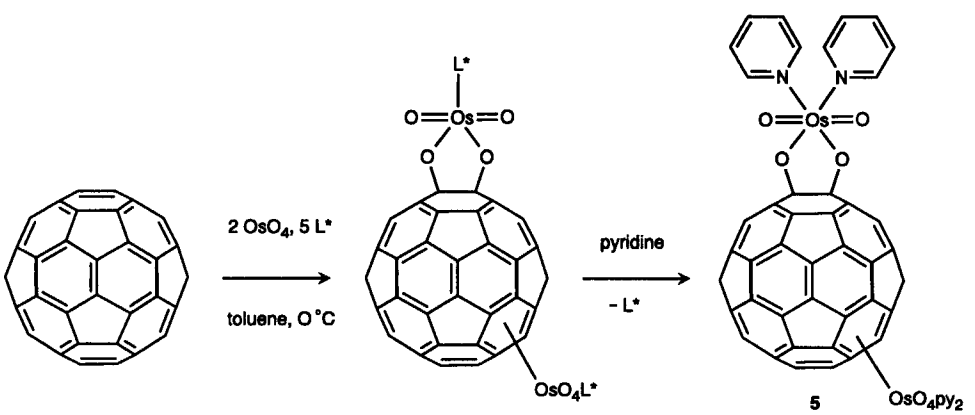

Scheme 8.6

These asymmetric bisosmylations are carried out by treating C_{60} with 2 equiv. of OsO_4 and 5 equiv. of the chiral ligand L* followed by the exchange of the chiral ligands for pyridine. Five regioisomers of **5** in varying ratios can be isolated after the exchange reactions [Table 8.2].

Table 8.2 Regioselectivity and stereoselectivity of the bisosmylation of C_{60}[24].

ligand[a]	ratio of $C_{60}(OsO_4py)_2$ isomers *trans*-1, *trans*-2, *trans*-3, *trans*-4, *e*	isomer *trans*-2 $[\alpha]_{436}$	isomer *trans*-3 $[\alpha]_{436}$
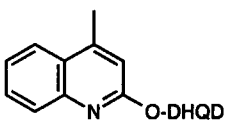	2:18:23:20:36	low	low
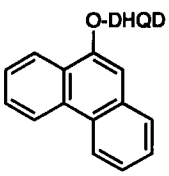	3:20:23:14:39	-707°	23°
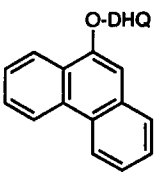	2:28:24:10:35	957°	-52°
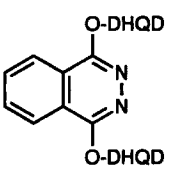	1:16:18:13:52	324°	-564°
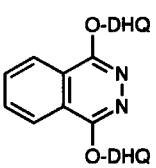	3:17:36:11:33	150°	3700°

[a] DHQD = dihydroquinidine, DHQ = dihydroquinine.

Significantly, the *trans*-3 and *e* isomers are in many cases the most abundant, which again is observed for $C_{62}(COOEt)_4$[23]. As *N*-donor ligands L* various Sharpless cinchona alkaloids, such as dihydroquinidine (DHQD) and dihydroquinine derivatives (DHQ), have been used[25]. The circular dichroism (CD) spectra of both enantiomers of *trans*-2-**5** and *trans*-3-**5** show a mirror image profile for the mirror image molecules. The highest enantioselectivities for *trans*-2-**5** and *trans*-3-**5** are always observed when the formation of the corresponding regioisomers are also favored[24], suggesting that attractive rather than repulsive electronic interactions are responsible for the enantioselectivity.

The osmylation of C_{70} with 0.75 equiv of OsO_4 in pyridine/toluene at 0 °C leads to the two regioisomers with **9** as a major and **10** as a minor product [Scheme 8.7][26]. The same regioselectivity was observed in the hydrogenation[27], nucleophilic additions[28] as well as in Ir-adduct formations[29] of C_{70} and is in line with the predicted stabilities[27,30] of C_{70} adducts. The reaction occurs at the most reactive 6–6 double bonds, with the closest geometric similarity to the 6–6 double bonds of C_{60}. These are the double bonds at the poles (1) and between two positions **C**(2) [Scheme 8.7].

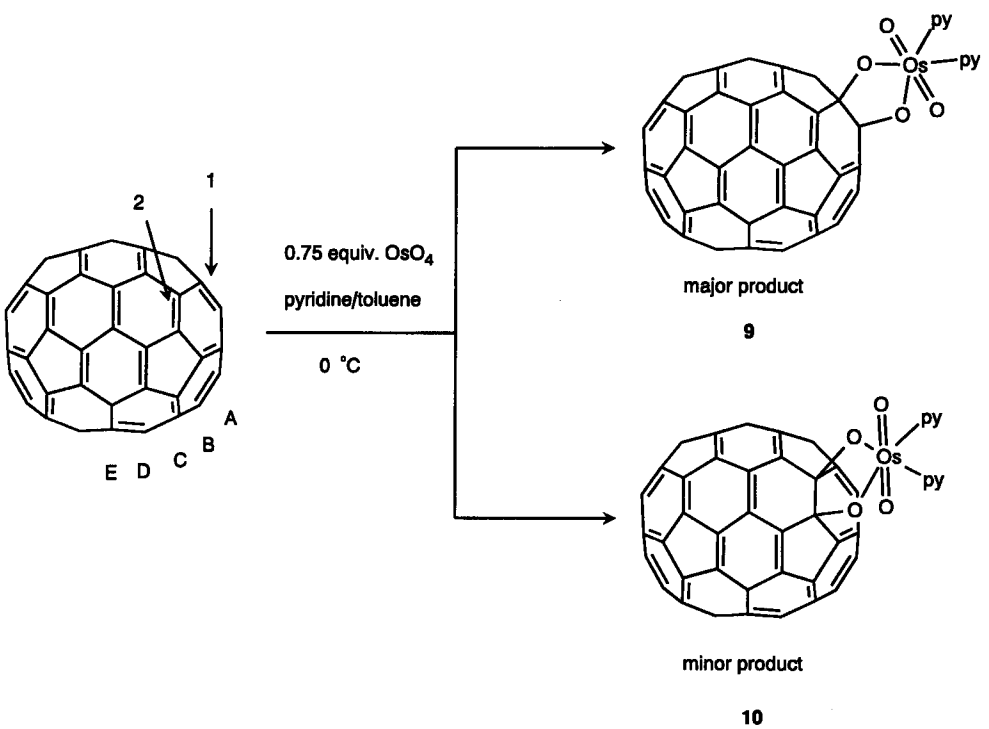

Scheme 8.7

The chiral fullerene C_{76} was also asymmetrically osmylated using the chiral ligands L^1 and L^2 [Scheme 8.8][31]. In this way an optically active allotrope of a pure element was prepared. C_{76} contains 15 different types of 6–6 bonds. The pronounced regioselectivity of C_{70} towards osmylation[26] suggests that specific bonds in C_{76} may be favored for an attack by OsO_4. An analysis of the ab initio calculated curvature of C_{76} shows that two of the five pyracylene-type bonds are particularly distorted,

which could enhance their reactivity[32]. Indeed the HPLC analysis of $C_{76}[OsO_4L^*]$ shows that two regioisomers are predominantly formed upon osmylation of C_{76}[31].

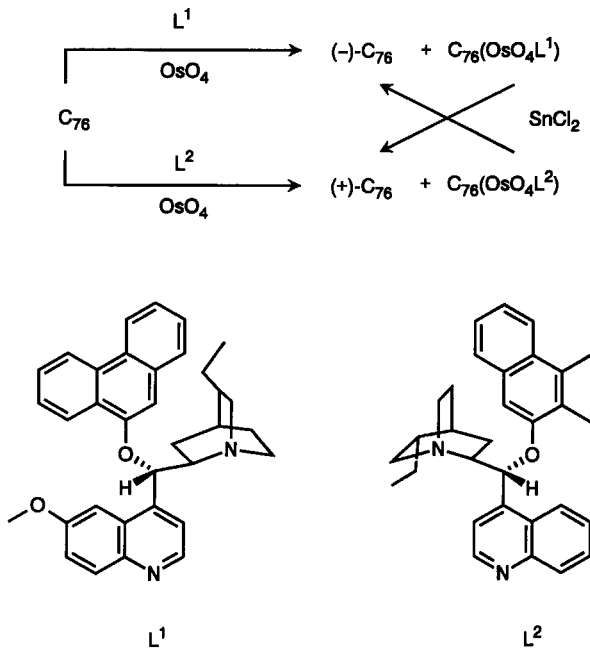

Scheme 8.8

During the kinetically controlled asymmetrical osmylation, one enantiomer reacts faster with the asymmetric reagent than the other. The starting material becomes enriched with the discriminated enantiomer of C_{76} and the reaction products $C_{76}[OsO_4L^*]$ are predominantly formed with the more reactive enantiomer. The C_{76}, recovered by HPLC from the treatment with OsO_4 and the chiral alkaloid ligands L^1 or L^2 with an enantiomeric excess of more than 97 %, shows a maximum specific rotation $[\alpha]_D$ of about -4000 °. The circular dichroism spectrum corresponds to the UV/Vis spectrum[31]. The regeneration of C_{76} from $C_{76}[OsO_4L^*]$ is possible by treatment with $SnCl_2$ [Scheme 8.8]. In this procedure the opposite enantiomer can also be generated. The two enantiomers of C_{76} show mirror image circular dichroism spectra[31]. The pronounced chiral discrimination observed in these asymmetric osmylation reactions were interpreted in terms of diastereotropic attractive π-π interactions between the phenanthryl units of L^1 and L^2 and the reactive part with the greatest local curvature of the fullerene surface[31].

The osmylation reaction of C_{60} has been used to covalently tether the fullerene to a silicon surface[33]. Self-assembled monolayers (SAMs), **12**, have been obtained by the reaction of C_{60} with OsO_4 in the presence of pyridyl-terminated alkylsiloxane monolayers on the surface of both quartz and Ge/Si materials. According to X-ray diffraction studies, the tethered C_{60} monolayer occurs as a primitive, planar hexagonal lattice.

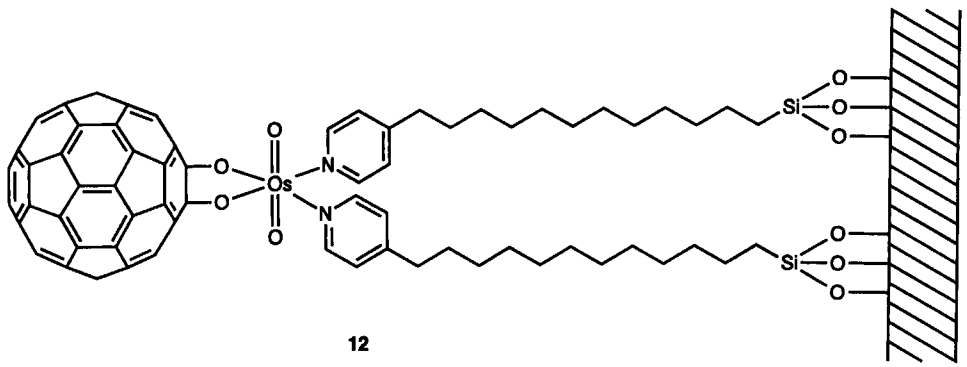

12

8.5 Halogenation

8.5.1 Fluorination

Calculations on fluorinated fullerenes[34,35,36,37,38] predict the fluorination to be a very exothermic process. The large stabilizations are due to the formation of strong C–F bonds and the breaking of weak F–F bonds. Similar to the hydrogenations of C_{60}, it is predicted that fluorinations in a 1,2-addition mode to form $C_{60}F_{2n}$ are favored over the 1,4-addition mode up to n = 6[37,38]. Among the eight possible regioisomers of $C_{60}F_4$, the isomer in which the addition to the second 6–6 double bond occurred at the *e* position relative to the first addition has the lowest MNDO heat of formation[37].

The fluorination of C_{60} can be achieved either by the treatment of dichloromethane solutions with XeF_2 [Scheme 8.9][39] or by allowing fluorine gas at low pressure to react with the solid fullerene [Scheme 8. 10][39,40,41].

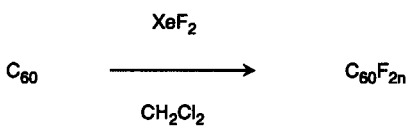

Scheme 8.9

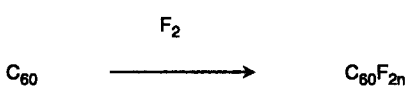

Scheme 8. 10

In the case of fluorination with fluorine gas, the fluorine uptake can be monitored with a suspension balance[40]. The uptake is almost complete within a few minutes after which it increases only very slowly. The average degree of fluorination after 2–4 weeks lies in the range between 35 to 44[41]. The resulting polyfluorofullerenes are mixtures of products with different degrees of fluorination. This can be seen inter alia from the ^{19}F NMR spectra showing very broad peaks at around $\delta = -150$[39].

Depending on the procedure and the degree of fluorination, the color of $C_{60}F_{2n}$ varies between brown and white. The polyfluorofullerenes $C_{60}F_{2n}$ are very soluble in nonpolar solvents, such as toluene, as well as in more polar solvents, such as THF and acetone, but they do not dissolve in water[41]. Mass spectrometry reveals a broad distribution of fluorination, peaking between n = 15–22[40]. The most intense peak in the mixture of polyfluorofullerenes is due to $C_{60}F_{36}$, which exhibits an enhanced stability and is similar to the polyhydrofullerenes (Chapter 5). Solid $C_{60}F_{2n}$ was found to sublime in vacuum at 300 °C[41]. With this method of further purification of $C_{60}F_{2n}$, a uniform yellow solid can be enriched. This material consists mainly of $C_{60}F_{42}$ and $C_{60}F_{40}$. Mass spectrometry and X-ray results show that crystalline polyfluorofullerenes prepared by this method do not contain the most highly fluorinated species[41]. The perfluorinated $C_{60}F_{60}$ was detected only in traces of 1 part in 10^5 relative to the dominant species[41].

Higher degrees of fluorination can be obtained by the reaction of prefluorinated fullerenes $C_{60}F_{2n}$ with fluorine under simultaneous UV irradiation at 85 °C[42]. As determined by mass spectrometry, the polyfluorofullerene $C_{60}F_{48}$ is the most abundant species in the reaction mixture and the amount of perfluorinated C_{60} is enhanced. The intensity of $C_{60}F_{60}^{\cdot+}$ is about 1.3 % of the base peak. Significantly, fluorinated fullerenes $C_{60}F_{2n}$ beyond n = 30 also are formed by this preparation method[42]. The most extensively hyperfluorinated C_{60}, that could be detected by mass spectrometry was $C_{60}F_{102}$. This hyperfluorination requires the rupture of σ-bonds of the fullerene framework. There are indications that the breaking of fullerene σ-bonds caused by fluorination and simultaneous UV irradiation occurs already at degrees of fluorination lower than 60. For example, there is a smooth transition between the section in the mass spectrum where the disruption of the fullerene framework may exist ($C_{60}F_{60}$ and below) and where it must exist (above $C_{60}F_{60}$)[42].

In the absence of any organic solvent $C_{60}F_{2n}$ does not react with boiling water because of its insolubility in this medium[41]. However, a very exothermic reaction together with the formation of HF takes place when THF is added to the suspension[43,44,45]. The fluorinated fullerenes are extremely susceptible to nucleophilic substitutions. During the reaction of polyfluorofullerenes with aqueous methanol, highly oxygenated derivatives $C_{60}F_xO_y$ with up to eighteen oxygen atoms attached to the fullerene cage are formed, as determined by mass spectrometry[45]. It was concluded that during the treatment of $C_{60}F_{2n}$ epoxides are produced by nucleophilic substitution of F by OH followed by the elimination of HF from adjacent OH and F groups[45] [Scheme 8.11]. Since a substitution with the more nucleophilic OMe groups was not observed in these experiments, epoxide formation is apparently favored

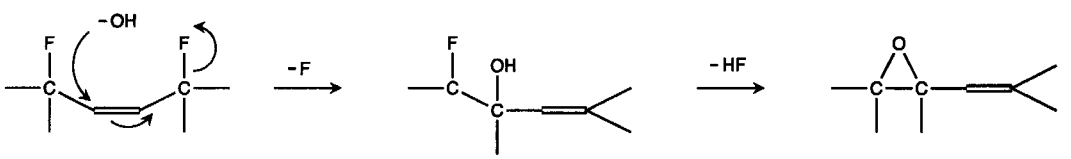

Scheme 8.11

The polyfluorofullerenes $C_{60}F_{2n}$ also undergo nucleophilic substitutions with a variety of other stronger nucleophiles [Scheme 8.12][44]. The reaction of $C_{60}F_{2n}$ with sodium methoxide was monitored over 140 h at room temperature by ^{19}F NMR spectroscopy[44]. It was observed that the replacement of fluorine by the nucleophile is very fast in the beginning and eventually slows down, indicating that the

rate of displacement diminishes as the fluorine content of C_{60} diminishes. The rate of replacement is also dependent on the reactivity of the nucleophile. Whereas the strong nucleophile diethylamine reacts very vigorously with $C_{60}F_{2n}$, the reaction with sodium acetate is very slow[44].

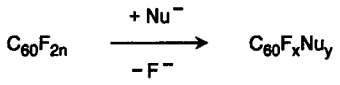

Nu = e.g. RO^-, R^-, NHRR', $RCOO^-$

Scheme 8.12

Also very vigorous reactions have been observed with methylmagnesium bromide, vinylmagnesium bromide, ethynylmagnesium bromide, phenyllithium, tris(trimethylsilyl)methyllithium and lithium aluminum hydride[44]. In the latter, an especially vigorous reaction with a total and instantaneous loss of fluorine was observed.

This reactivity is in contrast to the behavior of usual alkyl fluorides which are very resistant towards nucleophilic substitution. In addition, the cage structure of C_{60} makes an S_N2 mechanism impossible, and due to the expected electron-withdrawing character of the polyfluorofullerene cage, an S_N1 mechanism seems to be very unlikely[44]. Two mechanisms for the nucleophilic substitution of fluorine in $C_{60}F_{2n}$ have been suggested [Scheme 8.13, Scheme 8.14][44]. In an elimination–addition mechanism [Scheme 8.13] first the counterion for the nucleophile may first remove a fluoride and the resulting cation could then react in a non-rate-determining step with the nucleophile. Alternatively, since most of $C_{60}F_{2n}$ is only partly fluorinated, the addition to a fullerene double bond could take place in an initial step, after which an elimination of fluoride and a regeneration of a double bond occurs [Scheme 8.14]. The latter mechanism is very likely, because it is known that C_{60} itself readily reacts with nucleophiles[46,47,48,49,50,51,52] and a high degree of fluorination should even enhance the electrophilicity of the fullerene double bonds. Additional support for this mechanism comes from the fact that the rate of fluorine replacement diminishes as the degree of fluorination of C_{60} decreases and brominated C_{60} is less reactive towards nucleophilic substitutions[44].

Scheme 8.13

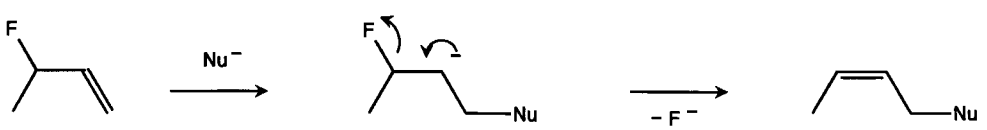

Scheme 8.14

8.5.2 Chlorination

Whereas the treatment of C_{60} with chlorine in organic solvents does not lead to any detectable reaction, a polychlorination to $C_{60}Cl_{2n}$ can be achieved by allowing a slow stream of chlorine gas to react with C_{60} in a hot glass tube at temperatures between 250 and 400 °C [Scheme 8.15][53]. The maximum uptake of chlorine was obtained within 5 h. An average of 24 chlorine atoms can be attached to C_{60} by this method. The polychlorofullerenes are a mixture of products that are light orange in color and soluble in many organic solvents[53].

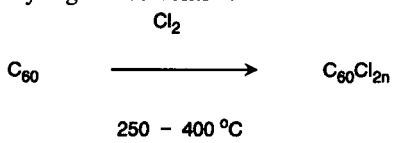

Scheme 8.15

Chlorofullerenes $C_{60}Cl_{2n}$ with a lower degree of chlorination ($n \approx 6$) can be synthesized by the treatment of solid C_{60} with liquid chlorine at - 35 °C [Scheme 8.16][54]. These reactions are completed in about one day after passing liquid chlorine continuously over C_{60} on a glass filter.

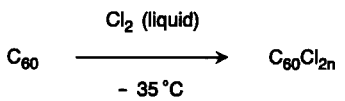

Scheme 8.16

The chlorofullerenes are less stable than their fluorine analogues. Ions deduced from $C_{60}Cl_{2n}$ cannot be observed in the mass spectra due to fragmentation to C_{60}[53,54]. The instability of the chlorofullerenes can also be seen from their behavior towards thermal, chemical and electrochemical manipulations. Heating $C_{60}Cl_{2n}$ at 400 °C under argon results in dechlorination and the parent fullerenes are recovered [Scheme 8.17][53]. The dechlorination starts at 200 °C[54]. The cyclic voltammogram of $C_{60}Cl_{2n}$ ($n \approx 6$) shows a broad irreversible wave near -0.2 V (vs Ag/AgCl) and three reversible waves due to the parent C_{60}[54], indicating that after reduction chloride anions dissociate from the chlorinated fullerene [Scheme 8.17]. The treatment of toluene solutions of $C_{60}Cl_{2n}$ with triphenylphosphine leads to a dechlorination to C_{60} in 80 % yield [Scheme 8.17][54].

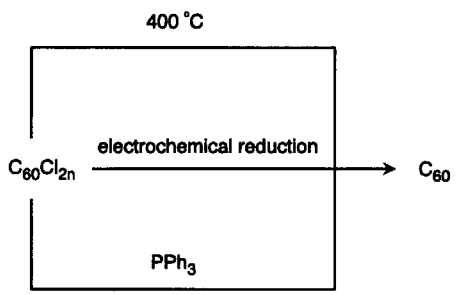

Scheme 8.17

Similar to their fluorinated analogues, the polychlorofullerenes also undergo substitution reactions with nucleophiles[53]. The treatment of $C_{60}Cl_{2n}$ with potassium methanolate under reflux for 3 h leads to the polymethoxylated species, $C_{60}(OMe)_{2n}$, in which all the chlorines are replaced [Scheme 8.18]. These polymethoxyfullerenes contain up to 26 methoxy groups.

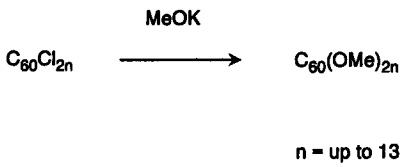

Scheme 8.18

Also Friedel-Crafts type reactions can be carried out with the polychlorofullerenes, $C_{60}Cl_{2n}$ [Scheme 8.19][53]. Upon stirring benzene solutions of $C_{60}Cl_{2n}$ with a catalytic amount of aluminum chloride at room temperature for 2 h, polyphenylated fullerenes can be obtained with at least 22 phenyl groups attached to the fullerene core. Polytoluation with toluene occurs similarly[53].

Scheme 8.19

The chlorofullerene, $C_{60}Cl_6$, as an isomerically pure single product was synthesized by the reaction of C_{60} with an excess of iodine monochloride in benzene or toluene at room temperature [Scheme 8.20][55]. The product is very soluble in benzene, carbon disulfide and tetrachloromethane. Deep orange crystals can be obtained by recrystallization from pentane. The synthesis of $C_{60}Cl_6$ using toluene as solvent proceeds slower than with benzene, which indicates, that radicals are involved and scavenged by the toluene[55].

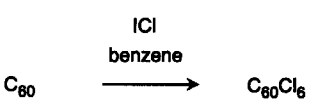

Scheme 8.20

The structure of $C_{60}Cl_6$ as 1,2,4,11,15,30-hexachlorofullerene-60 [Fig 8.1] was deduced from its ^{13}C NMR spectrum which shows 32 lines for 54 sp^2-hybridized and 6 sp^3-hybridized C-atoms demonstrating the C_s-symmetry. In this structure of $C_{60}Cl_6$, the same building principles seem to be important which also direct the formation of the radical $C_{60}R_5$, as shown by ESR spectroscopy[56]. In $C_{60}R_5$ the additions of the radicals R· also occurred in the positions 1,4,11,15,30. The regiochemistry of the chlorine addition leading to $C_{60}Cl_6$ therefore indicates that also in this case a radical mechanism is valid. For the chlorine addition to C_{60}, in contrast to that of hydrogen and fluorine, a 1,4-mode is predicted to be more favorable than a 1,2-mode[37]. This difference is mainly due to the enhanced steric requirement of the chlorine.

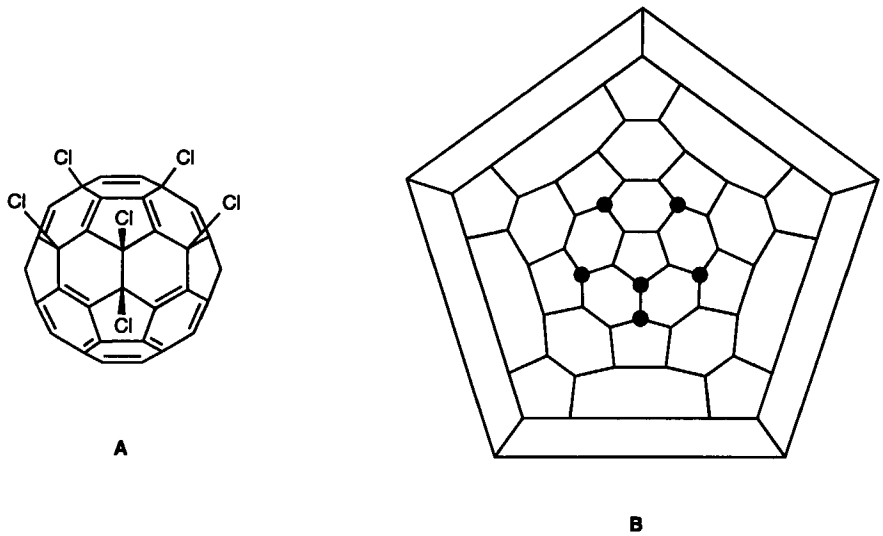

Figure 8.1 Schematic representation of the structure of $C_{60}Cl_6$: **(A)** front view, **(B)** Schlegel diagram.

8.5.3 Bromination

The bromination of C_{60} is predicted to be less exothermic than the chlorination or fluorination, and in general 1,4-additions should be favored over 1,2-additions[37]. C_{60} reacts with liquid bromine to form the bromofullerene, $C_{60}Br_{24}$, which is a yellow-orange crystalline compound and is obtained as a bromine solvate, $C_{60}Br_{24}(Br_2)_x$ [Scheme 8.21][57,58]. This compound has a simple IR spectrum indicating a highly symmetrical structure. Upon heating to 150 °C, all the bromine is eventually lost[58].

$$C_{60} \xrightarrow{Br_2\ (liquid)} C_{60}Br_{24}(Br_2)_x$$

Scheme 8.21

An X-ray crystal structure analysis shows that $C_{60}Br_{24}$ has T_h-symmetry[57]. This is the highest symmetry available for a brominated fullerene, $C_{60}Br_{2n}$. The addition pattern of the bromine atoms on the C_{60} surfaces arises from 1,4-additions to fused pairs of six membered rings with the closest Br,Br placement being 1,3 [Fig. 8.2]. Bromines attached to C-atoms in the 1 and 4 positions cause 12 of the hexagons to adopt boat conformations and the remaining eight hexagons to adopt chair conformations[57]. The addition of another two bromine atoms would require locations in 1,2-positions, which is very unfavorable for these bulky atoms[37].

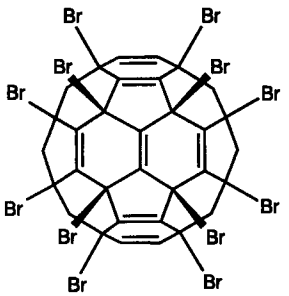

A

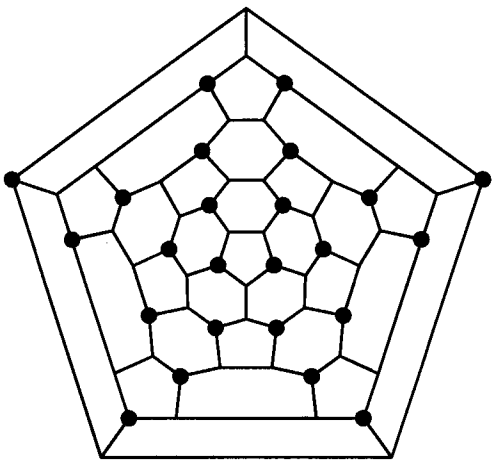

B

Figure 8.2 Schematic representation of the structure of $C_{60}Br_{24}$: (**A**) front view, (**B**) Schlegel diagram.

The bromination of C_{60} in CS_2 leads to the formation of dark brown crystals in 80 % yield after 24 h [Scheme 8.22][58].The single crystal X-ray diffraction analysis showed the crystals to be $C_{60}Br_8$ [Fig. 8.3]. The same compound can also be obtained in 58 % yield by brominating in chloroform [Scheme 8.22]. The octabromide is not very soluble in common organic solvents but it is soluble in bromine.

$$C_{60} \xrightarrow[CS_2 \text{ or } CHCl_3]{Br_2} C_{60}Br_8$$

Scheme 8.22

$$C_{60} \xrightarrow[\text{benzene or } CCl_4]{Br_2} C_{60}Br_6$$

Scheme 8.23

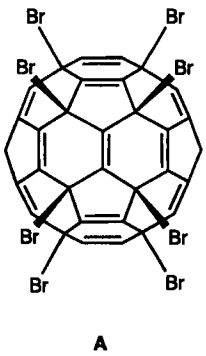

A

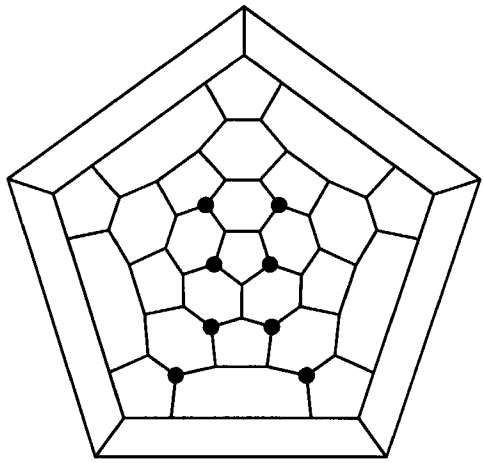

B

Figure 8.3 Schematic representation of the structure of $C_{60}Br_8$: (**A**) front view, (**B**) Schlegel diagram.

If the bromination of C_{60} is carried out in either benzene or tetrachloromethane, another bromide namely $C_{60}Br_6$ crystallizes out in magenta plates in 54 and 92 % yields, respectively [Scheme 8.23][58]. The structure of $C_{60}Br_6$ was also determined by single crystal X-ray analysis [Fig. 8.4]. This bromide is isostructural to $C_{60}Cl_6$[55].

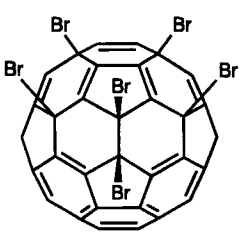

A

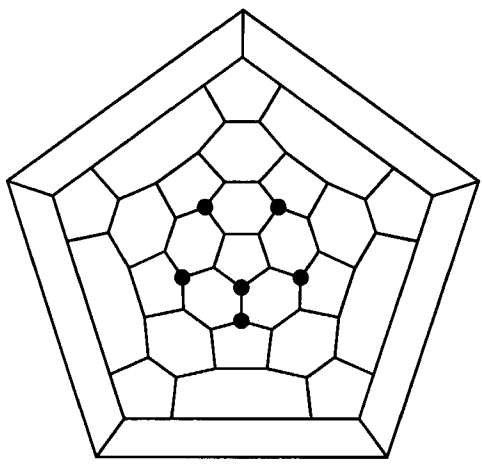

B

Figure 8.4 Schematic representation of the structure of $C_{60}Br_6$. (A) front view, (B) Schlegel diagram.

$C_{60}Br_6$ is moderately soluble in organic solvents. Each of the bromo derivatives is unstable when heated and loses bromine[58]. The most stable bromide is $C_{60}Br_{24}$. Upon heating in tetrachloromethane or benzene, $C_{60}Br_6$ disproportionates to give C_{60} and $C_{60}Br_8$ [Scheme 8.24][58].

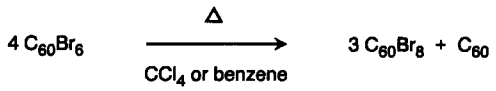

Scheme 8.24

The higher stability of $C_{60}Br_8$ compared to that of $C_{60}Br_6$ may be explained by the lack of the eclipsing interactions of $C_{60}Br_8$ present in $C_{60}Br_6$ [Fig. 8.4 and Fig. 8.5]. During the formation of $C_{60}Br_8$ from $C_{60}Br_6$, a sequence of 1,3-allylic bromine shifts may be involved[58]. The general instability of the bromides, especially $C_{60}Br_6$ and $C_{60}Br_8$, is related to the introduction of 5–6 double bonds. The fact that different bromides are formed in different solvents is due to the crystallization of insoluble bromofullerenes, such as $C_{60}Br_6$ in benzene, which inhibits further bromination.

Brominated fullerenes are also able to undergo a Friedel–Crafts fullerylation of benzene catalyzed by aluminum trichloride [Scheme 8.25][53].

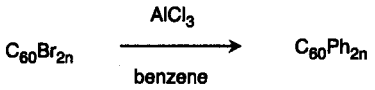

Scheme 8.25

8.5.4 Reaction with Iodine

A reaction of C_{60} with iodine was observed upon irradiating a C_{60}/I_2 mixture with Hg light at 130 °C for about 20 h[59]. The X-ray analysis of the resulting simple hexagonal structure revealed a $C_{60}I_2$ stoichiometry and an intercalation of iodine atoms[59,60]. The reaction, therefore has been described as a reaction with iodine radicals. During a period of 3 months, a relaxation of the compound into the initial FCC takes place. In contrast to alkali metal doped C_{60}, such as K_3C_{60}, no transition into a superconducting phase has been observed[59,60,61].

8.6 Reactions with Strong Oxidizing Reagents and Acids

The treatment of C_{60} with a large excess of the powerful oxidizing reagent, SbF_5/SO_2ClF, gives a dark green colored solution[62]. The broad peaks in the ^{13}C NMR spectra of these solutions recorded between −80 °C and room temperature were interpreted to indicate the formation of radical cations[62]. The presence of diamagnetic di- or polycations was excluded. Similar spectra were obtained by using SbF_5 and Cl_2 as an oxidant in SO_2ClF solution. Dark green colored solutions are also obtained upon dissolving C_{60} in oleum[62]. The formation of radical cations could be detected by ESR spectroscopy[63].

Persistent radical cations of C_{60} have been observed in super acidic media, for example in magic acid (FSO_3H, SbF_5)[64]. Multiply charged fullerene radical cations can be stabilized in a mixture of fuming sulfuric acid and SO_2ClF at low temperatures[65]. The ESR spectrum of these species shows triplet states, with the two spins mainly located on opposite sides of the molecule.

The reaction of C_{60} with sulfuric acid and nitric acid and the subsequent hydrolysis of the intermediates with aqueous base results in the formation of fullerols [Scheme 8.26][66,67]. Either nitric acid itself or nitric acid produced in situ from potassium nitrate and fuming sulfuric acid can be used.

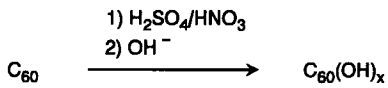

Scheme 8.26

The chemical composition of the water-soluble fullerols was found to consist of an average of 14–15 hydroxyl functional groups attached to the C_{60}[66]. The analysis of the XPS, IR and solid-state ^{13}C NMR spectra demonstrates the presence of hemiketal moieties in the fullerols [Fig. 8.5]. This was deduced from additional peaks in the XPS spectra characteristic for carbon in a higher oxidation state, the absence of a C=O stretching vibration in the IR spectra and additional downfield peaks in the ^{13}C NMR spectra at $\delta = 100.0$ and 170.5, which are due to the ketal and vinyl ether carbons respectively[67].

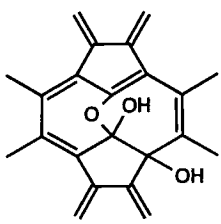

Figure 8.5 Schematic representation of a hemiketal moiety in a fullerol.

The presence of hemiketals, in addition to the tertiary hydroxy groups, is corroborated by the behavior toward acid, which leads to the formation of keto groups as shown by the appearance of C=O stretching vibrations in the IR spectra[67]. This formation of the keto groups is reversible. After the reaction with aqueous NaOH the hemiketal groups are recovered.

In a similar approach, fullerene derivatives with polar functional groups, namely polyhydroxy polyacyloxy C_{60} **11**, was synthesized by the reaction with nitronium tetrafluoroborate and carboxylic acids [Scheme 8.27][68]. After an initial electrophilic attack of the nitronium ion, a subsequent nucleophilic 1,3- or 1,5-substitution with acyloxy groups occurs. Treatment with water gives the mixed adducts **11**. An average of 13–15 hydroxyl groups and about 4–5 acyloxy groups are bound to the fullerene core. Hydrolysis of these derivatives in hydroxide solutions affords the corresponding water soluble fullerols **12**, consisting of 18–20 hydroxyl groups per C_{60} molecule on average [Scheme 8.27][68].

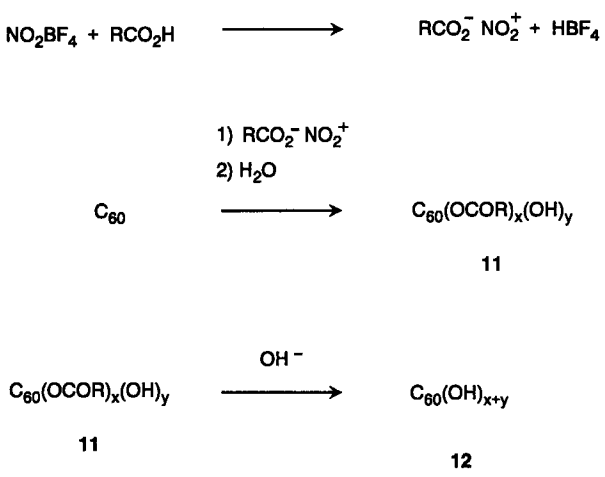

Scheme 8.27

8.7 Reactions with Lewis Acids and Fullerylation of Aromatics

The reaction of fullerenes with the Lewis acid, BH_3, was already discussed in Chapter 5. These hydroborations followed by hydolysis provide access to hydrogenated fullerenes[69]. Also, other Lewis acids have been allowed to react with C_{60} and C_{70}[62,70,71,72,73]. If these reactions are carried out in CS_2, fullerene-Lewis acid complexes precipitate[73]. The complexation behavior of C_{60} and C_{70} is different, with C_{70} complexing much stronger than C_{60}. This phenomenon was taken advantage of in separating the fullerene mixtures[73]. Other Lewis acids that form CS_2 insoluble complexes are $AlBr_3$, $TiCl_4$, $SnCl_4$ and $FeCl_3$. The parent fullerenes can be recovered from the Lewis acid complexes by reaction with ice water [Scheme 8. 28][73].

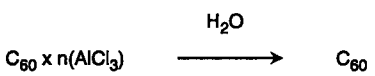

Scheme 8.28

If solutions of C_{60} in aromatic hydrocarbons are treated with Lewis acids, such as $AlCl_3$, $AlBr_3$, $FeBr_3$, $FeCl_3$, $GaCl_3$ or $SbCl_5$, then a fullerylation of aromatics takes place [Scheme. 8.29][62,70,72]. In this case, the Lewis acid serves as a catalyst and increases the electrophilicity of the fullerene. Mixtures of polyarylated fullerenes are obtained. Depending on the reaction conditions and the aromatics used for the fullerylation, up to 16 aryl groups are covalently bound to the fullerene core[62,70,72]. In the case of the phenyl addition to C_{60}, the highest intensity peak in the mass spectra was that for $C_{60}Ph_{12}$, indicating that this compound exhibits an enhanced stability[62].

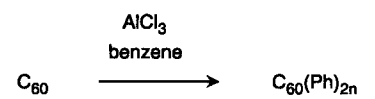

Scheme 8.29

The reaction takes place only with relatively strong Lewis acids as catalysts. No reaction was observed with weak Lewis acids, such as $SnCl_4$ and $TiCl_4$, and also $GeCl_4$, BF_3 and BCl_3 were found to be inactive[62]. The order of Lewis acid activity was found to be $AlBr_3 > AlCl_3 > FeCl_3 > GaCl_3 > SbCl_5$[62]. The polyarylated fullerenes appear to be unstable. On standing, partial decomposition was observed[72].

References

1 R. C. Haddon, L. E. Brus, K. Raghavachari *Chem. Phys. Lett.* **1986**, *125*, 459.
2 C. Jehoulet, A. J. Bard, F. Wudl *J. Am. Chem. Soc.* **1991**, *113*, 5456.
3 D. Dubois, K. M. Kadish, S. Flanagan, L. J. Wilson *J. Am. Chem. Soc.* **1991**, *113*, 7773.
4 K. Meerholz, P. Tschuncky, J. Heinze *J. Electroanal. Chem.* **1993**, *347*, 425.
5 Q. Xie, F. Arias, L. Echegoyen *J. Am. Chem. Soc.* **1993**, *115*, 9818.
6 F. Diederich, R. Ettl, Y. Rubin, R. L. Whetten, R. Beck, M. Alvarez, S. Anz, D. Sehsharma, F. Wudl, K. C. Khemani, A. Koch *Science* **1991**, *252*, 548.
7 J. M. Wood, B. Kahr, S. H. Hoke II, L. Dejarme, R. G. Cooks, D. Ben-Amotz *J. Am. Chem. Soc.* **1991**, *113*, 5907.
8 H. H. Thorp, W. A. Karlsbeck *J. Electroanal. Chem.* **1991**, *314*, 363
9 R. Taylor, J. P. Parsons, A. G. Avent, S. P. Rannard, T. J. Dennis, J. P. Hare, H. W. Kroto, D. R. M. Walton *Nature* **1991**, *351*, 277.
10 K. M. Creegan, J. L. Robbins, W. K. Robbins, J. M. Millar, R. D. Sherwood, P. J. Tindall, D. M. Cox, A. B. Smith III, J. P. McCauley Jr., D. R. Jones, R. T. Gallagher *J. Am. Chem. Soc.* **1992**, *114*, 1103.
11 A. M. Vassalo, L. S. K. Pang, P. A. Coke-Clarke, M. A. Wilson *J. Am. Chem. Soc.* **1991**, *113*, 7820.
12 K. Raghavachari, C. Sosa *Chem Phys. Lett.* **1993**, *209*, 223.
13 K. Raghavachari *Chem. Phys. Lett.* **1992**, *195*, 221.
14 Y. Elemes, S. K. Silverman, C. Sheu, M. Kao, C. S. Foote, M. M. Alvarez, R. L. Whetten *Angew. Chem.* **1992**, *104*, 364; *ibid Int. Ed. Engl.* **1992**, *31*, 351.
15 G. B. M. Vaughan, P. A. Heiney, D. E. Cox, A. R. McGhie, D. R. Jones, R. M. Strongin, M. A. Cichy, A. B. Smith III *Chem. Phys.* **1992**, *168*, 185.
16 C. Taliani, G. Ruani, R. Zamboni, R. Danieli, S. Rossini, V. N. Denisov, V. M. Burlakov, F. Negri, G. Orlandi, F. Zerbetto *J. Chem. Soc., Chem. Commun.* **1993**, 220.
17 J. W. Arbogast, A. P. Darmanyan, C. S. Foote, Y. Rubin, F. N. Diederich, M. M. Alvarez, S. J. Anz, R. L. Whetten *J. Phys. Chem.* **1991**, *95*, 11.
18 J. M. Hawkins, T. A. Lewis, S. D. Loren, A. Meyer, L. R. Heath, Y. Shibato, R. J. Saykally *J. Org. Chem.* **1990**, *55*, 6250.
19 J. M. Hawkins, A. Meyer, T. A. Lewis, S. Loren, F. J. Hollander *Science* **1991**, *252*, 312.
20 J. M. Hawkins, S. Loren, A. Meyer, R. Nunlist *J. Am. Chem. Soc.* **1991**, *113*, 7770.
21 J. M. Hawkins *Acc. Chem. Res.* **1992**, *25*, 150.
22 J. M. Hawkins, A. Meyer, T. A. Lewis, U. Bunz, R. Nunlist, G. E. Ball, T. W. Ebbesen, K. Tanigaki *J. Am. Chem. Soc.* **1992**, *114*, 7954.
23 A. Hirsch, I. Lamparth, H. R. Karfunkel *Angew. Chem.* **1994**, *106*, 453; *ibid. Int. Ed. Engl.* **1994**, *33*, 437.
24 J. M. Hawkins, A. Meyer, M. Nambu *J. Am. Chem. Soc.* **1993**, *115*, 9844.
25 K. B. Sharpless, W. Amberg, Y. L. Bennani, G. A. Crispino, J. Hartung, K. S. Jeong, H. L. Kwong, K. Morikawa, Z. M. Wang, D. Xu, X. L. Zhang *J. Org. Chem.* **1992**, *57*, 2768.
26 J. M. Hawkins, A. Meyer, M. A. Solow *J. Am. Chem. Soc.* **1993**, *115*, 7499.
27 C. C. Henderson, C. M. Rohlfing, P. A. Cahill *Chem. Phys. Lett.* **1993**, *213*, 383.
28 A. Hirsch, T. Grösser, A. Skiebe, A. Soi, *Chem. Ber.* **1993**, *126*, 1061
29 A. L. Balch, V. J. Catalano, J. W. Lee, M. M. Olmstead, S. R. Parkin *J. Am. Chem. Soc.* **1991**, *113*, 8953.
30 H.R. Karfunkel, A. Hirsch *Angew. Chem.* **1992**, *104*, 1529; *ibid. Int. Ed. Engl.* **1992**, *31*, 1468.
31 J. M. Hawkins, A. Meyer *Science* **1993**, *260*, 1918.
32 J. R. Colt, G. E. Scuseria *J. Phys. Chem.* **1992**, *96*, 10265.
33 J. A. Chupa, S. Xu, R. F. Fischetti, R. M. Strongin, J. P. McCauley, A. B. Smith III, J. K. Blasie, L. J. Peticolas, J. C. Bean *J. Am. Chem. Soc.* **1993**, *115*, 4383.

34 G. E. Scuseria *Chem. Phys. Lett.* **1991**, *176*, 423.
35 J. Cioslowski *Chem. Phys. Lett.* **1991**, *181*, 68.
36 B. I. Dunlap, D. W. Brenner, J. W. Mintmire, R. C. Mowrey, C. T. White *J. Phys. Chem.* **1991**, *95*, 5763.
37 N. Matsuzawa, T. Fukunaga, D. A. Dixon *J. Phys. Chem.* **1992**, *96*, 10747.
38 D.A. Dixon, N. Matsuzawa, T. Fukunaga, F. N. Tebbe *J. Phys. Chem.* **1992**, *96*, 6107.
39 J. H. Holloway, E. G. Hope, R. Taylor, G. L. Langley, A. G. Advent, T. J. Dennis, J. H. Hare, H. W. Kroto, D. M. Walton *J. Chem. Soc., Chem. Commun.* **1991**, 966.
40 H. Selig, C. Lifshitz, T. Peres, J. E. Fischer, A. R. McGhie, W. J. Romanov, J. P. McCauley Jr., A. B. Smith III *J. Am. Chem. Soc.* **1991**, *113*, 5475.
41 K. Kniaz, J. E. Fischer, H. Selig, G. B. M. Vaughan, W. J. Romanov, D. M. Cox, S. K. Chowdhury, J. P. McCauley, R. M. Strongin, A. B. Smith III *J. Am. Chem. Soc.* **1993**, *115*, 6060.
42 A. A. Tuinman, A. A. Gakh, J. L. Adcock, R. N. Compton *J. Am. Chem. Soc.* **1993**, *115*, 5885.
43 R. Taylor, A. G. Avent, T. J. Dennis, J. P. Hare, H. W. Kroto, D. R. M. Walton, J. Holloway, E. G. Hope, G. J. Langley *Nature* **1992**, *355*, 27.
44 R. Taylor, J. Holloway, E. C. Hope, A. G. Advent, G. J. Langley, T. J. Dennis, J. P. Hare, H. W. Kroto, D. R. M. Walton *J. Chem. Soc., Chem. Commun.* **1992**, 665.
45 R. Taylor, G. J. Langley, A. K. Brisdon, J. H. Holloway, E. G. Hope, H. W. Kroto, D. R. M. Walton *J. Chem. Soc., Chem. Commun.* **1993**, 875.
46 F. Wudl, A. Hirsch, K. C. Khemani, T. Suzuki, P.-M. Allemand, A. Koch, H. Eckert, H.; G. Srdanov, H. Webb In *Fullerenes: Synthesis, Properties, and Chemistry of Large Carbon Clusters;* G. S. Hammond, V. J. Kuck, Eds.; American Chemical Society Symposium Series 481; 1992; p 161.
47 A. Hirsch, A. Soi, H. R. Karfunkel *Angew. Chem.* **1992**, *104*, 808; *ibid. Int. Ed. Engl.* **1992**, *31*, 766.
48 A. Hirsch, T. Grösser, A. Skiebe, A. Soi *Chem. Ber.* **1993**, *126*, 1061.
49 A. Hirsch, *GIT Fachz. Lab.* **1993**, 764.
50 C. Bingel *Chem.Ber.* **1993**, *126*, 1957.
51 P.J. Fagan, P.J. Krusic, D.H. Evans, S.A. Lerke, E. Johnston, *J. Am. Chem. Soc.* **1992**, *114*, 9697.
52 A. Hirsch, Q. Li, F. Wudl, *Angew. Chem.* **1991**, *103*, 1339; *ibid. Int. Ed. Engl.* **1991**, *30*, 1309.
53 G. A. Olah, I. Bucsi, C. Lambert, R. Aniszfeld, N. J. Trivedi, D. K. Sensharma, G. K. S. Prakash *J. Am. Chem. Soc.* **1991**, *133*, 9385.
54 F. N. Tebbe, J. Y. Becker, D. B. Chase, L. E. Firment, E. R. Holler, B. S. Malone, P. J. Krusic, E. Wasserman *J. Am. Chem. Soc.* **1991**, *113*, 9900.
55 P. R. Birkett, A. G. Avent, A. D. Darwish, H. W. Kroto, R. Taylor, D. R. M. Walton *J. Chem. Soc., Chem. Commun.* **1993**, 1230.
56 P. J. Krusic, E. Wasserman, P. N. Keizer, J, R. Morton, K. F. Preston *Science*, **1991**, *254*, 1183.
57 F. N. Tebbe, R. L. Harlow, D. B. Chase, D. L. Thorn, G. C. Campbell Jr., J. C. Calabrese, N. Herron, R. J. Young, E. Wasserman *Science* **1992**, *256*, 822.
58 P. R. Birkett, P. B. Hitchcock, H. W. Kroto, R. Taylor, D. R. M. Walton *Nature* **1992**, *357*, 479.
59 T. Zenner, H. Zabel *J. Phys. Chem.* **1993**, *97*, 8690.
60 Q. Zhu, D. E. Cox, J. E. Fischer, K. Kniaz, A. R. McGhie, O. Zhou *Nature*, **1992**, *355*, 712.
61 M. Kobayashi, Y. Akahama, H. Kawamura, H. Shinohara, H. Sato, H. Saito *Solid State Commun.* **1992**, *81*, 93.
62 G. A. Olah, I. Bucsi, R. Aniszfeld, G. K. S. Prakash *Carbon*, **1992**, *30*, 1203.
63 G. A. Olah, I. Bucsi, G. K. S. Prakash, R. Anizfeld, *unpublished results.*
64 G. P. Miller *Mat. Res. Soc. Symp. Proc.* **1992**, *247*, 293
65 H. Thoman, M. Bernardo, G. P. Miller *J. Am. Chem. Soc.* **1992**, *114*, 6593.
66 L. Y. Chiang, J. W. Swirczewski, C. S. Hsu, S. K. Chowdhury, S. Cameron, K. Cressgan *J. Chem. Soc., Chem. Commun.* **1992**, 1791.
67 L. Y. Chiang, R. B. Upasani, J. W. Switczewski, S. Soled *J. Am. Chem. Soc.***1993**, *115*, 5453.
68 L. Y. Chiang, R. B. Upasani, J. W. Swirczewski *J. Am. Chem. Soc.* **1992**, *114*, 10154.
69 C. C. Henderson, P. A. Cahill *Science* **1993**, *259*, 1885.
70 S. H. Hoke, J. Molstad, G. L. Payne, B. Kahr, D. Ben-Amotz, R. G. Graham Cooks *Rap. Commun. Mass, Spec.* **1991**, *5*, 472.
71 G. A. Olah, I. Bucsi, C. Lambert, R. Aniszfeld, N. J. Trivedi, D. K. Sensharma, G. K. Prahash *J. Am. Chem. Soc.* **1991**, *113*, 9387.
72 R. Taylor, G. L. Langley, M. F. Meidine, J. P. Parsons, A. K. Abdul-Sada, T. J. Dennis, J. P. Hare, H. W. Kroto, D. R. M. Walton *J. Chem. Soc.,Chem. Commun.* **1992**, 667.
73 G. A. Olah, personal communication.

9 Principles and Perspectives of Fullerene Chemistry

9.1 Introduction

9.2 Reactivity

9.3 Regiochemistry of Addition Reactions

9.4 The Future of Fullerene Chemistry
9.4.1 Multiple Addition Products with a Defined Three-Dimensional Structure
9.4.2 Heterofullerenes
9.4.3 Ring-Opening and Degradation Reactions - Synthesis of Endohedrals
9.4.4 Chemistry with Higher Fullerenes

9.5 Perspectives for Practical Applications

9.6 Concluding Remarks

References

9.1 Introduction

The accessibility of the fullerenes in macroscopic quantities[1] opened up the unprecedented opportunity to develop a rich "three-dimensional" chemistry of spherical and polyfunctional all-carbon molecules. A large multitude of fullerene derivatives of both covalent addition products as well as of fullerene salts can be imagined; of which numerous examples have already been synthesized. As a consequence, new materials with outstanding biological[2,3] or material properties[4] have been discovered. Most of the chemistry of fullerenes has so far been carried out with C_{60} with little work on C_{70} and a few experiments with C_{76}. This is simply due to the fact that C_{60} is the most abundant fullerene. Principles of C_{60} chemistry can already be deduced from the analysis of the chemical transformations as well as from theoretical investigations of C_{60} and its derivatives. The chemical behavior of the higher homologs C_{70} and C_{76} tends to be similar, especially in those subunits of the molecules that are closely related to the C_{60} structural elements. To reveal the characteristics of fullerene chemistry[5,6,7,8,9,10,11,12] is not only challenging from an academic point of view; an understanding of the chemical behavior as well as the properties of this new class of compounds is an important requirement for the design of fullerene derivatives with technological applications.

9.2 Reactivity

Since all the C-atoms of the fullerenes are quarternary, and therefore contain no hydrogens, substitution reactions characteristic for aromatics are not possible with fullerenes. This leaves three main types of chemical transformations: (i) electron-transfer reactions resulting in the formation of fullerene salts; (ii) addition reactions and (iii) ring-opening and degradation reactions. Although defined degradation or ring-opening reactions of fullerenes would be of great importance, so far very little experimental material is available for these reactions. Thus, fullerene chemistry concentrates predominantly on addition reactions as well as on salt formation.

The sp^2 C-atoms in C_{60} exhibit a high degree of pyramidalization. The strain energy, which is estimated to be about 8 kcal/mol per carbon, is about 80 % of the heat of formation[13]. A major driving force for addition reactions leading to adducts with a low to moderate number of addents bound to C_{60} is the resulting *relief of strain in the fullerene cage*. Reactions leading to saturated tetrahedrally hybridized C-atoms are strongly assisted by the local strain of pyramidalization present in the fullerene[13]. Therefore, in most cases additions to C_{60} are exothermic reactions. The exothermicity of subsequent additions decreases with an increasing number of addents already bound to C_{60}. This holds also for the formation η^2-complexes. For example, the addition of one Pt-atom to C_{60} releases 17 kcal/mol of global strain energy, whereas in the hexaadduct less than 10 kcal/mol are released per Pt-atom[13].

The comparison of the chemical behavior with that of other classes of compounds reveals that *the reactivity of C_{60} is that of a fairly localized and electron-deficient polyolefin.* The electrophilicity per se is especially reflected by the ease of electrochemical and chemical reductions as well as by Michael-type nucleophilic additions [Scheme 9.1]. Also the reduction of C_{60} itself can be regarded as a strain-relief process[13], because many carbanions are known to prefer pyramidal geometries. Reductions, for example up to the dodecaanion (Chapter 2) as well as multiple nucleophilic additions (Chapter 3), are possible or unavoidable if an excess of reagent is used. The number of reduction steps or nucleophilic additions can be controlled by the stoichiometry of the reagent or sometimes in the case of nucleophilic additions by the size of the addent. The more addents already bound to C_{60}, the less

nucleophilic the fullerene becomes. For example, the longer reaction times required for the synthesis of $C_{66}(COOEt)_{12}$ (hexaadduct) by nucleophilic addition of diethyl bromomalonate starting from the pentadduct compared to that of the monoadduct $C_{61}(COOEt)_2$ from C_{60} are a consequence of both decreasing nucleophilicity of the fullerene cage and decreasing exothermicity of the addition[14,15]. The formation of the heptaadduct $C_{67}(COOEt)_{14}$ is almost completely suppressed at the same reaction conditions. In this case the sterical hindrance of the addents also becomes important.

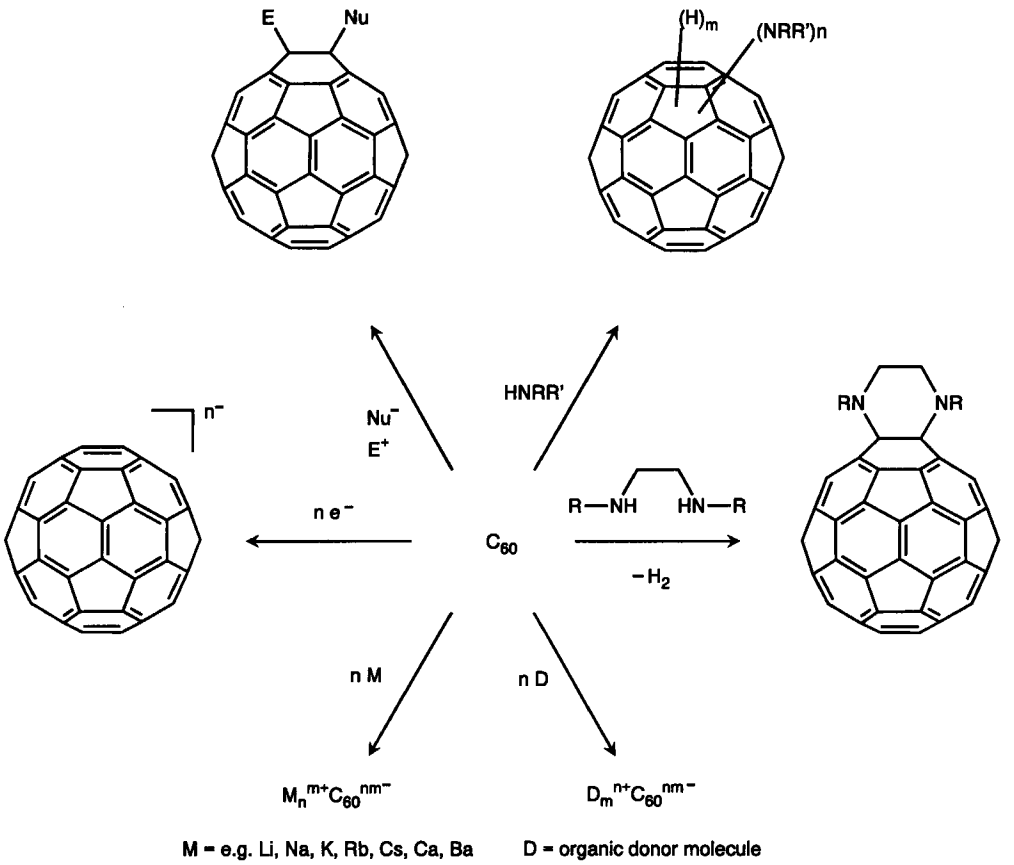

Scheme 9.1

With transition metal reagents, C_{60} undergoes either hydrometalations or forms η^2- rather than η^5- or η^6-π-complexes (Chapter 7). The latter would be typical reactions for planar aromatics [Scheme 9.2].

In analogy to olefins, C_{60} undergoes a broad variety of cycloadditions (Chapter 4) [Scheme 9.3]. In many cases cycloadducts of C_{60} exhibit a remarkable stability. These reactions are very useful for the introduction of functional groups. The fact that in the case of Diels-Alder reactions, C_{60} always reacts as the ene and that the benzyne addition proceeds in a [2+2]- rather than in an [4+2]-mode again demonstrates its electron-deficient olefin character.

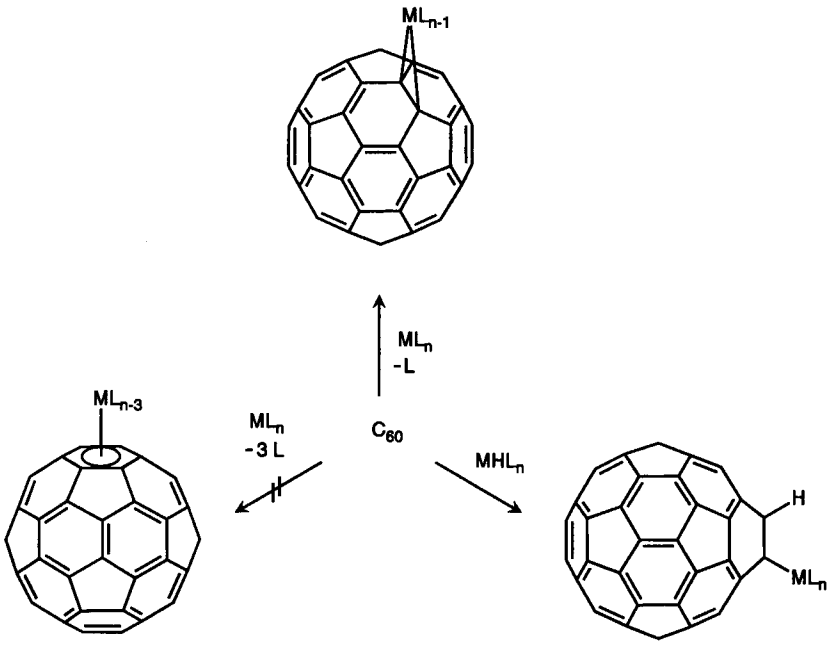

Scheme 9.2

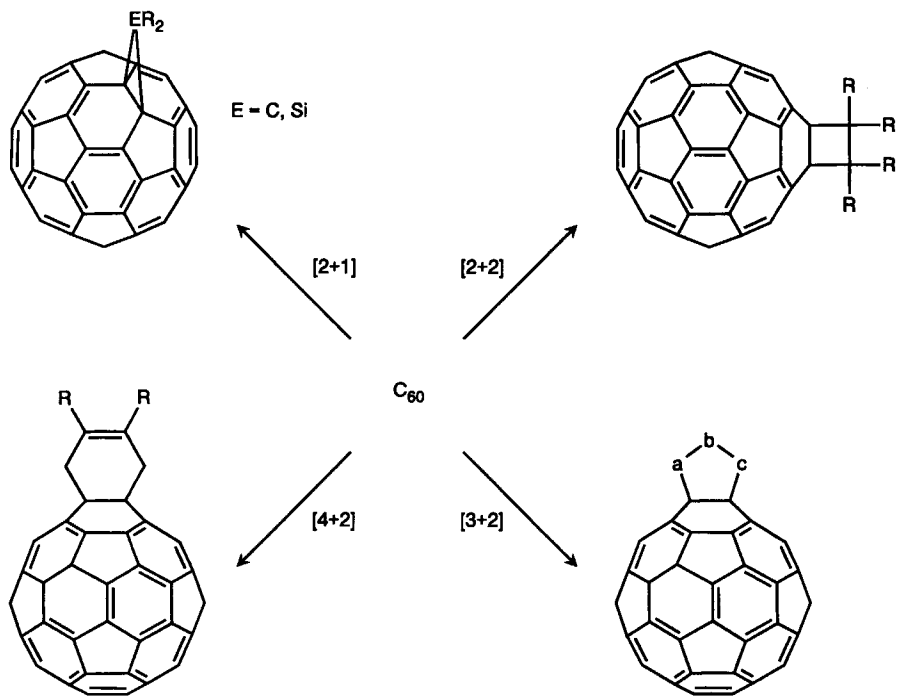

Scheme 9.3

C_{60} is a radical sponge [Scheme 9.4] and readily adds organic as well as inorganic radicals (Chapter 6). As in the case of nucleophilic additions, multiple additions take place if an excess of the free radical species is allowed to react with the fullerene.

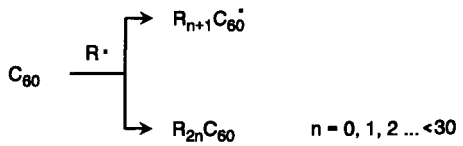

Scheme 9.4

Similar to usual olefins, C_{60} undergoes osmylations and epoxidations, as well as additions of Lewis acids (Chapter 8). In these cases, C_{60} acts as electron-donating species [Scheme 9.5].

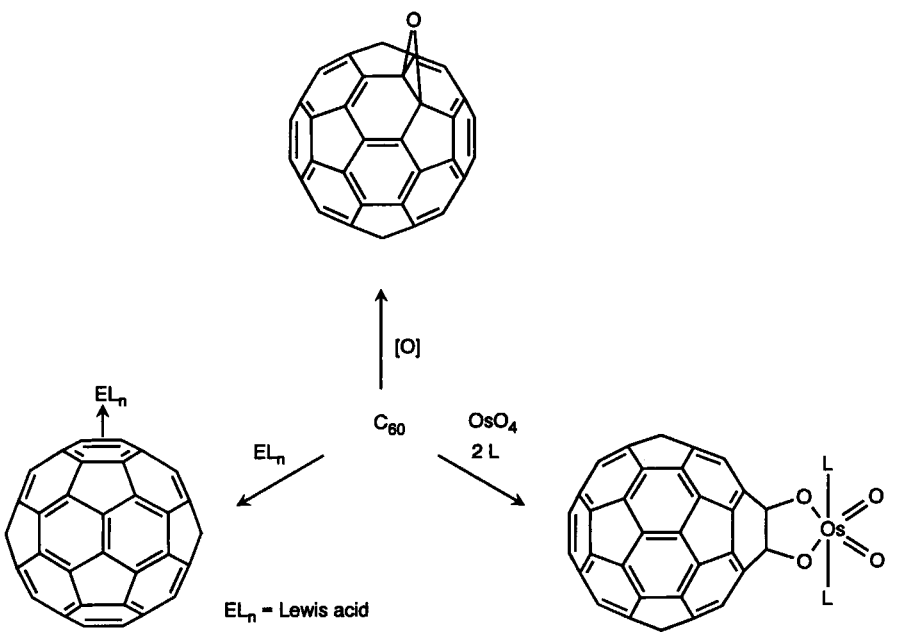

Scheme 9.5

Upon exhaustive hydrogenations (Chapter 5) or halogenations, (Chapter 8) the species $C_{60}X_{60}$ are not formed as major products [Scheme 9.6]. If formed at all, $C_{60}X_{60}$ is rather unstable or it is a ring-opened degraded product. This instability is due to another driving force in the fullerene chemistry, namely the *reduction of strain in polyadducts due to elimination*. The reason for these new types of strains are the increasing deviation from tetrahedral angles of sp^3-carbons (e.g. planar cyclohexane rings) as well as a cumulating amount of eclipsing interactions between the addents X bound in 1,2-positions. Eclipsing interactions between X are unfavorable, and increase with increasing size of X. Whereas for a small number of addents relief of strain in the parent fullerene cage caused by the addition is predominant; the opposite behavior is valid for polyadducts, because new types of strain are increasingly built up. Therefore, the degree of addition is a consequence of the balance of these two

opposing effects. In general exhaustive hydrogenations and halogenations lead to adducts $C_{60}X_{2n}$ with an intermediate number of addents bound to the fullerene, for example n = 12 and 18. These adducts, however, are thermally and chemically not very stable and tend to revert to C_{60}.

$$C_{60} \xrightarrow{X_2} C_{60}X_{2n} \qquad (X = H_2, F_2, Cl_2, Br_2)$$

Scheme 9.6

The chemical oxidation of C_{60} leading to free cationic species is possible under drastic conditions, for example in superacidic media (Chapter 8).

In general, addition products of C_{60} have a great propensity to revert to the parent fullerene by eliminating the addents. However, in the case of cycloadducts, such as Diels-Alder adducts or methanofullerenes, the elimination of the addent is often hindered, resulting in fullerene derivatives with a remarkable thermal and chemical stability. The higher homolog C_{70} exhibits an analogous reaction behavior.

9.3 Regiochemistry of Addition Reactions

It was calculated[16] that there are 12,500 Kekulé resonance structures possible for C_{60}. However, the two types of bonds in C_{60} have a different length, with the 6-6 bonds being shorter than the 5-6 bonds (Chapter 1). Thus, the lowest energy Kekulé structure of C_{60} is that with all the double bonds located at the junctions of the hexagons (6-6 double bonds) [Fig. 9.1].

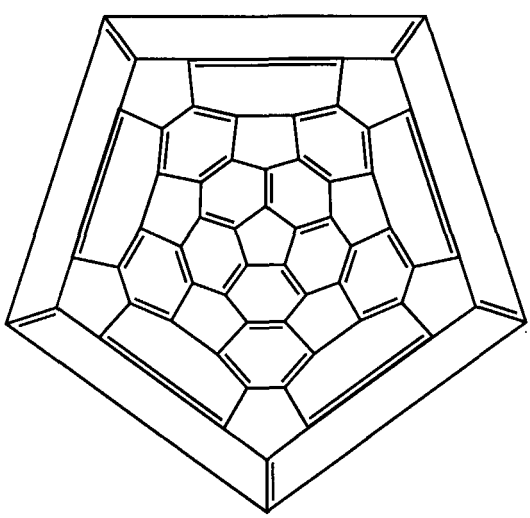

Figure 9.1 Lowest energy Kekulé structure of C_{60}.

This holds also for adducts with a few addents bound to C_{60} and leads directly to another principle of the fullerene chemistry namely *the minimization of 5-6 double bonds in the fullerene framework.*

The minimization of 5-6 double bonds is one factor that dictates the regiochemistry of addition reactions. No 5-6 double bonds are introduced into the lowest energy Kekulé structure of the fullerene framework upon 1,2-additions to 6-6 double bonds. In all cases of cycloadditions, a 1,2-mode is observed at least as the primary step. In many cases of the addition of segregated groups the 1,2-mode also prevails. In 1,2-additions, however, eclipsing interactions between the addents are introduced. Thus, if bulkier addents are allowed to react with C_{60}, a 1,4-mode avoiding eclipsing interactions may become important; this is observed in the synthesis of $C_{60}(CH_3)_2$ where both the 1,2- as well as the 1,4-adducts are formed simultaneously[17]. 1,2-Adducts are isolated predominantly or exclusively, for example, in hydroalkylation reactions leading to 1,2-$C_{60}HR$[18]. In a 1,4-addition product the lowest energy Kekulé structure contains one 5-6 double bond. The introduction of one 5-6 double bond costs about 8.5 kcal/mol[19]. In 1,2-$C_{60}H_2$, the eclipsing interaction was estimated to be about 3-5 kcal/mol. This value increases with an increasing size of the addent[20]. The relative product distribution is balanced by minimizing 5-6 double bonds on the one hand and eclipsing interactions on the other hand [Fig 9.2]. Adducts $C_{60}XY$, which have the addents attached further apart from each other and would require the introduction of even more 5-6 double bonds, have not been isolated.

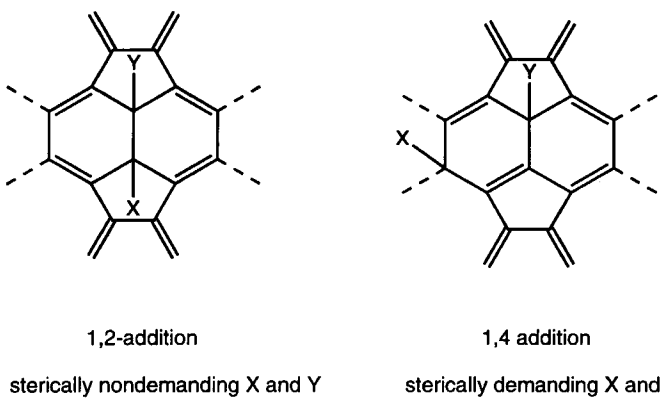

Figure 9.2 1,2- and 1,4-addition to C_{60}.

The charge density or spin density of primary adducts RC_{60}^- or RC_{60} formed by nucleophilic or radical additions is highest at position 2 and (4,11) for nucleophilic additions and at position 2, (4,11) and (6,9) for radical additions [Fig. 9.3]. This is also a result of the most efficient relief of strain (pyramidalization) as well as of avoiding formal 5-6 double bonds in the intermediates. Also from this point of view, an electrophilic attack or radical recombination process at the 2 position is favored, neglecting eclipsing interactions.

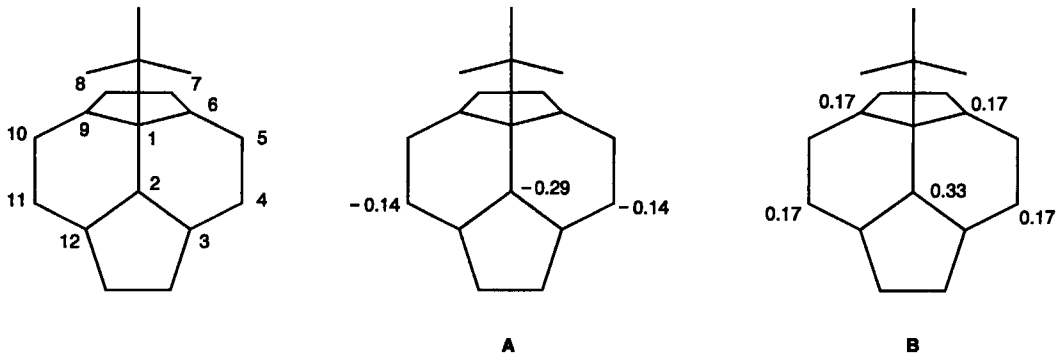

Figure 9.3 Charge distribution (**A**) (Mulliken charges) and spin distribution (**B**) in the intermediates *t*-BuC_{60}^- and *t*-Bu C_{60}.

In the case of methanofullerenes, either closed-ring 1,2-bridged structures or open-ring 1,6-bridged structures have been observed[21,22,23] [Fig. 9.4]. In both cases no 5-6 double bond has to be introduced into the lowest energy Kekulé structure. This is not valid for hypothetical open 1,2-bridged or closed 1,6-bridged structures. In both cases two 5-6 double bonds would be required. The open-ring 1,6-methanofullerenes (fulleroids) are formed upon diazomethane additions to C_{60} after a rearrangement of 1,2-bridged intermediates.

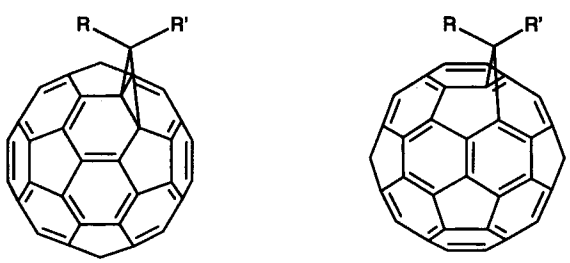

Figure 9.4 Stable ring-closed and ring-open methanofullerenes with no 5-6 double bonds.

The regiochemistry of subsequent additions of bulky segregated groups, such as alkyl radicals, seems also to be influenced by the possibility of electronic delocalization in open shell intermediates like **1** and **2**[24]. Presuming that a radical mechanism is also valid for the addition of bromine or chlorine, the formation of the regioisomers $C_{60}X_6$ (**3**) then becomes understandable[25,26].

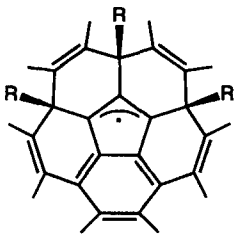

1

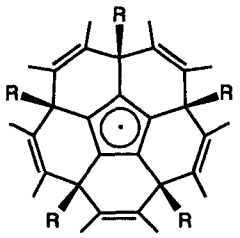

2

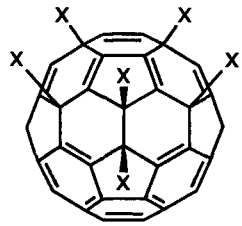

3

Additions to C_{70} take place predominantly at either the bonds between the carbons of set A and B (1,2-addition) or at those of set C (3,4-addition) [Fig. 9.5]. These are the most C_{60}-like bonds with the highest double-bond character and the corresponding carbons exhibit the highest degree of pyramidalization. In general 1,2-additions are preferred over 3,4-additions. Therefore, principles similar to those governing the regiochemistry of C_{60} are also valid for C_{70}.

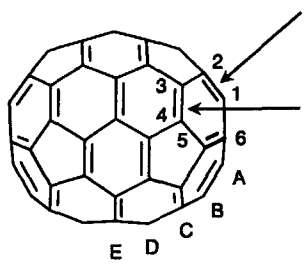

Figure 9.5 Preferred sites for additions to C_{70}.

Successive 1,2-additions to C_{60} show a remarkable regioselectivity. Among the eight possibilities for the position of a second attack to a monoadduct of C_{60}, the sites *e* and *trans*-3 are significantly favored [Fig. 9.6; Tab. 9.1][14,27,28]. If the addents are not sterically demanding, then the attack into the *cis*-1 position is also favored[28]. The *cis*-1 $C_{60}H_4$ is the major product obtained by hydroboration and subsequent protonation. However, if sterically requiring addents are used, attack at a *cis*-1 position is completely suppressed[14,27].

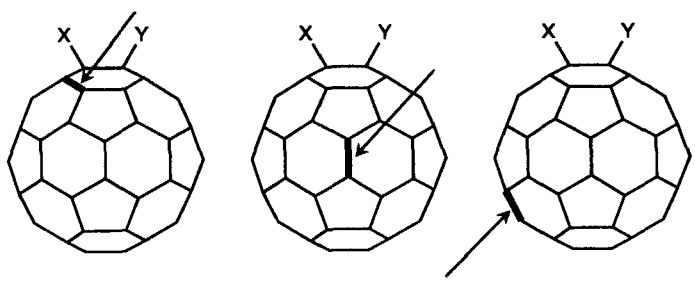

Figure 9.6 The most favored sites for a second 1,2-addition to C_{60}.

Table 9.1 Calculated stabilities and relative yields for different bisadducts of C_{60}

	$C_{60}H_4$[28]			$C_{60}(OsO_4py_2)$[27]	$C_{62}(COOEt)_4$[14]	
	(nondemanding addents)			(demanding addents)	(demanding addents)	
	relative stability		relative yield	relative yield	relative stability	relative yield
	AM1	3-31G*	(%)	(%)	AM1	(%)
	(kcal/mol)				(kcal/mol)	
cis-1	3.3	0.0	50	0	17.7	0
cis-2	3.5	6.0	-	0	1.8	2
cis-3	2.4	8.1	-	0	1.3	6
e	0.0	3.1	-	41	0.0	38
trans-4	0.2	4.0	-	13	0.0	9
trans-3	0.4	3.6	-	27	0.1	30
trans-2	0.6	3.8	-	17	0.2	13
trans-1	0.8	3.8	-	2	0.2	2

The *e* and *trans*-3 positions relative to addents already bound to C_{60} are also favored for the formation of higher adducts. Among the 14 regioisomers for $C_{63}(COOEt)_6$, which can be formed from $C_{62}(COOEt)_4$ with the addents in the *e* position, the C_3 symmetric *e,e,e*-regioisomer is obtained in a 40 % yield[14]. This preferred addition mode to octahedral sites (*e* additions) can be used for the controlled synthesis of very symmetric hexaadducts with T_h-symmetry [Scheme 9.7][29].

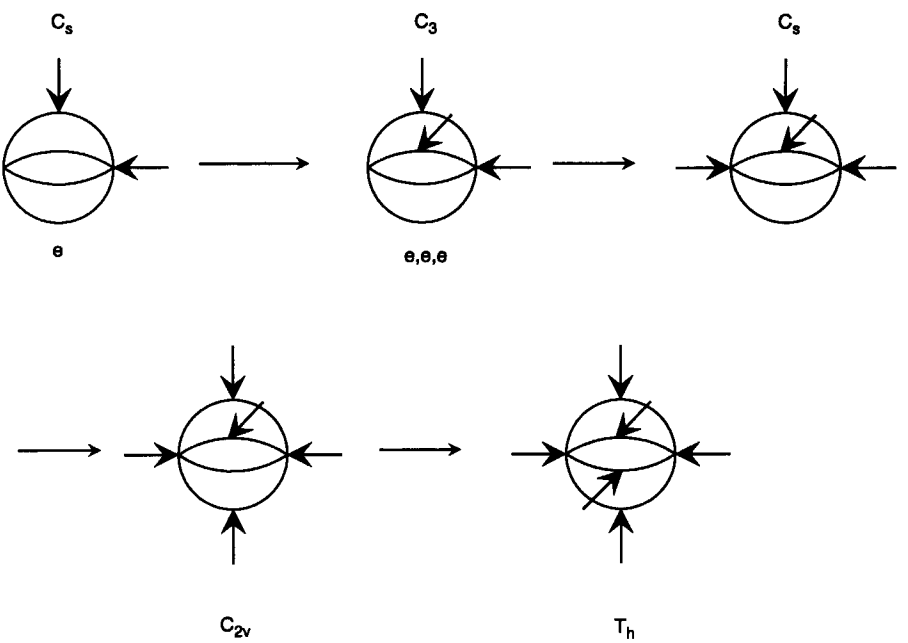

Scheme 9.7

To minimize side reactions, after each kinetically controlled and irreversible addition step to the fullerene core the right regioisomer has to be isolated from the reaction mixture, before the next addition is carried out. This is not necessary if the addition to the fullerene is thermodynamically controlled. For example, in the reaction of C_{60} with a 10-fold excess of $Pt(PEt_3)_4$, the most stable T_h symmetric hexaadduct, $[(Et_3P)_2Pt]_6C_{60}$, is formed as the only reaction product[30]. This is possible because the corresponding additions are reversible[31].

9.4 The Future of Fullerene Chemistry

The chemistry of the fullerenes has been dominated thus far by surveying the reactivity of C_{60} and C_{70} as well as by the synthesis and characterization of fulleride salts and exohedral addition products. Most of the work concentrated on the formation of monoaddition products of C_{60}. In a very short period of time a very rich chemistry developed in this respect. It is now possible to covalently bind almost any class of compounds to the fullerene core. As shown in Chapter 9.2 and 9.3 it is already possible, based on the present knowledge, to deduce rules for the chemical behavior of C_{60} and C_{70}. Despite this quick success, fullerene chemistry is still in an early stage. For synthetic chemists a lot of challenging work remains to be done. Since fullerene chemistry is moving very rapidly and accompanied with exciting surprises, it is impossible to predict precisely the future developments. In any case, the following partly solved or unsolved problems will be among the major topics for future fullerene chemistry.

9.4.1 Multiple Addition Products with a Defined Three-Dimensional Structure

The fullerenes exhibit a three-dimensional "workspace" with a comparatively large number of reactive double bonds. This polyfunctionality implies an enormous multitude of possible regioisomeric fullerene adducts. The regiochemistry of multiple additions to the fullerene core, which is the three-dimensional analog to the substitution reactions in benzene chemistry, will be a constituent of future chemistry textbooks. Stereochemically defined oligo- and polyadducts of fullerenes will also have a big potential for applications, like molecular recognition. Systematic studies on the regiochemistry of multiple additions have been done for transition metal complex formation reactions, hydrogenations, osmylations, radical additions and cyclopropanations (Chapter 9.3). The addition patterns and the regioselectivity depend on the reaction mechanism as well as on the nature of the addents. For most addition reactions presented in this book systematic investigations of multiple additions are still missing. For example, the structures as well as the pathway and reason for the decomposition of most of the polyhydrofullerenes and polyhalofullerenes are unknown. An interesting topic would be also to carry out combined additions like cycloadditions and then radical additions. The regiochemistry of the fulleroids (5-6-ring bridged fullerenes) is completely unknown. It is predicted[32] that a second addition step is by far less regioselective than that for a second addition to a 6-6-ring bridged fullerene, since a fulleroid retains the properties of the parent C_{60} much more. Thermal rearrangement reactions of bridged mono- and bisadducts have been investigated for only a few cases[33,34,35]. The scope of such "globe trotting" processes on the fullerene spheres as well as the potential for the rearrangements to preferred isomers of oligoadducts remains to be investigated. For practical applications it will be very important to synthesize stable oligoadducts of the fullerenes (e.g. cycloadducts) and then tailor make, by further side chain chemistry, defined molecules, for example with different functional groups.

These systems will have potential for catalysis and molecular recognition. Simply due to the addition pattern, many of the C_{60} adducts, for example those with C_1, C_2 or C_3 symmetry, are chiral. The separated enantiomers will be very useful for stereoselective synthesis (see Chapter 9.5).

9.4.2 Heterofullerenes

In heterofullerenes C-atoms are substituted with heteroatoms such as nitrogen and boron. These systems provide an extremely large structural multitude, chemical functionality and possibilities for electronic tuning of the fullerene properties. This three-dimensional analog of the transition from aromatics to heteroaromatics is therefore very attractive. Although the mass spectrometric detection of $C_{59}B$ (**4**) has been reported[36], a synthesis of heterofullerenes in macroscopic quantities is unknown. So far any attempts for their synthesis by the evaporation of carbon in the presence of heteroatoms failed, although it has been predicted[37,38] that many examples such as **4**, **5**, **6** or **7** have a similar stability to C_{60}. In addition to closed heterofullerenes, truncated systems such as **8** can be visualized[38]. The latter case would also provide the possibility of synthesizing endohedrals or, in analogy to the phthalocyanine chemistry, allow the introduction of a transition metal ion into the window by complexation with the four nitrogen atoms of the reduced truncated system. These few examples indicate the extensive possibilities for structural variation.

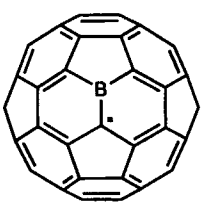

4

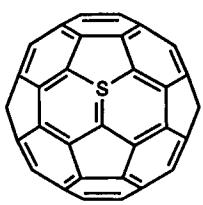

5

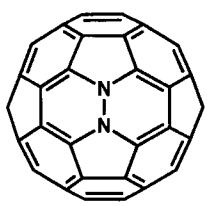

6

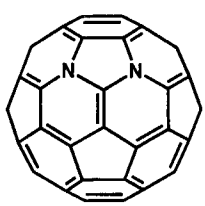

7

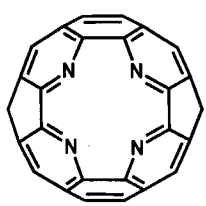

8

9.4.3 Ring-Opening and Degradation Reactions - Synthesis of Endohedrals

Defined ring-opening and degradation reactions would not only lead to new and exciting structures but would also allow the incorporation of atoms, ions and small molecules into the fullerene cages. The latter aspect becomes even more attractive if it is possible to reclose the spheres once the guest is located in the cage. Whereas the incorporation of small molecules or atoms like noble gases will lead to neutral systems, the encapsulation of ions will give salts. These salts are interesting in themselves

but by using electrochemical methods could also be converted into "molecular atoms", for example with a positively charged core (metal cation) and a negatively charged carbon shell. One can imagine encapsulating all elements of the periodic system in fullerenes. So far endohedral complexes have only been prepared in small quantities either with electropositive metals during fullerene formation or subsequently by the thermal incorporation of noble gases (Chapter 1). The latter results are already very exciting[39] but the yields of endohedrals are still low and the method seems to be restricted to the incorporation of noble gases. This could be overcome by using mild chemical opening reactions leading to defined products. Such reactions are so far unknown. Upon hyperfluorination[40] and treatment of solid C_{60} with singlet oxygen[41], however, first examples of ring opened and degraded but not completely characterized products have been obtained. In the fulleroids one 5-6 bond is open but the methano bridge above the nine-membered ring prevents an atom from penetrating through the sphere. A challenge for the future would be to open just one or a few bonds of the fullerene, for example by ozonolysis or a similar reaction, then allow an atom to penetrate through nine- or ten-membered rings into the cage and finally reclose the cage.

9.4.4 Chemistry with Higher Fullerenes

An extensive development of the chemistry of the higher fullerenes has been prevented by the fact that only small amounts of material are available. Once methods which provide larger quantities have been developed, additional possibilities for fullerene chemistry will arise. The regioselectivity of additions to higher fullerenes depending on the isomer will be an important topic. It can be predicted that the regions of the corresponding spheres with the highest curvature (corannulene subunits) will have the most C_{60} - like properties.

9.5 Perspectives for Practical Applications

Ever since the method for the preparation of macroscopic quantities of fullerenes was discovered in 1990, one of the questions most frequently asked was: What are the possible practical applications? The answer to this question, given about four years later, has not changed very much compared to earlier ones: There is no practical use at present but since fullerenes and their derivatives exhibit a variety of remarkable properties, for example, superconductivity, molecular magnetism, as well as catalytic and biological activity, a lot of important applications may arise in the future. A critical evaluation[42,43] of some possible applications based on the present knowledge is given.

From the very beginning of the "fullerene era" it was speculated that there is a potential for uses as lubricants, either for parent or fluorinated fullerenes. This view turned out to be unrealistic, because compared to other lubricants like graphite the fullerenes are either too expensive or the compounds, for example $C_{60}F_n$, are unstable (Chapter 8). Detailed results on the lubrication properties of perfluoroalkylated fullerenes[44] (Chapter 6) are not published.

The possibility of using fullerenes for containers for drugs is also unrealistic, since either the cavity is too small (C_{60} - C_{84}) or the abundance of the fullerenes is too low (giant fullerenes). In addition, the incorporation and release of drugs would require defined opening and closing reactions of the fullerene cages which up to now are unknown.

The application of fullerenes as superconductors or magnets is doubtful (Chapter 2). Although the fullerene superconductors, for example K_3C_{60}, exhibit some favorable properties like an isotropic charge transport, a comparatively large coherence length as well as a facile method of preparation, they

are extremely sensitive towards moisture and air. The only known fullerene material with ferromagnetic properties ([TDAE]C_{60}) on the other hand exhibits no magnetic remanence making it useless for applications.

More realistic seems to be the development of specific electronic and optical devices[43]. Solid C_{60} is a semiconductor with a band gap of about 2 eV. The conductivity can be varied by doping between $<10^{-7}$ and 10 S/cm[43]. The construction of semiconducting fullerene devices with an improved radiation and heat resistivity as well as of more efficient light sensors could be possible. Thin layers of C_{60} show fluorescence between 650 and 750 nm and phosphorescence between 780 and 950 nm. The first light emitting diodes have already been developed[43]. The multitude of derivatization reactions also allows the synthesis of fullerene polymers, monolayers of fullerenes covalently bound to a surface or of Langmuir–Blodgett films. This can be of additional importance for the development of electronic and optical devices, because many of the C_{60} properties are retained in these materials, while the processibility is improved.

Free standing C_{60} films could be used for X-ray lithography. This has been demonstrated by the preparation of mechanically stable C_{60} membranes[45]. Below 300 eV the membranes are much more transparent than conventional silicon discs. Solid C_{60} as well as solutions show a strong dependence of the absorption coefficients on the intensity of the incoming light[43]. This could be used for the development of "intelligent" laser protection glasses. Other nonlinear optical effects, for example the $\chi^{(3)}$ coefficient of C_{60} is about one order of magnitude smaller than those of conventional materials. It cannot be excluded, however, that fullerene derivatives may have better properties.

The fact that C_{60} can be reversibly reduced by up to 6 electrons (Chapter 2) stimulated the investigation of fullerene batteries[43]. The charge densities per volume, however, are so far lower than those of conventional batteries[43].

A more promising potential for fullerenes is their use as catalysts[46]. A variety of catalytic effects of the parent C_{60}, for example C–C bond formation, bond cleavage as well as dehydrogenation reactions have been discovered[47]. An additional, even more potent and selective impact is expected from fullerene derivatives. In particular the investigation of the regiochemistry of multiple additions to the fullerene core and synthesis of oligoadducts with a defined three-dimensional structure[14] could provide useful catalysts for the stereoselective synthesis.

Applications as pharmaceuticals are also intriguing[48]. Recently, it has been shown that some fullerene derivatives exhibit biological activity[49,50,51,52]. In this respect two properties of C_{60} are of special significance. The first is its spherical shape, which can be used for molecular recognition, for example the inhibition of HIV protease (HIVP)[49,50], and the second is the ability of the fullerene core to efficiently photosensitize the conversion of triplet oxygen to singlet oxygen, which can be used for DNA cleavage[51,52]. An important requirement for the investigation of the biological activity of a fullerene derivative is its water solubility. This can be achieved by the attachment of polar functional groups.

Although there is a lot of effort in the synthesis and characterization of endohedral complexes, applications of these interesting materials are hampered by the fact that so far only extremely low quantities can be isolated.

Other possible uses for fullerenes that have been discussed are, for example, the production of diamonds, molecular sieves, gas and hydrogen storage, solar cells, chemical sensors and fuel for satellites as well as several applications for nanotubes[42,43].

The following summarizing evaluation[43] shows that there is a potential for possible technological applications of fullerenes. On the other hand, it is impossible to predict whether even one of these applications will lead to a real innovation.

I) Considered to be promising:

- Electronic and optical devices based on fullerenes and fullerene polymers (electrical and photoconductivity)
- Photo and electroluminescing materials
- Catalysts
- Pharmaceuticals

II) Evaluation not clear based on the present knowledge:

- Diamond synthesis - thin films and in bulk
- Batteries
- Molecular sieves and gas storage media
- Materials for the nonlinear optics
- Solar cells
- Super conductors
- Applications for nanotubes

III) Not competitive with conventional materials based on the present knowledge:

- Magnetic materials
- Lubricants
- Giant fullerenes as containers for drugs
- Fuel for satellites

9.6 Concluding Remarks

Despite the beauty of the fullerenes and the fascinating results that have been obtained in a short time, fullerene chemistry still faces some resistance from organic chemists. "The majority of organic chemists are not turned on by C_{60} because, in a way, it is an insult to organic chemistry because it was not synthesized from scratch" Wudl says[48] but on the bright side he believes, that the situation is changing: "Recently I have found a lot less resistance from chemists in general, and organic chemists in particular, toward C_{60}". Scientists, who are involved in the fullerene chemistry themselves are usually very enthusiastic about this field. As was stated by Diederich[53]: "Within a few years C_{60} became an essential building block in organic chemistry. Michael Faraday discovered benzene in the early 19th century. It took 100 years to fully develop benzene chemistry. In 10 years, we will have developed a chemistry of C_{60} analogous to benzene chemistry, and chemists will utilize it routinely in their synthesis". This view seems to be realistic and is supported by the summarizing presentation of the fullerene chemistry given in this book. A sentence of Kroto plastically describes the additional aspect that the fullerenes introduced into the synthetic chemistry: "Five hundred years after Columbus reached the West Indies, flat carbon has gone that way of the flat earth"[54].

References

1 W. Krätschmer, L. D. Lamb, K. Fostiropoulos, D. R. Huffman *Nature* **1990**, *347*, 354.
2 S. M. Friedman, D. L. DeCamp, R. P. Sijbesma, G. Srdanov, F. Wudl, G. L. Kenyon *J. Am. Chem. Soc.* **1993**, *115*, 6506.
3 H. Tokuyama, S. Yamago, E. Nakamura, T. Shiraki, Y. Sugiura *J. Am. Chem. Soc.* **1993**, *115*, 7918.
4 *The Fullerenes;* H. W. Kroto, J. E. Fischer, D. E. Cox, Eds.; Pergamon: Oxford, 1993.
5 F. Wudl *Acc. Chem. Res.* **1992**, *25*, 157.
6 F. Wudl In *Buckminsterfullerenes*; W. E. Billups, M. A. Ciufolini, Eds; VCH: Weinheim, 1993; pp 317-335.
7 P. J. Fagan, B. Chase, J. C. Calabrese, D. A. Dixon, R. Harlow, P. J. Krusic, N. Matsuzawa, F. N. Tebbe, D. L. Thorn, E. Wasserman *Carbon* **1992**, *30*, 1213.
8 G. A. Olah, I. Bucsi, R. Aniszfeld, G. K. S. Prakash *Carbon*, **1992**, *30*, 1203.
9 P. J. Fagan, J. C. Calabrese, B. Malone *Acc. Chem. Res.* **1992**, *25*, 134.
10 J. M. Hawkins *Acc. Chem. Res.* **1992**, *25*, 150.
11 R. Taylor, D. R. M. Walton *Nature* **1993**, *363*, 685.
12 A. Hirsch *Angew. Chem.* **1993**, *105*, 1189; *ibid. Int. Ed. Engl.* **1993**, *32*, 1138.
13 R. C. Haddon *Science* **1993**, *261*, 1545.
14 A. Hirsch, I. Lamparth, H. R. Karfunkel *Angew. Chem.* **1994**, *106*, 453; *ibid Int. Ed. Engl.* **1994**, *33*, 437.
15 A. Hirsch, I. Lamparth *unpublished results.*
16 D. J. Klein, T. G. Schmalz, T. G. Hite, W. A. Seitz *J. Am. Chem. Soc.* **1986**, *108*, 1301.
17 C. Caron, R. Subramanian, F. D'Souza, J. Kim, W. Kutner, M. T. Jones, K. M. Kadish *J. Am. Chem. Soc.* **1993**, *115*, 8505.
18 A. Hirsch, T. Grösser, A. Skiebe, A. Soi *Chem.Ber.* **1993**, *126*, 1061.
19 N. Matsuzawa, D. A. Dixon, T. Fukunaga *J. Phys. Chem.* **1992**, *96*, 7594.
20 N. Matsuzawa, T. Fukunaga, D. A. Dixon *J. Phys. Chem.* **1992**, *96*, 10747.
21 M. Prato, V. Lucchini, M. Maggini, E. Stimpfl, G. Scorrano, M. Eiermann, T. Suzuki, F. Wudl *J. Am. Chem. Soc.* **1993**, *115*, 8479.
22 L. Isaacs, A. Wehrsig, F. Diederich *Helv. Chim. Acta* **1993**, *76*, 1231.
23 L. Isaacs, F. Diederich *Helv. Chem. Acta* **1993**, *76*, 2454.
24 P. J. Krusic, E. Wasserman, P. N. Keizer, J. M.Morton, K. F. Preston *Science* **1991**, *254*, 1183.
25 P. R. Birkett, A. G. Avent, A. D. Darwish, H. W. Kroto, R. Taylor, D. R. M. Walton *J. Chem. Soc., Chem. Commun.* **1993**, 1230.
26 P. R. Birkett, P. B. Hitchcock, H. W. Kroto, R. Taylor, D. R. M. Walton *Nature* **1992**, *357*, 479.
27 J. M. Hawkins, A. Meyer, M. Nambu *J. Am. Chem. Soc.* **1993**, *115*, 9844.
28 C. C. Henderson, C. M. Rohlfing, R. A. Assink, P. A. Cahill *Angew. Chem.* **1994**, 106, 803; *ibid Int. Ed. Engl.* **1994**, *33*, 786.
29 A. Hirsch, I. Lamparth, unpublished results.
30 P. J. Fagan, J. C. Calabrese, B. Malone *Acc. Chem. Res.* **1992**, *25*, 134.
31 S. A. Lerke, B. A. Parkinson, D. H. Evans, P. J. Fagan *J. Am. Chem. Soc.* **1992**, *114*, 7807.
32 A. Hirsch, unpublished results.
33 M. Prato, V. Lucchini, M. Maggini, E. Stimpfl, G. Scorrano, M. Eiermann, T. Suzuki, F. Wudl *J. Am. Chem. Soc.* **1993**, *115*, 8479.
34 F. Diederich, L. Isaacs, D. Philp *J. Chem. Soc., Perkin Trans. 2* **1994**, 391.
35 A. Hirsch, I. Lamparth, unpublished results.
36 R. E. Smalley In *Fullerenes: Synthesis, Properties, and Chemistry of Large Carbon Clusters;* G. S. Hammond, V. J. Kuck, Eds.; American Chemical Society Symposium Series 481; 1992; p 141.
37 N. Kurita, K. Kobayashi, H. Kumahora, K. Tago, K. Ozawa *Chem. Phys. Lett.* **1992**, *198*, 95.
38 H. R. Karfunkel, T. Dressler, A. Hirsch *J. Comp. Aid. Mol. Design* **1992**, *6*, 521.
39 M. Saunders, H. A. Jimenez-Vazquez, R. James Cross, S. Mroczkowski, M. L. Gross, D. E. Giblin, R. J. Poreda *J. Am. Chem. Soc.* **1994**, *116*, 2193.
40 A. A. Tuinman, A. A. Gakh, J. L. Adcock, R. N. Compton *J. Am. Chem. Soc.* **1993**, *115*, 5885.
41 C. Taliani, G. Ruani, R. Zamboni, R. Danieli, S. Rossini, V. N. Denisov, V. M. Burlakov, F. Negri, G. Orlandi, F. Zerbetto *J. Chem. Soc., Chem. Commun.* **1993**, 220.
42 R. Baum *Chem.& Eng. News* **1993**, *22*, 8.
43 H. Eickenbusch, P. Härtwich *Fullerene*: *Analyse & Bewertung Zukünftiger Technologien;* VDI Technologiezentrum: Düsseldorf; 1993.
44 P. J. Fagan, P. J. Krusic, C. N. McEven, L. Lazar, D. H. Parker, N. Herron, E. Wasserman *Science* **1993**, *262*, 404.
45 C. B. Eom, A. F. Hebard, L. E. Trimble, G. K. Cellar, R. C. Haddon *Science* **1993**, *259*, 1887.

46 R. Baum *Chem.& Eng. News* **1993,** *22*, 8, quoting R. Malhorta.
47 R. Malhorta, D. F. McMillen, D. S. Tse, D. L. Lorents, R. S. Ruoff, D. M. Keegan *Energy & Fuels* **1993**, *7*, 685.
48 R. Baum *Chem.& Eng. News* **1993,** *22*, 8, quoting F. Wudl.
49 S. M. Friedman, D. L. DeCamp, R. P. Sijbesma, G. Srdanov, F. Wudl, G. L. Kenyon, *J. Am. Chem. Soc.* **1993**, *115*, 6506.
50 R. Sijbesma, G. Srdanov, F. Wudl, J. A. Castoro, C. Wilkins, S. H. Friedman, D. L. DeCamp, G. L. Kenyon, *J. Am. Chem. Soc.* **1993**, *115*, 6510.
51 H. Tokuyama, S. Yamago, E. Nakamura, T. Shiraki, Y. Sugiura, *J. Am. Chem. Soc.* **1993**, *115*, 7918.
52 C. B. Chen, Y. Z. An, D. S. Sigman, Y. Rubin, *J. Am. Chem. Soc.* **1994** in press.
53 R. Baum *Chem.& Eng. News* **1993,** *22*, 8, quoting F. Diederich.
54 H. W. Kroto *Nature*, **1992**, *359*, 670.

Index

Adams' catalyst, 81
N-(1-adamantyl)bis(trifluoromethyl)sulfin imide, 106
alkoxy radicals, 140
7-alkylidene-2,3-diazabicycloheptene, 99
alkylthio radicals, 140
allylic radicals, 143
allyltributyltin, 100
1-aminobenzotriazole, 107
arc heating, 1, 10
arc vaporization, 15
bis(ethylenedithio)tetrathiafulvalene, 32
benchtop reactor, 8
7*H*-benz[*de*]anthracene, 128
benzenesulfenyl chloride, 109
benzo[18]crown-6, 82
benzocyclobutenes, 82
1*H*-benzotriazol-1-ol, 97
benzyl *N*-(*tert*-butoxycarbonyl)-L-glutamate, 86
N-(benzyloxycarbonyl)-L-alanine, 86
benzyl radicals, 143
benzyne, 107
Bingel, C., 66
Birch–Hückel reduction, 115, 125, 126, 129
1,6-bis(aminomethyl)hexane, 83
bis(2,6-diisopropylphenyl)silylene, 111
bis-*o*-quinodimethane, 81
bromination, 162, 177, 178, 179, 180
bromoacetophenone, 66
Buckyclutcher HPLC, 107, 117
carbenes, 111
catalytic hydrogenation, 115, 125, 129
chlorination, 162, 175, 176
chlorofullerenes, 175
Columbus, 200
corannulene, 5, 26, 144, 197
18-crown-6, 107
cyanopolyynes, 5
cyclo[n]carbons, 19, 20
cycloadditions, 116
[2+1] cycloadditions, 111
[2+2] cycloadditions, 107
[3+2] cycloadditions, 87, 90, 99
[4+2] cycloadditions, 80, 87
cyclodextrin, 23
dangling bonds, 17, 18
dansyl chloride, 104
decachlorocorannulene, 16
desyl chloride, 66
dialkyl peroxides, 140
1,8-diazabicyclo[5.4.0]undec-7-ene, 66, 73, 106
4,13-diaza-[18]-crown-6, 83
dicyanopolyynes, 16
dicyclohexylcarbodiimide, 97
Diederich, F., 23, 54, 199
Diels–Alder adducts, 81, 92
Diels–Alder reactions, 80
N,N-diethylpropynylamine, 109
9,10-dihydroanthracene, 127
1,2-dihydro-1,2-(carboxymethano)fullerene-60, 96
2,5-dihydro-2,2-dimethoxy-5,5-dimethyl-1,3,4-oxadiazole, 111
1,4-dihydro-1,4-epoxy-3-phenylisoquinoline, 80
dihydroquinidine, 169, 170
dihydroquinine, 169, 170
diisobutylaluminium hydride, 100
1,3-dimercaptobenzene, 83
2,3-dimethylbuta-1,3-diene, 87
4-(dimethylamino)pyridine, 100
5,6-dimethylene-1,4-dimethyl-2,3-diphenylnorborn-2-en-7-one, 85
dimethyldihydrofullerene-60, 44
dimethyldioxirane, 164
1,2-dioxetane, 165
1,3-dioxolane, 164
1,3-diphenylisobenzofuran, 80
disiliranes, 106
DNA, 198
electrocrystallization, 37, 42, 43
endohedral complexes, 1, 12, 14, 21, 29, 185, 186, 197, 198
ethylene-propylene terpolymer, 75
Euler 's theorem, 2, 25
Fagan, P. J., 151
Faraday, M., 199
Fermi level, 50
ferrocene, 14, 32, 104
ferromagnets, 53, 198
flagellanes, 65
fluorination, 162, 172, 173, 174, 177
fluoroacyl peroxides, 145
fluoroalkyl iodides, 145
4-(4-fluoro-3-nitrobenzoyl)benzocyclobutene, 83
Fowler, P. W., 27
fulleranes, 116
fulleroid, 88, 192, 195, 197
fullerylation, 162, 180, 182
giant fullerenes, 5, 21, 197, 199
Gomberg radical, 141
gravity feed generators, 8
Grignard reagents, 57, 58, 174
Gutmann solvent donicity number, 39
halofluorocarbons, 145
halogenation, 162, 172
Hawkins, J. M., 166
heterofullerenes, 12, 185, 196
hexamethylene diisocyanate, 94
higher fullerenes, 2, 16, 21, 23, 28, 29, 31, 38, 40, 185, 197
HIV protease, 95, 198
HIV reverse transcriptase, 95
Hückel calculations, 5, 153
Huffman, D. R., 7, 20
hydroalkylation, 56, 57, 62, 116, 118, 191
hydroarylation, 56, 57, 62

hydroboration, 115, 116, 117, 118
hydrofullerenes, 12, 57, 116, 117, 129, 130
hydrogenation, 115, 116, 118, 125, 127, 128, 129, 130, 131, 132
hydrometalation reactions, 150, 151, 159
hydrostannylation, 136, 148
hydrozirconation, 115, 116
hyperfluorination, 173, 197
inductive heating, 1, 11
isoamyl nitrite, 107
isobenzofuran, 80, 81
3-isochromanone, 82
isolated pentagon rule, 17, 18, 19, 25, 26, 27
isoxazoline, 105
Jahn–Teller distortion, 40, 52
Jahn–Teller ground state, 40
Jones, D. E. H., 5
Kekulé structure, 119
Krätschmer, W., 7, 20
Kroto, H. W., 5, 6, 200
Langmuir–Blodgett films, 56, 63, 198
lanthanum fullerenes, 13
laser vaporization, 5, 6, 12, 13
Lewis acids, 162, 163, 182, 183
living polystyrene, 65
lubricants, 197, 199
magic acid, 180
Manolopoulos, D. E., 27
Meißner–Ochsenfeld Effect, 50
metallofullerenes, 14
(*p*-methoxyphenyl)diazoethane, 90
methyl 2-chloroacetylacetate, 66
N-methylglycine, 103, 104
7-methyl-3-methylideneocta-1,6-diene, 87
N-methylpyrrolidine, 103
molecular ferromagnetism, 38
Müllen, K., 81
Mulliken charges, 59
myrcene, 87
nanotubes, 21
nitrile oxides, 105
norbornene, 109
nucleophilic additions, 75, 116, 170, 186, 189, 191
1-organo-1,2-dihydrofullerenes-60, 58, 60
oligohydrofullerenes, 115, 116
organolithium reagents, 57, 58, 174
organopalladium polymers, 150, 160
Osawa, E., 5
osmylation, 162, 166, 170, 171
oxygenation, 162, 163, 189
ozonolysis, 197
pentacarbonylrhenium radicals, 136, 146
1-phenyl-1,2-dihydrofullerene-70, 62
phenylene-bis(diazomethane), 93
phenylthiyl radical adducts, 140
Pirkle-type phases, 23
poly(bisphenol A hexamethyleneurethane), 94
polyaromatic hydrocarbons, 11, 16
polyfluorofullerenes, 172, 173
polyhydrofullerenes,5, 115, 116, 125, 126, 127, 128, 129, 130, 131, 132, 194
polymethoxyfullerenes, 176
polynaphthyls, 12
polystyrene gel, 23
pyracylene, 170
pyramidalization, 186, 191, 193
pyrazoline, 87, 90
pyridinium chlorochromate, 100
pyridinium *p*-toluenesulfonate, 100
quadricyclane, 108
o-quinodimethanes, 82
[5]radialene, 89
radical additions, 136, 137, 143, 145
regiochemistry, 185, 190, 191, 192, 193, 195, 198
resistive heating, 7, 9, 10
retro-Diels–Alder, 80
Rubin, Y., 85
Schlegel diagram, 3, 4, 5, 26, 177, 178, 179, 190
sebacoyl chloride, 93
self-assembled monolayers, 75
Sharpless cinchona alkaloids, 170
Smalley, R. E., 5, 6, 10
solar generators, 1, 10, 198, 199
Soxhlet chromatography, 22, 23
spectroelectrochemistry, 40
Stone–Wales rearrangement, 17, 20
strain energy, 186
sulfinimides, 106
superconductors, 38, 45, 47, 49, 50, 51, 53, 198, 199
tetrahydrofullerene-60, 117, 123, 124
tetrakis(dimethylamino)ethylene, 52, 53, 198
1,1,2,2-tetrakis(2,6-dimethylphenyl)disilirane, 106
1,1,2,2-tetramesityldisilirane, 106
1,1,3,3-tetramesityl-1,3-disilolane, 106
transfer hydrogenation, 127
transition metal complex formation, 150, 151
transition metal complexes, 150, 151, 159
tri-*O*-acetylglycal, 100
trimethylenemethanes, 99
2-trimethylsilyloxy-1,3-butadiene, 86
3-triphenylmethyl-5-oxazolidinone, 104
Vaska's complex, 155, 157
Wudl, F., 8, 199
X-ray lithography, 198
yttrium fullerenes, 13